Environmental Geochemistry and petrology of the recent sediments from lakes in the vicinity of the coal-fired power plants in central Alberta, Canada

By

Hamed Sanei
B.Sc., Shiraz University, 1994

A Dissertation Submitted in Partial Fulfillment of the
Requirements for the Degree of

DOCTOR OF PHILOSOPHY

in the School of Earth and Ocean Sciences

Supervisors: Drs. F. Goodarzi & E. van der Flier-Keller

ABSTRACT

This study utilizes geochemical and petrological approaches to characterize recent sediments and their porewaters from the central Alberta lakes to elucidate the possible impact from coal utilization in this region. A multi-elemental analysis of recent sediments in conjunction with other inorganic and organic geochemical approaches are applied to determine the sources, quantity, and processes involved in the temporal and spatial distribution of trace elements in the study region.

Concentration versus depth profiles in the sediments and the associated porewaters suggest that geochemical processes impact the mobility and vertical distribution of trace elements in these sediments. Although inputs of trace elements to ecosystems have clearly been elevated by emissions from the coal-fired power plants, diagenetic processes and natural inputs cannot be ignored in determining the temporal and spatial distribution of lake sediments. A combination of various biogeochemical processes may control the distribution of elements and nutrients in sediment and porewater. However, because of the alkalinity and eutrophic conditions of the studied lakes, and in particular Wabamun Lake, the Ca-OM fraction plays the most important role as substrate for trace elements and nutrients (e.g., P). The higher input of calcareous fly ash in Wabamun Lake as compared to the other studied lakes may cause higher scavenging of trace metals.

The size of fly ash particles tends to decrease towards the more recent part of the sediment profile indicating the effect of particle emission control measures adopted by

the power plants. There is no evidence of fly ash particles in the sediments deposited prior to the commencement of coal-fired power plants in Wabamun Lake (before 1956). Fly ash particles can be also found in the post-industrial sediments of Isle Lake. However, the sediment of Lac Ste. Anne shows no evidence of fly ash deposition.

The affinity of various rare earths elements (REEs) to the labile organic matter (S1-OM) in porewater causes preferential fractionation of REEs throughout the porewater profile during the diagenesis process. In contrast, the sediments show little fractionation as a result of high clastic input of REE-enriched clay minerals in the sediment that mask the patterns caused by diagenetic processes.

The relationships between the temporal distribution of organic matter and concentrations of trace elements indicate that the significant positive correlation between TOC and metals in recent sediments arises mainly from the portion of organic matter related to the thermally labile compounds released during pyrolysis at 300°C (S1-compounds). In contrast, the higher molecular, kerogen-derived hydrocarbons show a consistently lesser correlation with trace elements. The strong affinity between temporal distribution of metals and thermally labile compounds is due to both the chemical reactivity and petrological characteristics of these amorphous compounds. The S1-compounds are derived mainly from 'bitumen stain-like' amorphous organic matter. The fluid-like nature of the S1-compounds provides surface coating for the sediments grains, which accounts for the strong grain surface adsorption of organic matter.

Supervisors: Drs. F. Goodarzi & E. van der Flier-Keller, (School of Earth and Ocean Sciences)

TABLE OF CONTENTS

LIST OF TABLES

LIST OF FIGURES

ACKNOWLEDGEMENTS

This dissertation is a joint project between Geological Survey of Canada (GSC), Calgary (Alberta) and School of Earth and Ocean Sciences, University of Victoria (British Columbia). The entire project was funded by the Environmental Study Group of the GSC-Calgary.

I would like to express my deepest gratitude to Dr. Fariborz Goodarzi, who supervised this research project and provided the financial support that has made the completion of this project possible. This dissertation is indeed dedicated to him; besides his scientific guidance, he has been a source of inspiration in all aspects of my personal life.

I am also indebted to the following individuals for their invaluable support in the completion of this dissertation.

- Dr. Eileen van der Flier-Keller (University of Victoria), for supervision of my Ph.D. program.

- Dr. Kevin Telmer (University of Victoria), member of my supervising committee, whose invaluable scientific advise was instrumental for provoking further examination of the topics I chose for this study.

- Dr. R.M. Bustin (University of British Columbia) for accepting to be my external examiner.

- Dr. L.D.Stasiuk of GSC-Calgary, whose scientific advise on Organic Petrology provided an avenue for the exploration of a new topic in this field. He provided me with unlimited access to the lab facilities as well as ongoing encouragement and personal support throughout my evolving course of study.

- Dr. L.R. Snowdon (University of Calgary) who always generously donated his valuable time for scientific discussions, technical assistance, and reviewing my dissertation. He also provided me with unlimited access to Organic Geochemistry lab.

- Mr. J Budahn (U.S. Geological Survey) for undertaking the isotopic dating and Neutron Activation Analyses of the samples in Phase 1 of this research. The author also benefited from his invaluable scientific advise for the calculation of isotopic data.

- Mr. Labonté (GSC, Calgary) for creating a computer program providing me with a unique way of presenting the multiple sediment profiles based on their similarity indices. His very useful discussions on the statistical analyses of my data were also a great asset during the course of this study.

- Dr. G. Hall and Dr. S. Alpay (GSC, Ottawa) for their very useful scientific recommendations on the field techniques and laboratory methodology.

- Ms. B. Kerr (GSC, Calgary) for editing the earlier draft of this dissertation and her great help in presentation of graphics and the production of the maps.

- Ms. B Balfour (Calgary Herald) for her remarkable task of reviewing and editing the final version of my dissertation.

- Mr. J. Reyes (GSC, Calgary) and Mr. P. Klassen (University of Calgary) for their assistance in the coring project and their extensive contribution in the sample preparation and presentation of data in this dissertation.

- Ms. J. Wong (GSC, Calgary) for her exceptional quality of work in the SEM/EDX analyses of my samples and for her scientific input.

- Mr. R. Dureau (CANMET, Ottawa) for mercury analysis of the samples and his invaluable scientific discussions.

- Mr. R Stewart (GSC, Calgary) for providing technical assistance for Rock-Eval analyses.

- Ms. S. Ashal (GSC, Calgary) for providing training for extraction of organic compounds.

- Dr. A.A. Goodarzi (University of Calgary) for his useful advise on the preparation of my dissertation.

- Ms. S. Gilbert (GSC, Calgary) for assistance in preparation of some of the graphics used in my dissertation.

- Mr. P. Errmann (GSC, Calgary) and his assistants Mr. B. Walker; R.B. Elahee and Mr. K. Vanzeeventer for their construction of the sub-sampling devise and for their technical support of the field project.

- Ms. T. Jeanson (GSC, Calgary) and her assistant Mr. D. Landers for their enormous help with the logistics of the project.

- Mr. P. Houvardas (GSC, Calgary) for his exceptional computer technical support.

- Ms. K. Grundmann for her technical assistance with carbon/sulphur analyzer.

- Becquerel Laboratories Inc. and ACME Analytical Laboratories Ltd. for the analyses of trace elements in the samples.

I would like to express my appreciation to Mr. D. Sargent (GSC, Calgary) for his great assistance in the final production of my dissertation and his editorial help

Finally, I would like to thank Barbara for her love, encouragement and patience throughout the difficult time of my study.

PREFACE

The research presented herein is part of a comprehensive, multidisciplinary project conducted by a joint team of members from the Geological Survey of Canada and the University of Victoria. The entire content of this dissertation has been conceived and written by Hamed Sanei under the supervision and direction of Dr. Fariborz Goodarzi of Geological Survey of Canada (Calgary division), Professor Eileen van der Flier-Keller, and Professor Kevin Telmer of School of Earth and Ocean Sciences, University of Victoria.

This dissertation is written in separate research manuscripts, which are intended for publication in the relevant peer-reviewed scientific journals at a future date. The manuscript presented in Chapter 8 has been accepted, and currently in press for publication in Organic Geochemistry. This paper is co-authored with Dr. Lavern Stasiuk of Geological Survey of Canada and has benefited from the cooperation of Dr. Lloyd R. Snowdon of Geological Survey of Canada (currently at the University of Calgary).

The geochemical study of the recent sediments from Pigeon Lake, Alberta, was initially started as the author's M.Sc. thesis. This study was later upgraded into a Ph.D. thesis containing a greater number of lakes in the central Alberta region. The results of the Pigeon Lake study were published as Sanei et. al, (2000) and (2001), which are attached with this dissertation.

CHAPTER 1: INTRODUCTION

1.1. OVERVIEW

Elements in the environment originate from various natural and anthropogenic sources. Naturally occurring elements may be derived from geogenic sources (e.g., chemical and physical weathering of rocks, volcanic activity), forest fires, and various biological processes (bioaccumulation of trace elements by biota). However, anthropogenic releases of trace elements, particularly those of metals, result partially from the mining, metal smelting plants, incineration of waste/sludge, and fossil fuel combustion (e.g., Nriagu and Pacyna, 1988; Nriagu, 1990; 1994; Rasmussen, 1996; Rassmussen, 1998, Goodarzi et al., 2003; and Telmer et al., 2004).

The main pathways of trace elements to lake ecosystems are surface runoff, groundwater, waste outlets, and atmospheric deposition (Håkanson and Jansson, 1983; Horowitz, 1991). Subsequently, trace elements can be scavenged from lake water to surface sediments during various geochemical processes (Murray,1975; Davis,1984; Ali and Dzomback, 1996; Tessier et al.,1996). Therefore, the geochemical study of recent lacustrine sediments can be used as a tool to monitor levels of trace elements in the environment.

The temporal variation of trace elements in a vertical profile of recent lacustrine sediments offers a key to the pollution history of the lake (Shirahata et al., 1980; Swain et al., 1992). Additionally, the spatial distribution of trace elements in sediments of various lakes have been used to evaluate the transport pattern of trace elements as related to the

extent of impact from the anthropogenic sources (e.g., Telmer et al., 1999; in press a; Anderson, 2003). However, only a few studies have considered the role of geochemical processes involved in the distribution of trace metals and their affinity to organic or inorganic fractions when interpreting metal concentration data in lake sediments (e.g., Telmer et al., 1999; in press a; El Bilali et al., 2002).

Several coal-fired power plants are located in the Wabamun area in central Alberta (Figure 1.1). Emissions from these facilities can be a significant source of elements deposited in the local environment, and as a result are a subject of environmental concern. This study utilizes the geochemical and petrological approaches to characterize the recent sediments from the central Alberta Lakes as related to the possible impact from coal-utilization in this region.

1.2. BACKGROUND

The coal-fired power plants in central Alberta have been in operation for half a century. Their activities have long raised public concern about the atmospheric deposition of contaminants in the nearby bodies of water (Mitchell, 1990, Anderson, 2003). The Wabamun region in Central Alberta is located in the focal point of four major power plants (Figure 1.1). The Wabamun, Sundance, Keephills and Genesee Power Plants have been implicated by some studies as being the main sources of trace elements accumulation in the region (e.g., Donahue 2002).

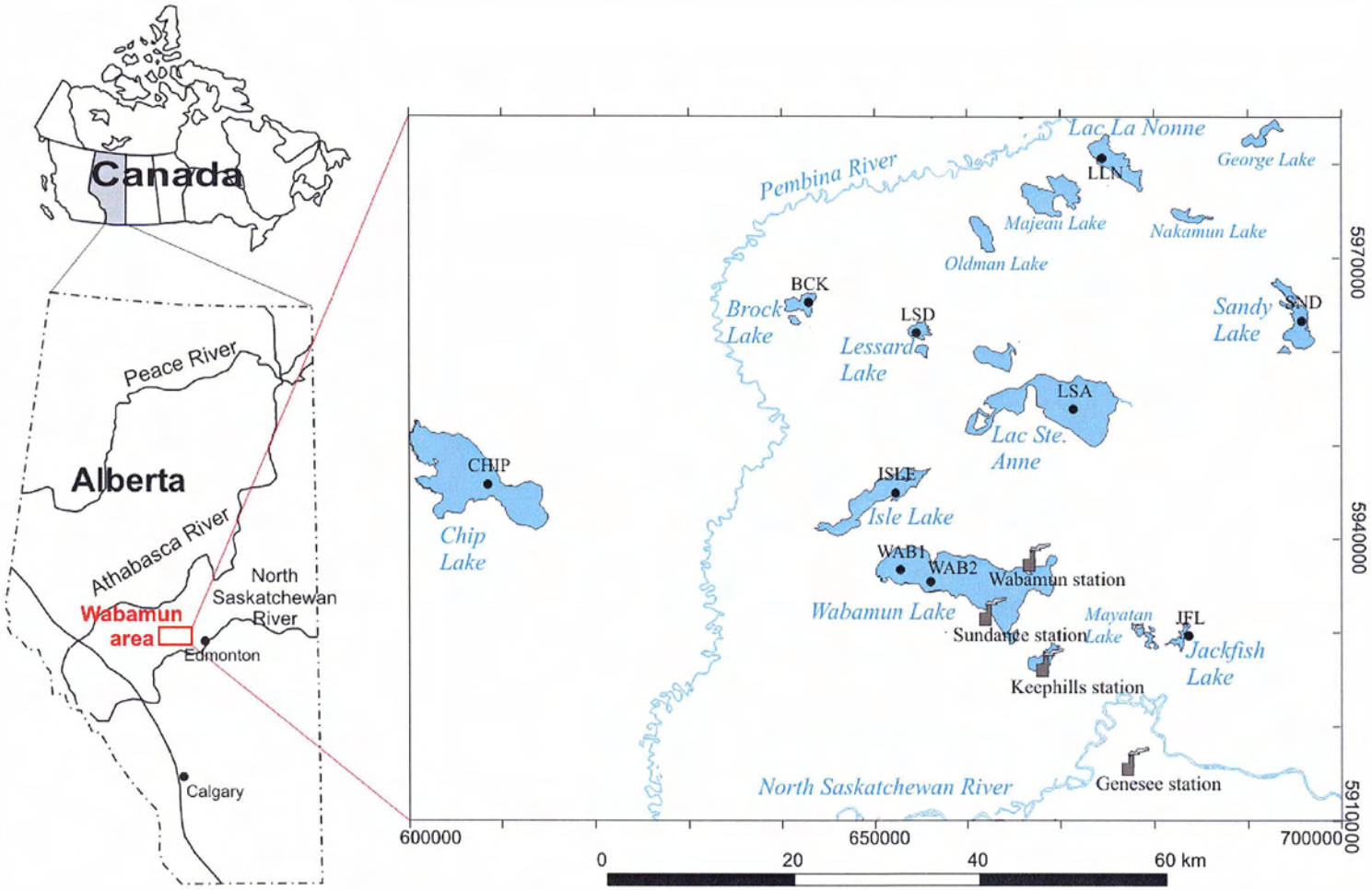

Figure 1.1: Map of the studied lakes in Central Alberta, locations of the sediment cores in each lake, and locations of the coal-fired power plants in Wabamun area.

Lake basins cover large portions of land in the Wabamun region, and may act as sinks for emitted particles/elements from the coal-fired power plants. Therefore, sediment quality sampling has been carried out in the lakes in the Wabamun region as part of a variety of research or monitoring initiatives to determine contaminant levels in sediments deposited over the past decades. There has been great interest expressed by the government, local residents, and industry stakeholders (coal-fired power generating companies) in such studies since they would indicate the possible effects of the industrialization and urbanization of the region. Many of these studies have been focused on Wabamun Lake due to the controversy concerning the effect of the power plants and their associated coal mines on the lake sediment and water quality (Reid Crowther Partners Ltd., 1973; Noton, 1974; Beak Consult. Ltd., 1980; Habgood, 1983; AENV, 2002, Golder Associates, 2002; Donahue, 2002; HydroQual Laboratories, 2003; Anderson, 2003). Almost all sediment studies in the Wabamun region attempt to link the temporal and spatial variation of trace elements and other contaminants to the coal-utilization activities in the study area. These studies typically use a monitoring approach by reporting the total concentration of trace elements in the sediment as a way of determining the sediment quality. There is, however, insufficient information to understand the factors/processes that influence the distribution of trace elements in the Wabamun region.

The vertical profile of the elements in conjunction with the age of the sediments is typically used to interpret the history of the Wabamun lake as related to the coal-utilizing activities in its watershed (e.g., Donahue 2002). This type of study uses the "forensic

approach" to establish a correlation between the emission history of the power plant and the age of a sediment profile as a way to establish the impact of the power plant on the lake. Based on such an approach, an enrichment of trace elements in surface sediments relative to deep sediments is regarded as a degree of impact by coal-fired power plants in Wabamun Lake (Donahue 2002). In contrast, there are other studies, which suggest mainly natural geochemical sources for the metals in the Lake Wabamun sediment (e.g., Anderson, 2003). These types of studies, however, do not address the geochemical interactions between sediment and porewater during early diagenesis in the recent sediments. The interaction between sediment and water is a very important factor in the biogeochemical cycling of elements in their natural aquatic environment. These processes are known to significantly alter the temporal variation of elements throughout the sediment profile. (Eck and Smits, 1986; Gobeil et al., 1987; Morfett et al., 1988; Jahnke et al., 1989; Gerringa, 1990; Ivert, 1990; Carignan and Lean, 1991; Dahmke et al., 1991; Barbanti et al., 1992a; Williams, 1992). Therefore, the proper interpretation of the elemental data, in terms of historical events, requires careful examination of the sediments in relation to the porewater found within the sediments. Furthermore, it is important to preserve the natural anoxic environment of sediments during the coring/sampling procedure. Oxidation of the sediment during sampling may alter the distribution pattern of trace elements throughout the sediment column (Song and Müller, 1999).

This study uses geochemical and petrological approaches to reveal more detailed information on the processes involved in the distribution of trace elements in the

sediment in the Wabamun region. The results of this study may provide a new insight into the way that the sediment data can be interpreted, especially in the Wabamun area.

1.3. OBJECTIVES

A multi-elemental analysis of the recent sediments in conjunction with other inorganic and organic geochemical factors provides valuable information on the sources, quantity, and processes involved in the distribution of trace elements in the study region. In this study, a wide range of analytical techniques and petrographic methods (Chapter 1.7) assist us to characterize the recent sediments and their porewater from the Wabamun region in central Alberta. This comprehensive study includes 9 lakes, which cover an expansive geographical area in the study region (Figure 1.).

The main objectives of this study are (i) to determine the age of sediments and sedimentation rate in all studied lakes; (ii) to investigate the temporal variation and spatial distribution of trace elements in the recent sediments from the Wabamun area; (iii) to determine the possible mobility of trace elements during the early diagenetic processes and geochemical interactions between sediments and porewater; (iv) to study the affinity of trace elements with organic and inorganic compounds and the geochemical factors influencing metal distribution; (v) to characterize mineralogy and morphology of sediment particles; and (vi) to characterize the organic compounds in the sediment using organic geochemistry/petrology approaches.

1.4. PROJECT DESCRIPTION AND SAMPLING STRATEGY

Valid quantitative measures of the geochemical parameters in the sediments require a uniform sediment size fraction (Håkanson and Jansson, 1983). This is especially important where the study involves the inter-comparison among sediments obtained from various locations in the lake(s). A direct comparison between the sediments obtained from the littoral zone and those from deep, off-shore parts of the lake can often be misleading (Håkanson and Jansson, 1983). For example, sediments from the shallow parts of Pigeon Lake showed lower concentrations of most elements as compared to those from the deepest parts (Sanei et al., 2000; 2001). The reason for this is that grain size, which varies at different depths in a lake, largely influences the bulk concentration of inorganic/organic matter in the sediments (Premuzic et al., 1982; Tyson, 1995; Håkanson and Jansson, 1983; Horowitz 1991; Sanei et al., 2000; 2001). This is due to the greater surface area of fine-grained sediments, allowing greater adsorptive accumulation of elements and organic matter by smaller sediments (Weiler and Mills, 1965; Suess, 1973; Tanoue and Handa, 1979; Mayer et al., 1985; 1988; Horowitz 1991; Sanei et al., 2000; 2001).

To establish a common base for the comparison among sediments obtained from various parts of the lakes with different grain sizes, wet sieving is suggested (Håkanson and Jansson, 1983). The wet sieving method attempts to isolate the < 63 μm size fraction of the sediment to limit the variability of the sediment size and provide a representative

sample. However, there is a large contamination risk involved while sieving the samples in the field, as well as the potential loss of porewater and colloidal fractions, both of which carry a substantial portion of elements and organic matter in the sediment.

The alternative method for isolating the uniform and comparable sediment size fraction is to rely on the natural capability of a lake to sort the sediment grains itself. The sediment grain size can be naturally sorted due to the wave action within the lake. The finest sediment particles tend to remain suspended in the water column until they are finally deposited in the deeper, less disturbed part of the lake, well away from the shore. In contrast, heavy particles cannot travel long distances from the littoral zone and gradually accumulate in the shallow part of the lake (Håkanson and Jansson, 1983). This natural phenomenon is common in shallow lakes with large surface area to mean depth ratios, such as the lakes in this study (Mitchell and Prepas, 1990). As a result, the grain size distribution of the bottom sediments is spatially sorted, ranging from coarse-grained sediments in the littoral zone, to fine-grained sediments in the deeper part of a lake. The sediment samples in the deepest part of the lake are presumably sorted to the finest grain size fraction (the silt-clay fraction) with the least variability in the grain size.

Obtaining several sediment cores from each lake following the statistical gridding method would satisfy the proper representative sampling protocol (Håkanson and Jansson, 1983). However, statistically valid sampling strategies can often require a number of samples and sample tests that are prohibitively expensive and time consuming. Hence, a decision was made to obtain a representative sediment core from the deepest

portion of each lake (two deep-hole cores were obtained in the Wabamun lake) (Figure 1.1). The deep-hole sediments are the best available choice for representative sampling, especially when the study involves comparisons between various cores/lakes in a general aquatic pollution study. This is because the sediments obtained from the deep-hole are: (i) naturally sorted to the finest grain size fraction (the silt-clay fraction), which has the highest ability for adsorption of contaminants; (ii) less disturbed with respect to the historical profile, as the least turbidity occurs in this area; and (iii) show the most representative data reflecting the sum of allogenic, authogenic, and endogenic processes in the lake (Dean and Gorham, 1976; Garrett and Hornbrook, 1976; Mitchell and Prepas, 1990).

The coring project was conducted in two phases. The first phase (Phase I) took place in the winter of 2001 (late February), when all the studied lakes were covered with 60 to 80 cm of the ice. Phase I included nine lakes, Lac La Nonne (LLN), Lessard Lake (LSD), Chip Lake (CHIP), Brock Lake (BCK), Isle Lake (ISLE), Jackfish Lake (JFL), Lac St Anne (LSA), Sandy Lake (SND), and Wabamun Lake (WAB) (Figure 1.1). The studied lakes are located various radial distances from the coal-utilization installations in the Wabamun region (Figure 1.1). One representative core was taken from the deepest part of each lake, except Wabamun Lake where two cores were obtained from the deepest parts (Figure 1.1).

The second phase (Phase II) of the lake-coring project was conducted in October 2002, during the open water period (not frozen). The focus of study in Phase II of the

project was on the interaction between porewater and sediments and included more detailed temporal geochemistry of the lake sediments. It was essential to study the interaction between porewater and sediments under the same geochemical condition as the bottom of the lake. For this reason, the entire sub-sampling and sample preparation in Phase II was carried out under anoxic conditions (N_2-filled glove bag). The porewater samples were also retrieved under a N_2 atmosphere (Chapter 1.7).

The phase II project covered only the Wabamun Lake, Isle Lake, and Lac Ste. Anne, which are all exposed to the same prevailing wind direction. The lakes chosen for Phase II of the study represent proximal (Wabamun), short (Isle Lake), and medium distances (Lac Ste. Anne) from the Wabamun coal-utilizing facilities. The same coring locations from Phase I (winter 2000; Figurer 1.1) were revisited by tracing the previously registered coordinates for each coring site using the Global Positioning System (GPS). A core was collected from each of the two deepest regions (west side) of Wabamun Lake (WAB1 and WAB2), as well as from the deepest regions (east side) of Isle Lake (ISLE) and Lac Ste. Anne (LSA) (Figure 1.1).

In this dissertation, the results of the Phase II project are discussed in detail (Chapter 3, 5, 6, 7, 8, and Appendix A) but only a portion of the Phase I results related to the sediment dating (Chapter 2) and spatial comparison of elements (Hg in particular; Chapter 4) are presented. In this dissertation, special attention is given to the Wabamun Lake due to health and environmental concern for this lake.

1.5. ADDITIONAL RESEARCH

In addition to this study, the author was involved in an investigation of the geochemistry of recent sediments from Pigeon Lake, also located in central Alberta. Pigeon Lake serves as site-specific natural background for the study region due to its longer distance from the coal-fired power plants as compared to the other lakes in the Wabamun area. The results of this study are published as Sanei et. al, (2000) and (2001) (attachment). Some of the geochemical interpretations in this current study are based on concepts developed by Sanei et al., (2000) and (2001).

1.6. STUDY AREA

Nine lakes from two major drainage basins located in central Alberta have been chosen for this study (Figure 1.1). The selected lakes are as follows:

- Athabasca River Basin: Lac La Nonne, Lessard Lake, Chip Lake, and Brock Lake.

- North Saskatchewan River Basin: Isle Lake, Jackfish Lake, Lac St Anne, Sandy Lake, and Wabamun Lake.

Lakes on the Boreal Plain of western Canada are essential for domestic, municipal and industrial water sources, and are often used for recreation and urban development (Murphy et al., 1990; Prepas et al., 1997). These lakes are influenced by a variety of anthropogenic as well as geogenic and natural activities in central Alberta. A substantial increase in Alberta's population over the past century has had a definite impact on the drainage basins of most Alberta lakes (Mitchell and Prepas, 1990). All the lakes in central Alberta are likely to receive local and long-range industrial fallout. The major local industrial sources of atmospheric emissions in this region are coal-fired power plants and gas refining plants.

The mean depths of the lakes are the indicators of the morphology, limnology and water quality characteristics. Lake Wabamun has the greatest mean depth (6.3 m) as compared to Lac Ste. Anne (4.8 m) and Isle Lake (4.1 m) (Mitchell and Prepas, 1990). The order of mean depth in the lakes is inversely proportional to the amount of nutrients (total phosphorous: Isle Lake> Lac Ste. Anne > Wabamun Lake) and hence productivity (as indicated by amount of Chlorophyll a: Isle Lake> Lac Ste. Anne > Wabamun Lake). This indicates that the lake water with the shallow mean depth will mix from the surface to the bottom on windy days. The bottom sediments may be a source of nutrients, which will enhance productivity and reduce the dissolved oxygen level (Mitchell and Prepas, 1990).

Drainage basin sizes relative to lake areas within each basin are highly variable in this study, thus influencing the water quality of each studied lake. For instance, lakes with proportionately larger drainage basins usually receive more runoff and consequently

greater amounts of nutrients and suspended sediment than lakes with small basins (Mitchell and Prepas, 1990). The ratios of the drainage basin area to the lake area are greater in Lac Ste. Anne and Isle Lake (11.4 and 10.7, respectively) as compared to that of Wabamun Lake (3.2) (Mitchell and Prepas, 1990). This is also proportional with amount of nutrients (total phosphorous) and degree of productivity, which is greater in Lac Ste. Anne and Isle Lake relative to Wabamun Lake (Mitchell and Prepas, 1990).

Bedrock in Alberta is primarily sedimentary and consists of layers of sandstone, siltstone, shale, coal, and limestone. The current geomorphology of the study area is formed because of the ice ages during the Quaternary period, when huge ice caps formed in the Arctic regions and began to flow southward over large areas of North America. As the ice sheets advanced and retreated over Alberta, they reshaped the land, eroding the mountains, moving rocks and depositing gravel and silts. The last retreat of the ice, beginning 12,000 years ago, formed a blanket of glacial till of up to 100 m thick over almost all of Alberta east of the mountains. In central Alberta, the terrain is more hummocky and rolling such as that seen west of Stony Plain. Most of the studied lakes were formed by the retreating glacier and till pile, where holes or kettles were left in the landscape due to the melting ice (Mitchell and Prepas, 1990).

In this study, more attention was given to Wabamun Lake, Isle Lake, and Lac Ste. Anne (Figure 1.1). Wabamun Lake hosts the Sundance and Wabamun generating stations upon its shore (Figure 1.1) so it will likely show the strongest influence of the stations within its sediments. Moreover, Isle Lake and Lac Ste. Anne were selected due to their

proximities to power plants and large surface areas (Figure 1.1). Prevalent wind direction in the region is from the northwest (Environment Canada, 1982), and as a result the greatest deposition of elements will likely be downwind of generating plants.

The following are brief descriptions of the lakes given the most attention in this study:

1.6.1. Wabamun Lake

Wabamun Lake is a large (total surface area: 81.8 km^2), shallow lake (average depth: 6.3 m), located at 53°33'N 114°36'W (Lat/Long), west of the city of Edmonton, Alberta, Canada (Mitchell, 1990a) (Figures 1.1; 1.2).

The first settlements in the Wabamun area occurred in 1912. Since that time, about half of the land in the basin has been either cleared or used for agricultural purposes (Reid, Crowther Partners Ltd. 1973) (Figure 1.2). Presently, Wabamun Lake itself is also used extensively for recreational activities. The first underground coalmine operation began in 1910 in the lake's watershed. Subsequently, strip coal mines have run operations since 1948 (Mitchell, 1990a). The Wabamun and Sundance power plants were built on Wabamun Lake and have been operating since 1956 and 1970, respectively (Figures 1.1; 1.2). A third plant, Keephills, is located just outside the watershed southeast of the lake, but its cooling pond lies within the watershed boundary (Figures 1.1; 1.2).

The runoff from the watershed is conveyed into the lake through at least 35 intermittent drainage streams, which flow only during snowmelt in spring and rainstorms in summer. There are some streams on the north side of the lake, which have a continuous base flow from groundwater (Mitchell 1990a; Figures 1.2). The lake's outlet, Wabamun Creek, flows intermittently towards the North Saskatchewan River (Mitchell, 1985; Figures 1.2).

Wabamun Lake is a fresh water lake with total dissolved solids (TDS) of 235 mg/L) (Mitchell, 1990a). Bicarbonate and sodium are the dominant ions in Wabamun lake water (Mitchell, 1990a). The water is well mixed showing similar temperatures from the top to the bottom of the water column. As well, the water column is normally well oxygenated from May through October. This is due to the large surface area of the lake relative to its depth and the orientation of the lake with respect to the prevailing wind (Mitchell, 1990a). In hot weather, rapid surface warming promotes temporary thermal stratification, and dissolved oxygen levels decline in the hypolimnon. Under frozen water conditions in winter, the main basin of the lake remains well oxygenated near the surface, although oxygen levels gradually decline at the bottom. Total oxygen depletion under ice occurs in some years due to the shallowness of the Wabamun Lake and abundant plant growth. A region in the east end of the lake remains unfrozen all winter due to heated effluent from the Wabamun Power Plant (Gallup and Hickman, 1973; Mitchell, 1990a).

Wabamun Lake is mildly eutrophic (Hamilton and Reynoldson, 1981). Diatoms (Bacillariophyta) and blue-green algae (Cyanophyta: *Anabaena* spp. and *Aphanizomenon*

flos-aquae) form the dominant phytoplankton biomass in Wabamun Lake (Mitchell, 1990a).

The bottom of Wabamun Lake is relatively flat, with a gradual slope towards the deepest area located at the western end of the lake, where the sampling sites are located. The surficial deposits in the southern and western regions of the lake consist of discontinuous glacial till or Paleocene sedimentary bedrock. In some parts of the lake bottom, and along the shoreline, coal outcrops contribute significantly to the sediment compositions. This is apparent as some beach sands along the lake are black (Mitchell, 1990a). Coal seams in Wabamun Lake occur in the lowermost portion of the Paskapoo Formation or in the uppermost Cretaceous bedrock. The surficial deposits to the east of the lake consist of fine-grained glaciolacustrine materials. Bedrock underlying the eastern part of the lake was formed during the Cretaceous age (Andriashek et al. 1979).

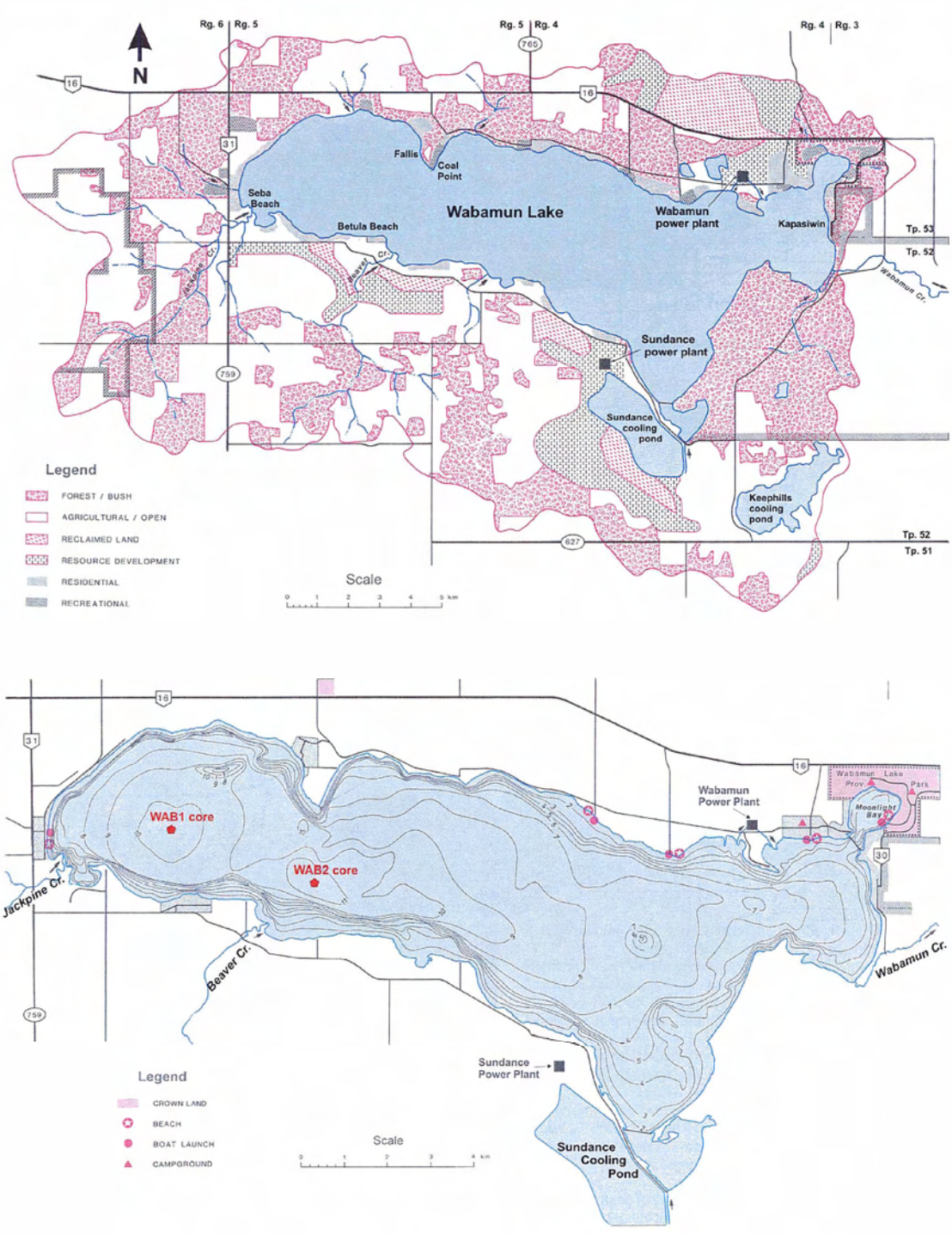

Figure 1.2: Map of Wabamun Lake drainage basin, land use, the bathymetry map of the lake, and location of its sediment core. After Mitchell and Prepas, (1990).

1.6.2. Isle Lake

Isle Lake is classified as hyper-eutrophic and is located west of Edmonton, Alberta, in the counties of Parkland and Lac Ste. Anne (Lat/Long: 53°38'N 114°44'W) (Figures 1.1; 1.3). Isle Lake is shallow with a maximum depth of only 7.5 m, occurring at the middle of the lake (Figure 1.3). The lake is made up of a small, shallow western basin and a slightly larger and deeper eastern basin (Figure 1.3). The total surface area of the Isle Lake is 23 km^2 (Buckland-Nicks and Mitchell, 1990).

Isle Lake contains freshwater (Total dissolved solids: 155 mg/L) dominated by calcium and bicarbonate ions (Alberta Environment, 1989; Mitchell 1984; R.L. & L. Environmental Services Ltd., 1987). Because the lake is shallow, large, and exposed to prevailing westerly winds, its waters mix from the surface to the bottom on most days during the open-water season. The water column is weakly thermally stratified on hot, calm days. Dissolved oxygen concentrations in the lake are frequently very low during winter (R.L. & L. Environmental Services Ltd., 1987).

The drainage basin of Isle Lake is about 11 times the size of the lake (Buckland-Nicks and Mitchell, 1990; Figure 1.3). Most surface water flows into the lake from the Sturgeon River in the southwest (Figure 1.3). Several intermittent streams drain the remainder of the drainage basin. The lake's outlet, also the Sturgeon River, is located at the eastern end and flows eastward from Isle Lake to the North Saskatchewan River via

Lac Ste. Anne, Matchayaw Lake, and Big Lake (Buckland-Nicks and Mitchell, 1990; Figure 1.3).

Four bedrock formations underlie Isle Lake. The lowermost, Horseshoe Canyon Formation, is lithologically complex resulting in groundwater conditions that differ markedly from region to region. Overlying the Horseshoe Canyon Formation are the relatively impermeable Whitemud and Battle formations. The Paskapoo Formation lies nearest to the surface and offers the most reliable source of groundwater. This formation contains the Ardley coal zone, which is mined at nearby Wabamun Lake. Surficial deposits appear to be closely related to the underlying bedrock. The undulating ground moraine that covers most of the drainage basin is composed of glacial till, and lesser amounts of glaciolacustrine deposits. Organic deposits occur in depressions throughout the basin, and beach sands occur around the shoreline (Twardy and Brocke 1978; Buckland-Nicks and Mitchell, 1990).

Settlement around Isle Lake began in 1905 after the clear cutting of forested lands for agriculture. The most rapid development of land around the lake occurred between 1955 and 1964. About 54% of the drainage basin is forested, while 45% is open or has been cleared for agriculture. The remaining 1 % has been developed with cottages and permanent residences (Buckland-Nicks and Mitchell, 1990). Trembling aspen is the dominant tree on well-drained sites, while balsam poplar, white spruce, and willow are prevalent in more poorly drained areas (Edmonton Regional Planning Commission. 1983).

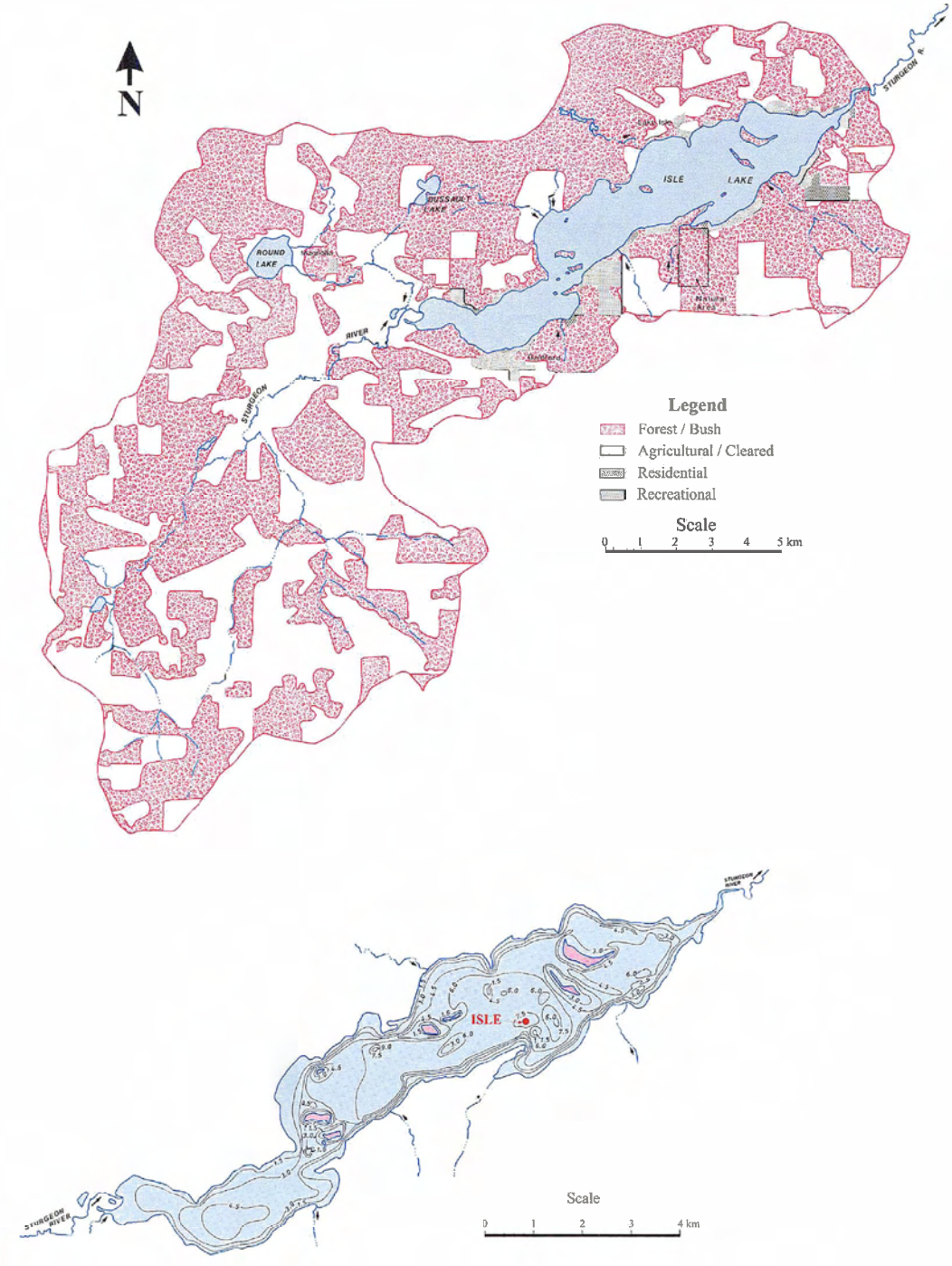

Figure 1.3: Map of Isle Lake drainage basin, land use, the bathymetry map of the lake, and location of its sediment core. After Mitchell and Prepas, (1990).

1.6.3. Lac Ste. Anne

Lac Ste. Anne is located in the county of Lac Ste. Anne, approximately 46 km northwest of the city of Edmonton (53°42'N 114°25'W Lat/Long) (Mitchell, 1990b; Figures 1.1; 1.4).

Lac Ste. Anne is made up of two basins connected by a narrow passage. The east basin is larger and contains the deepest water (9 m). The west basin is smaller with a maximum depth of 6 m (Mitchell, 1990b). The sediment core was obtained from the deepest part (9 m) of the east basin.

Lac Ste. Anne is a freshwater lake with low total dissolved solids (156-165 mg/L). The dominant ions in Lac Ste. Anne are bicarbonate and calcium (Nelson and Mitchell 1988). The water column is well mixed in the summer, except on calm days when the lake may thermally stratify. This stratification results in an anoxic condition at the hypolimnon/sediment-water interface. In winter, oxygen depletion is rapid in the deepest regions of both basins (Mitchell, 1990b).

In terms of trophic status, Lac Ste. Anne is classified as eutrophic. Blue-green algae and diatoms are the dominant phytoplankton biomass in Lac Ste. Anne (Mitchell, 1990b).

The drainage basin of Lac Ste. Anne is more than 11 times larger than the area of the lake and includes Isle and Birch lakes (Mitchell, 1990b; Figure 1.4). There are several small intermittent creeks produced by runoff from the watershed into the lake. However, the main inlet is the Sturgeon River, which flows from Isle Lake into the west end of Lac Ste. Anne (Mitchell, 1990b; Figure 1.4). The outflow is also the Sturgeon River, which leaves the lake at the east end. The Sturgeon River eventually flows into Big Lake and then into the North Saskatchewan River (Mitchell, 1990b; Figure 1.4).

Lac Ste. Anne is extensively used both recreationally and residentially. As well, there are mining activities conducted in the watershed, as a small portion of the Whitewood coal mine extends into the southern part of the basin (Mitchell, 1990b).

The drainage basin is covered by glacial moraine. Sand lenses occur throughout the watershed, with beach sands present at the east end of the lake, and at a few other areas along the shoreline (Macyk and Veauvy 1977). The vegetation in Lac Ste. Anne watershed consists of trembling aspen, balsam poplar, willow, black spruce, and small areas of coniferous dominated forest (Renewable Resources Consulting Services Ltd., 1971).

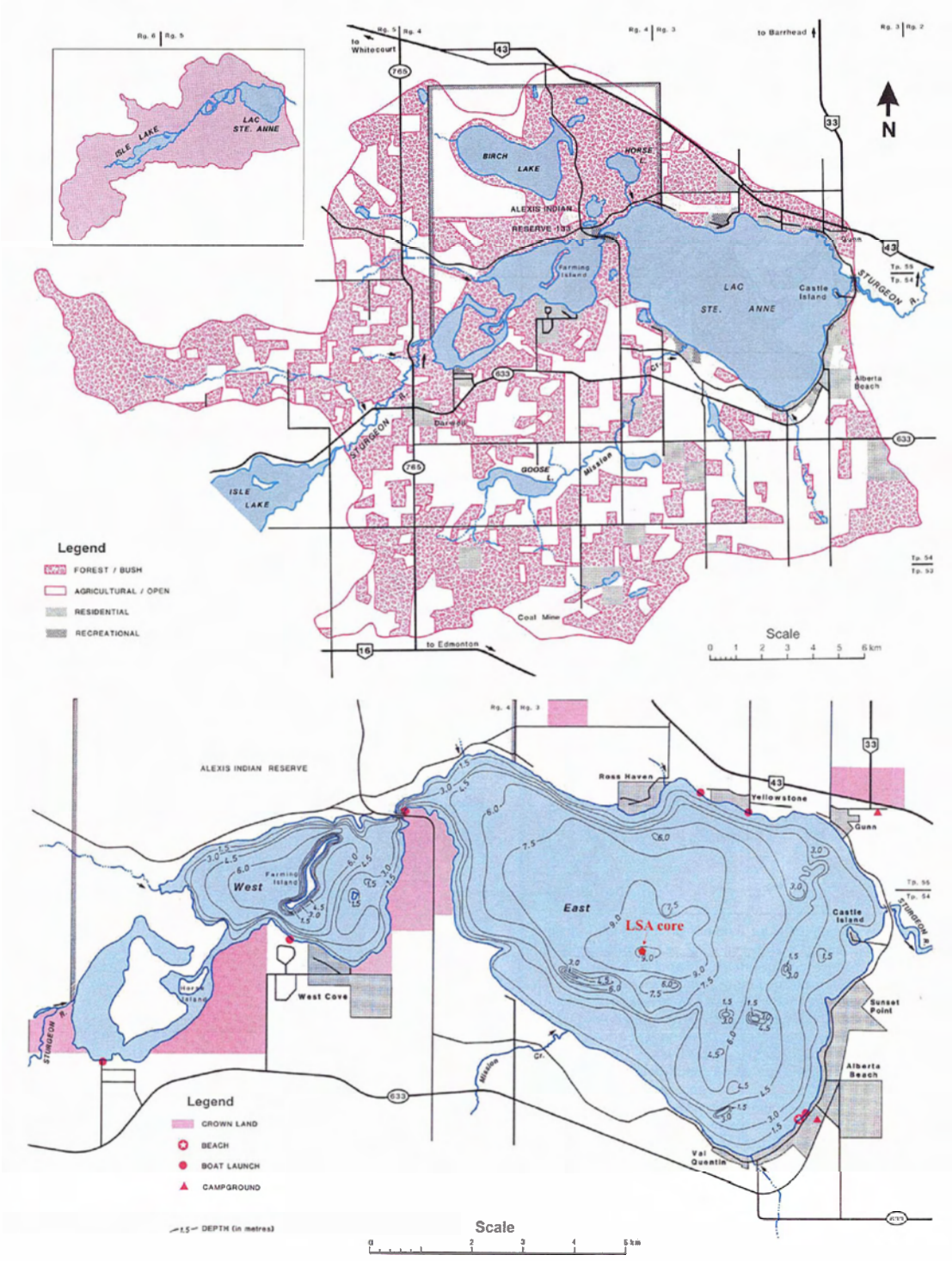

Figure 1.4: Map of Lac Ste. Anne drainage basin, land use, the bathymetry map of the lake and location of its sediment core. After Mitchell and Prepas, (1990).

1.7. METHODOLOGY

1.7.1. Field Methodology

1.7.1.1. Coring project

The deepest location in the lakes was navigated using a Garmin GPS unit and the published bathymetry maps for each studied lake (Mitchell, and Prepas, 1990). Once the position was located, anchors were dropped to stabilize the position of the motorboat.

A modified Kajak-Brinkhurst (KB) core sampler was used to retrieve an undisturbed sediment sample (Figure 1.5a). This coring device was constructed by Telmer et al., (in press b) at the School of Earth and Ocean Sciences of the University of Victoria and is specifically designed to minimize disturbance of the sediment-water interface. The coring device was slowly lowered into the water using a nylon rope with depth interval markings. Once on the lake bottom, the weight of the coring device drove the one-meter polyvinyl chloride (PVC) coring pipe into the sediments to a desired depth (between 60 cm to 85 cm), leaving a 20 cm to 30 cm water column over the extracted sediments to prevent atmospheric exposure. The coring device was then retracted with sediments being held in placed by capillary forces created by a rubber seal. The retracted coring device and PVC pipe were held upright and promptly returned to shore for sub-sampling. Upon arrival to the shore, the coring device was separated from the PVC coring pipe to ease transport from the boat to the sub-sampling station.

1.7.1.2. Sub-Sampling

The sediment cores were sub-sampled in the field using an extrusion device. This reduces the disturbance of the sediments due to the transportation and handling of the cores (e.g., core cutting). The sub-sampling tray was mounted on the top section of the sediment-filled PVC coring pipe. Attached to the sub-sampling tray was a centrifuge tube holding a platform loaded with a sufficient number of pre-labeled 60 ml Fisherbrand centrifuge tubes. The next step involved placing a modified polyethylene glove bag over the sub-sampling tray and the centrifuge holding platform. The existing air in the glove bag was evacuated from the base of the bag, which was connected to the nozzle of a 12-volt vacuum pump. Once the air was removed, the glove bag was filled with nitrogen (Figure 1.5b).

Excess water in the PVC pipe was evacuated using the extruder, where the weight of the core pushes on the extruder forcing the supernatant water out. A metal pin placed in the 1cm interval holes of the extruder is removed and placed one hole down, allowing a portion of the sediment to rise to a level on the sub-sampling platform where it can be scraped and put into a centrifuge tube. This step is repeated until there is no more sediment in the PVC tube. Before dismantling the N_2-glove bag, the centrifuge tubes filled with the sediments and nitrogen headspace were air-tight sealed and placed into vacuum-sealed nitrogen bags. The samples were transported immediately to the lab under temperature conditions of +1 to –4 $^{\circ}$C.

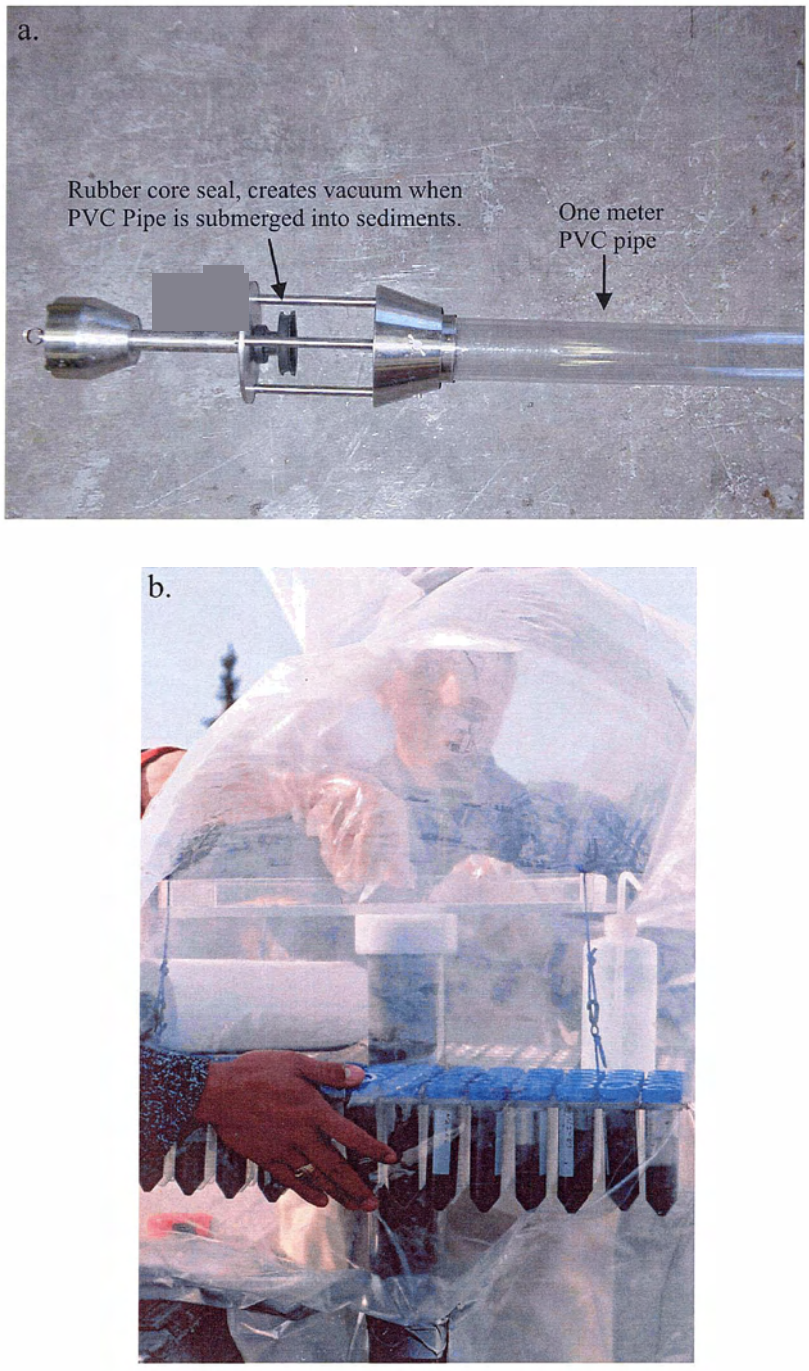

Figure 1.5: (a) A modified KB (Kajak-Brinkhurst) core sampler with PVC pipe attachment (constructed by Telmer et al. (in press b), School of Earth and Ocean Sciences), (b) Complete sub-sampling station insides a nitrogen glove-bag.

1.7.2. Sample preparations

1.7.2.1. Separation of sediment and porewater

Since the goal of the study is to conduct the analysis of both porewater and sediments, the separation of the two is necessary to avoid early co-precipitation of some elements along with iron and manganese oxides. The porewater samples were retrieved by centrifuging the wet sediment sample at 5000 rpm inside the sealed centrifuge tube filled with N_2 headspace. The advantage of the centrifuging method is that it provides direct relationships between the sediment interval and its porewater. The centrifuged samples, along with all the necessary equipment (a sufficient number of 30 ml syringes, an equal number of < 0.45μm syringe filters and several pre-labeled, loosened cap, 15ml Nalgene bottles), were transferred into the nitrogen glove bag. The supernatant water in each centrifuge tube was decanted into a 30 ml syringe fitted with a < 0.45 μm Millipore® syringe filter (Hall 1998; Hall et al., 2002). The porewater from each sediment interval was filtered evenly and split into two 15 ml Nalgene bottles, one meant for mercury analyses and the other for conducting analyses of the rest of the elements. The remaining sediments were freeze-dried and ground finely before the geochemical analyses.

1.7.2.2. Porewater Acidification

While the porewater samples were still in the nitrogen chamber, each split sample was treated using different reagents. A calculated amount of 0.5% Bromine monochloride (BrCl) solution was used to fix and preserve Hg as bivalent mercury in the solution (EPA, 1996; Hall 1998; Hall et al., 2002). The other porewater split was acidified using 1% HNO_3 to preserve the remaining metals in the solution.

1.7.3. Analytical

The porewater and sediment sample were subjected to various geochemical analyses, which are discussed further in this paper. In all analytical methods, duplicate samples and laboratory standards were used to monitor analytical accuracy and precision. For porewater samples, both the laboratory and field blanks were tested to insure the quality of the analyses.

1.7.3.1. Multi-elemental analyses

The concentrations of elements in sediment samples were analyzed using both Inductively Coupled Plasma-Mass Spectrometry (ICP-MS) and Instrumental Neutron Activation Analysis (INAA). The two sets of data were compared against analytical standards, and the elemental results with the best detection limit/precision were chosen. The presented sediment data is given in concentration per gram of dry substance.

The quantitative measurements of all elements (except Hg) in porewater samples were carried out using ICP-MS.

1.7.3.1.1. ICP-MS

The geochemical analyses of elements in collected sediment and porewater samples were conducted using a Perkin-Elmer Elan 6000 Inductively Coupled Plasma-Mass Spectrometry (ICP-MS) unit located in ACME Analytical Laboratories Ltd (Vancouver, British Columbia, Canada). The sediment samples were introduced to ICP-MS following a hot digestion with nitric, perchloric, and hydrofluoric acids. However, the porewater samples were directly injected into ICP-MS without any acid digestions. The reader is referred to Stoeppler (1992) and Sloss and Gardner (1995) for further details on sample preparation and instrumentation used in ICP-MS methods.

1.7.3.1.2. INAA

Instrumental Neutron Activation Analyses (INAA) were also used to determine the bulk concentrations of element in the sediment samples. This method was carried out using McMaster University's (Hamilton, Ontario) nuclear reactor followed by Gamma Spectrometry conducted by Becquerel Laboratories Inc. Instrumental Neutron Activation Analysis (INAA) involves irradiating samples with neutrons to produce unstable radioactive nuclides. The sediment samples (100 mg) were irradiated at 2 MW with a

flux of 8×10^{12} neutrons $cm^{-2}s^{-1}$ in the core of the nuclear reactor. Neutrons are absorbed by various elements in the sample to produce unstable radioactive isotopes (radio-nuclides). Many of these radionuclides emit gamma-rays of characteristic energies that can be measured utilizing high-resolution semiconductor detectors. Therefore, after a waiting period, the sample was placed close to a high resolution instrinsic germanium coaxial detector coupled through a Canberra model 2024 fast spectroscopy amplifier to a model 8715 ADC nuclear data ND599 loss free counting module. Interactions between the gamma-rays (which continue to radiate from the sample) and the detector, lead to discrete voltage pulses proportional in height to the incident gamma-ray energies. An Aptec 8K channel multi-channel analyzer sorts out the voltage pulses from the detector and digitally constructs a spectrum of gamma-ray energies versus intensities. By comparing spectral peak positions and areas with library standards, the elements were identified both qualitatively and quantitatively.

1.7.3.1.3. Mercury analyses

An analysis of the total mercury in porewater was conducted using a Tekran® 2600 mercury analyzer by CANMET lab in Ottawa. This method uses an ultra-sensitive atomic fluorescence detector, which is capable of measuring waters with a detection limit of much less than the required < 0.5 ng/L (ppt). The analytical process followed the U.S. EPA method 1631 (EPA, 1996).

The concentration of mercury in sediments was determined using Cold Vapor Atomic Absorption (CVAA) by ACME Analytical Laboratories Ltd (Vancouver, British

Columbia, Canada). In this method, the sediments were digested with Aqua Regia (HCl-HNO_3) before being introduced to the mercury analyzer.

1.7.3.1.4. Total carbon and sulphur analyses

The analyses of total bulk concentrations of carbon and sulphur in the sediment samples were conducted using fully automated LECO®-SC42 sulphur-carbon analyzer in Geological Survey of Canada, Calgary division. The inorganic carbon was calculated by subtracting the organic carbon (measured by Rock-Eval; Chapter 1.7.3.2) from the total carbon.

1.7.3.2. Organic geochemistry (Rock-Eval analyses)

The quantity and quality of the organic matter present in the sediments is useful to interpret the results obtained from multi-elemental analyses. Sanei et al., (2000) have applied the Rock-Eval method to study recent sediments, and reconstruct the environmental history of a lake. This method is conventionally used in petroleum geoscience for identifying the quantity and quality of the organic matter as well as the maturity of source rocks (Sykes and Snowdon, 2002; Lafargue et al., 1998; Tissot and Welte, 1985).

The new version, high resolution Rock-Eval® 6, manufactured by Vinci Technologies (France), was used for quantitative and qualitative study of OM in the recent sediments. The Rock-Eval® 6 method consists of pyrolysis and oxidation ovens,

both performing the temperature programmed heating of the sediments (20 mg) and standard samples (100 mg) at a heating rate of 25 °C per minute.

In the oven, the pyrolysis stage occurs between 100 °C and 650 °C under an inert atmosphere (He). During the pyrolysis process, the quantity of free, 'volatile' hydrocarbons present in the sample (S1 peak, mg Hydrocarbons/g of sample) and the amount of hydrocarbons released by the thermal cracking of OM (S2; mg hydrocarbons/g of sample) are detected by the Flame Ionization Detector (FID) (Figure 8.1a). Simultaneously, the CO and CO_2 released during thermal cracking of oxygen-bearing organic compounds (S3; mg CO-CO_2/g of sample) are measured by online Infrared (IR) detectors (Figures 8.1b-c). The measurement of CO is conducted up to the temperature 570 °C, while the measurement of CO_2 is conducted up to the temperature of 400 °C. This is to avoid interference by releases of inorganic CO and CO_2 at temperatures higher than 570 °C and 400 °C, respectively (Figures 8.1b-c).

Following the pyrolysis stage, the sample is automatically transferred to the oxidation oven where it is heated from 400 °C to 850 °C, incinerating all the residual organic carbon in the sample. At this step, the CO and CO_2 released during the combustion of residual organic carbon (S4; mg CO-CO_2/g of sample) are measured by online Infrared (IR) detectors (Figure 8.1d). The quantity of all OM released during pyrolysis (Pyrolysable carbon; 100 °C – 650 °C) and oxidation (Residual carbon; 400 °C – 850 °C) accounts for the total organic carbon (TOC; wt.%) in the sediment sample.

The reader is referred to Lafargue et al., (1998) and references therein for further details on instrumentation, detection techniques, advantages, and limitations.

1.7.3.3. Mineralogy and morphology of the sediments

The morphological and mineralogical/chemical composition of the sediments were studied using the Scanning Electron Microscope equipped with Energy Dispersive X-ray in back-scattered mode (SEM/EDX) at the Geological Survey of Canada (Calgary division). The SEM/EDX study was carried out on gold-coated, surface polished, sediment pellets.

1.7.3.4. Organic petrology

The sediment samples were placed in 3 cm diameter teflon molds and then impregnated with a cold-setting EPOTECH® epoxy-resin mixture. After curing, the sample pellets were then ground using carborundum grit and polished on Pelon® and then on a silk-covered lap using alumina-water slurries of 0.3 μm and 0.05 μm, respectively, in final preparation for microscopy (Mackowsky, 1982).

Organic petrography was conducted using an incident light Zeiss Axioplan II microscope system equipped with white and fluorescent light sources, a J & M® photometer, and a spectrometer (300-1100 nm). Oil-immersion objectives of various magnifications were used to assist in OM characterizations (total magnification ranging

from 100 to 2500x). Fluorescence of OM, as seen in the photomicrographs in this paper, represent ultraviolet G 365 nm excitation with a 420 nm barrier filter, although other excitation-emission combinations were also used. Digital images were captured using Zeiss Axiocam® and Axiovision® software.

Relative fluorescence intensity measurements of liptinite macerals (sporinites, alginites, cutinites,) were made every 2.5 nm (420-720 nm). An epiplan-neofluor 40x water immersion objective (N.A. = 0.95), ultraviolet G 365 nm excitation filter, 395 nm beam splitter and 420 nm barrier filter (HBO 100W Hg UV-light source) was used during spectral analysis. A black body curve was used to correct spectra for background. A standard tungsten lamp (3100 K) was used as a reference radiator during background correction.

1.7.3.5. Gamma-ray spectrometry analyses

The natural decay of uranium produces a series of radionuclides with different half-lives that can be used to determine the absolute ages and accumulation rates of sediments. The gamma-ray emission rates from the ^{238}U series radionuclides (^{238}U, ^{226}Ra, ^{210}Pb, ^{214}Pb, and ^{214}Bi) were measured on 2 to 5 grams of the sediment samples using a high precision, low energy gamma-ray spectrometry. In addition, gamma-ray spectrometry is used to identify the presence of man-made radionuclide ^{137}Cs originating in the sediments from radioactive fallout.

Each of the three samples was combined for the gamma-spec in order to get enough radiation. This makes each depth interval 3 cm as calculated by 3 × 1cm (for each sample). The sediment samples were packaged in colourless acrylic petri dishes (8.5 cm diameter × 3.8 cm high). The dishes were sealed with black electrical tape to prevent the loss of radon gas and stored for 3 weeks to establish radioactive equilibrium between ^{226}Ra and its short-lived daughter nuclei (^{222}Rn, ^{218}Po, ^{214}Pb, ^{214}Bi, ^{214}Po) within the ^{238}U decay series.

The gamma photons were measured using an EG and G Ortec GLP series low energy photon (LEP) detector in US Geological Survey (USGS). In this method, the Gamma-ray emissions of 0 to 400 keV (kiloelectron-volt) of energy were detected. The detector crystal was a high purity germanium semiconductor (16 mm diameter x 10 mm sensitive depth). Detector resolution at gamma-ray energy of 122 keV was 0.489 keV (peak width at half-maximum peak height). Gamma-ray spectra were accumulated in a 2048-channel Nuclear Data ND6600 multi-channel analyzer (0.2 keV/channel), with times ranging from 24 to 72 hours per sample. Ambient background counts were reduced by placing lead shielding around the detector and covering the samples with lead foil enclosed by a Cu-Cd shield.

Total counts recorded under the gamma-ray photopeaks of interest were calculated by summing the total recorded counts under the peak and subtracting background counts. The measured count-per-minute (cpm) data for each photopeak were converted to the desired values of disintegration-per-minute/gram (dpm/g) using

parameters such as absolute efficiency of the detector, absorption correction factor, branching ratio, and sample weight (g) (Zielinski and Budahn, 1998) [1].

The absolute efficiency of the detector (Eff.) was determined using a planar National Institute of Standards and Technology (NIST)-traceable source (SRM-4275). The standard source contains several nuclides of certified activity (dpm) that emit multiple gamma-rays within the energy range of interest. Estimated precision of individual efficiency curves is based on counting statistics for the SRM standard. Counting of the standard was carried out for a sufficient amount of time to obtain a precision better than 2% (Zielinski and Budahn, 1998).

The absorption correction factor accounts for the self-absorption of gamma rays by the sample, which is especially important for low-energy (< 100 keV) gamma rays. In consideration of the low energy gamma rays measured in the variety of sample types, absorption correction factors were estimated for each gamma-ray photopeak of interest in each sample. The absorption of gamma rays of varying energies was determined by comparing the counts recorded when the SRM-4275 source was placed on top of a container containing a sample, versus an empty container. The estimated precision of absorption corrections is based on counting statistics for attenuated and unattenuated gamma rays from the SRM standard (Zielinski and Budahn, 1998).

---

[1] dpm/g = (cpm - background)/Eff. × Abs. × B.R. × w
where Eff. = absolute efficiency of the detector; Abs. = absorption correction factor; B.R. = branching ratio; and w = sample weight (g)

Detection limits for each nuclide were estimated using the standard deviation of average background counts near the best-determined photopeak. Detection limits for the sediment samples were 0.4 dpm/g for ^{214}Pb and ^{226}Ra and 0.2 dpm/g for ^{210}Pb.

CHAPTER 2: SEDIMENT AGE AND SEDIMENTATION RATE FOR LAKES IN CENTRAL ALBERTA, CANADA

2.1. LEAD-210 ISOTOPE DATING

2.1.1. Introduction

Lead-210 (^{210}Pb) geochronology is based on the decay of ^{210}Pb (half life: 22.26 yr) following its burial in sediments, which is often used to study environmental changes over the past 100 years (Goldberg, 1963; Robbins, 1978; Robbins et al., 1978; Evans and Rigler, 1983; Nittrouer et al., 1984; Dukat and Kuehl, 1995).

^{210}Pb is a member of the uranium-238 (^{238}U) decay series, which decays via α and β-decays to ^{226}Ra (half life = 1622 yr) in the earth's crust. The radium isotope ^{226}Ra subsequently decays to inert gaseous ^{222}Rn (half life = 3.8 days). A fraction of the gaseous ^{222}Rn formed by ^{226}Ra decay in soils escapes from the earth's crust to the atmosphere, where it undergoes a series of very short-lived decays to ^{210}Pb (Appleby and Oldfield, 1983). ^{210}Pb is rapidly removed from the atmosphere either by precipitation or by settling under the influence of gravity or electrostatic forces (Turekian et al., 1977; Brunskill and Wilkinson, 1987). Aerial ^{210}Pb may be deposited directly into a water body where it will be rapidly scavenged by particulates or indirectly deposited on surface soil and then carried to the aquatic basins (Robbins, 1978).

Aerially deposited ^{210}Pb onto surface sediments is called unsupported ^{210}Pb ($^{210}Pb_{excess}$) since it is disconnected from its decay source (^{226}Ra) following burial. Therefore, unsupported ^{210}Pb generally decreases with depth in the recent sediment profile. In contrast, the in-situ ^{210}Pb is constantly produced in the sediments as the result of the decay by some

portion of ^{226}Ra in the sediments. This portion of ^{210}Pb is called supported (background) ^{210}Pb, which is constant with sediment depth. The sum of supported ^{210}Pb and unsupported ^{210}Pb at any depth in the sediment is equal to total ^{210}Pb.

Total ^{210}Pb = supported ^{210}Pb + unsupported ^{210}Pb ($^{210}Pb_{excess}$)

The ^{210}Pb geochronology estimates the extent of unsupported ^{210}Pb decay in each layer of sediment. Hence, for ^{210}Pb dating, an estimate of supported ^{210}Pb must be obtained and subtracted from total ^{210}Pb to estimate unsupported ^{210}Pb (Goldberg, 1963; Appleby et al., 1978; Appleby and Oldfield, 1978; Robbins, 1978; Appleby and Oldfield, 1983; Appleby et al., 1988).

2.1.2. Measurement of supported and unsupported ^{210}Pb

The total ^{210}Pb concentration is directly measured (Table 2.1a-d) using a low energy photon (LEP) detector (Chapter 1.7.3.5). In contrast, the supported ^{210}Pb were indirectly measured by achieving the radioactive equilibrium between ^{226}Ra and its short-lived daughter nuclei (^{222}Rn, ^{218}Po, ^{214}Pb, ^{214}Bi, ^{214}Po) within the ^{238}U decay series (Table 2.1a-d). Once radioactive equilibrium is established, the forward and reverse rates of disintegration and formation between parent and daughters are equal. Therefore, the concentration of any of the short-lived ^{238}U decay series nuclides is a measure for the supported ^{210}Pb (Table 2.1a-d).

Table 2.1.a. The concentration (dpm/g) of ^{238}U-series radionuclides and calculated $^{210}Pb_{excess}$ in Wabamun Lake, core WAB1.

WAB1 core combined intervals	Middle depth*	$^{210}Pb_{total}$	^{226}Ra	^{214}Pb	^{214}Bi	Average ^{214}Pb & ^{214}Bi	$^{210}Pb_{excess}$
	cm	dpm/g	dpm/g	dpm/g	dpm/g	dpm/g	dpm/g
WAB1 (1-3 cm)	4.5	15.5	5.71	1.47	1.82	1.65	13.8
WAB1 (4-6 cm)	7.5	13.5	4.65	1.21	0.96	1.09	12.4
WAB1 (7-9 cm)	10.5	11.2	3.24	0.72	0.78	0.75	10.4
WAB1 (10-12 cm)	13.5	7.61	3.38	0.85	0.97	0.91	6.70
WAB1 (13-15 cm)	16.5	3.15	3.03	0.37	0.46	0.42	2.74
WAB1 (16-18 cm)	19.5	3.23	3.75	0.73	0.96	0.85	2.39
WAB1 (19-21 cm)	22.5	2.63	2.74	0.61	0.67	0.64	1.99
WAB1 (22-24 cm)	25.5	1.49	4.99	0.93	1.09	1.01	0.48
WAB1 (25-27 cm)	28.5	1.89	4.19	0.64	0.47	0.56	1.34
WAB1 (28-30 cm)	31.5	0.62	3.40	0.79	0.85	0.82	***0.25***
WAB1 (31-33 cm)	34.5	1.01	3.20	1.12	0.86	0.99	0.02
WAB1 (34-36 cm)	37.5	0.52	3.58	0.78	0.78	0.78	***0.25***
WAB1 (37-39 cm)	40.5	1.50	2.55	1.22	1.30	1.26	0.24
WAB1 (40-42 cm)	43.5	1.31	3.37	0.93	1.16	1.05	0.27
WAB1 (43-45 cm)	46.5	1.33	5.63	0.94	0.72	0.83	0.50
WAB1 (46-48 cm)	49.5	0.57	3.49	0.88	0.88	0.88	***0.25***
WAB1 (49-51 cm)	52.5	2.11	3.24	1.03	0.95	0.99	1.12
WAB1 (52-54 cm)	55.5	0.72	3.65	1.00	1.14	1.07	***0.25***

* top 3 cm of sediment were lost during sampling therefore 3 cm is added to the middle depth values.

Values in bold fonts were below detection limit (0.5 dpm/g) and hence were assigned a value equivalent to one-half of the detection limit.

Table 2.1.b. The concentration (dpm/g) of ^{238}U-series radionuclides and calculated $^{210}Pb_{excess}$ in Wabamun Lake, core WAB2.

WAB2 core combined intervals	Middle depth	$^{210}Pb_{total}$	^{226}Ra	^{214}Pb	^{214}Bi	Average ^{214}Pb & ^{214}Bi	$^{210}Pb_{excess}$
	cm	dpm/g	dpm/g	dpm/g	dpm/g	dpm/g	dpm/g
WAB2 (1-3 cm)	1.5	13.6	3.50	2.21	2.76	2.49	11.1
WAB2 (4-6 cm)	4.5	15.7	2.99	0.75	1.02	0.89	14.9
WAB2 (7-9 cm)	7.5	10.8	4.34	0.67	1.01	0.84	9.94
WAB2 (10-12 cm)	10.5	4.89	3.68	0.87	0.67	0.77	4.12
WAB2 (13-15 cm)	13.5	3.48	3.68	0.68	0.90	0.79	2.69
WAB2 (16-18 cm)	16.5	1.87	2.53	0.51	0.85	0.68	1.19
WAB2 (19-21 cm)	19.5	1.66	2.16	0.77	0.80	0.79	0.88
WAB2 (22-24 cm)	22.5	1.92	2.97	0.72	0.65	0.69	1.24
WAB2 (25-27 cm)	25.5	1.40	2.61	0.93	0.96	0.95	0.46
WAB2 (28-30 cm)	28.5	1.67	2.98	0.79	0.77	0.78	0.89
WAB2 (31-33 cm)	31.5	1.41	3.15	0.65	0.78	0.72	0.70
WAB2 (34-36 cm)	34.5	2.42	2.95	0.70	0.83	0.77	1.66
WAB2 (37-39 cm)	37.5	2.95	3.44	0.88	0.62	0.75	2.20
WAB2 (40-42 cm)	40.5	1.76	3.59	0.79	1.10	0.95	0.82
WAB2 (43-45 cm)	43.5	1.61	3.90	1.15	1.20	1.18	0.44
WAB2 (46-48 cm)	46.5	1.10	2.17	1.07	1.05	1.06	0.04
WAB2 (49-52 cm)	50	1.34	4.64	1.28	1.17	1.23	0.12
WAB2 (53-56 cm)	54	2.05	2.74	1.07	1.07	1.07	0.98
WAB2 (57-59 cm)	57.5	1.44	4.24	0.88	0.96	0.92	0.52
WAB2 (60-62 cm)	60.5	1.31	3.31	1.14	0.80	0.97	0.34

Table 2.1.c. The concentration (dpm/g) of ^{238}U-series radionuclides and calculated $^{210}Pb_{excess}$ in Isle Lake sediment core (ISLE).

ISLE core combined intervals	Middle depth	$^{210}Pb_{total}$	^{226}Ra	^{214}Pb	^{214}Bi	Average ^{214}Pb & ^{214}Bi	$^{210}Pb_{excess}$
	cm	dpm/g	dpm/g	dpm/g	dpm/g	dpm/g	dpm/g
ISLE (1-3 cm)	1.5	16.7	4.07	1.90	1.76	1.83	14.9
ISLE (4-6 cm)	4.5	14.2	2.96	1.71	1.97	1.84	12.4
ISLE (7-9 cm)	7.5	11.3	3.58	1.58	1.65	1.62	9.70
ISLE (10-12 cm)	10.5	11.3	2.16	1.48	1.63	1.56	9.79
ISLE (13-15 cm)	13.5	7.61	5.18	1.82	1.82	1.82	5.79
ISLE (16-18 cm)	16.5	4.57	2.04	1.40	1.32	1.36	3.21
ISLE (19-21 cm)	19.5	3.68	3.45	1.47	1.66	1.57	2.12
ISLE (22-24 cm)	22.5	1.83	2.82	1.14	1.23	1.19	0.65
ISLE (25-27 cm)	25.5	2.86	2.06	1.60	1.67	1.64	1.23
ISLE (28-30 cm)	28.5	1.82	2.81	1.69	1.66	1.68	0.15
ISLE (31-33 cm)	31.5	1.97	3.91	1.74	1.60	1.67	0.30
ISLE (34-36 cm)	34.5	2.42	3.04	1.49	1.69	1.59	0.83
ISLE (37-39 cm)	37.5	1.77	2.34	1.21	1.23	1.22	0.55
ISLE (40-42 cm)	40.5	2.40	2.99	1.27	1.22	1.25	1.16
ISLE (43-45 cm)	43.5	2.68	3.35	1.56	1.59	1.58	1.11
ISLE (46-48 cm)	46.5	1.92	3.13	1.34	1.38	1.36	0.56

Table 2.1.d. The concentration (dpm/g) of 238U-series radionuclides and calculated 210Pbexcess in Lac Ste. Anne sediment core.

LSA core combined intervals	Middle depth	$^{210}Pb_{total}$	^{226}Ra	^{214}Pb	^{214}Bi	Average ^{214}Pb & ^{214}Bi	$^{210}Pb_{excess}$
	cm	dpm/g	dpm/g	dpm/g	dpm/g	dpm/g	dpm/g
LSA (1-3 cm)	1.5	15.0	2.55	2.66	2.64	2.65	12.4
LSA (4-6 cm)	4.5	11.7	2.14	1.61	1.89	1.75	9.92
LSA (7-9 cm)	7.5	11.9	1.95	1.83	2.23	2.03	9.89
LSA (10-12 cm)	10.5	9.12	2.10	1.92	2.13	2.03	7.10
LSA (13-15 cm)	13.5	8.08	1.92	1.27	1.26	1.27	6.82
LSA (16-18 cm)	16.5	5.41	1.81	1.23	1.33	1.28	4.13
LSA (19-21 cm)	19.5	4.43	1.97	1.19	1.40	1.30	3.14
LSA (22-24 cm)	22.5	3.42	2.63	1.65	1.25	1.45	1.97
LSA (25-27 cm)	25.5	2.31	2.58	1.16	1.43	1.30	1.02
LSA (28-30 cm)	28.5	2.88	1.83	1.49	1.15	1.32	1.56
LSA (31-33 cm)	31.5	2.77	2.86	1.57	1.52	1.55	1.23
LSA (34-36 cm)	34.5	2.98	2.06	1.46	1.54	1.50	1.48
LSA (37-39 cm)	37.5	2.32	1.51	1.30	1.32	1.31	1.01
LSA (40-42 cm)	40.5	2.12	2.06	1.45	1.19	1.32	0.80
LSA (43-45 cm)	43.5	2.23	2.88	1.53	1.54	1.54	0.70
LSA (46-48 cm)	46.5	1.99	1.98	1.45	1.23	1.34	0.65
LSA (49-51 cm)	49.5	1.95	1.97	1.51	1.48	1.50	0.46
LSA (52-54 cm)	52.5	2.47	2.32	1.52	1.41	1.47	1.01

The best nuclides are daughters such as ^{214}Pb and ^{214}Bi in order to determine the disintegration rates of their respective parent ^{226}Ra (Table 2.1a-d). This is because ^{214}Pb and ^{214}Bi can be measured more conveniently and with high accuracy. Therefore, in this study the average disintegration rates of ^{214}Pb and ^{214}Bi are used as measures of supported ^{210}Pb (Table 2.1a-d).

The isotopic dating of the sediments was carried out on all ten studied sediment cores (LLN, LSD, CHIP, BCK, ISLE, JFL, LSA, SND, WAB1 and WAB2) during the phase I survey (Figure 1.1; Chapter 1.4). However, only the resulting isotopic data for the sediment profiles from Wabamun Lake (WAB1 and WAB2), Isle Lake (ISLE), and Lac Ste. Anne (LSA) are discussed in this Chapter.

2.1.3. Sediment age determination model

The two geochronological models used for dating sediments by ^{210}Pb are the Constant Rate of Supply (CRS) model and the Constant Initial Concentration (CIC) model (Goldberg, 1963; Appleby et al., 1978; Appleby and Oldfield, 1978; Robbins, 1978; Appleby and Oldfield, 1983; Appleby et al., 1988). The CRS model assumes that the supply of unsupported ^{210}Pb to the sediment is the same for all time intervals, while the CIC model assumes a constant concentration in the top layer of the sediment.

In this study, the CRS model is applied because the declines in unsupported ^{210}Pb activity with depth for all the studied cores are non-monotonous (Appleby and Oldfield,

1983). This is due to the variations in the accumulation rates, since faster net sediment accumulation will tend to depress initial unsupported ^{210}Pb concentrations (Appleby and Oldfield, 1983).

In the CRS model, it can be presumed that the cumulate residual $^{210}Pb_{excess}$ activity, A, below sediments of age, t, varies according to the following formula:

$$A = A_0 e^{-\lambda t}$$

Where "A_0" is cumulated specific activity of unsupported ^{210}Pb integrated over the whole profile (residuals $^{210}Pb_{excess}$), "A" represents cumulated activity integrated for the part of the profile below the depth "x", and "λ" is the radioactive decay constant for ^{210}Pb ($0.03114\ yr^{-1}$).

By re-arranging the above equation, the age (t) at a particular sediment depth can be calculated using the following formula (Table 2.2a-d):

$$t = \frac{1}{\lambda} \ln(\frac{A_0}{A})$$

The estimated age of the sediments from the four cores, WAB1, WAB2, ISLE, and LSA are also shown in the age-depth diagram shown in Figures 2.1a-d.

Table 2.2.a. The calculation of sediment age, sedimentation rates, and mass accumulation rates in sediment core WAB1.

WAB1 core combined intervals	Middle depth	Interval thickness	Water content	TOC	Grain density	Dry mass	$^{210}Pb_{excess}$ Inventory	A	Sediment age (t)*	^{210}Pb dates	Linear sedimentation rates	Sediment cumulative mass	Average MAR	Incremental MAR
	cm	cm	%	%	g/cm^3	g/cm^2	dpm/cm^2	dpm/cm^2	yr		cm/yr	g/cm^2	$g/cm^2.yr$	$g/cm^2.yr$
WAB1 (1-3)	4.5*	3	88.5	15.4	2.44	0.84	11.7	41.3	4	1997	1.06	0.42	0.10	0.10
WAB1 (4-6)	7.5	3	88.6	15.9	2.43	0.83	10.3	30.3	14	1987	0.53	1.26	0.09	0.08
WAB1 (7-9)	10.5	3	88.9	17.7	2.40	0.80	8.32	21.0	26	1975	0.40	2.08	0.08	0.07
WAB1 (10-12)	13.5	3	88.2	18.5	2.39	0.85	5.67	14.0	39	1962	0.35	2.90	0.07	0.06
WAB1 (13-15)	16.5	3	88.4	17.8	2.40	0.84	2.29	10.0	50	1951	0.33	3.74	0.08	0.08
WAB1 (16-18)	19.5	3	88.3	17.3	2.41	0.85	2.02	7.87	57	1944	0.34	4.58	0.08	0.11
WAB1 (19-21)	22.5	3	88.1	16.6	2.42	0.86	1.72	6.00	66	1935	0.34	5.44	0.08	0.10
WAB1 (22-24)	25.5	3	87.1	15.7	2.43	0.94	0.45	4.92	73	1928	0.35	6.34	0.09	0.14
WAB1 (25-27)	28.5	3	86.9	15.0	2.44	0.96	1.28	4.05	79	1922	0.36	7.29	0.09	0.15
WAB1 (28-30)	31.5	3	86.6	14.8	2.45	0.99	0.25	3.29	86	1915	0.37	8.26	0.10	0.15
WAB1 (31-33)	34.5	3	86.3	14.9	2.45	1.01	0.02	3.16	87	1914	0.40	9.26	0.11	0.75
WAB1 (34-36)	37.5	3	86.4	14.4	2.45	1.00	0.25	3.02	88	1913	0.42	10.3	0.12	0.71
WAB1 (37-39)	40.5	3	85.7	14.4	2.45	1.05	0.25	2.77	91	1910	0.44	11.3	0.12	0.37
WAB1 (40-42)	43.5	3	85.8	13.2	2.48	1.05	0.28	2.50	94	1907	0.46	12.3	0.13	0.32
WAB1 (43-45)	46.5	3	85.2	15.1	2.44	1.08	0.54	2.09	100	1901	0.46	13.4	0.13	0.19
WAB1 (46-48)	49.5	3	85.0	14.3	2.46	1.10	0.28	1.68	107	1894	0.46	14.5	0.14	0.16
WAB1 (49-51)	52.5	3	84.9	14.5	2.45	1.11	1.25	0.92	126	1875	0.42	15.6	0.12	0.06
WAB1 (52-54)	55.5	3	83.9	13.7	2.47	1.19	0.30	0.15	185	1816	0.30	16.8	0.09	0.02
SUM						**17.4**	**47.2 = Ao**							

* top 3 cm of sediment were lost during sampling; sediment age is estimated since sampling time at year 2001.

MAR: Mass Accumulation Rates.

Ao: Cumulated specific activity of $^{210}Pb_{excess}$ integrated over the whole profile (residuals $^{210}Pb_{excess}$)

A: Cumulated activity of $^{210}Pb_{excess,}$ integrated below depth x.

Table 2.2.b. The calculation of sediment age, sedimentation rates, and mass accumulation rates in sediment core WAB2.

WAB2 core combined intervals	Middle depth	Interval thickness	Water content	TOC	Grain density	Dry mass	$^{210}Pb_{excess}$ Inventory	A	Sediment age (t)*	^{210}Pb dates	Linear sedimentation rates	Sediment cumulative mass	Average MAR	Incremental MAR
	cm	cm	%	%	g/cm^3	g/cm^2	dpm/cm^2	dpm/cm^2	yr		cm/yr	g/cm^2	$g/cm^2.yr$	$g/cm^2.yr$
WAB2 (1-3)	1.5	3	88.8	13.9	2.46	0.83	9.18	51.0	3	1998	0.54	0.41	0.15	0.15
WAB2 (4-6)	4.5	3	88.0	13.6	2.47	0.89	13.2	39.8	11	1990	0.42	1.27	0.12	0.11
WAB2 (7-9)	7.5	3	86.7	10.7	2.52	1.00	9.96	28.3	22	1979	0.35	2.22	0.10	0.09
WAB2 (10-12)	10.5	3	86.0	13.0	2.48	1.04	4.28	21.1	31	1970	0.34	3.24	0.10	0.11
WAB2 (13-15)	13.5	3	85.8	12.0	2.50	1.06	2.86	17.6	37	1964	0.36	4.29	0.12	0.18
WAB2 (16-18)	16.5	3	85.1	11.8	2.50	1.12	1.33	15.5	41	1960	0.40	5.38	0.13	0.27
WAB2 (19-21)	19.5	3	84.6	11.3	2.51	1.16	1.01	14.3	44	1957	0.45	6.52	0.15	0.45
WAB2 (22-24)	22.5	3	84.0	10.8	2.52	1.21	1.49	13.0	47	1954	0.48	7.70	0.17	0.40
WAB2 (25-27)	25.5	3	83.6	10.6	2.52	1.24	0.56	12.0	49	1952	0.52	8.92	0.18	0.46
WAB2 (28-30)	28.5	3	83.5	11.2	2.51	1.24	1.10	11.2	51	1950	0.55	10.2	0.20	0.54
WAB2 (31-33)	31.5	3	83.5	11.4	2.51	1.24	0.86	10.2	54	1947	0.58	11.4	0.21	0.42
WAB2 (34-36)	34.5	3	83.5	11.2	2.51	1.24	2.06	8.74	59	1942	0.58	12.6	0.21	0.25
WAB2 (37-39)	37.5	3	83.4	11.6	2.50	1.24	2.74	6.35	70	1931	0.54	13.9	0.20	0.12
WAB2 (40-42)	40.5	3	82.9	11.0	2.51	1.29	1.05	4.45	81	1920	0.50	15.2	0.19	0.11
WAB2 (43-45)	43.5	3	82.4	10.6	2.52	1.33	0.58	3.64	88	1913	0.50	16.5	0.19	0.20
WAB2 (46-48)	46.5	3	81.7	10.2	2.53	1.39	0.06	3.32	90	1911	0.51	17.8	0.20	0.46
WAB2 (49-52)	50	4	82.0	11.1	2.51	1.81	0.21	3.19	92	1909	0.54	19.4	0.21	1.23
WAB2 (53-56)	54	4	81.7	10.9	2.52	1.84	1.80	2.19	104	1897	0.52	21.2	0.20	0.15
WAB2 (57-59)	57.5	3	80.2	10.2	2.53	1.50	0.78	0.90	133	1868	0.43	22.9	0.17	0.06
WAB2 (60-62)	60.5	3	80.7	8.2	2.56	1.49	0.51	0.25	173	1828	0.35	24.4	0.14	0.04
SUM						**25.1**	**55.6 = Ao**							

* Sediment age is estimated since sampling time at year 2001.

MAR: Mass Accumulation Rates.

Ao: Cumulated specific activity of $^{210}Pb_{excess}$ integrated over the whole profile (residuals $^{210}Pb_{excess}$)

A: Cumulated activity of $^{210}Pb_{excess,}$ integrated below depth x.

Table 2.2.c. The calculation of sediment age, sedimentation rates, and mass accumulation rates in sediment core ISLE.

ISLE core combined intervals	Middle depth	Interval thickness	Water content	TOC	Grain density	Dry mass	$^{210}Pb_{excess}$ Inventory	A	Sediment age (t)*	^{210}Pb dates	Linear sedimentation rates	Sediment cumulative mass	Average MAR	Incremental MAR
	cm	cm	%	%	g/cm^3	g/cm^2	dpm/cm^2	dpm/cm^2	yr		cm/yr	g/cm^2	$g/cm^2.yr$	$g/cm^2.yr$
ISLE (1-3)	1.5	3	88.3	19.6	2.37	0.83	12.4	57.5	3	1998	0.46	0.42	0.13	0.13
ISLE (4-6)	4.5	3	86.9	19.4	2.37	0.93	11.6	45.5	11	1990	0.42	1.30	0.12	0.12
ISLE (7-9)	7.5	3	85.3	18.7	2.38	1.05	10.2	34.6	20	1981	0.38	2.29	0.12	0.11
ISLE (10-12)	10.5	3	85.7	18.3	2.39	1.03	10.0	24.5	31	1970	0.34	3.33	0.11	0.09
ISLE (13-15)	13.5	3	85.0	18.0	2.39	1.07	6.22	16.4	44	1957	0.31	4.38	0.10	0.08
ISLE (16-18)	16.5	3	84.9	17.6	2.40	1.09	3.50	11.5	55	1946	0.30	5.47	0.10	0.10
ISLE (19-21)	19.5	3	84.0	18.0	2.39	1.15	2.43	8.53	65	1936	0.30	6.59	0.10	0.12
ISLE (22-24)	22.5	3	84.4	18.0	2.39	1.12	0.72	6.96	71	1930	0.32	7.72	0.11	0.17
ISLE (25-27)	25.5	3	83.8	18.3	2.39	1.16	1.42	5.89	76	1925	0.33	8.86	0.12	0.21
ISLE (28-30)	28.5	3	85.0	19.0	2.38	1.07	0.16	5.10	81	1920	0.35	9.98	0.12	0.24
ISLE (31-33)	31.5	3	84.9	18.9	2.38	1.08	0.32	4.86	83	1918	0.38	11.1	0.13	0.70
ISLE (34-36)	34.5	3	84.0	19.1	2.38	1.14	0.94	4.22	87	1914	0.40	12.2	0.14	0.25
ISLE (37-39)	37.5	3	84.2	19.0	2.38	1.13	0.62	3.44	94	1907	0.40	13.3	0.14	0.17
ISLE (40-42)	40.5	3	85.3	19.4	2.37	1.05	1.21	2.53	104	1897	0.39	14.4	0.14	0.11
ISLE (43-45)	43.5	3	83.6	19.7	2.37	1.16	1.28	1.28	125	1876	0.35	15.5	0.12	0.05
ISLE (46-48)	46.5	3	84.0	19.3	2.37	1.14	0.64	0.32	170	1831	0.27	16.6	0.10	0.03
SUM						**17.2**	**63.7 = Ao**							

* Sediment age is estimated since sampling time at year 2001.

MAR: Mass Accumulation Rates.

Ao: Cumulated specific activity of $^{210}Pb_{excess}$ integrated over the whole profile (residuals $^{210}Pb_{excess}$)

A: Cumulated activity of $^{210}Pb_{excess,}$ integrated below depth x.

Table 2.2.d. The calculation of sediment age, sedimentation rates, and mass accumulation rates in sediment core LSA.

LSA core combined intervals	Middle depth	Interval thickness	Water content	TOC	Grain density	Dry mass	$^{210}Pb_{excess}$ Inventory	A	Sediment age (t)*	^{210}Pb dates	Linear sedimentation rates	Sediment cumulative mass	Average MAR	Incremental MAR
	cm	cm	%	%	g/cm^3	g/cm^2	dpm/cm^2	dpm/cm^2	yr		cm/yr	g/cm^2	$g/cm^2.yr$	$g/cm^2.yr$
LSA (1-3)	1.5	3	87.2	13.7	2.47	0.95	11.7	67.6	3	1998	0.56	0.48	0.18	0.18
LSA (4-6)	4.5	3	86.0	13.5	2.47	1.04	10.3	56.5	8	1993	0.54	1.47	0.18	0.17
LSA (7-9)	7.5	3	85.0	14.0	2.46	1.11	10.9	45.9	15	1986	0.50	2.54	0.17	0.16
LSA (10-12)	10.5	3	84.6	13.4	2.47	1.14	8.08	36.4	23	1978	0.47	3.66	0.16	0.15
LSA (13-15)	13.5	3	84.3	13.1	2.48	1.17	7.96	28.4	31	1970	0.44	4.82	0.16	0.14
LSA (16-18)	16.5	3	83.5	12.5	2.49	1.23	5.07	21.9	39	1962	0.42	6.02	0.15	0.14
LSA (19-21)	19.5	3	83.5	12.4	2.49	1.24	3.87	17.4	46	1955	0.42	7.25	0.16	0.17
LSA (22-24)	22.5	3	83.3	12.0	2.50	1.25	2.46	14.2	53	1948	0.43	8.49	0.16	0.19
LSA (25-27)	25.5	3	83.3	11.9	2.50	1.25	1.27	12.4	57	1944	0.45	9.74	0.17	0.28
LSA (28-30)	28.5	3	83.5	12.6	2.49	1.23	1.92	10.8	62	1939	0.46	11.0	0.18	0.28
LSA (31-33)	31.5	3	83.6	12.2	2.49	1.23	1.50	9.07	67	1934	0.47	12.2	0.18	0.22
LSA (34-36)	34.5	3	82.9	11.3	2.51	1.29	1.91	7.36	74	1927	0.47	13.5	0.18	0.19
LSA (37-39)	37.5	3	82.5	10.8	2.52	1.32	1.33	5.74	82	1919	0.46	14.8	0.18	0.16
LSA (40-42)	40.5	3	81.3	10.4	2.52	1.41	1.13	4.51	90	1911	0.45	16.1	0.18	0.18
LSA (43-45)	43.5	3	81.2	10.9	2.51	1.42	0.98	3.45	98	1903	0.44	17.6	0.18	0.16
LSA (46-48)	46.5	3	82.4	12.0	2.50	1.32	0.86	2.53	108	1893	0.43	18.9	0.17	0.14
LSA (49-51)	49.5	3	82.1	11.7	2.50	1.35	0.61	1.80	119	1882	0.42	20.2	0.17	0.12
LSA (52-54)	52.5	3	80.3	11.3	2.51	1.48	1.49	0.75	147	1854	0.36	21.7	0.15	0.05
SUM						**22.4**	**73.4 = Ao**							

* Sediment age is estimated since sampling time at year 2001.

MAR: Mass Accumulation Rates.

Ao: Cumulated specific activity of $^{210}Pb_{excess}$ integrated over the whole profile (residuals $^{210}Pb_{excess}$)

A: Cumulated activity of $^{210}Pb_{excess,}$ integrated below depth x.

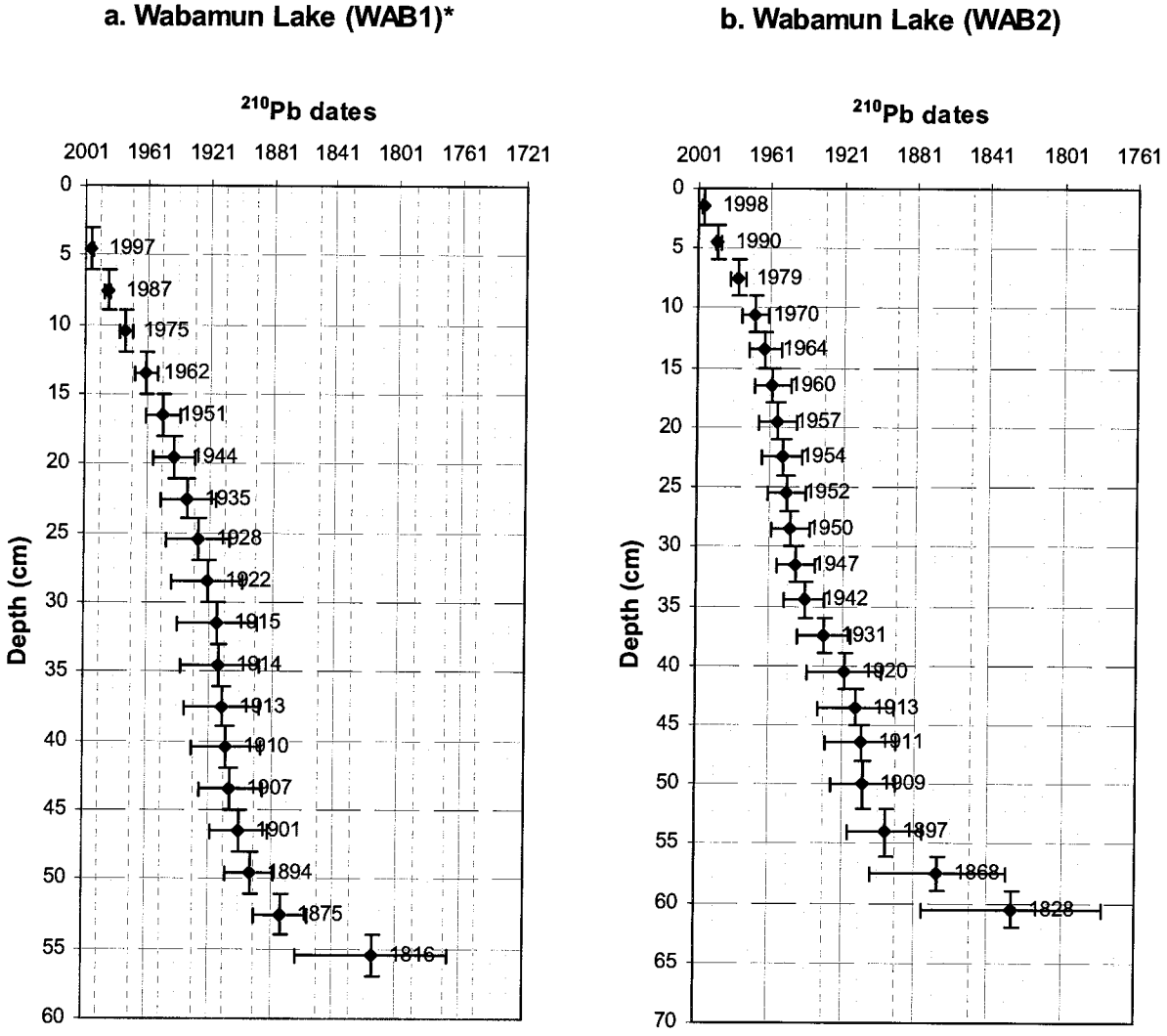

Figures 2.1.a-b: Profiles of ages of the sediment cores WAB1 (a) and WAB2 (b) from Wabamun Lake (*top 3 cm of sediments were lost during sampling).

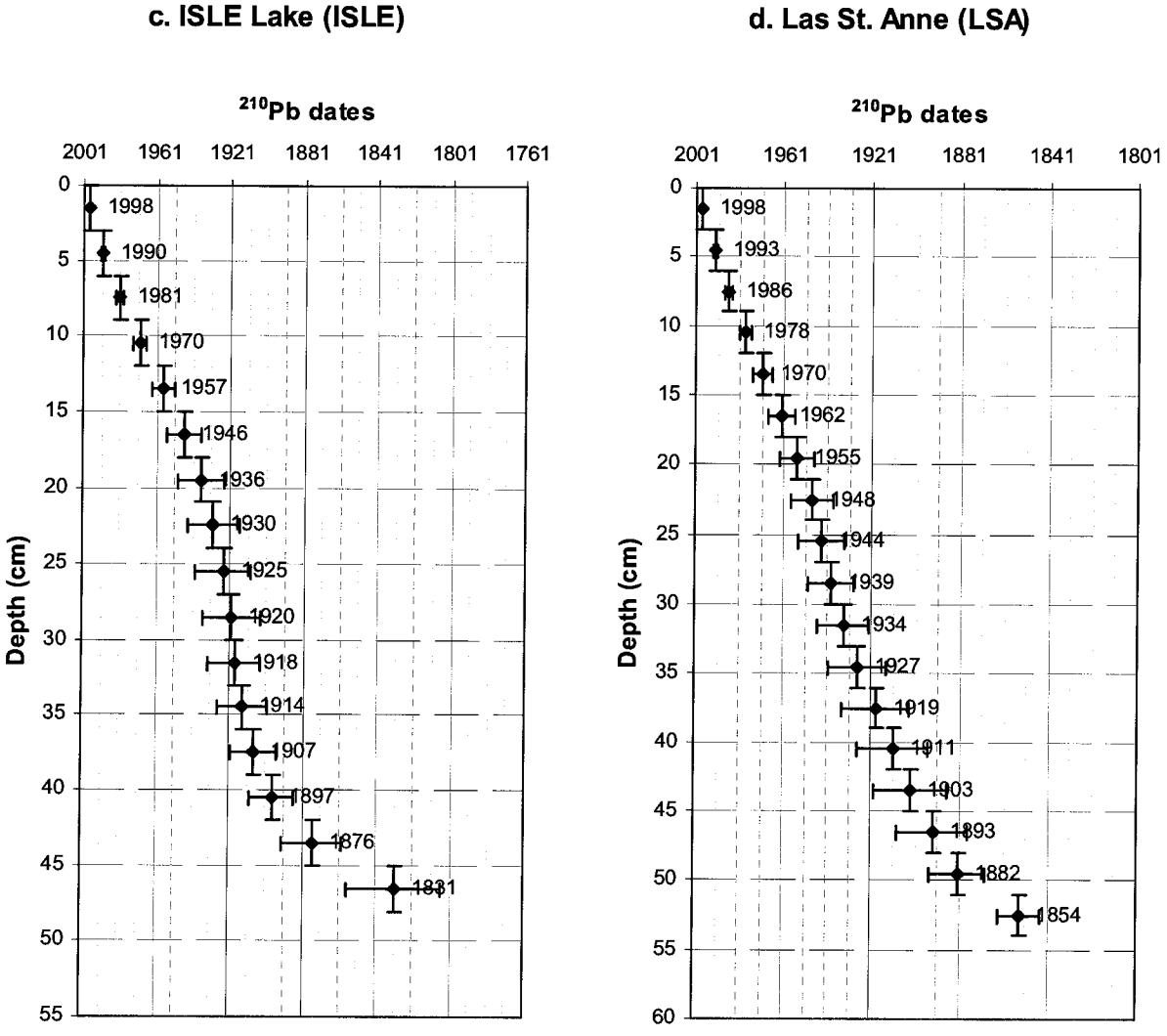

Figures 2.1.c-d: Profiles of ages of the sediment cores from Isle Lake (c) and Lac Ste. Anne (d).

The event horizons corresponding to the coal-utilization events in the study region for all sediment cores are shown in Table 2.3. The major events relate to the starting of the Wabamun, Sundance, Keephills, and Genesee power stations, in 1956, 1970, 1983, and 1989, respectively (Table 2.3). The results indicate the similar sediment age for the top 11-12 cm for cores WAB1 and WAB2 (Table 2.3). However, there is a marked difference between the depth representing the 1956 horizon in core WAB1 (15 cm) and WAB2 (21 cm) (Table 2.3). Both WAB1 and WAB2 cores were obtained from the same lake and similarly from the deep, off-shore part of the Wabamun lake, where a similar depositional environment exists (Figure 1.2). Therefore, it is expected that both cores would show very similar results with respect to the depth representing 1956-horizon. The elemental data (Chapter 3 and 4) and evidences from flyash in the sediment column (as determined by SEM/EDX; Chapter 6) suggest a possible error in determining the 1956 horizon in core WAB2 (Table 2.3). Based on elemental and petrological data, it appears that the 1956 horizon for WAB2 occurs at approximately the same depth as WAB1 core (depth 15 cm) (Table 2.3).

Table 2.3. The depth representing the commencement of the Wabamun, Sundance, Keephills, and Genesee stations in central Alberta.

	Wabamun station in 1956	Sundance Station in 1970	Keephills Station in 1983	Genesee Station in 1989
Interval depth	cm	cm	cm	cm
Wabamun Lake (WAB1 core)	15	12	8.5	7
Wabamun Lake (WAB2 core)	21	10.5	6.5	5
Isle Lake (ISLE core)	14	10.5	7	5
Lac Ste. Anne (LSA core)	19	13.5	8.8	6

The key to the resolution of the age-estimate lies in the error associated with the measurement of unsupported ^{210}Pb. In this study, the error bars in age-depth graphs are calculated based on ±0.4 dpm/g analytical error for $^{210}Pb_{excess}$ (Figures 2.1a-d).

2.1.4. Linear sedimentation rates

The estimated ages of sediment layers (t) were used to calculate apparent sedimentation rates (linear sedimentation rate) for each layer. It was assumed that the calculated age corresponds to the centre of the layer. Sedimentation rates were calculated according to the following formula (Table 2.2a-d):

$$r_n = (x - x\text{-}1) / (t_x - t_{x-1}),$$

Where r_n is sedimentation rate (cm/yr) for the interval between centers of depth x and (x-1) layer and t_x and t_{x-1} are age of the x layers.

The linear deposition rate (or sedimentation rate, cm/yr) in the sediment cores from Wabamun Lake, Isle Lake and Lac Ste. Anne are shown in Figures 2.2a-d. The highest sedimentation rate (0.5 to 1 cm/yr) occurs in the top 10 cm of the sediment profile from WAB1 (Figure 2.2a; Table 2.2a). Below the depth of 10 cm, the deposition rate varies within a narrow range of 0.3 to 0.5 cm/yr (Figure 2.2a; Table 2.2a). WAB2 core shows the periodical high and low sedimentation rate cycles throughout its profile (Figure 2.2b). The

sedimentation rate in WAB2 ranges between 0.35 and 0.58 cm/yr, with the highest deposition rates at the uppermost portion of the profile, as well as at a depth of 31.5 to 34.5 cm (Figure 2.2b; Table 2.2b).

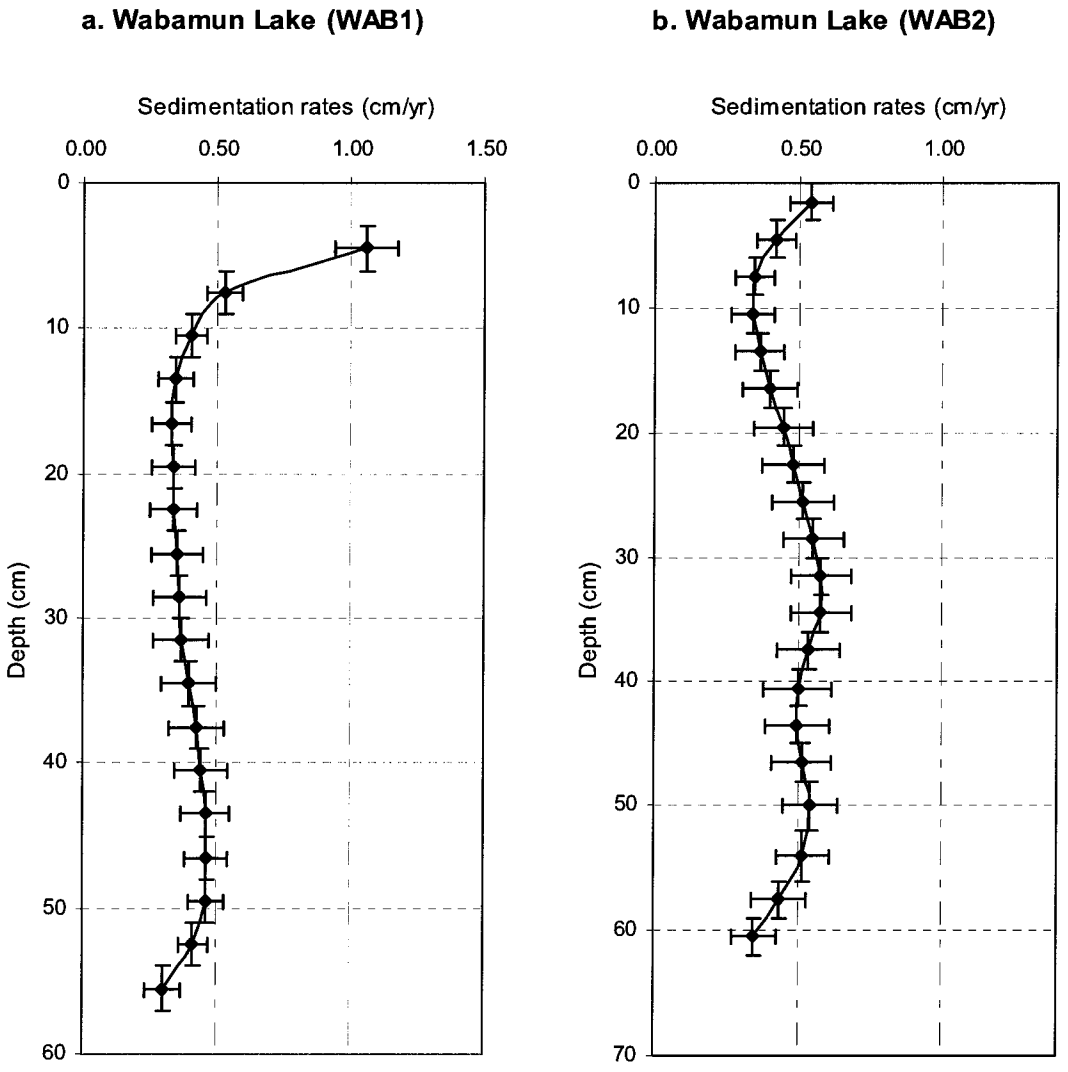

Figures 2.2.a-b: Profiles of the linear sedimentation rates for WAB1 (a) and WAB2 (b) cores from Wabamun Lake.

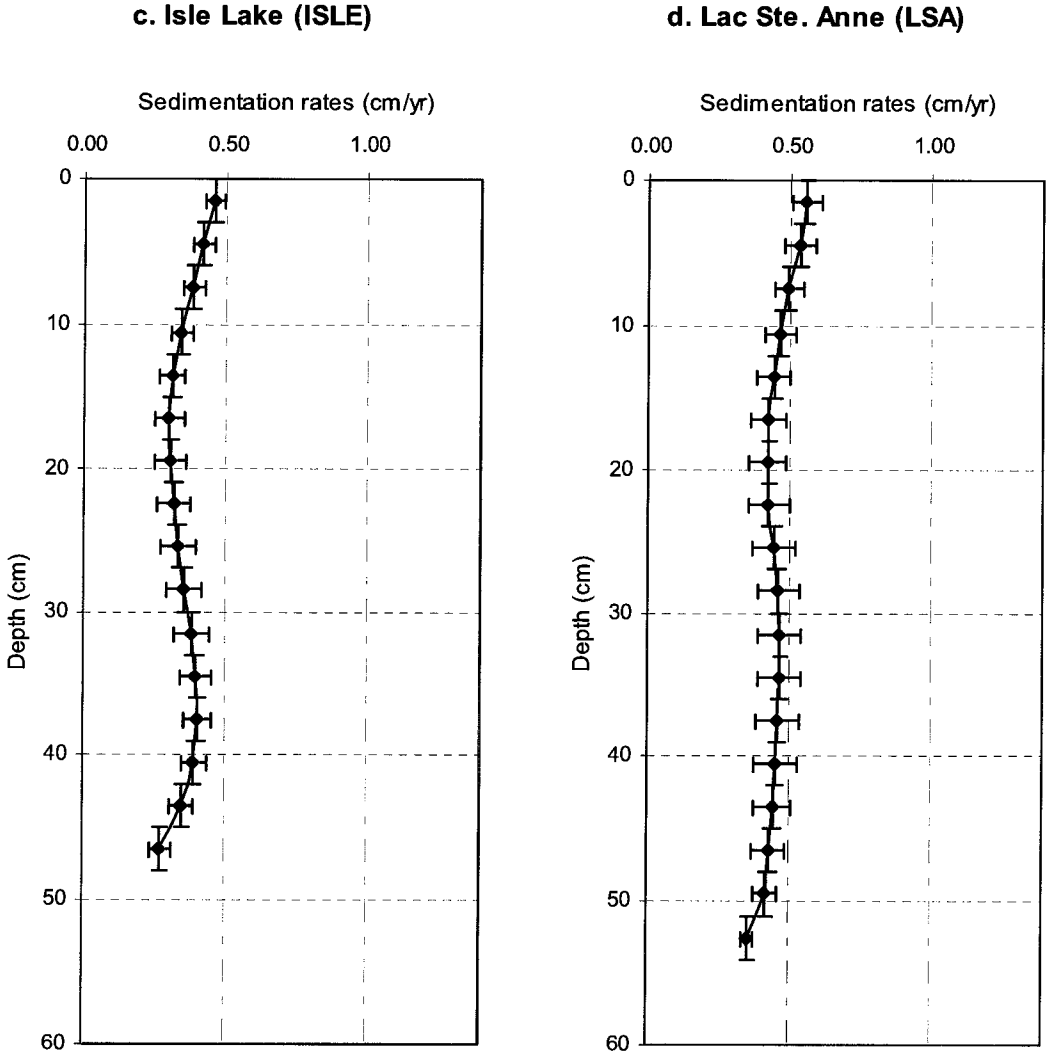

Figures 2.2.c-d: Profiles of the linear sedimentation rates for Isle Lake (c) and Lac Ste. Anne (d).

The linear sedimentation rates in cores ISLE (Figure 2.2c) and LSA (Figure 2.2d) show a gradual increase towards upper part of the sediment profile (Figures 2.2c-d). The estimated sedimentation rates in ISLE and LSA cores are within the ranges of 0.27 to 0.56 and 0.36 to 0.56 cm/yr, respectively (Tables 2.2c-d). General increase of the sedimentation rates in the upper part of the studied cores may reflect the increasing trend of soil erosion in the lakes watershed due to clear cutting caused by human settlement during the past century (Mitchell and Prepas, 1990).

2.1.5. Mass Accumulation Rates (MAR)

The Mass Accumulation Rates (MAR; g/cm^2yr) of the sediments were calculated following the equation (Tables 2.2a-d):

$$MAR = m / t$$

Where "m" is the cumulative dry mass (g/cm^2) at any depth, and "t" is the calculated age of the sediment.

The cumulative dry mass (g/cm^2) of the sediment was calculated using the following formula (Table 2.2a-d):

$$\rho_b = \rho_g (1 - \Phi)$$

Where "ρ_b" is the bulk density (sediment grains + organic matter + porosity filled with water under saturated system), and "ρ_g" is the grain density. The grain density is calculated using the grain density of quartz particles corrected for percent TOC of the sediments as shown in the following formula (Table 2.2a-d):

$$\rho_g = \rho_{quartz} \times (1\text{-}TOC/100) + \rho_{organic} \times (TOC/100)$$

$$\rho_{quartz} = 2.65\ g/cm^3$$

$\rho_{organic} = \sim 1\ g/cm^3$

Φ = porosity, which is equivalent to the water content under the saturated system as seen in the unconsolidated recent sediments.

The estimated mass accumulation rate (MAR) in all four sediment cores suggests periods of high and low mass accumulation rates throughout the history of the sediment profiles (Figures 2.3a-d). These fluctuations in MAR are due to factors such as water levels, flooding events, and deforestation in the drainage basin. In Wabamun Lake, core WAB2 shows a substantially higher average MAR ($0.17 \pm 0.02\ g/cm^2.yr$) than core WAB1 ($0.1 \pm 0.01\ g/cm^2.yr$) (Tables 2.2a-b and Figures 2.3a-b). On average, core LSA has a higher MAR ($0.17 \pm 0.00\ g/cm^2.yr$) than ISLE ($0.12 \pm 0.01\ g/cm^2.yr$) (Tables 2.2c-d and Figures 2.3c-d).

In order to identify the high and low MAR events throughout the sediment core, the incremental mass accumulation rates (IMAR: $g/cm^2.yr$) were estimated for each studied core. The IMAR ($g/cm^2.yr$) at any given depth (x) in the sediment core were calculated using the following formula (Tables 2.2a-d):

$$IMAR\ (g/cm^2.yr) = (MAR_x - MAR_{x-1}) / (t_x - t_{x-1})$$

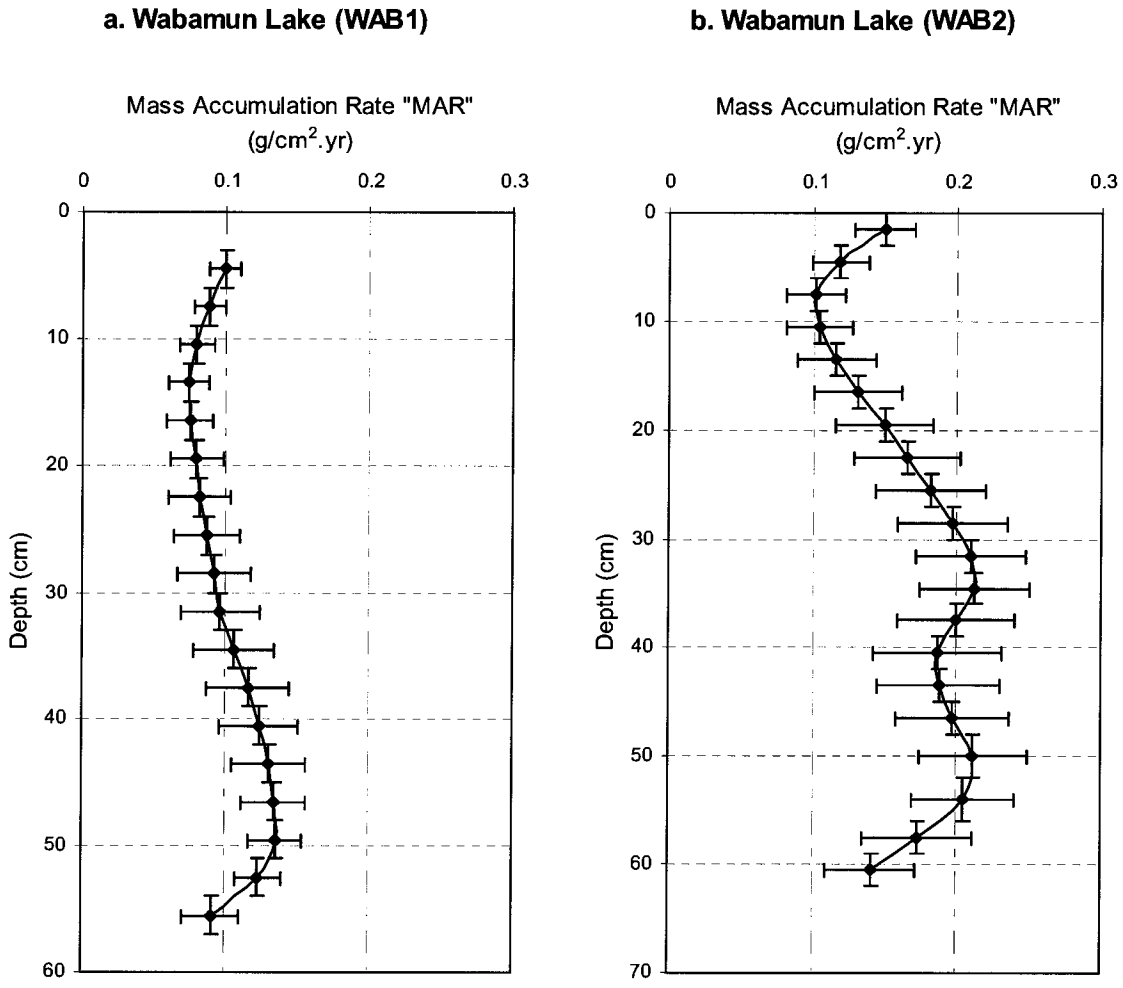

Figures 2.3a-b: Profiles of mass accumulation rates (MAR) for WAB1 (a) and WAB2 (b) cores from Wabamun Lake.

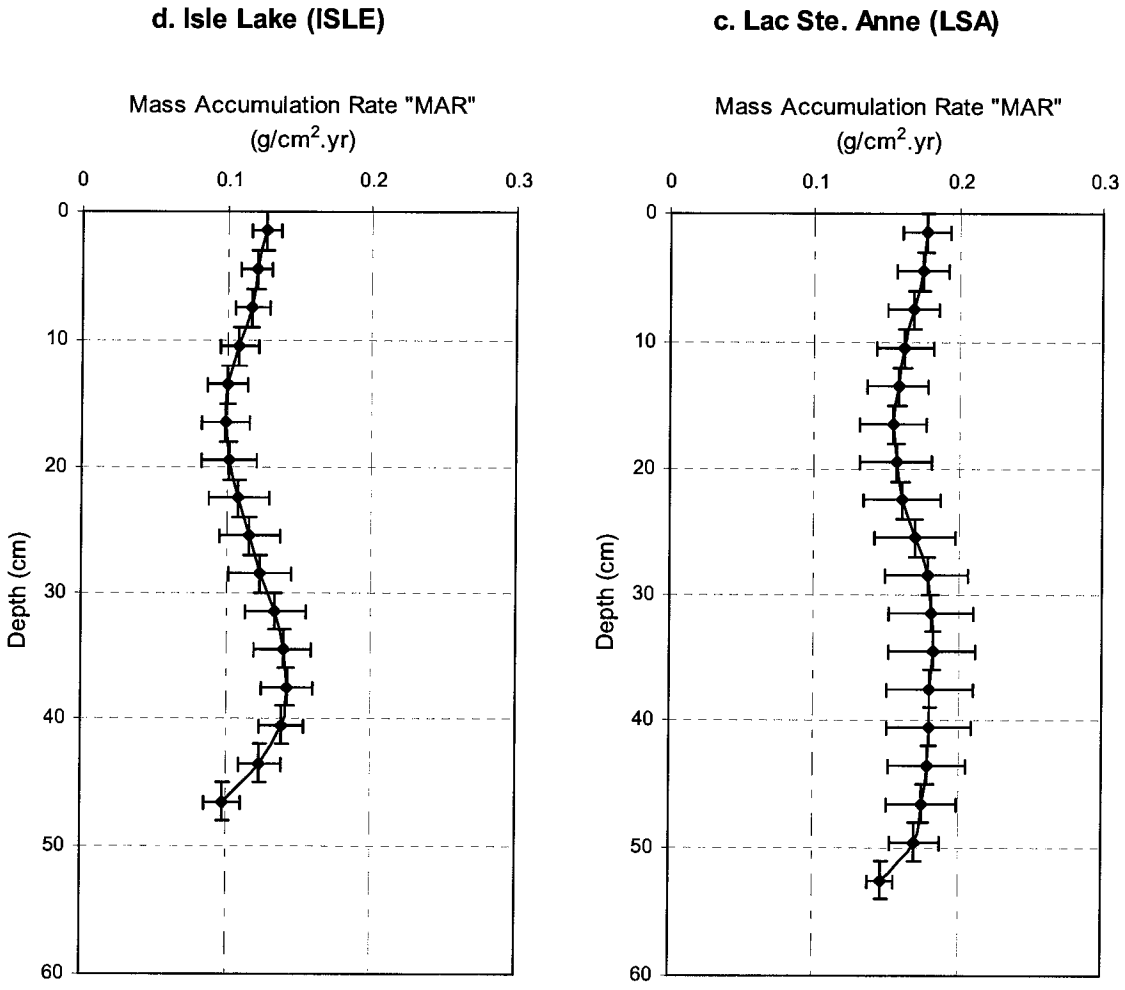

Figure 2.3c-d: Profiles of mass accumulation rates (MAR) for Isle Lake (c) and Lac Ste. Anne (d).

The IMAR versus depth graphs for sediment cores WAB1, WAB2, ISLE, and LSA are shown in Figures 2.4a-d. The results indicate a rapid sedimentation event at the depths of 34.5 to 37.5 cm in WAB1 and 50 cm in WAB2 (Tables 2.2a-b and Figures 2.4a-b). This event is chronologically consistent in both WAB1 and WAB2 cores from Wabamun Lake (Figures 2.4a-b). Such an event may correspond to a widespread, major flooding/high water event in Wabamun Lake in the early 1900's (approx. 1904-1909). Similarly, core LSA shows

a marked IMAR increase event at the depth of 25.5 cm to 28.5 cm, which corresponds to the years 1939 to 1944 (Figure 2.4d). Furthermore, the Isle lake core shows a rapid increase in MAR at depth 31.5 cm coinciding with the year 1918 (Figure 2.4c) (Buckland-Nicks and Mitchell, 1990).

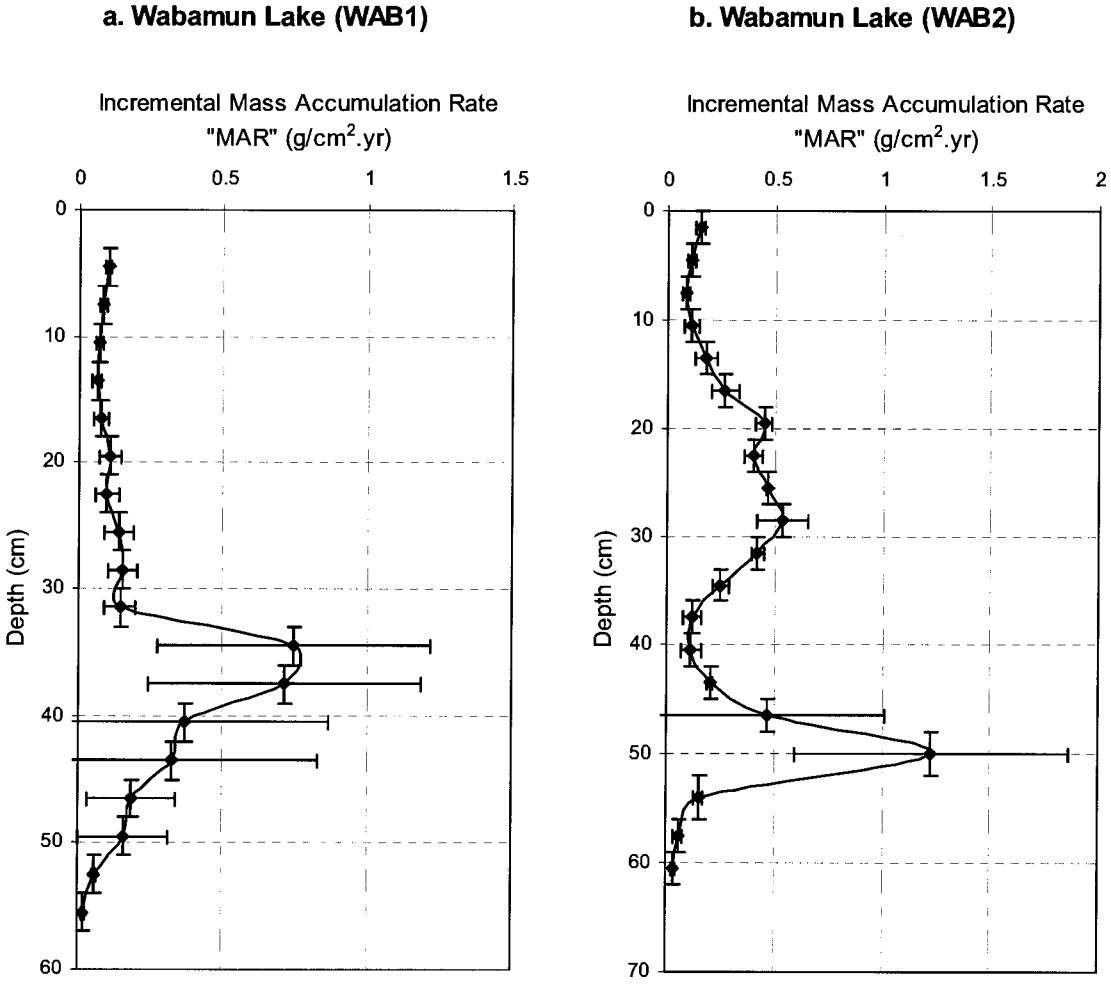

Figures 2.4a-b: Profiles of incremental mass accumulation rates (MAR) for WAB1 (a) and WAB2 (b) cores from Wabamun Lake.

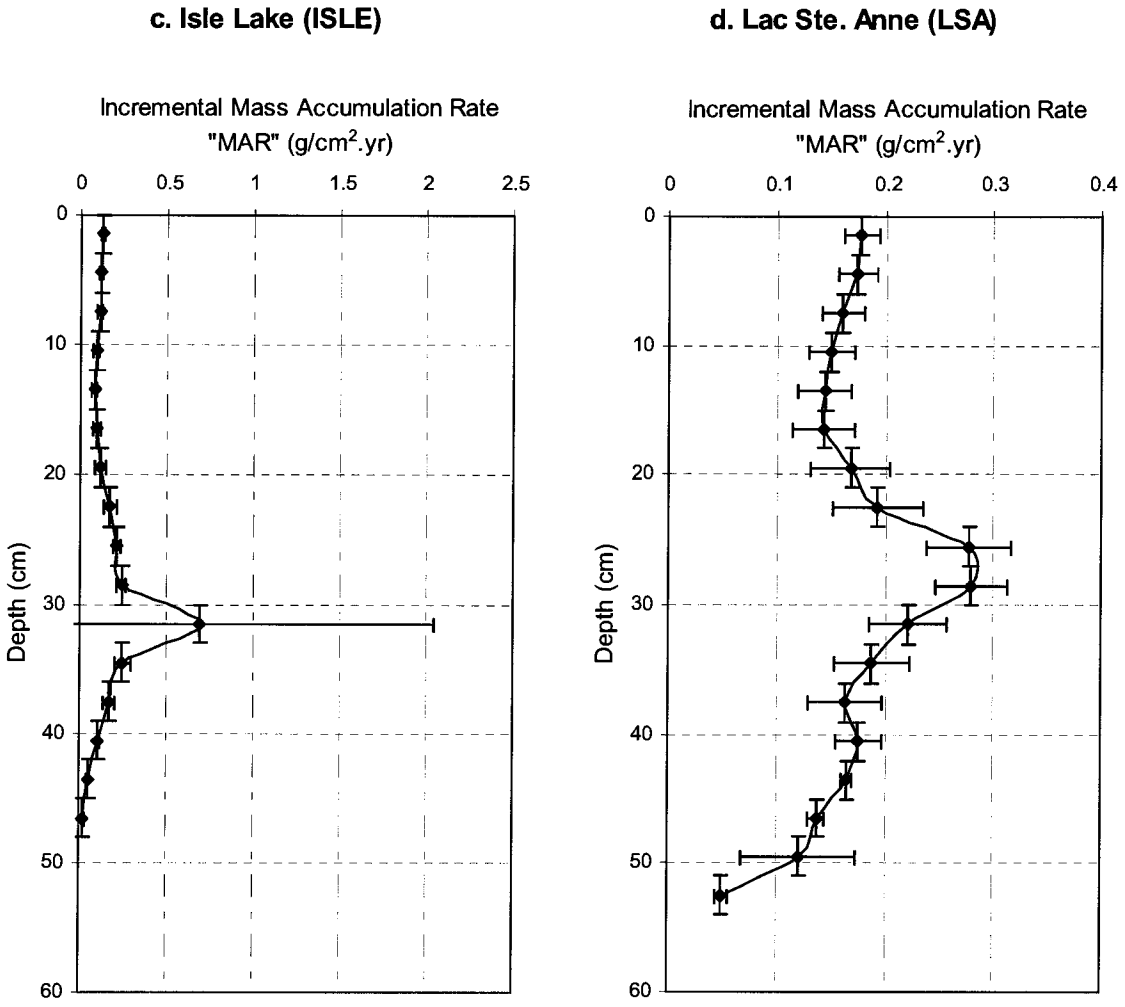

Figure 2.4c-d: Profiles of mass accumulation rates (MAR) for Isle Lake (c) and Lac Ste. Anne (d).

It appears that in all four studied cores, a high MAR period or event occurred in the first half of the twentieth century (Figures 2.4a-d). Following the high accumulation periods, the accumulation rates of sediments decline and remain constant towards the second half of the century (Figures 2.4a-d). The high rate of clear cutting upon the arrival of settlers and the commencement of agricultural/residential activities in the region enhanced the runoff and increased the erosion, leading to higher sediment accumulation rates (Mitchell and Prepas,

1990). The recent decrease or stabilization of MAR in the studied lakes is likely the result of the reduction in the deforestation rate and/or other anthropogenic activities responsible for increasing the runoff.

2.1.6. ^{210}Pb flux

The yearly flux of ^{210}Pb was estimated for each core using the following equation:

$$^{210}\text{Pb flux (Bq/cm}^2\text{.yr)} = \lambda \times A_o$$

The calculated ^{210}Pb flux were 0.02 to 0.03 Bq/cm^2.yr for Wabamun cores and 0.03 and 0.04 Bq/cm^2.yr for ISLE and LSA cores, respectively. The results indicate that the ^{210}Pb flux for all four studied cores with similar depositional environments are quite similar, varying within a narrow range. This confirms the validity of CRS model for geochronology of the sediment cores in the study area (Appleby and Oldfield, 1983). Additionally, the estimated ^{210}Pb flux for the studied lakes reflect the global range of ^{210}Pb fallout (0.0074 to 0.0333 Bq/cm^2.yr), which is another required condition outlined by CRS model (Appleby and Oldfield, 1983).

2.2. CESIUM-137 NUCLEAR FALLOUT

Physical and geochemical processes may affect a ^{210}Pb profile and hence cause misinterpretation of the data. For this reason, radionuclides with different input functions, or input sources, are often used to provide reasonable estimates in the sediment cores. In this

study, ^{137}Cs is used in conjunction with ^{210}Pb, because these radionuclides provide independent estimates of sedimentation rates and mixing depths (Robbins and Herche, 1993). Unlike lead-210 geochronology, which relies on the isotopic decay of ^{210}Pb in sediments, the Cesium-137 dating is based on the identification of known horizons.

The ^{137}Cs method may provide less detail on sedimentation processes than ^{210}Pb. This is because the sedimentation rates calculated by ^{137}Cs are average estimates, based only on two depth horizons. Moreover, the location of the ^{137}Cs horizons is sensitive to loss or disturbance of surface sediments with coring, erosion, or sediment reworking (Robbins et al., 1978).

Cesium-137 (^{137}Cs) is a product of nuclear fission, which originates primarily from global atmospheric nuclear bomb testing, and has a half-life (t½) of 30 years (e.g., McCallan et al., 1980; Longmore et al., 1983). The global fallout of ^{137}Cs to the environment began with high-yield thermonuclear tests in 1952 (Perkins and Thomas, 1980). As a result of the nuclear tests in this period, ^{137}Cs was released into the stratosphere, where it circulated globally (Longmore, 1982). The globally transported ^{137}Cs returned to the earth's surface through local precipitation (Longmore, 1982). The year of initial input of ^{137}Cs into the global atmosphere is estimated to be 1952 ± 2 yr (Health and Safety Laboratory, 1972; Robbins et al., 1978). The detectable amounts of ^{137}Cs in soils began appearing around 1954 (Longmore, 1982). Suspended aquatic particles continue to adsorb the fallout ^{137}Cs deposited on water surfaces and remove the ^{137}Cs out of the water column within a few years after the

initial fallout. However, small portions of ^{137}Cs continue to be reintroduced through the re-suspension of surface sediments (Robbins et al., 1978).

Cesium-137 is typically associated with very fine atmospheric dust particles (Lockhart et al., 1965). Once ^{137}Cs reaches the earth's surface, it is preferentially adsorbed into the clay fraction of sediments (Francis and Brinkley, 1976; Tamura, 1964; Comans et al., 1991; Lomenick and Tamura, 1965). There are two important pathways resulting in ^{137}Cs presence in aquatic sediments. The first is through direct deposition of ^{137}Cs at the site, while the second involves indirect transportation of ^{137}Cs deposited in the watershed due to erosion processes (Ritchie and McHenry, 1990).

Cesium-137 is also an important tracer of hydrophobic contaminants since it follows a behavior similar to some non-degradable contaminants (e.g., PCBs) circulating in the aquatic environment.

In a well-preserved sedimentary profile, the shape of the ^{137}Cs profile (concentration versus depth) can be used to identify the major periods of global deposition of ^{137}Cs fallout. The first detectable ^{137}Cs activity in the sediment profile is dated to 1954 corresponding to the onset of atmospheric nuclear weapons testing. Atmospheric deposition of ^{137}Cs was greatest in 1963, with a smaller peak occurring between 1958 and 1959. These peaks correspond to the most intense periods of nuclear testing (Robbins et al., 1978). The ^{137}Cs input declined in the 1970s until it reached below detection limits by the early 1980s due to bans on nuclear testing. In some sedimentary profiles, the ^{137}Cs peak corresponding to the

Chernobyl accident in 1986 can be detected (Comans et al., 1989; Albrecht et al., 1998; Johnson-Pyrtle et al., 2000; Ritchie and McHenry, 1990). Therefore, the sedimentation rates can be estimated by comparing the vertical distribution of ^{137}Cs in sediments with the temporal deposition of fallout ^{137}Cs from the atmosphere to locate sediment horizons (Ritchie and McHenry, 1990).

2.2.1. Nuclear fallout of ^{137}Cs in central Alberta lakes

In this study, the concentration of ^{137}Cs was determined in nine recent sediment cores from eight Central Alberta lakes as part of the Phase I survey. However, only the results of the four cores, which are related to the Phase II survey, are presented in this dissertation (Tables 2.4a-d; Figures 2.5a-d). The sedimentation rates obtained from the ^{137}Cs profile in each core were compared with those of the ^{210}Pb profile (Table 2.5).

The comparisons between the ^{210}Pb and ^{137}Cs ages show some discrepancies, particularly for the 1954 and 1964 horizons corresponding to the radionuclide fallout events in ^{137}Cs profiles (Table 2.5). The results indicate much younger ^{210}Pb ages for the ^{137}Cs 1964 peak in the profiles of all four cores. In other words, the 1964 horizon in ^{137}Cs profile occurs below the assigned age based on ^{210}Pb dating (Table 2.5; Figures 2.5a-d). In contrast, the 1954 peak in ^{137}Cs--profile occurs above that in ^{210}Pb profile. This may partially be because ^{210}Pb data are corrected for the compaction but ^{137}Cs profile is not. The estimated linear sedimentation rate based on the occurrence depths of 1954 and 1964 events in ^{137}Cs depth are shown in Table 2.5. Low sedimentation rates of 0.12-0.28 cm/yr are calculated based on ^{137}Cs data in the upper section of the sediment profiles (above 1964-marker) (Table 2.5).

Table 2.4.a-d: The concentration (dpm/g) of ^{137}Cs in Wabamun Lake (WAB1 and WAB2 cores), Isle Lake (ISLE core), and Lac Ste. Anne (LSA core).

a.

WAB1 core combined intervals	Middle depth	^{137}Cs
	cm	dpm/g
WAB1 (1-3 cm)	4.5*	8.87
WAB1 (4-6 cm)	7.5	11.00
WAB1 (7-9 cm)	10.5	7.85
WAB1 (10-12 cm)	13.5	1.60
WAB1 (13-15 cm)	16.5	1.04
WAB1 (16-18 cm)	19.5	0.68
WAB1 (19-21 cm)	22.5	0.40
WAB1 (22-24 cm)	25.5	0.10
WAB1 (25-27 cm)	28.5	0.28
WAB1 (28-30 cm)	31.5	0.11
WAB1 (31-33 cm)	34.5	***0.05***
WAB1 (34-36 cm)	37.5	***0.05***
WAB1 (37-39 cm)	40.5	***0.05***
WAB1 (40-42 cm)	43.5	***0.05***
WAB1 (43-45 cm)	46.5	***0.05***
WAB1 (46-48 cm)	49.5	***0.05***
WAB1 (49-51 cm)	52.5	***0.05***
WAB1 (52-54 cm)	55.5	***0.05***

* top 3 cm of sediment were lost during sampling.

b.

WAB2 core combined intervals	Middle depth	^{137}Cs
	cm	dpm/g
WAB2 (1-3 cm)	1.5	6.09
WAB2 (4-6 cm)	4.5	8.53
WAB2 (7-9 cm)	7.5	7.47
WAB2 (10-12 cm)	10.5	4.23
WAB2 (13-15 cm)	13.5	1.67
WAB2 (16-18 cm)	16.5	0.78
WAB2 (19-21 cm)	19.5	0.64
WAB2 (22-24 cm)	22.5	0.20
WAB2 (25-27 cm)	25.5	0.28
WAB2 (28-30 cm)	28.5	***0.05***
WAB2 (31-33 cm)	31.5	***0.05***
WAB2 (34-36 cm)	34.5	***0.05***
WAB2 (37-39 cm)	37.5	0.22
WAB2 (40-42 cm)	40.5	0.15
WAB2 (43-45 cm)	43.5	***0.05***
WAB2 (46-48 cm)	46.5	***0.05***
WAB2 (49-52 cm)	50	***0.05***
WAB2 (53-56 cm)	54	***0.05***
WAB2 (57-59 cm)	57.5	0.12
WAB2 (60-62 cm)	60.5	***0.05***

c.

ISLE core combined intervals	Middle depth	^{137}Cs
	cm	dpm/g
ISLE (1-3 cm)	1.5	6.50
ISLE (4-6 cm)	4.5	7.21
ISLE (7-9 cm)	7.5	7.27
ISLE (10-12 cm)	10.5	7.99
ISLE (13-15 cm)	13.5	6.62
ISLE (16-18 cm)	16.5	2.43
ISLE (19-21 cm)	19.5	1.45
ISLE (22-24 cm)	22.5	0.51
ISLE (25-27 cm)	25.5	0.49
ISLE (28-30 cm)	28.5	0.09
ISLE (31-33 cm)	31.5	0.14
ISLE (34-36 cm)	34.5	0.15
ISLE (37-39 cm)	37.5	0.14
ISLE (40-42 cm)	40.5	0.20
ISLE (43-45 cm)	43.5	***0.05***
ISLE (46-48 cm)	46.5	***0.05***

d.

LSA core combined intervals	Middle depth	^{137}Cs
	cm	dpm/g
LSA (1-3 cm)	1.5	5.81
LSA (4-6 cm)	4.5	5.98
LSA (7-9 cm)	7.5	7.46
LSA (10-12 cm)	10.5	7.80
LSA (13-15 cm)	13.5	5.25
LSA (16-18 cm)	16.5	2.44
LSA (19-21 cm)	19.5	0.92
LSA (22-24 cm)	22.5	0.44
LSA (25-27 cm)	25.5	0.36
LSA (28-30 cm)	28.5	0.16
LSA (31-33 cm)	31.5	0.20
LSA (34-36 cm)	34.5	0.21
LSA (37-39 cm)	37.5	0.05
LSA (40-42 cm)	40.5	0.14
LSA (43-45 cm)	43.5	***0.05***
LSA (46-48 cm)	46.5	***0.05***
LSA (49-51 cm)	49.5	***0.05***
LSA (52-54 cm)	52.5	***0.05***

Values in Italic font are below detection limit and hence were assigned a value equivalent to one-half of the detection limit.

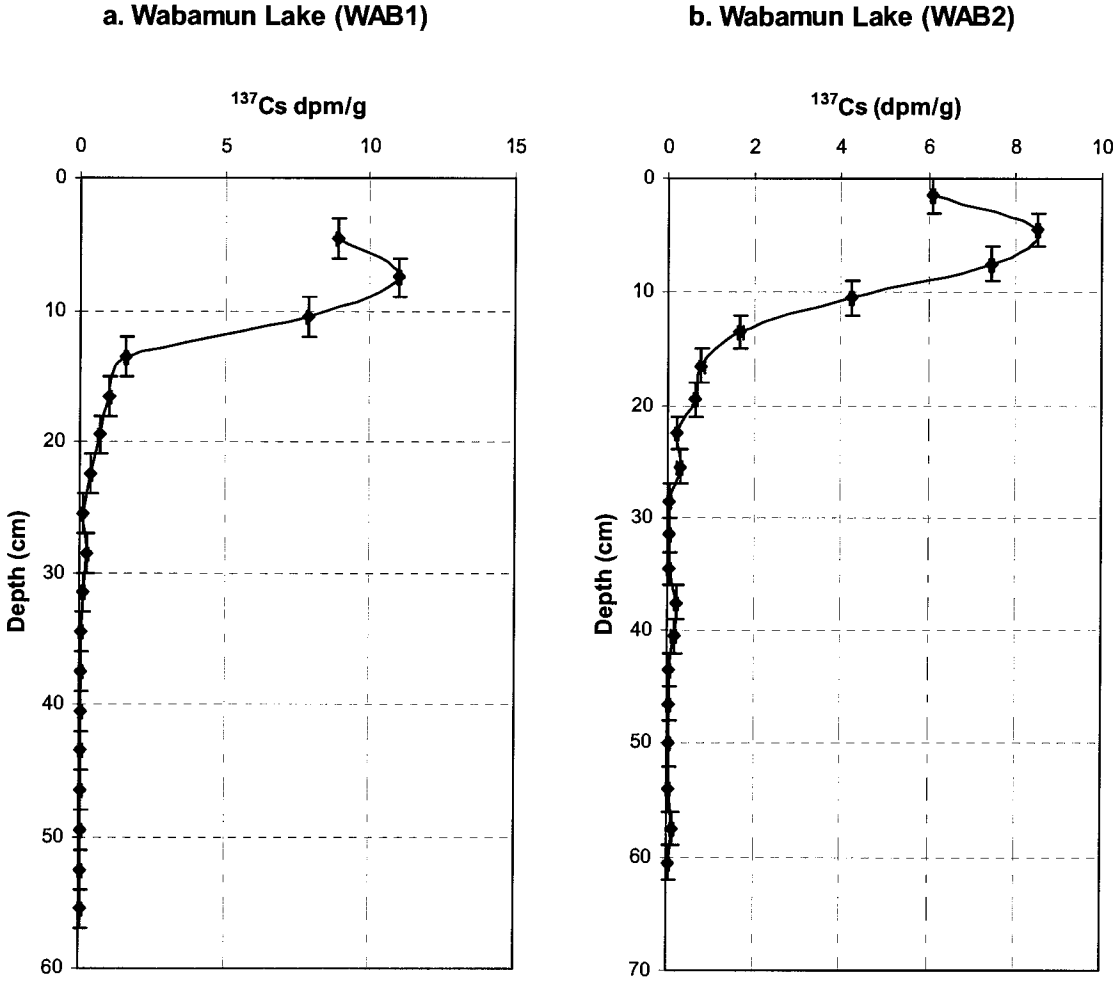

Figures 2.5a-b: Profiles of the specific activity of ^{137}Cs in the sediment cores WAB1 (a) and WAB2 (b) from Wabamun Lake.

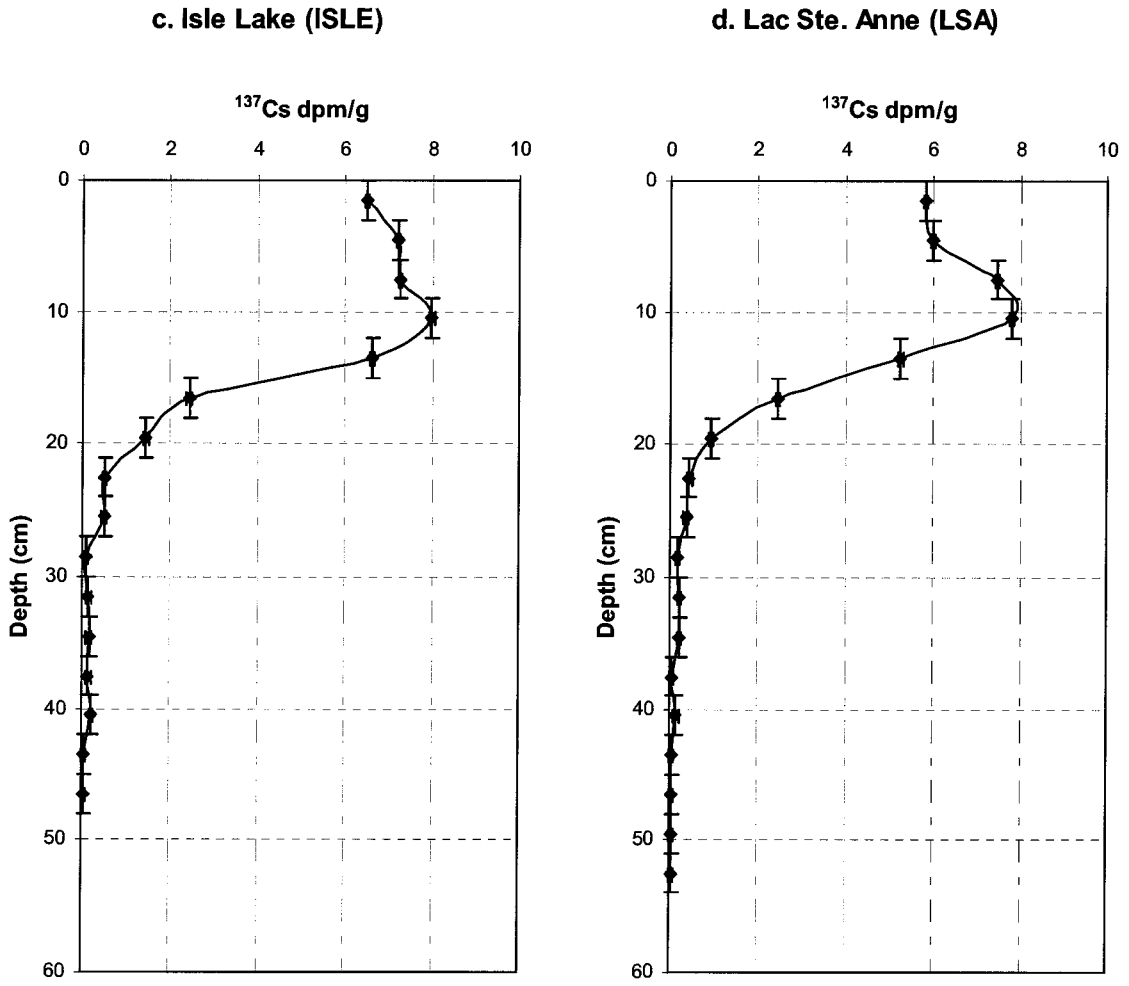

Figures 2.5c-d: Profiles of the specific activity of ^{137}Cs in the sediment cores from Isle Lake (c) and Lac Ste. Anne (d).

WAB2 and LSA cores show a very similar sedimentation rates in both ^{137}Cs and ^{210}Pb methods (Table 2.5). However, WAB1 and ISLE cores show different results (Table 2.5).

Table 2.5. The comparison between estimated sedimentation rates obtained from the ^{137}Cs profile in each core versus those of the ^{210}Pb profile.

	^{210}Pb dating		^{137}Cs dating		^{210}Pb sedimentation rates*	^{137}Cs sedimentation rates		
	1954 marker	1964 marker	1954 marker	1964 marker		since 1954	since 1964	average
	cm	cm	cm	cm	cm/yr	cm/yr	cm/yr	cm/yr
Wabamun Lake (WAB1)	22.5	13.5	28.5	4.5	0.53	0.61	0.12	0.36
Wabamun Lake (WAB2)	15.0	12.8	28.5	7.5	0.42	0.61	0.20	0.40
Isle Lake (ISLE)	14.5	12.0	28.5	10.5	0.38	0.61	0.28	0.45
Lac Ste. Anne (LSA)	20.0	16.0	28.5	10.5	0.48	0.61	0.28	0.45

*Average sedimentation rates above 1954-marker horizons in the sediment columns

The discrepancies between the two geochronology methods are due in part to differences in mobility of the two radionuclides in aquatic sediments. Mixing of sediments can redistribute ^{137}Cs within the sediments, spreading ^{137}Cs activity over the top portion of the vertical profile and broadening ^{137}Cs peaks (i.e., Robbins and Edgington, 1975; Robbins et al., 1978; Krezoski and Robbins, 1985). Surficial sediments can be also mixed by biological activity or other physical processes (e.g., waves, high flow events). The secondary transportation of ^{137}Cs from the watershed to the lake may also alter the ^{137}Cs record by broadening the 1963 ^{137}Cs peak or by completely obscuring its appearance (Boudreau, 1994; Dellapenna et al., 1998).

CHAPTER 3: TEMPORAL DISTRIBUTION OF TRACE ELEMENTS IN SEDIMENTS AND POREWATER FROM LAKES IN CENTRAL ALBERTA, CANADA

3.1. INTRODUCTION

The temporal variation of trace elements in recent lake sediments has been used for many years as a monitoring tool in the environment, and offers excellent insights into the pollution history of a lake (Shirahata et al., 1980; Swain et al., 1992; Vile et al., 2000; Sanei et al., 2000; 2001; El Bilali et al., 2002). However, the proper interpretation of the elemental data in a sediment column requires careful examination of the sediment-porewater interaction. Interaction between sediment and water during early diagenesis is very important in biogeochemical cycling of elements in the natural aquatic environment (Eck and Smits, 1986; Gobeil et al., 1987; Morfett et al., 1988; Jahnke et al., 1989; Gerringa, 1990; Ivert, 1990; Carignan and Lean, 1991; Dahmke et al., 1991; Barbanti et al., 1992a; Williams, 1992). This exchange of elements between sediments and porewater throughout the sediment profile in early diagenesis may alter the historical record of elements.

Several coal-fired power plants are located in central Alberta (Figure 1.1). Emissions from these facilities can be a significant source of the elements found in the local environment, and as a result, are a subject of environmental concern. A multi-elemental analysis of the recent sediments and their porewater in conjunction with other inorganic and organic geochemical parameters can provide valuable information on the sources, quantity, and processes involved in the distribution of trace elements in the recent sediments.

The objective of this study is to investigate temporal distribution of trace elements in the sediment cores from Wabamun Lake, Isle Lake, and Lac Ste. Anne in central Alberta as

related to activities of the coal-fired power plants in the study region. Furthermore, this study focuses on the biogeochemical processes involved between sediments and porewater and the possible mobility of elements during early diagenesis.

3.2. STUDY AREA

This study was conducted on four sediment cores obtained from Wabamun Lake (WAB1 and WAB2), Isle Lake (ISLE), and Lac Ste. Anne (LSA). Detailed information on the study area and location of the sediment cores can be found in Chapter 1.6.

3.3. METHODOLOGY

The information regarding the coring method, sample preparation, and analytical procedures is discussed in Chapter 1.7.

3.4. RESULTS AND DISCUSSION

The results of the elemental analyses for sediment and porewater profiles from Wabamun Lake (WAB1 and WAB2), Isle Lake (ISLE), and Lac Ste. Anne (LSA) are shown in Tables 3.1-3.8. In this chapter, the elemental data are used to study the vertical distribution of elements in sediment and porewater and their interaction during post-deposition geochemical processes.

Table 3.1. The concentration of elements and organic matter (TOC and S1) in the sediments from WAB1 core.

Sediment intervals (cm)	Al	As		Ba	Bi	Br	Ca	Cd	Co		Cr		Cs		Cu	Fe		Ga	Hf		Hg	K	Li	Mg	Mn	Mo	
	L	*C*		*L*	*C*	*A, L*	*L*	*C*	*C, S*		*L*		*L*		*C*	*C, S*		C	*L*		*C*	*L*	*L*	*L*	*L*	*C, S*	
	IMS	NAA*	IMS	IMS	IMS	NAA	IMS	IMS	NAA*	IMS	NAA*	IMS	NAA*	IMS	IMS	NAA	IMS*	IMS	NAA*	IMS	CVAA	IMS	IMS	IMS	IMS	NAA	IMS*
	%	ppm	ppm	ppm	ppm	ppm	%	ppm	ppm	ppm	ppm	ppm	ppm	ppm	ppm	%	%	ppm	ppm	ppm	ppm	%	ppm	%	ppm	ppm	ppm
Wab1-01	6.49	11	11	99	0.24	31	1.27	0.42	11.3	10.7	68	63	4.1	4.5	30	2.87	2.88	14	4.4	2.7	0.02	1.09	27	0.70	515	2	3.0
Wab1-02	4.19	16	13	99	0.23	30	3.23	0.30	6.8	6.3	50	46	3.1	2.9	97	1.73	1.83	12	2.3	1.8	0.10	0.74	19	0.62	375	24	22
Wab1-03	4.31	16	13	93	0.23	31	3.14	0.34	6.9	6.3	54	47	3.1	3.0	103	1.84	1.87	12	2.4	1.8	0.08	0.72	18	0.62	372	25	23
Wab1-04	4.42	17	14	81	0.23	31	3.20	0.30	6.7	6.7	52	50	2.3	3.0	105	1.82	1.92	12	2.5	1.8	0.06	0.80	20	0.63	395	28	25
Wab1-05	4.50	18	15	143	0.22	29	3.20	0.34	6.9	7.2	52	50	3.0	3.1	108	1.88	1.94	12	2.5	1.8	0.06	0.74	19	0.63	380	28	29
Wab1-06	4.62	19	17	113	0.24	29	3.18	0.32	7.6	6.8	56	54	3.0	3.1	118	1.92	2.01	13	2.5	1.9	0.08	0.78	20	0.63	377	31	32
Wab1-07	4.75	20	18	118	0.24	29	3.07	0.37	7.8	7.4	58	56	2.7	3.2	121	2.02	2.07	14	2.4	2.0	0.06	0.79	21	0.64	382	34	34
Wab1-08	4.98	21	19	109	0.24	29	2.95	0.36	7.4	7.2	60	58	3.1	3.2	132	2.06	2.14	14	2.8	1.9	0.06	0.77	21	0.65	385	34	34
Wab1-09	4.96	23	20	100	0.28	31	2.70	0.42	7.3	8.2	61	59	3.1	3.5	157	2.05	2.15	15	2.7	2.0	0.06	0.86	23	0.63	380	33	36
Wab1-10	4.94	24	22	91	0.28	33	2.40	0.42	7.7	7.9	62	59	3.6	3.5	176	2.08	2.17	15	2.7	2.1	0.08	0.82	22	0.61	368	33	35
Wab1-12	4.80	25	23	75	0.27	34	2.18	0.46	7.6	8.1	55	53	3.2	3.3	149	2.06	2.19	13	2.7	2.0	0.06	0.82	21	0.59	365	30	30
Wab1-14	4.74	20	19	68	0.27	38	1.71	0.54	7.8	7.4	46	45	2.7	3.2	64	2.14	2.18	11	2.7	2.0	0.05	0.81	21	0.57	360	16	14
Wab1-16	4.55	17	16	63	0.28	40	1.72	0.47	7.4	7.7	42	41	2.8	3.1	41	2.08	2.16	10	2.9	1.8	0.05	0.75	20	0.54	362	11	10
Wab1-18	4.37	16	15	67	0.32	42	1.88	0.50	7.2	7.1	42	41	2.9	3.1	37	2.16	2.21	10	2.7	1.8	0.05	0.76	19	0.51	363	8	7.8
Wab1-20	4.52	15	14	74	0.32	41	2.34	0.50	7.5	7.9	41	39	2.7	3.1	38	2.32	2.43	10	2.4	1.9	0.05	0.72	18	0.52	382	7	6.4
Wab1-23	4.98	15	14	70	0.31	42	2.08	0.49	7.9	8.9	44	43	3.2	3.4	34	2.24	2.41	10	3.0	2.1	0.02	0.81	20	0.55	384	5	4.8
Wab1-26	4.64	12	12	83	0.24	39	2.12	0.40	7.5	7.4	42	40	3.2	3.2	31	2.10	2.20	10	2.7	2.0	0.03	0.74	19	0.50	358	2	3.8
Wab1-30	5.08	12	11	98	0.23	40	2.09	0.39	8.5	8.9	49	44	3.3	3.5	32	2.30	2.36	11	3.1	2.2	0.05	0.80	21	0.54	385	4	4.1
Wab1-34	5.42	10	10	106	0.23	38	1.83	0.38	9.1	9.4	52	48	3.6	3.9	31	2.62	2.66	11	3.3	2.3	0.04	0.91	23	0.58	394	3	3.6
Wab1-39	5.59	11	10	86	0.24	36	1.76	0.40	9.9	10.3	51	51	4.0	4.1	34	2.62	2.78	12	3.1	2.3	0.02	0.95	23	0.60	387	4	3.0
Wab1-44	5.57	12	12	93	0.25	37	1.90	0.44	9.4	10.2	51	49	4.0	3.9	34	2.71	2.77	12	3.3	2.3	0.03	0.87	23	0.58	443	4	4.0
Wab1-50	5.61	12	11	66	0.26	36	1.26	0.42	9.4	10.1	52	48	4.2	3.9	34	2.63	2.73	12	3.3	2.5	0.05	0.89	23	0.57	399	6	4.1
Wab1-56	5.93	9	12	60	0.26	27	1.06	0.43	8.3	11.0	48	50	3.7	4.3	34	2.54	3.07	12	2.9	2.6	0.04	0.93	26	0.62	389	3	3.6
Wab1-64	5.76	13	11	93	0.26	38	1.14	0.43	10.0	10.9	53	50	3.8	4.2	34	2.76	2.90	12	3.2	2.5	0.05	0.98	25	0.63	383	6	3.7
Min	4.19	9	10	60	0.22	27	1.06	0.30	6.7	6.3	41	39	2.3	2.9	30	1.73	1.83	10	2.3	1.8	0.02	0.72	18	0.50	358	2	3.0
Median	4.87	16	14	92	0.25	35	2.11	0.42	7.7	7.9	52	50	3.2	3.3	40	2.12	2.20	12	2.7	2.0	0.05	0.81	21	0.61	382	9	8.8
Max	6.49	25	23	143	0.32	42	3.23	0.54	11.3	11.0	68	63	4.2	4.5	176	2.87	3.07	15	4.4	2.7	0.10	1.09	27	0.70	515	34	35.5
Mean	4.99	16	15	89.5	0.26	35	2.23	0.41	8.1	8.3	52	49	3.3	3.5	74	2.23	2.33	12	2.9	2.1	0.05	0.83	21	0.59	387	16	15.7

Table 3.1. Continued.

Sediment intervals (cm)	Na		Nb	Ni	P	Pb	Rb	S		Sb		Sc		Se	Sr	Th		Ti	U		V	W	Zn		Zr	TOC	S1
	L		*L*	*C, S*	*B, L, S*	*C*	*L*	*B, C*		*C*		*L*		*C*	*L*	*L*		*L*	*L*		*L*	*L, S*	*C*		*L*		
	NAA*	IMS	IMS	IMS	IMS	IMS	IMS	SA*	IMS	NAA*	IMS	NAA*	IMS	IMS	IMS	NAA*	IMS	IMS	NAA*	IMS	IMS	IMS	NAA	IMS*	IMS	REVL	REVL
	%	%	ppm	ppm	%	ppm	ppm	%	%	ppm	ppm	ppm	ppm	ppm	ppm	ppm	ppm	%	ppm	ppm	ppm	ppm	ppm	ppm	ppm	%	
Wab1-01	0.57	0.57	7.1	42	0.09	16	54	1.859	1.7	1.3	1.3	10.9	9.5	*-0.2*	122	9.6	9.0	0.30	5.9	5.1	91	1.1	97	105	87	18.19	34.62
Wab1-02	0.35	0.35	4.5	25	0.25	25	35	1.784	1.9	1.8	1.7	6.7	6.2	0.9	165	5.8	5.8	0.17	4.5	4.4	70	2.4	105	106	52	18.06	34.66
Wab1-03	0.36	0.35	4.6	24	0.24	22	36	1.743	1.8	2.0	1.9	7.0	6.3	1.0	163	6.3	6.1	0.17	5.5	4.9	75	2.4	106	109	53	17.38	31.74
Wab1-04	0.37	0.37	4.6	25	0.23	23	36	1.737	1.8	2.1	2.1	7.0	6.6	1.2	162	6.0	6.2	0.18	5.7	5.3	78	2.4	109	108	54	17.93	34.08
Wab1-05	0.35	0.37	4.8	25	0.21	23	37	1.676	1.7	2.3	2.4	7.1	6.5	1.2	164	6.3	6.2	0.18	6.2	6.0	84	2.5	104	113	56	16.87	29.40
Wab1-06	0.36	0.36	4.9	27	0.19	24	39	1.607	1.8	2.6	2.5	7.4	7.2	1.6	163	6.4	6.6	0.19	6.7	6.8	89	2.5	114	116	58	16.18	26.07
Wab1-07	0.37	0.36	5.2	28	0.18	25	40	1.576	1.7	2.5	2.6	7.7	7.0	1.5	166	6.8	6.6	0.19	7.5	7.1	92	2.4	109	125	61	16.60	29.73
Wab1-08	0.35	0.37	5.2	28	0.17	27	39	1.541	1.6	2.8	2.8	7.7	7.3	1.8	152	6.7	6.6	0.20	7.4	7.2	95	2.5	114	123	60	16.36	27.68
Wab1-09	0.36	0.37	5.3	30	0.17	30	42	1.516	1.6	3.2	3.1	7.8	7.4	2.5	146	6.8	7.0	0.20	7.6	7.7	99	2.4	131	135	62	15.64	24.71
Wab1-10	0.38	0.37	5.2	29	0.16	32	41	1.552	1.7	3.4	3.5	8.0	7.8	2.8	133	6.8	7.1	0.20	8.0	8.0	102	2.6	124	143	62	17.20	28.19
Wab1-12	0.37	0.38	5.2	31	0.16	30	42	1.607	1.7	3.2	3.3	7.9	7.6	2.4	128	6.5	6.5	0.20	8.4	8.2	97	2.4	123	140	62	17.42	28.79
Wab1-14	0.38	0.39	5.1	29	0.16	26	40	1.711	1.8	2.1	2.0	7.8	7.3	*-0.2*	112	6.3	6.3	0.20	6.8	6.3	76	1.7	108	119	59	18.25	27.73
Wab1-16	0.37	0.37	4.8	30	0.16	23	40	1.759	1.9	1.8	1.7	7.6	7.0	*-0.2*	111	6.3	6.1	0.19	6.1	5.6	70	0.9	98	112	57	18.76	27.68
Wab1-18	0.37	0.36	4.7	29	0.16	20	38	1.845	2.0	1.7	1.6	7.6	7.0	*-0.2*	109	6.3	6.1	0.19	5.9	5.4	67	0.8	103	112	55	18.74	27.20
Wab1-20	0.35	0.36	4.7	31	0.15	18	38	2.056	2.2	1.6	1.5	7.5	7.2	*-0.2*	117	6.3	6.3	0.19	4.5	4.5	67	0.9	95	112	58	18.68	26.29
Wab1-23	0.36	0.39	5.3	34	0.15	16	40	1.819	2.0	1.5	1.4	8.0	7.8	*-0.2*	109	6.8	7.0	0.21	5.3	5.1	72	0.9	106	113	64	17.59	23.93
Wab1-26	0.35	0.36	4.8	31	0.13	14	36	1.685	1.8	1.0	1.0	7.8	7.3	*-0.2*	99	6.7	6.7	0.20	4.2	4.0	64	0.8	102	110	58	16.81	22.24
Wab1-30	0.38	0.37	5.4	33	0.13	14	41	1.684	1.8	1.4	1.3	8.7	8.1	*-0.2*	102	7.5	7.1	0.22	6.2	5.9	74	0.8	103	108	62	16.19	20.04
Wab1-34	0.39	0.40	5.9	36	0.13	14	48	1.872	2.0	1.1	1.0	9.2	8.6	*-0.2*	104	7.7	7.6	0.23	5.3	5.1	75	0.9	107	108	70	15.29	18.69
Wab1-39	0.39	0.39	6.0	38	0.12	14	49	1.881	2.0	1.1	0.9	9.3	8.9	*-0.2*	103	7.7	7.9	0.24	4.8	4.9	80	0.9	93	112	70	15.04	17.36
Wab1-44	0.39	0.40	6.2	37	0.12	14	46	2.041	2.1	1.2	1.2	9.5	8.7	*-0.2*	105	7.8	7.8	0.24	6.0	5.9	80	0.9	95	104	72	15.31	17.56
Wab1-50	0.39	0.39	6.5	38	0.11	15	47	2.005	2.0	1.3	1.3	9.7	9.1	*-0.2*	92	8.5	8.1	0.24	6.2	5.8	81	0.9	94	107	74	14.35	14.25
Wab1-56	0.35	0.40	6.5	42	0.10	15	51	1.893	2.3	0.9	1.2	8.7	9.6	*-0.2*	93	7.3	8.4	0.25	4.9	5.4	85	1.1	81	102	78	11.03	11.27
Wab1-64	0.39	0.40	6.1	41	0.11	14	51	2.08	2.1	1.3	1.2	9.7	9.5	*-0.2*	93	8.2	8.1	0.25	6.5	6.1	84	1.0	98	107	72	14.57	15.61
Min	0.35	0.35	4.5	24	0.09	14	35	1.516	1.6	0.9	0.9	6.7	6.2	*-0.2*	92	5.8	5.8	0.17	4.2	4.0	64	0.8	81	102	52	11.03	11.27
Median	0.37	0.37	5.2	30	0.16	21	40	1.751	1.8	1.7	1.6	7.8	7.4	1.6	115	6.7	6.7	0.20	6.0	5.7	80	1.1	105	112	61	16.84	26.75
Max	0.57	0.57	7.1	42	0.25	32	54	2.080	2.3	3.4	3.5	10.9	9.6	2.8	166	9.6	9.0	0.30	8.4	8.2	102	2.6	131	143	87	18.76	34.66
Mean	0.38	0.38	5.4	32	0.16	21	42	1.772	1.9	1.9	1.8	8.2	7.7	1.7	126	7.0	7.0	0.21	6.1	5.9	81	1.6	105	114	63	16.60	24.98

Analytical methods: IMS: Inductively Coupled Plasma-Mass Spectrometry
NAA: Instrumental Neutron Activation Analysis
CVAA: Cold Vapor Atomic Absorption
SA: LECO® Sulphur Analyser CA: LECO® Carbon Analyser
REVL: Rock Eval 6 ® * : Preferred method

Elemental affinities: L: Lithophile
C: Chalcophile
A: Atmophile
B: Biophile
S: Siderophile

Table 3.2. The concentration of elements and organic matter (TOC and S1) in the sediments from WAB2 core.

Sediment intervals (cm)	Al	As		Ba	Bi	Br	Ca	Cd	Co		Cr		Cs		Cu	Fe		Ga	Hf		Hg	K	Li	Mg	Mn	Mo	
	L	*C*		*L*	*C*	*A, L*	*L*	*C*	*C, S*		*L*		*L*		*C*	*C, S*		*C*	*L*		*C*	*L*	*L*	*L*	*L*	*C, S*	
	IMS	NAA*	IMS	IMS	IMS	NAA	IMS	IMS	NAA*	IMS	NAA*	IMS	NAA*	IMS	IMS	NAA	IMS*	IMS	NAA*	IMS	CVAA	IMS	IMS	IMS	IMS	NAA	IMS*
	%	ppm	ppm	ppm	ppm	ppm	%	ppm	ppm	ppm	ppm	ppm	ppm	ppm	ppm	%	%	ppm	ppm	ppm	ppm	%	ppm	%	ppm	ppm	ppm
Wab2-01	5.01	16	14	196	0.24	36	3.15	0.39	6.3	7.8	62	52	3.1	3.3	92	1.81	1.89	12	3.2	2.1	0.06	0.84	21	0.67	788	5	4.7
Wab2-02	5.01	15	14	164	0.21	37	3.05	0.40	8.3	7.9	64	57	3.3	3.3	90	1.93	1.86	12	3.4	2.1	0.07	0.84	21	0.66	731	5	5.0
Wab2-03	5.08	14	14	200	0.22	37	2.92	0.37	8.0	8.0	63	54	3.3	3.4	95	1.87	1.83	13	3.4	2.3	0.06	0.83	22	0.65	691	4	4.9
Wab2-04	5.29	15	15	160	0.24	37	2.99	0.38	7.7	8.5	66	57	3.6	3.5	104	1.86	1.90	13	3.2	2.3	0.07	0.84	23	0.69	705	4	4.6
Wab2-05	4.63	15	14	158	0.24	38	2.92	0.39	8.3	8.9	67	56	3.3	3.6	104	1.91	1.86	13	3.4	2.2	0.06	0.88	23	0.68	690	2	4.4
Wab2-06	5.22	16	15	180	0.23	39	2.87	0.40	8.3	8.3	64	55	3.2	3.6	102	1.83	1.87	13	3.7	2.2	0.07	0.84	22	0.67	678	4	4.4
Wab2-07	5.27	18	16	145	0.23	39	2.81	0.38	8.6	8.9	60	56	3.4	3.5	102	1.88	1.90	13	3.4	2.2	0.05	0.87	23	0.67	672	3	4.5
Wab2-08	5.27	19	18	150	0.23	39	2.79	0.41	8.2	8.2	64	54	3.5	3.6	99	1.99	1.99	13	3.2	2.3	0.04	0.89	22	0.67	654	3	5.2
Wab2-09	5.39	21	19	143	0.23	40	2.76	0.41	8.3	8.3	60	54	3.7	3.5	88	2.05	2.08	13	3.6	2.3	0.02	0.86	23	0.68	625	6	5.9
Wab2-10	5.59	21	20	149	0.24	40	2.91	0.43	8.4	8.3	61	56	3.5	3.4	77	2.10	2.25	14	3.5	2.3	0.10	0.83	23	0.70	621	6	6.1
Wab2-12	5.29	19	17	146	0.24	38	2.87	0.44	8.9	8.7	56	49	3.6	3.5	46	2.28	2.33	13	3.4	2.3	0.08	0.84	22	0.66	562	4	6.0
Wab2-14	5.59	15	15	152	0.22	37	2.79	0.44	9.1	8.6	55	50	3.9	3.9	36	2.41	2.45	14	3.8	2.4	0.09	0.96	24	0.68	578	6	5.9
Wab2-16	4.27	12	12	162	0.23	35	2.73	0.43	9.2	9.4	58	50	3.7	4.2	30	2.37	2.44	14	3.7	2.6	0.07	1.01	25	0.67	569	3	4.3
Wab2-18	5.90	12	10	137	0.19	38	2.62	0.35	9.8	8.5	59	52	3.9	3.7	28	2.56	2.61	13	3.8	2.4	0.06	0.95	24	0.69	563	4	3.9
Wab2-20	5.80	10	9	138	0.2	35	2.56	0.37	9.4	9.3	58	53	3.6	3.8	26	2.61	2.69	13	3.7	2.5	0.07	0.94	22	0.68	565	2	3.3
Wab2-23	5.03	10	9	131	0.21	37	2.46	0.37	10.0	10.2	60	53	4.2	4.0	27	2.66	2.73	14	3.8	2.7	0.06	1.00	25	0.68	571	*-3*	3.0
Wab2-26	5.12	10	9	136	0.22	32	2.28	0.42	9.5	10.3	58	54	3.7	4.1	28	2.51	2.70	14	4.1	2.7	0.07	0.94	25	0.67	589	3	2.9
Wab2-30	5.98	10	10	194	0.22	34	1.65	0.40	10.1	9.9	62	56	4.2	4.2	28	2.67	2.74	15	4.3	2.8	0.06	1.04	26	0.69	555	2	2.8
Wab2-35	4.97	9	10	115	0.23	32	1.43	0.44	10.4	10.6	61	56	4.5	4.4	29	2.76	2.81	16	4.2	2.8	0.06	1.07	27	0.68	541	2	3.0
Wab2-41	5.74	9	10	150	0.21	33	1.93	0.45	9.9	11.0	61	58	3.7	4.4	30	2.50	2.76	16	3.8	2.8	0.06	1.10	27	0.71	584	2	2.9
Wab2-47	5.81	8	9	154	0.21	36	1.92	0.41	9.9	9.6	57	54	3.9	4.2	27	2.46	2.63	14	3.9	2.6	0.05	1.04	24	0.65	530	1	2.5
Wab2-54	6.42	8	9	195	0.21	34	2.23	0.41	9.8	10.1	60	59	4.3	4.2	28	2.45	2.65	15	4.2	2.8	0.06	1.08	26	0.69	537	5	2.7
Min	4.27	8	9	115	0.19	32	1.43	0.35	6.3	7.8	55	49	3.1	3.3	26	1.81	1.83	12	3.2	2.1	0.02	0.83	21	0.65	530	*-3*	2.5
Median	5.28	15	14	151	0.23	37	2.78	0.41	9.0	8.8	61	54	3.7	3.7	41	2.33	2.39	13	3.7	2.3	0.06	0.92	23	0.68	587	4	4.4
Max	6.42	21	20	200	0.24	40	3.15	0.45	10.4	11.0	67	59	4.5	4.4	104	2.76	2.81	16	4.3	2.8	0.10	1.10	27	0.71	788	6	6.1
Mean	5.35	14	13	157	0.22	36	2.57	0.40	8.9	9.1	61	54	3.7	3.8	60	2.25	2.32	14	3.7	2.4	0.06	0.93	24	0.68	618	4	4.2

Table 3.2. Continued.

Sediment intervals (cm)	Na		Nb	Ni	P	Pb	Rb	S		Sb		Sc		Se	Sr	Th		Ti	U		V	W	Zn		Zr	TOC	S1
	L		*L*	*C, S*	*B, L, S*	*C*	*L*	*B, C*		*C*		*L*		*C*	*L*	*L*		*L*	*L*		*L*	*L, S*	*C*		*L*		
	NAA*	IMS	IMS	IMS	IMS	IMS	IMS	SA*	IMS	NAA*	IMS	NAA*	IMS	IMS	IMS	NAA*	IMS	IMS	NAA*	IMS	IMS	IMS	NAA	IMS*	IMS	REVL	REVL
	%	%	ppm	ppm	%	ppm	ppm	%	%	ppm	ppm	ppm	ppm	ppm	ppm	ppm	ppm	%	ppm	ppm	ppm	ppm	ppm	ppm	ppm	%	
Wab2-01	0.46	0.43	5.7	26	0.18	20	41	1.278	1.4	2.3	2.3	8.0	7.2	0.4	175	7.3	6.9	0.21	4.6	4.0	82	2.2	84	100	63	14.88	24.17
Wab2-02	0.42	0.43	5.7	28	0.17	20	42	1.254	1.3	2.6	2.3	8.2	7.4	*-0.2*	169	7.5	6.7	0.21	4.8	4.1	83	2.2	96	102	64	14.73	18.79
Wab2-03	0.44	0.42	5.9	26	0.17	21	40	1.241	1.3	2.8	2.4	8.2	7.3	0.3	166	7.8	7.1	0.22	4.9	4.5	86	2.2	104	104	64	14.67	20.62
Wab2-04	0.44	0.44	6.1	28	0.17	22	45	1.233	1.4	3.0	2.7	8.4	7.7	0.2	170	7.6	7.3	0.23	5.2	4.8	91	2.3	99	108	67	13.34	15.75
Wab2-05	0.44	0.44	6.2	27	0.16	23	44	1.22	1.3	2.8	2.6	8.5	7.8	0.7	168	7.7	7.1	0.23	5.0	4.8	90	2.3	105	109	69	14.38	19.44
Wab2-06	0.45	0.44	6.3	26	0.16	21	42	1.21	1.3	2.7	2.6	8.3	7.5	0.6	169	7.5	7.4	0.22	5.6	5.1	89	2.3	102	105	70	14.82	23.06
Wab2-07	0.45	0.45	6.1	27	0.16	21	42	1.272	1.4	2.9	2.7	8.3	7.7	0.3	162	7.3	7.3	0.22	5.7	5.4	88	2.3	104	108	67	13.88	17.63
Wab2-08	0.44	0.47	6.1	28	0.16	22	44	1.334	1.5	2.9	2.6	8.4	7.6	0.2	163	7.4	7.2	0.22	5.9	5.5	89	2.3	100	109	66	14.89	22.79
Wab2-09	0.47	0.48	6.1	28	0.15	21	45	1.335	1.5	2.8	2.6	8.5	7.8	0.4	163	7.6	7.4	0.23	6.4	6.0	89	2.5	97	107	69	15.15	22.81
Wab2-10	0.46	0.50	5.8	27	0.14	21	42	1.322	1.4	2.7	2.6	8.5	6.7	1.1	157	7.4	6.8	0.24	7.2	6.1	94	2.1	96	99	67	14.10	19.50
Wab2-12	0.49	0.48	6.0	27	0.12	17	44	1.434	1.5	1.9	1.8	8.7	7.0	0.2	156	7.7	6.9	0.24	6.1	5.4	80	1.6	83	93	68	13.51	17.84
Wab2-14	0.49	0.51	6.3	30	0.11	16	47	1.419	1.5	1.5	1.3	9.2	7.5	*-0.2*	157	8.0	7.5	0.25	5.2	4.9	80	1.4	93	94	72	12.66	13.95
Wab2-16	0.49	0.50	6.8	32	0.11	16	51	1.328	1.5	1.2	1.2	9.5	8.2	*-0.2*	162	8.0	8.3	0.26	5.0	4.9	78	1.2	84	94	77	13.24	15.56
Wab2-18	0.49	0.50	6.2	30	0.10	15	46	1.442	1.5	1.2	1.1	9.7	7.7	*-0.2*	140	8.4	7.3	0.26	5.0	4.4	79	1.2	89	86	70	12.38	15.02
Wab2-20	0.47	0.50	6.3	31	0.09	15	48	1.455	1.6	1.1	1.0	9.7	7.8	*-0.2*	135	8.6	7.5	0.27	4.8	4.4	82	1.1	89	85	71	12.42	14.64
Wab2-23	0.49	0.51	6.8	32	0.10	16	47	1.468	1.7	1.1	1.0	9.9	8.3	*-0.2*	144	8.4	8.3	0.27	5.2	4.9	81	1.1	75	89	77	12.50	13.39
Wab2-26	0.49	0.51	7.1	33	0.10	16	51	1.372	1.6	1.1	1.1	9.7	8.6	*-0.2*	138	8.4	8.3	0.28	5.0	5.1	83	1.0	86	90	81	12.36	13.12
Wab2-30	0.51	0.54	7.4	34	0.09	17	53	1.428	1.5	1.3	1.2	10.6	8.9	*-0.2*	131	9.3	8.5	0.29	5.3	5.0	87	1.1	84	94	85	10.92	10.50
Wab2-35	0.51	0.53	7.7	35	0.09	17	55	1.536	1.8	1.1	1.2	10.5	9.0	*-0.2*	128	9.3	8.8	0.28	4.9	5.0	85	1.2	88	96	88	11.68	11.65
Wab2-41	0.52	0.56	7.3	35	0.10	16	53	1.308	1.5	1.2	1.1	10.0	8.8	*-0.2*	134	9.0	8.5	0.29	5.4	5.3	89	1.1	82	98	85	11.51	11.46
Wab2-47	0.48	0.51	7.0	34	0.09	15	52	1.402	1.5	1.3	1.1	9.7	8.8	*-0.2*	125	8.4	8.2	0.27	4.9	4.6	83	1.0	87	94	79	11.75	11.46
Wab2-54	0.50	0.57	7.4	33	0.09	16	53	1.319	1.4	1.1	1.1	10.0	9.1	*-0.2*	143	8.7	8.3	0.29	5.0	5.0	89	1.0	94	97	82	11.41	11.74
Min	0.42	0.42	5.7	26	0.09	15	40	1.21	1.3	1.1	1.0	8.0	6.7	*-0.2*	125	7.3	6.7	0.21	4.6	4.0	78	1.0	75	85	63	10.92	10.50
Median	0.48	0.50	6.2	29	0.12	17	46	1.331	1.5	1.7	1.5	8.9	7.8	0.4	157	7.9	7.4	0.25	5.1	5.0	86	1.5	91	98	70	13.29	15.66
Max	0.52	0.57	7.7	35	0.18	23	55	1.536	1.8	3.0	2.7	10.6	9.1	1.1	175	9.3	8.8	0.29	7.2	6.1	94	2.5	105	109	88	15.15	24.17
Mean	0.47	0.49	6.5	30	0.13	18	47	1.346	1.5	1.9	1.8	9.1	7.9	0.4	153	8.1	7.6	0.25	5.3	5.0	85	1.7	92	98	73	13.24	16.59

Analytical methods: IMS: Inductively Coupled Plasma-Mass Spectrometry
NAA: Instrumental Neutron Activation Analysis
CVAA: Cold Vapor Atomic Absorption
SA: LECO® Sulphur Analyser CA: LECO® Carbon Analyser
REVL: Rock Eval 6 ® * : Preferred method

Elemental affinities: L: Lithophile
C: Chalcophile
A: Atmophile
B: Biophile
S: Siderophile

Table 3.3. The concentration of elements and organic matter (TOC and S1) in the sediments from ISLE core.

Sediment intervals (cm)	Al	As		Ba	Bi	Br	Ca	Cd	Co		Cr		Cs		Cu	Fe		Ga	Hf		Hg	K	Li	Mg	Mn	Mo	
	L	*C*		*L*	*C*	*A, L*	*L*	*C*	*C, S*		*L*		*L*		*C*	*C, S*		*C*	*L*		*C*	*L*	*L*	*L*	*L*	*C, S*	
	IMS	NAA*	IMS	IMS	IMS	NAA	IMS	IMS	NAA*	IMS	NAA*	IMS	NAA*	IMS	IMS	NAA	IMS*	IMS	NAA*	IMS	CVAA	IMS	IMS	IMS	IMS	NAA	IMS*
	%	ppm	ppm	ppm	ppm	ppm	%	ppm	ppm	ppm	ppm	ppm	ppm	ppm	ppm	%	%	ppm	ppm	ppm	ppm	%	ppm	%	ppm	ppm	ppm
ISLE-01	3.61	8	8	248	0.16	76	2.32	0.39	4.9	8.7	37	38	2.4	2.4	21	2.43	2.77	8	3.3	1.6	0.06	0.86	21	0.59	1881	*-4*	1.0
ISLE-02	3.63	7	6	302	0.15	78	2.37	0.39	8.6	8.1	40	34	2.2	2.3	21	2.65	2.66	8	3.2	1.6	0.07	0.86	20	0.58	1097	2	0.9
ISLE-03	3.06	7	6	197	0.16	82	2.05	0.35	8.4	7.9	41	35	2.4	2.3	21	2.56	2.63	8	3.0	1.6	0.06	0.89	19	0.59	985	*-3*	0.9
ISLE-04	3.64	6	6	229	0.16	80	1.91	0.40	8.5	8.7	39	36	2.2	2.3	22	2.64	2.57	8	3.4	1.6	0.07	0.89	20	0.58	974	2	0.9
ISLE-05	3.83	6	6	201	0.16	82	1.85	0.39	8.7	9.2	41	38	2.2	2.4	23	2.53	2.60	8	3.1	1.8	0.07	0.91	21	0.61	1017	*-3*	0.9
ISLE-06	3.71	7	6	262	0.16	77	1.70	0.40	8.5	8.9	40	39	2.1	2.4	22	2.50	2.60	8	3.3	1.6	0.08	0.87	21	0.59	1092	3	0.9
ISLE-07	3.81	7	7	167	0.17	80	1.66	0.44	8.8	9.1	43	38	2.3	2.5	23	2.47	2.60	9	3.3	1.7	0.08	0.90	22	0.61	1085	3	1.0
ISLE-08	3.76	7	7	153	0.17	80	1.63	0.38	8.8	9.0	41	39	2.6	2.5	24	2.46	2.58	8	3.2	1.6	0.07	0.87	21	0.59	1104	*-3*	1.0
ISLE-09	3.69	7	6	199	0.15	81	1.56	0.41	8.8	8.5	44	36	1.8	2.3	21	2.47	2.41	8	3.3	1.6	0.07	0.88	19	0.58	978	*-3*	0.9
ISLE-10	3.91	8	7	108	0.16	80	1.64	0.41	8.5	9.1	42	40	2.6	2.6	24	2.42	2.52	8	3.6	1.8	0.07	0.90	21	0.61	1013	2	1.0
ISLE-12	3.86	8	7	117	0.17	80	1.54	0.39	8.8	8.8	44	40	2.2	2.5	22	2.41	2.38	8	3.4	1.7	0.06	0.93	21	0.60	905	2	1.1
ISLE-14	3.65	14	12	60	0.16	74	1.45	0.45	9.0	8.6	43	39	2.5	2.4	23	2.46	2.45	8	3.4	1.8	0.07	0.93	19	0.59	789	1	1.4
ISLE-16	4.07	16	15	66	0.18	76	1.48	0.46	8.9	10.1	46	42	2.7	2.7	26	2.47	2.64	9	3.5	1.9	0.05	0.97	22	0.63	752	*-3*	1.7
ISLE-18	3.94	15	14	53	0.18	78	1.44	0.46	10.0	10.7	45	43	2.5	2.7	27	2.47	2.64	9	3.4	1.8	0.06	0.97	23	0.64	677	*-3*	1.7
ISLE-21	4.37	15	13	93	0.18	82	1.46	0.41	10.9	11.8	46	45	2.8	2.9	29	2.56	2.66	10	3.6	2.0	0.05	0.96	23	0.65	599	1	1.9
ISLE-24	4.40	14	13	85	0.18	81	1.45	0.45	11.0	11.4	44	45	3.4	3.1	31	2.54	2.66	10	3.7	2.1	0.04	0.98	25	0.65	525	*-3*	1.9
ISLE-27	4.31	14	13	65	0.18	87	1.46	0.40	11.2	11.9	48	45	3.1	3.0	31	2.57	2.67	10	3.5	2.1	0.04	0.96	24	0.64	497	2	2.0
ISLE-30	4.14	15	13	55	0.16	83	1.39	0.37	10.5	10.9	46	41	2.9	2.8	28	2.39	2.50	9	3.5	2.0	0.05	0.94	24	0.61	439	1	1.8
ISLE-33	4.33	15	14	59	0.17	87	1.45	0.44	11.2	11.4	48	44	3.0	3.0	31	2.48	2.66	10	3.4	2.2	0.05	1.00	24	0.64	454	2	2.1
ISLE-36	4.28	15	14	69	0.17	88	1.47	0.47	10.7	11.6	45	44	2.4	2.9	30	2.37	2.54	9	3.4	2.0	0.05	0.97	24	0.63	448	2	2.1
ISLE-40	4.04	17	15	70	0.16	87	1.41	0.48	10.7	10.4	44	41	2.2	2.6	27	2.66	2.63	9	3.8	2.0	0.05	0.85	22	0.58	412	2	2.1
ISLE-44	4.01	15	12	71	0.16	90	1.39	0.52	12.0	11.5	49	42	2.8	2.8	33	2.75	2.64	9	3.7	2.1	0.06	0.86	24	0.57	422	2	2.1
ISLE-48	3.85	16	13	73	0.16	96	1.37	0.46	11.3	11.1	44	40	3.1	2.5	31	2.56	2.44	8	3.3	2.0	0.05	0.81	21	0.55	414	*-3*	2.1
Min	3.06	6	6	53	0.15	74	1.37	0.35	4.9	7.9	37	34	1.8	2.3	21	2.37	2.38	8	3.0	1.6	0.04	0.81	19	0.55	412	*-4*	0.9
Median	3.86	14	12	93	0.16	81	1.48	0.41	8.9	9.2	44	40	2.5	2.5	24	2.48	2.60	8	3.4	1.8	0.06	0.90	21	0.60	789	2	1.4
Max	4.40	17	15	302	0.18	96	2.37	0.52	12.0	11.9	49	45	3.4	3.1	33	2.75	2.77	10	3.8	2.2	0.08	1.00	25	0.65	1881	3	2.1
Mean	3.91	11	10	131	0.17	82	1.63	0.42	9.5	9.9	43	40	2.5	2.6	26	2.51	2.58	9	3.4	1.8	0.06	0.91	22	0.60	807	2	1.4

Table 3.3. Continued.

Sediment intervals (cm)	Na		Nb	Ni	P	Pb	Rb	S		Sb		Sc		Se	Sr	Th		Ti	U		V	W	Zn		Zr	TOC	S1
	L		*L*	*C, S*	*B, L, S*	*C*	*L*	*B, C*		*C*		*L*		*C*	*L*	*L*		*L*	*L*		*L*	*L, S*	*C*		*L*		
	NAA*	IMS	IMS	IMS	IMS	IMS	IMS	SA*	IMS	NAA*	IMS	NAA*	IMS	IMS	IMS	NAA*	IMS	IMS	NAA*	IMS	IMS	IMS	NAA	IMS*	IMS	REVL	REVL
	%	%	ppm	ppm	%	ppm	ppm	%	%	ppm	ppm	ppm	ppm	ppm	ppm	ppm	ppm	%	ppm	ppm	ppm	ppm	ppm	ppm	ppm	%	
ISLE-01	0.43	0.38	4.1	30	0.26	17	40	0.883	0.8	0.5	0.5	5.8	5.6	*-0.2*	143	4.9	5.4	0.16	2.3	2.2	60	0.5	57	78	50	20.77	22.51
ISLE-02	0.35	0.43	4.0	29	0.20	16	40	0.861	0.8	0.5	0.5	6.3	5.3	*-0.2*	140	4.9	5.1	0.16	2.8	2.4	59	0.5	89	76	52	20.35	23.34
ISLE-03	0.35	0.40	4.0	30	0.20	17	39	0.851	0.8	0.7	0.5	6.3	5.6	*-0.2*	128	5.1	4.9	0.16	2.5	2.5	62	0.6	75	78	51	19.72	22.50
ISLE-04	0.36	0.39	4.0	30	0.21	17	41	0.807	0.8	0.5	0.5	6.5	5.5	*-0.2*	126	5.5	5.0	0.17	2.7	2.6	63	0.5	75	78	51	19.96	21.97
ISLE-05	0.36	0.43	4.2	33	0.21	18	42	0.775	0.8	0.5	0.5	6.5	5.8	*-0.2*	129	5.3	5.4	0.17	2.9	2.8	65	0.5	71	83	56	20.39	23.36
ISLE-06	0.37	0.41	4.1	32	0.21	17	41	0.749	0.8	0.5	0.6	6.3	5.6	*-0.2*	124	5.3	5.2	0.17	2.7	2.7	64	0.6	66	78	52	20.58	23.03
ISLE-07	0.37	0.41	4.2	33	0.20	18	43	0.727	0.8	0.6	0.6	6.4	5.9	*-0.2*	120	5.2	5.3	0.17	2.5	2.7	67	0.6	69	82	53	19.32	23.13
ISLE-08	0.36	0.38	4.3	32	0.20	18	42	0.769	0.8	0.6	0.6	6.5	5.8	*-0.2*	118	5.3	5.3	0.17	2.8	2.7	66	0.6	74	82	54	18.94	20.88
ISLE-09	0.36	0.42	4.0	30	0.18	17	39	0.759	0.8	0.7	0.5	6.7	5.5	*-0.2*	116	5.4	4.9	0.17	2.8	2.5	63	0.6	74	79	51	19.83	23.38
ISLE-10	0.39	0.43	4.2	33	0.20	18	42	0.819	0.8	0.7	0.6	6.6	5.9	*-0.2*	122	5.4	5.2	0.18	3.3	2.8	66	0.6	73	84	56	20.10	23.82
ISLE-12	0.39	0.45	4.3	31	0.18	17	43	0.847	0.9	0.7	0.6	6.7	5.8	*-0.2*	121	5.7	5.4	0.17	3.4	3.0	65	0.6	92	84	54	20.57	24.40
ISLE-14	0.42	0.49	4.2	32	0.14	15	43	1.274	1.2	0.7	0.6	6.6	5.7	*-0.2*	120	5.4	5.2	0.18	3.9	3.5	65	0.5	75	83	55	19.17	18.96
ISLE-16	0.43	0.45	4.6	37	0.15	14	44	1.344	1.5	0.7	0.6	6.8	6.4	*-0.2*	118	5.8	5.7	0.19	3.5	3.7	71	0.6	92	90	61	18.81	18.31
ISLE-18	0.40	0.42	4.7	37	0.14	12	46	1.334	1.4	0.7	0.6	7.2	6.6	*-0.2*	118	6.0	5.9	0.19	3.8	4.1	75	0.6	80	96	60	19.79	18.05
ISLE-21	0.38	0.41	4.9	41	0.14	12	48	1.319	1.4	0.8	0.6	7.6	7.0	*-0.2*	112	6.3	6.1	0.20	4.7	4.9	81	0.6	90	99	64	19.37	17.60
ISLE-24	0.38	0.39	5.1	42	0.14	12	49	1.323	1.4	0.7	0.7	7.8	7.5	*-0.2*	115	6.1	6.3	0.20	4.7	4.9	83	0.7	92	97	66	21.15	17.36
ISLE-27	0.37	0.39	5.0	45	0.14	12	49	1.368	1.5	0.7	0.7	8.0	7.2	*-0.2*	115	6.4	6.3	0.20	5.3	5.0	82	0.6	83	98	64	22.92	18.74
ISLE-30	0.38	0.42	4.8	40	0.13	11	46	1.388	1.4	0.7	0.6	7.4	6.7	*-0.2*	114	6.2	5.7	0.19	4.8	4.5	76	0.6	71	87	64	21.60	17.88
ISLE-33	0.38	0.41	4.9	45	0.13	11	48	1.421	1.6	0.7	0.6	7.7	7.2	*-0.2*	111	6.6	6.2	0.20	5.1	4.8	81	0.7	86	94	65	20.58	18.47
ISLE-36	0.35	0.42	4.8	42	0.13	11	47	1.358	1.5	0.6	0.6	7.3	6.8	*-0.2*	111	6.0	5.9	0.19	5.1	4.7	79	0.6	76	96	63	20.20	16.12
ISLE-40	0.38	0.42	4.5	40	0.13	9	45	1.804	1.8	0.7	0.5	7.3	6.7	*-0.2*	112	6.4	6.1	0.18	4.8	4.7	71	0.5	82	95	60	19.60	15.87
ISLE-44	0.35	0.38	4.5	42	0.12	10	45	1.716	1.9	0.8	0.6	8.1	6.9	0.5	108	6.7	6.6	0.18	5.8	5.4	77	0.6	90	97	64	21.47	18.09
ISLE-48	0.34	0.37	4.0	44	0.12	9	40	1.793	1.8	0.7	0.5	7.5	6.6	0.3	100	6.2	5.8	0.17	5.7	5.0	71	0.5	94	92	58	20.94	17.77
Min	0.34	0.37	4.0	29	0.12	9	39	0.727	0.8	0.5	0.5	5.8	5.3	*-0.2*	100	4.9	4.9	0.16	2.3	2.2	59	0.5	57	76	50	18.81	15.87
Median	0.37	0.41	4.3	33	0.15	15	43	1.274	1.2	0.7	0.6	6.7	5.9	0.4	118	5.7	5.4	0.18	3.5	3.5	67	0.6	76	84	56	20.20	18.96
Max	0.43	0.49	5.1	45	0.26	18	49	1.804	1.9	0.8	0.7	8.1	7.5	0.5	143	6.7	6.6	0.20	5.8	5.4	83	0.7	94	99	66	22.92	24.40
Mean	0.38	0.41	4.4	36	0.17	14	43	1.143	1.2	0.6	0.6	6.9	6.2	0.4	119	5.7	5.6	0.18	3.8	3.7	70	0.6	79	87	57	20.27	20.24

Analytical methods: IMS: Inductively Coupled Plasma-Mass Spectrometry
NAA: Instrumental Neutron Activation Analysis
CVAA: Cold Vapor Atomic Absorption
SA: LECO® Sulphur Analyser CA: LECO® Carbon Analyser
REVL: Rock Eval 6 ® * : Preferred method

Elemental affinities: L: Lithophile
C: Chalcophile
A: Atmophile
B: Biophile
S: Siderophile

Table 3.4. The concentration of elements and organic matter (TOC and S1) in the sediments from LSA core.

Sediment intervals (cm)	Al	As		Ba	Bi	Br	Ca	Cd	Co		Cr		Cs		Cu	Fe		Ga	Hf		Hg	K	Li	Mg	Mn	Mo	
	L	*C*		*L*	*C*	*A, L*	*L*	*C*	*C, S*		*L*		*L*		*C*	*C, S*		*C*	*L*		*C*	*L*	*L*	*L*	*L*	*C, S*	
	IMS	NAA*	IMS	IMS	IMS	NAA	IMS	IMS	NAA*	IMS	NAA*	IMS	NAA*	IMS	IMS	NAA	IMS*	IMS	NAA*	IMS	CVAA	IMS	IMS	IMS	IMS	NAA	IMS*
	%	ppm	ppm	ppm	ppm	ppm	%	ppm	ppm	ppm	ppm	ppm	ppm	ppm	ppm	%	%	ppm	ppm	ppm	ppm	%	ppm	%	ppm	ppm	ppm
LSA-01	4.01	6	-	-	-	62	7.49	-	6.3	-	43	-	2.4	-	48	2.01	-	*-8*	3.8	-	-	1.06	-	0.73	1340	*-4*	-
LSA-02	3.44	5	5	462	0.12	59	5.92	0.31	6.3	5.2	41	34	2.3	2.4	14	1.95	1.94	8	3.1	1.7	0.05	0.86	21	0.58	973	*-3*	0.8
LSA-03	3.44	4	5	459	0.12	60	5.69	0.30	6.6	5.8	39	35	2.8	2.4	14	1.94	1.88	7	3.5	1.7	0.04	0.86	21	0.58	895	*-3*	0.9
LSA-04	3.47	4	5	453	0.12	62	5.63	0.27	6.6	5.4	41	34	2.4	2.5	14	1.95	1.88	7	3.1	1.7	0.04	0.86	22	0.59	840	*-3*	0.8
LSA-05	3.65	4	5	475	0.12	66	5.49	0.30	6.8	5.0	41	37	2.5	2.6	14	1.95	1.94	8	3.6	1.8	0.05	0.90	21	0.62	774	*-3*	1.0
LSA-06	3.54	5	5	443	0.13	62	5.19	0.33	6.9	5.6	40	35	2.2	2.5	14	1.80	1.80	8	3.7	1.7	0.04	0.85	21	0.58	692	*-3*	1.1
LSA-07	3.61	5	5	451	0.13	65	5.12	0.34	7.2	5.3	42	35	2.5	2.5	15	1.83	1.80	8	3.7	1.9	0.05	0.90	21	0.60	643	*-3*	1.2
LSA-08	3.71	4	5	458	0.13	63	4.96	0.37	7.2	5.6	43	35	2.5	2.6	15	1.77	1.81	8	3.7	1.9	0.06	0.92	22	0.61	613	*-3*	1.3
LSA-09	3.84	5	6	470	0.14	65	5.09	0.38	7.1	5.4	45	38	2.6	2.8	16	1.87	1.90	9	3.6	2.0	0.05	0.96	23	0.63	633	2	1.5
LSA-10	3.91	5	6	468	0.14	62	4.97	0.35	6.8	6.3	43	39	2.7	2.7	15	1.75	1.87	8	3.5	1.9	0.05	0.95	22	0.64	611	*-3*	1.5
LSA-12	3.95	7	7	424	0.15	64	5.02	0.36	7.0	6.1	44	38	3.1	2.8	16	2.02	2.09	9	3.8	1.9	0.04	0.98	23	0.64	560	2	1.8
LSA-14	3.88	8	8	367	0.15	62	4.95	0.39	7.5	6.2	45	38	2.8	2.7	14	2.15	2.15	9	4.1	1.9	0.04	0.94	23	0.62	569	2	2.3
LSA-16	4.04	8	8	328	0.16	65	5.01	0.36	7.2	6.5	44	39	2.7	2.7	15	2.09	2.19	9	3.9	1.9	0.05	1.01	24	0.64	590	*-3*	2.1
LSA-18	4.05	7	7	396	0.15	62	4.88	0.38	7.4	7.4	42	40	2.6	2.8	15	1.97	2.03	9	3.9	2.0	0.04	1.01	24	0.64	599	*-3*	1.8
LSA-20	4.05	6	8	463	0.16	64	4.88	0.38	7.7	6.9	46	39	2.6	2.7	14	1.88	1.96	9	4.4	2.1	0.05	1.00	24	0.64	612	2	1.5
LSA-23	3.95	7	7	469	0.15	59	4.79	0.34	7.6	6.4	43	39	2.8	2.7	13	1.77	1.80	8	4.3	2.1	0.05	1.00	22	0.62	586	2	1.5
LSA-26	3.98	10	10	444	0.14	59	4.47	0.31	7.3	6.6	45	39	2.8	2.7	14	1.87	1.88	9	4.3	2.1	0.04	1.01	23	0.63	563	3	1.6
LSA-29	3.89	12	12	240	0.13	55	4.46	0.34	7.1	6.2	43	38	2.6	2.8	14	2.05	2.08	9	4.4	2.1	0.03	0.99	24	0.61	558	*-3*	1.6
LSA-32	3.88	11	9	230	0.12	53	4.95	0.30	7.3	6.3	45	37	2.5	2.8	15	2.12	2.16	9	4.2	2.0	0.04	1.00	24	0.61	580	*-3*	1.9
LSA-36	4.02	8	7	343	0.12	53	5.44	0.28	7.3	7.4	43	39	2.7	2.7	15	1.90	2.00	9	4.1	2.0	0.02	1.02	23	0.63	586	2	2.5
LSA-40	3.93	5	5	450	0.11	52	4.85	0.30	7.2	6.4	44	39	2.3	2.6	13	1.65	1.68	9	4.7	2.0	0.02	1.01	23	0.62	530	*-3*	1.6
LSA-45	4.06	5	6	465	0.12	50	4.85	0.31	7.4	6.0	44	40	2.6	2.7	14	1.63	1.71	9	4.7	2.1	0.02	1.03	23	0.63	537	*-3*	1.6
LSA-50	4.01	8	8	207	0.12	48	4.10	0.31	7.3	6.1	46	38	2.6	2.7	13	2.15	2.10	9	5.3	2.1	0.02	1.07	23	0.61	511	2	2.0
LSA-56	4.17	9	8	180	0.13	57	2.42	0.34	8.2	7.8	48	42	2.7	3.0	14	2.06	2.03	10	5.0	2.3	0.03	1.10	25	0.62	489	2	2.0
LSA-65	4.07	9	8	193	0.13	56	5.26	0.30	7.5	6.3	48	41	2.6	2.8	15	2.21	2.15	9	4.5	2.1	*-0.01*	1.04	25	0.62	522	*-3*	2.1
Min	3.44	4	0	0	0	48	2.42	0.00	6.3	0.0	39	0	2.2	0.0	13	1.63	0.00	*-8*	3.1	0.0	*-0.01*	0.85	0	0.58	489	*-4*	0.0
Median	3.93	6	7	447	0.13	62	4.97	0.34	7.2	6.2	43	38	2.6	2.7	14	1.95	1.94	9	3.9	2.0	0.04	1.00	23	0.62	590	2	1.6
Max	4.17	12	12	475	0.16	66	7.49	0.39	8.2	7.8	48	42	3.1	3.0	48	2.21	2.19	10	5.3	2.3	0.06	1.10	25	0.73	1340	3	2.5
Mean	3.86	7	7	389	0.13	59	5.04	0.33	7.2	6.2	43	38	2.6	2.7	16	1.93	1.95	8	4.0	2.0	0.04	0.97	23	0.62	656	2	1.6

Table 3.4. Continued.

Sediment intervals (cm)	Na		Nb	Ni	P	Pb	Rb	S		Sb		Sc		Se	Sr	Th		Ti	U		V	W	Zn		Zr	TOC	S1
	L		*L*	*C, S*	*B, L, S*	*C*	*L*	*B, C*		*C*		*L*		*C*	*L*	*L*		*L*	*L*		*L*	*L, S*	*C*		*L*		
	NAA*	IMS	IMS	IMS	IMS	IMS	IMS	SA*	IMS	NAA*	IMS	NAA*	IMS	IMS	IMS	NAA*	IMS	IMS	NAA*	IMS	IMS	IMS	NAA	IMS*	IMS	REVL	REVL
	%	%	ppm	ppm	%	ppm	ppm	%	%	ppm	ppm	ppm	ppm	ppm	ppm	ppm	ppm	%	ppm	ppm	ppm	ppm	ppm	ppm	ppm	%	
LSA-01	0.36	-	-	-	-	-	-	-	-	0.4	-	6.1	-	-	-	5.3	-	0.21	2.0	-	79	-	51	-	-	-	-
LSA-02	0.34	0.34	4.0	16	0.20	16	44	0.584	0.6	0.6	0.4	6.0	5.4	*-0.2*	190	5.4	5.2	0.17	2.2	2.2	60	0.5	68	67	47	15.52	23.81
LSA-03	0.33	0.36	4.1	18	0.20	16	44	0.615	0.7	0.6	0.4	6.1	5.2	*-0.2*	193	5.1	5.4	0.17	2.4	2.4	59	0.6	64	67	49	15.41	24.28
LSA-04	0.34	0.35	4.1	16	0.20	17	44	0.659	0.7	0.5	0.5	6.1	5.3	*-0.2*	189	4.9	5.3	0.16	2.8	2.4	60	0.5	64	66	49	15.32	21.14
LSA-05	0.36	0.38	4.3	18	0.20	18	45	0.702	0.7	0.5	0.5	6.2	5.6	*-0.2*	182	5.3	5.4	0.18	3.2	2.7	64	0.6	64	67	53	15.45	22.10
LSA-06	0.37	0.35	4.2	18	0.19	18	44	0.712	0.7	0.5	0.5	6.1	5.7	*-0.2*	181	5.4	5.5	0.17	3.0	2.8	61	0.7	62	69	51	15.63	22.53
LSA-07	0.35	0.37	4.4	18	0.19	18	46	0.768	0.8	0.7	0.5	6.3	5.5	*-0.2*	180	5.3	5.6	0.18	3.5	2.9	64	0.5	65	72	54	16.59	26.24
LSA-08	0.37	0.38	4.5	18	0.18	18	47	0.81	0.8	0.7	0.5	6.3	5.8	*-0.2*	181	5.4	5.6	0.18	3.2	3.0	65	0.5	66	74	55	15.46	23.92
LSA-09	0.37	0.39	4.6	20	0.19	19	49	0.841	0.9	0.7	0.6	6.5	6.0	*-0.2*	183	5.5	5.9	0.19	3.6	3.5	69	0.6	72	75	56	16.33	25.26
LSA-10	0.35	0.41	4.5	19	0.17	18	48	0.821	0.8	0.6	0.6	6.3	6.1	*-0.2*	176	5.1	5.7	0.19	3.6	3.3	69	0.5	76	75	56	15.52	23.10
LSA-12	0.40	0.40	4.7	20	0.16	18	50	0.97	1.0	0.7	0.7	6.5	6.0	*-0.2*	181	5.7	6.1	0.19	4.8	4.2	71	0.6	70	78	56	15.17	22.09
LSA-14	0.38	0.40	4.7	19	0.15	16	47	1.078	1.1	0.8	0.6	6.6	5.8	*-0.2*	176	5.7	5.8	0.19	3.8	3.5	69	0.7	70	76	55	14.70	19.50
LSA-16	0.39	0.43	4.9	20	0.15	20	50	1.074	1.2	0.6	0.6	6.6	6.2	*-0.2*	181	5.9	6.0	0.20	3.9	3.5	72	0.7	76	80	61	14.00	16.66
LSA-18	0.40	0.41	5.0	19	0.15	14	51	0.934	1.0	0.7	0.6	6.7	6.1	*-0.2*	178	5.6	6.2	0.20	3.3	3.2	72	0.6	70	78	61	13.46	16.03
LSA-20	0.41	0.43	4.9	20	0.15	13	50	0.815	0.9	0.6	0.5	6.8	6.1	*-0.2*	180	6.1	6.3	0.20	3.2	3.1	73	0.6	72	79	61	14.55	17.60
LSA-23	0.42	0.46	4.8	19	0.15	12	47	0.776	0.8	0.6	0.5	6.6	5.8	*-0.2*	178	5.6	6.2	0.20	3.0	3.0	69	0.5	69	75	60	13.70	15.83
LSA-26	0.41	0.47	4.8	19	0.14	11	49	0.912	1.0	0.6	0.5	6.6	6.0	*-0.2*	179	5.8	6.3	0.20	3.3	3.2	69	0.6	69	76	62	13.36	16.15
LSA-29	0.43	0.43	4.8	20	0.15	9	49	1.142	1.3	0.4	0.5	6.3	5.8	*-0.2*	173	5.6	5.7	0.19	3.3	3.1	69	0.6	68	76	62	13.59	16.98
LSA-32	0.41	0.40	4.8	20	0.15	10	47	1.285	1.4	0.5	0.6	6.4	5.9	*-0.2*	173	5.5	6.2	0.19	3.3	3.3	71	0.6	63	73	62	13.32	15.96
LSA-36	0.40	0.44	5.2	20	0.14	9	50	1.07	1.2	0.6	0.5	6.4	6.1	*-0.2*	188	5.5	5.9	0.20	3.8	3.3	72	0.7	72	70	64	13.56	17.33
LSA-40	0.43	0.47	4.9	19	0.13	9	48	0.824	0.9	0.5	0.4	6.3	5.9	*-0.2*	181	5.4	6.0	0.20	3.7	3.4	68	0.6	62	66	65	13.20	15.82
LSA-45	0.43	0.48	4.9	20	0.14	10	49	0.806	0.9	0.4	0.5	6.4	5.9	*-0.2*	179	5.7	6.1	0.20	3.4	3.2	71	0.6	66	72	64	12.32	14.12
LSA-50	0.46	0.49	5.0	19	0.13	9	49	1.372	1.4	0.6	0.5	6.6	5.9	*-0.2*	168	6.1	6.2	0.20	3.5	3.2	70	0.6	72	72	64	11.38	13.06
LSA-56	0.47	0.49	5.6	23	0.14	9	53	1.223	1.3	0.6	0.5	7.1	6.3	*-0.2*	129	6.0	6.3	0.21	3.7	3.6	73	0.7	70	79	67	13.68	15.06
LSA-65	0.41	0.46	5.2	21	0.13	9	51	1.369	1.5	0.5	0.5	6.8	5.9	*-0.2*	187	5.8	6.3	0.21	4.5	4.3	73	0.6	65	74	63	11.94	14.07
Min	0.33	0.34	4.0	16	0.13	9	44	0.584	0.6	0.4	0.4	6.0	5.2	*-0.2*	129	4.9	5.2	0.16	2.2	2.2	59	0.5	62	66	47	11.38	13.06
Median	0.40	0.41	4.8	19	0.15	15	48	0.833	0.9	0.6	0.5	6.4	5.9	*-0.2*	181	5.5	6.0	0.19	3.3	3.2	69	0.6	68	74	60	14.28	17.47
Max	0.47	0.49	5.6	23	0.20	20	53	1.372	1.5	0.8	0.7	7.1	6.3	0.0	193	6.1	6.3	0.21	4.8	4.3	79	0.7	76	80	67	16.59	26.24
Mean	0.39	0.42	4.7	19	0.16	14	48	0.923	1.0	0.6	0.5	6.4	5.8	*-0.2*	179	5.5	5.9	0.19	3.4	3.2	68	0.6	67	73	58	14.30	19.11

Analytical methods: IMS: Inductively Coupled Plasma-Mass Spectrometry
NAA: Instrumental Neutron Activation Analysis
CVAA: Cold Vapor Atomic Absorption
SA: LECO® Sulphur Analyser CA: LECO® Carbon Analyser
REVL: Rock Eval 6 ® * : Preferred method

Elemental affinities: L: Lithophile
C: Chalcophile
A: Atmophile
B: Biophile
S: Siderophile

Table 3.5. The total dissolved concentration of elements throughout the porewater profile from WAB1 core.

Sediment intervals (cm)	Al	As	Ba	Br	Ca	Cd	Co	Cr	Cs	Cu	Fe	Hg	K	Li	Mg	Mn	Mo	Na	Ni	P	Pb	Rb	S	Sb	Sc	Se	Sr	Th	Ti	U	V	W	Zn	Zr
	ppb	ppb	ppb	ppb	ppm	ppb	ppb	ppb	ppb	ppb	ppb	ppt	ppb	ppb	ppb	ppb	ppb	ppb	ppb	ppb	ppb	ppb	ppm	ppb	ppb	ppb	ppb	ppb	ppb	ppb	ppb	ppb	ppb	ppb
Wab1-01	3	5.2	135	23	< 50	< .05	0.03	1	< .01	0.8	13	< 2	11013	43	19520	199	18.7	76479	< .2	< 20	< .1	5.38	15	0.16	3.26	< .5	301	< .05	< 10	1.3	0.3	0.27	0.5	0.03
Wab1-02	2	4.7	134	21	< 50	< .05	0.04	2.8	< .01	0.7	32	< 5	10917	36.5	19057	240	3	76568	< .2	27	< .1	6.02	9	0.17	3.76	< .5	305	< .05	< 10	0.42	0.6	0.28	< .5	0.03
Wab1-03	4	3.9	140	22	< 50	< .05	0.04	2.4	< .01	0.7	22	< 2	10957	39.1	19519	250	8.9	75730	< .2	34	< .1	6.56	13	0.17	3.75	< .5	329	< .05	< 10	0.53	0.4	0.33	< .5	0.03
Wab1-04	8	3.2	172	22	< 50	< .05	0.05	< .5	< .01	6.3	64	< 8	10976	41	20889	284	20.5	73198	1.2	38	< .1	6.31	16	0.22	3.78	< .5	337	< .05	< 10	0.49	0.6	0.37	1	0.02
Wab1-05	6	3	142	21	< 50	< .05	0.05	2.3	< .01	0.7	24	< 2	10744	36.1	17871	296	7.7	72927	< .2	57	< .1	6.24	9	0.13	3.72	< .5	313	< .05	< 10	0.47	0.3	0.34	< .5	0.04
Wab1-06	6	3	143	22	< 50	< .05	0.07	1.8	< .01	0.7	< 10	< 2	11448	38	19066	334	16.7	73661	< .2	120	< .1	6.46	11	0.19	4.17	< .5	327	< .05	< 10	0.53	0.6	0.37	< .5	0.05
Wab1-07	9	3.2	143	24	< 50	< .05	0.07	1.5	0.01	0.8	45	< 2	11408	37.2	19008	242	21.9	71822	< .2	174	3.4	6.81	11	0.17	4.35	< .5	341	< .05	< 10	0.59	0.7	0.35	0.5	0.06
Wab1-08	11	2.8	150	25	< 50	< .05	0.09	1.8	0.01	0.8	16	24	11006	39.4	17666	248	12.4	71212	< .2	380	< .1	6.18	5	0.07	4.73	< .5	313	< .05	< 10	0.34	0.4	0.33	0.7	0.06
Wab1-09	14	2.9	158	24	< 50	< .05	0.11	2.1	< .01	1.5	< 10	16	11282	37	18678	264	10.6	73663	< .2	387	0.1	6.32	4	0.08	5.30	< .5	330	< .05	< 10	0.41	0.5	0.28	0.6	0.07
Wab1-10	15	2.4	176	25	< 50	< .05	0.21	2.9	0.01	0.9	< 10	10	10943	36.5	18932	289	2.2	73208	< .2	884	< .1	6.30	< 1	< .05	6.25	< .5	333	< .05	< 10	0.08	0.6	0.25	< .5	0.08
Wab1-12	15	3.2	165	29	< 50	< .05	0.18	1.5	0.01	0.9	< 10	10	11117	38.3	20032	294	10.4	72847	< .2	886	< .1	6.70	3	0.15	6.70	< .5	347	< .05	< 10	0.44	0.8	0.21	< .5	0.08
Wab1-14	14	2.3	183	30	< 50	< .05	0.22	2.9	0.01	0.9	15	< 2	11490	38.9	20422	341	3.2	71970	< .2	1092	< .1	6.69	2	< .05	7.31	< .5	354	< .05	< 10	0.1	0.4	0.1	< .5	0.07
Wab1-16	13	2.5	188	31	< 50	< .05	0.25	2.5	0.01	0.8	11	11	11728	38.5	20170	339	5.1	75446	< .2	1306	0.1	6.87	3	0.11	8.40	< .5	369	< .05	< 10	0.2	0.4	< .02	< .5	0.08
Wab1-18	13	1.7	191	30	< 50	< .05	0.24	2.4	0.01	0.8	21	10	11665	39.6	20004	347	2	73064	< .2	1598	0.1	6.63	1	< .05	8.79	< .5	378	< .05	< 10	0.1	0.4	0.02	0.7	0.08
Wab1-20	11	1.8	185	32	< 50	< .05	0.26	3.5	0.01	0.8	10	< 5	12208	39.9	19641	368	1.7	70948	< .2	1829	0.1	6.59	1	0.07	9.44	< .5	367	< .05	< 10	0.09	0.4	< .02	< .5	0.09
Wab1-23	11	3.3	191	36	51	< .05	0.18	1	0.01	1.1	< 10	< 6	11779	42.4	19519	251	1.8	74043	< .2	2015	0.1	6.39	3	0.28	10.5	< .5	369	< .05	< 10	0.25	0.8	< .02	0.8	0.1
Wab1-26	8	3.9	200	35	54	< .05	0.21	2.7	0.01	0.9	< 10	10	11805	44.2	19690	236	1.6	74333	< .2	2365	1.2	6.51	2	0.35	11.0	< .5	360	< .05	< 10	0.28	0.7	< .02	0.9	0.11
Wab1-30	12	2.9	208	40	56	< .05	0.22	2.4	0.01	1	10	< 5	11919	43.4	20300	326	1.3	73167	< .2	2464	0.4	6.62	2	0.32	12.0	< .5	379	< .05	< 10	0.51	0.9	< .02	4.3	0.13
Wab1-34	10	6.7	228	38	57	< .05	0.13	0.5	0.01	0.9	< 10	< 6	11906	43.2	20758	32.2	2.2	70105	< .2	2648	0.9	6.91	2	0.86	12.2	< .5	393	< .05	< 10	0.84	2.1	< .02	1.4	0.08
Wab1-39	9	10	257	41	64	< .05	0.13	4.6	0.01	1.1	15	< 6	11843	42.8	21239	24.7	2.7	75695	< .2	2907	0.1	7.37	2	1.07	11.8	< .5	399	< .05	11	1.13	2.3	< .02	1.6	0.16
Wab1-44	9	20	271	42	65	< .05	0.12	2.9	0.02	5	22	< 4	12136	43.2	21843	15.2	5.6	73964	< .2	3121	0.1	7.46	1	2.33	11.8	< .5	429	< .05	10	2.01	2.7	0.02	0.9	0.16
Wab1-50	11	38	284	28	67	< .05	0.23	3.9	0.02	1.4	24	< 5	12441	46.6	22670	10.7	10.4	82045	0.3	3210	0.1	8.05	2	4.24	12.7	< .5	430	< .05	12	5.49	13.8	0.05	0.9	0.28
Wab1-56	11	13.2	284	53	69	< .05	0.13	2.5	0.01	1.4	< 10	< 5	11671	52.5	24566	24.3	2.9	84953	< .2	3707	0.1	6.92	0	1.18	13.5	< .5	433	< .05	13	1.35	0.2	0.02	1	0.21
Wab1-64	38	19	317	57	68	< .05	0.12	4.1	0.01	3.2	< 10	< 5	11431	50.8	26780	22.8	4.2	89503	0.8	4107	0.1	6.50	0	1.74	12.5	< .5	472	< .05	13	2.71	2.7	0.04	1.6	0.21
Min	2	1.7	134	21	51	*ND*	0.03	0.5	0.01	0.7	10	10	10744	36.1	17666	10.7	1.3	70105	0.3	27	0.1	5.38	0	0.07	3.26	*ND*	301	*ND*	10	0.08	0.2	0.02	0.5	0.02
Median	11	3.2	184	30	64	*ND*	0.13	2.4	0.01	0.9	21	10	11469	39.8	19847	251	4.7	73662	0.8	1306	0.1	6.58	3	0.19	7.86	*ND*	357	*ND*	12	0.48	0.6	0.27	0.9	0.08
Max	38	38	317	57	69	*ND*	0.26	4.6	0.02	6.3	64	24	12441	52.5	26780	368	21.9	89503	1.2	4107	3.4	8.05	16	4.24	13.5	*ND*	472	*ND*	13	5.49	13.8	0.37	4.3	0.28
Mean	11	6.8	194	31	61	*ND*	0.14	2.4	0.01	1.4	23	13	11493	41.2	20327	220	7.4	75023	0.8	1537	0.5	6.62	5	0.67	7.99	*ND*	363	*ND*	12	0.86	1.4	0.21	1.16	0.10

"<" denotes values below detection limits *ND*: Not detected

Table 3.6. The total dissolved concentration of elements throughout the porewater profile from WAB2 core.

Sediment intervals (cm)	Al	As	Ba	Br	Ca	Cd	Co	Cr	Cs	Cu	Fe	Hg	K	Li	Mg	Mn	Mo	Na	Ni	P	Pb	Rb	S	Sb	Sc	Se	Sr	Th	Ti	U	V	W	Zn	Zr
	ppb	ppb	ppb	ppb	ppb	ppb	ppb	ppb	ppb	ppb	ppb	ppt	ppb	ppb	ppb	ppb	ppb	ppb	ppb	ppb	ppb	ppb	ppm	ppb	ppb	ppb	ppb	ppb	ppb	ppb	ppb	ppb	ppb	ppb
Wab2-01	6	9.8	174	26	< 50	< .05	0.02	1.5	< .01	0.8	< 10	< 5	12055	46.7	23115	271	26.6	79685	< .2	27	0.1	6.11	21	0.3	2.61	< .5	347	< .05	< 10	4.01	< .2	0.4	1.6	0.04
Wab2-02	5	11.7	182	24	< 50	< .05	0.02	2.6	< .01	0.6	26	< 5	12106	43.5	22956	767	19.2	76066	< .2	65	0.1	6.51	18	0.16	3.22	< .5	362	< .05	< 10	0.89	< .2	0.52	< .5	0.04
Wab2-03	5	7.7	172	22	< 50	< .05	0.03	2.5	< .01	0.6	16	< 5	12218	44	23120	375	11.2	76322	< .2	154	0.1	6.77	18	0.13	3.86	< .5	363	< .05	< 10	0.43	< .2	0.52	< .5	0.06
Wab2-04	4	6	179	23	< 50	< .05	0.03	1.7	< .01	0.6	13	< 4	11990	43.8	23723	315	8.6	74391	< .2	182	< .1	6.65	20	0.17	3.75	< .5	382	< .05	< 10	0.36	< .2	0.49	< .5	0.06
Wab2-05	6	7.3	172	23	< 50	< .05	0.04	2.5	< .01	0.6	20	< 4	12281	43.4	22325	661	8.1	72998	< .2	251	< .1	6.7	12	0.14	4.05	< .5	341	< .05	< 10	0.33	< .2	0.58	< .5	0.07
Wab2-06	6	7.1	180	26	34794	< .05	0.03	0.9	< .01	1	< 10	< 4	11092	34	19651	390	9.1	79085	< .2	193	0.2	7.52	21	0.23	2.32	< .5	344	0.07	< 10	0.54	1.1	0.54	< .5	0.07
Wab2-07	5	7.3	178	25	31485	< .05	0.03	0.9	< .01	1	11	< 6	10910	35.6	19471	343	9.8	77361	< .2	211	0.2	7.71	19	0.19	2.1	< .5	332	< .05	< 10	0.49	0.9	0.55	< .5	0.08
Wab2-08	6	6.4	167	25	31261	< .05	0.03	0.9	0.01	0.9	10	< 4	10845	37.2	19646	305	10.1	77201	< .2	243	0.2	7.65	18	0.26	2.16	< .5	323	< .05	< 10	0.49	1.1	0.51	< .5	0.07
Wab2-09	5	6.7	165	24	29141	< .05	0.03	0.8	< .01	0.9	19	< 3	11001	33.4	18489	294	9.4	76485	< .2	276	0.1	7.54	14	0.17	2.15	< .5	299	< .05	< 10	0.38	1	0.49	< .5	0.05
Wab2-10	5	7.4	167	24	31212	< .05	0.02	0.5	0.01	0.8	< 10	< 5	11566	37.9	18849	174	11.2	77435	< .2	231	0.2	7.79	17	0.24	1.97	< .5	321	< .05	< 10	0.55	1.6	0.39	0.9	0.04
Wab2-12	6	7.6	163	24	30872	< .05	0.03	0.8	0.01	1	< 10	< 5	11810	36.3	18312	254	8.4	78405	< .2	341	0.1	7.85	9	0.19	2.24	< .5	306	< .05	< 10	0.33	0.9	0.31	< .5	0.08
Wab2-14	6	7.8	166	22	31435	< .05	0.04	0.6	0.01	1	< 10	< 2	12036	36.4	18057	201	9.5	78393	< .2	340	0.3	8.07	8	0.31	2.34	< .5	286	< .05	< 10	0.39	1.2	0.21	< .5	0.08
Wab2-16	8	6.7	169	25	33099	< .05	0.05	0.6	0.01	1.1	< 10	< 4	12541	37.2	18183	324	5.4	74242	< .2	448	0.1	7.89	7	0.2	2.47	< .5	293	< .05	< 10	0.21	0.6	0.19	< .5	0.1
Wab2-18	7	5.6	168	22	33102	< .05	0.06	0.7	0.01	1.1	< 10	< 3	12113	39.3	17815	160	6.2	76046	< .2	402	0.1	7.67	8	0.27	2.42	< .5	287	< .05	< 10	0.29	1.3	0.14	0.5	0.12
Wab2-20	6	3.2	156	27	33970	< .05	0.07	0.7	0.01	1.2	< 10	< 3	12681	40.1	17819	407	2.8	75391	< .2	567	0.1	7.08	6	0.08	2.63	< .5	296	< .05	< 10	0.16	0.4	0.12	1.1	0.14
Wab2-23	10	3.8	162	26	37975	< .05	0.11	< .5	0.01	1.2	< 10	< 4	12708	40	17188	290	2.9	75051	< .2	576	0.3	7.44	7	0.41	3.04	< .5	304	< .05	< 10	0.32	0.9	0.08	< .5	0.17
Wab2-26	8	5.8	161	21	37957	< .05	0.1	< .5	0.01	1.2	< 10	< 4	12015	42.3	16621	209	2.8	75636	< .2	603	0.3	7.05	8	0.5	2.94	< .5	282	< .05	< 10	0.48	1.5	0.05	0.5	0.19
Wab2-30	8	4.9	161	25	38940	< .05	0.09	< .5	0.01	1.2	< 10	< 3	11941	39.7	16180	221	2.7	73808	< .2	667	0.3	7.03	6	0.45	3.26	< .5	287	< .05	< 10	0.41	1.2	0.07	0.5	0.19
Wab2-35	6	5.5	156	28	40142	< .05	0.05	0.7	0.01	2.1	< 10	< 3	10768	39.9	17245	250	3	74729	< .2	734	0.2	6.04	6	0.54	3.69	< .5	282	< .05	< 10	0.54	0.6	0.03	6.9	0.15
Wab2-41	10	5.7	163	23	41962	< .05	0.06	0.5	0.01	2.2	< 10	< 2	10752	37.6	16443	164	2.3	77397	< .2	875	0.4	6.39	4	0.64	4.06	< .5	287	< .05	< 10	0.51	1	0.04	10.3	0.15
Wab2-47	10	11.9	182	25	45016	< .05	0.07	< .5	0.01	2.6	< 10	< 3	10990	37.5	16776	56.0	2.5	74861	< .2	996	0.3	6.74	4	1.36	4.51	< .5	294	< .05	< 10	0.72	1.6	0.03	6.2	0.17
Wab2-54	10	5.6	176	33	44769	< .05	0.07	< .5	0.01	1.5	< 10	< 4	9907	36.7	16622	59.9	1.8	76667	< .2	1346	0.3	5.91	1	0.92	5.06	< .5	302	< .05	< 10	0.35	1	0.04	2.9	0.2
Min	4	3.2	156	21	29141	*ND*	0.02	0.5	0.01	0.6	10	*ND*	9907	33.4	16180	56.0	1.8	72998	*ND*	27	0.1	5.91	1	0.08	1.97	*ND*	282	0.07	*ND*	0.16	0.4	0.03	0.5	0.04
Median	6	6.7	168	25	33970	*ND*	0.04	0.8	0.01	1.0	16	*ND*	11966	38.6	18248	281	8.3	76194	*ND*	341	0.2	7.07	8.5	0.25	2.79	*ND*	303	0.07	*ND*	0.42	1	0.26	1.35	0.08
Max	10	11.9	182	33	45016	*ND*	0.11	2.6	0.01	2.6	26	*ND*	12708	46.7	23723	767	26.6	79685	*ND*	1346	0.4	8.07	21	1.36	5.06	*ND*	382	0.07	*ND*	4.01	1.6	0.58	10.3	0.2
Mean	7	6.9	169	25	35714	*ND*	0.05	1.1	0.01	1.1	16	*ND*	11651	39.2	19028	295	7.9	76257	*ND*	442	0.2	7.10	11	0.36	3.04	*ND*	315	0.07	*ND*	0.60	1.1	0.29	3.14	0.11

"<" denotes values below detection limits *ND*: Not detected

Table 3.7. The total dissolved concentration of elements throughout the porewater profile from ISLE core.

Sediment intervals (cm)	Al	As	Ba	Br	Ca	Cd	Co	Cr	Cs	Cu	Fe	Hg	K	Li	Mg	Mn	Mo	Na	Ni	P	Pb	Rb	S	Sb	Sc	Se	Sr	Th	Ti	U	V	W	Zn	Zr
	ppb	ppb	ppb	ppb	ppb	ppb	ppb	ppb	ppb	ppb	ppb	ppt	ppb	ppb	ppb	ppb	ppb	ppb	ppb	ppb	ppb	ppb	ppm	ppb	ppb	ppb	ppb	ppb	ppb	ppb	ppb	ppb	ppb	ppb
ISLE-01	1	3.8	200	25	51466	< .05	0.1	0.5	< .01	0.3	435	< 2	12359	19.2	15855	3070	1.5	34234	< .2	321	< .1	5.23	7	0.07	3.13	< .5	320	< .05	< 10	0.76	0.2	< .02	1	0.04
ISLE-02	1	2.6	160	17	41869	< .05	0.04	0.5	< .01	0.3	487	< 2	11575	18.3	13545	1491	0.8	32948	< .2	187	0.1	4.31	2	< .05	2.84	< .5	258	< .05	< 10	0.16	< .2	< .02	2.6	0.03
ISLE-03	4	2.5	176	20	41802	< .05	0.05	< .5	< .01	0.7	615	13	12293	19	12902	1526	0.8	32352	< .2	145	0.1	4.5	4	0.06	3.13	< .5	259	< .05	< 10	0.23	< .2	< .02	2	0.04
ISLE-04	2	2.5	164	22	45077	< .05	0.06	< .5	< .01	0.4	968	< 4	11711	18.9	13424	1496	0.8	32369	< .2	140	0.1	4.44	4	0.06	3.3	< .5	279	< .05	< 10	0.21	< .2	< .02	1.0	0.04
ISLE-05	3	2.7	170	23	46821	< .05	0.07	< .5	< .01	0.4	926	< 2	12142	19.1	13240	1424	0.7	33593	< .2	178	0.1	4.76	4	0.06	3.42	< .5	274	< .05	< 10	0.23	< .2	< .02	2.2	0.05
ISLE-06	2	2.4	161	23	41856	< .05	0.05	< .5	< .01	0.5	666	< 4	11904	19.3	12668	1787	0.6	31285	< .2	141	0.1	4.58	3	0.06	3.24	< .5	256	< .05	< 10	0.16	< .2	< .02	0.6	0.04
ISLE-07	3	2.8	166	24	43432	< .05	0.05	< .5	< .01	0.4	1302	< 2	11549	20	12180	1839	0.4	31500	< .2	218	0.2	4.99	1	< .05	3.94	< .5	261	< .05	< 10	0.11	< .2	< .02	1.0	0.05
ISLE-08	3	3.3	176	24	44396	< .05	0.06	< .5	< .01	0.6	1487	< 2	11598	19.4	13309	2125	0.4	33081	< .2	292	0.1	5.46	1	< .05	4.39	< .5	273	< .05	< 10	0.10	< .2	< .02	3.1	0.06
ISLE-09	3	2.2	152	22	41116	< .05	0.06	< .5	< .01	0.4	1355	10	11293	18.5	12101	1808	0.2	31757	< .2	170	0.1	5.15	1	< .05	4.91	< .5	266	< .05	< 10	0.06	< .2	< .02	5.2	0.06
ISLE-10	6	2.7	154	22	44097	< .05	0.06	< .5	< .01	0.4	1763	< 2	11462	19.3	13133	1987	0.2	31469	< .2	251	0.1	5.43	0	< .05	4.6	< .5	266	< .05	< 10	0.05	< .2	< .02	6.3	0.05
ISLE-12	3	2.5	151	24	43698	< .05	0.06	< .5	< .01	0.4	1390	< 2	11471	20.9	13797	1872	0.1	32419	< .2	269	0.1	5.92	0	< .05	5.43	< .5	281	< .05	< 10	0.07	< .2	< .02	3.5	0.06
ISLE-14	4	2.1	141	26	43375	< .05	0.05	< .5	< .01	0.6	634	< 5	11135	20.8	14107	1522	0.4	32576	< .2	114	0.2	6.0	1	< .05	5.56	< .5	274	< .05	< 10	0.07	< .2	< .02	4.5	0.07
ISLE-16	5	1.5	113	22	36696	0.23	0.03	< .5	< .01	0.5	323	< 2	8231	13.1	13350	1060	0.4	24163	< .2	105	0.4	5.65	1	< .05	2.48	< .5	208	< .05	< 10	0.06	< .2	0.16	1.9	0.05
ISLE-18	7	1.6	106	24	39624	< .05	0.03	< .5	< .01	1.3	129	10	8782	14.9	12780	774	0.5	25097	10.5	44	0.3	5.66	< 1	< .05	2.44	< .5	205	< .05	< 10	0.10	< .2	0.13	2.8	0.06
ISLE-21	8	1.6	115	29	39883	< .05	0.03	< .5	< .01	1.3	82	< 2	8900	15.7	12843	760	0.7	26046	< .2	48	0.2	5.7	1	0.09	2.45	< .5	215	< .05	< 10	0.23	< .2	0.09	6.7	0.08
ISLE-24	6	1.1	110	31	42081	< .05	0.03	< .5	< .01	0.8	59	< 2	8233	15.3	12650	674	0.4	25908	< .2	37	0.1	5.07	< 1	< .05	2.45	< .5	213	< .05	< 10	0.16	< .2	0.06	2.3	0.07
ISLE-27	6	1.6	130	35	50842	< .05	0.03	< .5	< .01	1.7	299	< 2	8625	17.2	14597	700	0.4	28957	< .2	90	0.4	4.79	0	< .05	2.38	< .5	235	< .05	< 10	0.22	< .2	0.06	4.8	0.1
ISLE-30	6	0.9	119	36	44026	< .05	0.03	< .5	< .01	1.7	367	< 2	7590	16.8	12265	684	0.3	26160	< .2	50	0.2	3.84	0	< .05	2.42	< .5	210	< .05	< 10	0.13	< .2	0.04	7.0	0.1
ISLE-33	8	1.3	113	40	43697	< .05	0.04	< .5	< .01	2	349	< 2	7344	17.1	12337	581	0.5	27094	< .2	48	0.8	4.11	0	< .05	2.6	< .5	212	< .05	< 10	0.30	< .2	0.04	13.7	0.08
ISLE-36	9	1.7	112	45	42479	< .05	0.05	< .5	< .01	1.5	116	< 2	7411	21.5	11680	329	0.6	28688	< .2	55	0.4	4.37	0	0.06	2.85	< .5	199	< .05	< 10	0.20	0.3	0.03	0.9	0.12
ISLE-40	9	2.3	135	54	47319	< .05	0.04	< .5	< .01	1.2	117	< 2	7740	21.8	12261	398	0.7	28258	< .2	54	0.2	4.45	1	0.06	3.19	0.5	238	< .05	< 10	0.22	0.3	0.02	0.7	0.12
ISLE-44	36	2.1	135	63	51893	< .05	0.05	< .5	< .01	32.8	135	< 2	7028	23.1	13789	452	0.6	29262	17.1	58	2.9	4.13	1	0.07	3.34	0.6	264	< .05	< 10	0.24	0.3	0.03	17.7	0.14
ISLE-48	11	3.3	136	77	58052	< .05	0.05	< .5	< .01	1.3	68	< 2	7150	28.5	14903	454	0.7	32090	< .2	72	0.2	4.29	1	0.1	4.13	0.7	277	< .05	< 10	0.31	0.5	0.02	2.2	0.15
Min	1	0.9	106	17	36696	0.23	0.03	0.5	*ND*	0.3	59	10	7028	13.1	11680	329	0.1	24163	10.5	37	0.1	3.84	0	0.06	2.38	0.5	199	*ND*	*ND*	0.05	0.2	0.02	0.6	0.03
Median	5	2.3	141	24	43697	0.23	0.05	0.5	*ND*	0.6	435	10	11135	19.1	13133	1424	0.5	31469	13.8	114	0.2	4.79	1	0.06	3.19	0.6	259	*ND*	*ND*	0.16	0.3	0.04	2.6	0.06
Max	36	3.8	200	77	58052	0.23	0.1	0.5	*ND*	32.8	1763	13	12359	28.5	15855	3070	1.5	34234	17.1	321	2.9	6	7	0.1	5.56	0.7	320	*ND*	*ND*	0.76	0.5	0.16	17.7	0.15
Mean	6	2.2	143	32	44591	0.23	0.05	0.5	*ND*	2.2	612	11	9892	19.0	13205	1253	0.6	30057	13.8	134	0.3	4.91	2	0.07	3.42	0.6	250	*ND*	*ND*	0.19	0.3	0.06	4.1	0.07

"<" denotes values below detection limits *ND*: Not detected

Table 3.8. The total dissolved concentration of elements throughout the porewater profile from LSA core.

Sediment intervals (cm)	Al	As	Ba	Br	Ca	Cd	Co	Cr	Cs	Cu	Fe	Hg	K	Li	Mg	Mn	Mo	Na	Ni	P	Pb	Rb	S	Sb	Sc	Se	Sr	Th	Ti	U	V	W	Zn	Zr
	ppb	ppb	ppb	ppb	ppb	ppb	ppb	ppb	ppb	ppb	ppb	ppt	ppb	ppb	ppb	ppb	ppb	ppb	ppb	ppb	ppb	ppb	ppm	ppb	ppb	ppb	ppb	ppb	ppb	ppb	ppb	ppb	ppb	ppb
LSA-01	2	0.9	79	19	39906	0.08	< .02	< .5	< .01	0.6	< 10	< 16	8551	14.6	14645	8.64	0.6	21988	< .2	< 20	0.3	4.33	7	< .05	1.33	< .5	206	< .05	< 10	0.61	< .2	0.06	2.2	< .02
LSA-02	2	1.4	125	22	50286	< .05	< .02	< .5	< .01	0.4	246	< 2	10209	15.8	17484	1249	0.9	21290	< .2	47	0.2	6.42	9	0.06	2.19	< .5	290	< .05	< 10	0.89	< .2	0.04	1.7	0.02
LSA-03	5	1.3	117	19	50499	< .05	< .02	< .5	< .01	0.5	398	12	10314	15.8	18078	1177	0.8	22011	< .2	51	0.1	6.87	10	< .05	2.84	< .5	269	< .05	< 10	0.34	< .2	0.04	4.0	< .02
LSA-04	4	1.4	111	19	52349	< .05	< .02	< .5	< .01	0.3	259	< 3	10361	16.7	17968	1223	1	22755	< .2	62	0.3	6.31	8	< .05	2.82	< .5	264	< .05	< 10	0.34	< .2	0.04	5.1	0.02
LSA-05	4	1.5	115	19	51181	< .05	< .02	< .5	< .01	0.1	384	15	11153	17.3	16695	1199	1.2	21674	< .2	61	0.1	6.08	7	< .05	2.37	< .5	270	< .05	< 10	0.33	< .2	0.05	2.0	0.02
LSA-06	4	1.1	104	18	48769	< .05	< .02	< .5	< .01	0.6	141	< 2	10092	16.9	16566	831	1	23074	< .2	40	0.1	5.33	8	< .05	2.29	< .5	240	< .05	< 10	0.19	< .2	0.04	1.4	< .02
LSA-07	4	1.1	96	16	47597	< .05	< .02	< .5	< .01	0.6	121	< 4	10125	17.1	16078	592	1.2	23173	< .2	40	0.4	5.14	7	< .05	2.16	< .5	230	< .05	< 10	0.09	< .2	0.04	3.7	< .02
LSA-08	4	1.1	99	17	44432	0.06	< .02	< .5	< .01	5.1	216	< 3	9981	15.9	14227	833	1.8	21262	12.2	56	0.2	4.94	5	< .05	1.98	< .5	234	< .05	< 10	0.08	< .2	0.05	3.5	< .02
LSA-09	5	1.2	92	16	47695	< .05	< .02	< .5	< .01	1.1	114	< 2	10123	17.1	15084	739	1.7	22499	< .2	63	0.2	5.08	5	< .05	2.06	< .5	218	< .05	< 10	0.08	< .2	0.05	2.8	0.02
LSA-10	5	1	99	18	52130	< .05	< .02	< .5	< .01	0.7	108	28	10142	16.8	14712	749	1.7	21584	< .2	150	2	5.27	8	< .05	2.11	< .5	245	< .05	< 10	0.12	< .2	0.05	2.4	0.02
LSA-12	5	1	91	18	50656	0.08	< .02	< .5	< .01	0.6	227	< 2	9415	15.6	14424	776	1.5	22657	< .2	35	0.2	5.15	2	< .05	2.13	< .5	230	< .05	< 10	0.12	< .2	0.04	4.9	< .02
LSA-14	8	0.8	106	23	61407	< .05	< .02	< .5	< .01	0.4	152	< 2	9364	16.4	14725	813	1.4	22532	< .2	30	0.4	5.72	2	< .05	2.67	< .5	251	< .05	< 10	0.1	< .2	0.05	2.3	0.02
LSA-16	3	0.8	120	27	65968	0.08	< .02	< .5	< .01	0.9	113	12	9929	17.5	15589	910	0.9	21266	< .2	45	5.7	6.22	1	< .05	3.31	< .5	288	< .05	< 10	0.11	< .2	0.04	2.9	0.02
LSA-18	3	0.9	127	30	67254	0.07	< .02	< .5	< .01	1.4	504	< 2	10429	15	15596	1168	0.5	21323	< .2	48	0.2	6.42	0	< .05	3.62	< .5	283	< .05	< 10	0.07	< .2	0.03	7.2	0.03
LSA-20	4	0.8	128	30	68770	0.08	< .02	< .5	< .01	0.8	193	11	11031	16.1	15574	1077	0.8	21675	< .2	57	0.4	7.9	1	< .05	4.18	< .5	288	< .05	< 10	0.1	< .2	0.03	3.8	0.03
LSA-23	4	0.9	135	34	74007	< .05	< .02	< .5	< .01	0.9	325	< 2	10821	16.7	15824	904	0.8	21574	< .2	90	0.3	8.02	0	< .05	4.18	< .5	293	< .05	< 10	0.09	< .2	0.03	43	0.04
LSA-26	8	0.9	144	40	77741	< .05	< .02	< .5	< .01	1.7	103	< 2	11424	16.7	15574	988	0.6	20955	< .2	61	0.2	8.14	0	< .05	4.73	< .5	317	< .05	< 10	0.08	< .2	0.02	13.4	0.03
LSA-29	4	1.6	164	40	85366	< .05	0.03	< .5	< .01	0.1	501	12	11319	17.4	18919	1513	0.5	23067	< .2	108	0.2	8.18	0	< .05	5.21	0.5	339	< .05	< 10	0.07	< .2	0.02	< .5	0.05
LSA-32	2	1.8	171	40	68095	< .05	< .02	< .5	0.01	1	21	12	8596	16.9	15214	611	1.1	21232	< .2	55	< .1	7.36	1	< .05	2.61	< .5	284	< .05	< 10	0.17	< .2	0.3	12.2	0.06
LSA-36	3	1.5	169	43	69555	< .05	< .02	< .5	< .01	0.7	117	< 2	8825	17.2	15084	740	1.4	19998	< .2	64	< .1	7.02	2	< .05	2.52	< .5	287	< .05	< 10	0.12	< .2	0.19	< .5	0.07
LSA-40	2	1.6	168	44	69761	< .05	< .02	< .5	< .01	0.7	10	< 2	8424	18.5	15672	807	0.9	20049	< .2	62	0.1	6.51	1	< .05	2.66	< .5	286	< .05	< 10	0.14	< .2	0.07	16.5	0.07
LSA-45	2	1.3	165	50	72437	< .05	< .02	< .5	< .01	1.3	59	< 2	7990	18.6	15914	766	0.7	20083	< .2	71	0.4	6.13	1	< .05	2.87	< .5	284	< .05	< 10	0.1	< .2	0.02	1.6	0.06
LSA-50	3	2.6	190	56	85312	< .05	< .02	0.6	< .01	0.8	< 10	< 2	8058	21.9	15637	381	1.3	19685	< .2	77	0.2	6.3	2	< .05	2.6	< .5	323	< .05	< 10	0.16	< .2	< .02	1.9	0.07
LSA-56	4	3.1	176	61	72339	< .05	< .02	< .5	< .01	1.5	< 10	< 2	8230	21.1	14381	789	1.2	18972	< .2	75	< .1	6.29	1	< .05	2.74	< .5	286	< .05	< 10	0.14	< .2	< .02	< .5	0.08
LSA-65	5	8.4	199	69	76669	< .05	< .02	< .5	< .01	2	< 10	< 7	8301	23.4	15466	177	2.3	19121	< .2	181	0.1	6.87	1	0.1	2.7	< .5	318	< .05	< 10	0.53	< .2	< .02	9.1	0.1
Min	2	0.8	79	16	39906	0.06	0.03	0.6	0.01	0.1	10	11	7990	14.6	14227	8.64	0.5	18972	12.2	30	0.1	4.33	0	0.06	1.33	0.5	206	*ND*	*ND*	0.07	*ND*	0.02	1.4	0.02
Median	4	1.2	125	27	65968	0.08	0.03	0.6	0.01	0.7	152	12	10092	16.9	15589	813	1	21574	12.2	61	0.2	6.30	2	0.08	2.66	0.5	284	*ND*	*ND*	0.12	*ND*	0.04	3.6	0.03
Max	8	8.4	199	69	85366	0.08	0.03	0.6	0.01	5.1	504	28	11424	23.4	18919	1513	2.3	23173	12.2	181	5.7	8.18	10	0.1	5.21	0.5	339	*ND*	*ND*	0.89	*ND*	0.3	43	0.1
Mean	4	1.6	132	32	62007	0.08	0.03	0.6	0.01	1.0	205	15	9728	17.3	15805	841	1.1	21420	12.2	68	0.6	6.32	4	0.08	2.84	0.5	273	*ND*	*ND*	0.21	*ND*	0.06	6.7	0.04

"<" denotes values below detection limits *ND*: Not detected

The vertical variation of elements throughout the sediment and profiles are compared and statistically sorted based on their similarity indices. Furthermore, the non-parametric, rank correlation (Spearman correlation) is applied to construct a correlation matrix for the elements in sediment and porewater samples in each of the studied lakes. The elements linked to important geochemical fractions are discussed for all sediment cores to investigate the prevailing geochemical processes occurring in each lake. Furthermore, the concentration data for trace metals are discussed in detail for Wabamun Lake (Appendix A) due to environmental concerns surrounding this specific lake.

3.4.1. Trace elements in the sediments and porewater from Wabamun Lake

The temporal distributions of trace elements As, Sb, U, V, Cr, Cu, Mo, Pb, Se, Hg, and Zn in the Wabamun Lake sediment cores show different concentrations between the younger sediment layers and the older sediment layers, as characterized by an episode of high concentrations in the upper section of the WAB1 and WAB2 sediment profiles (Figures 3.1-3.2). There are several scenarios for enrichment of trace elements in surficial sediments from Wabamun Lake, which are discussed as follows:

3.4.1.1. Anthropogenic input

The enrichment of these elements may be due in part to increased external input in recent time. The depth profiles of As, Sb, Cu, Cr, Mo, Pb, Se, Hg, and Zn in the Wabamun Lake sediment cores show significant correlation with those of Ca, U, V, and W, which are known

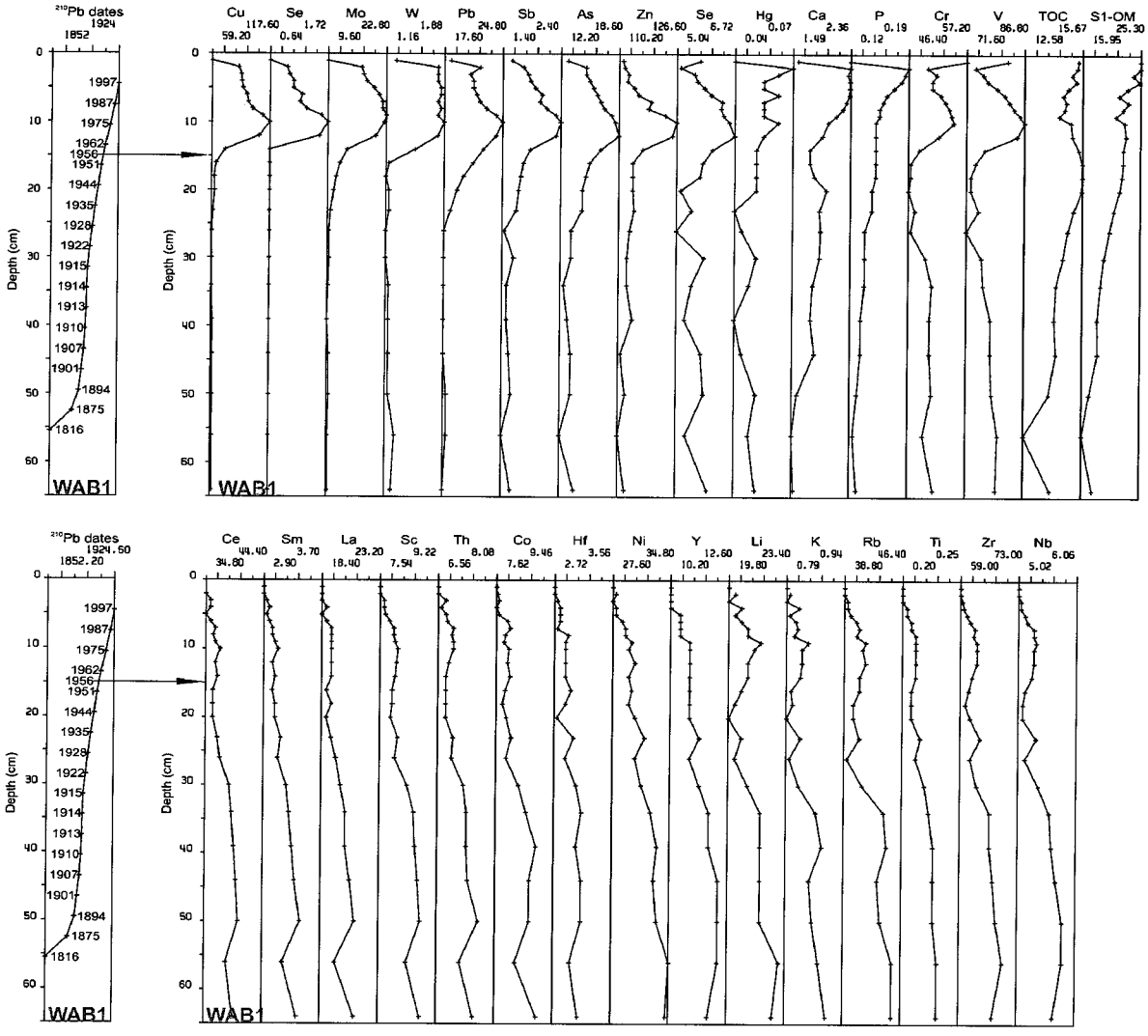

Figure 3.1. The temporal distribution of elements and organic matter throughout the WAB1 sediment profile as related to the ^{210}Pb-dates of the sediments.

to enrich in power plant fly ash (Tables 3.9-3.10). This suggests that the concentrations of metals in the sediment profiles from Wabamun Lake are likely controlled by the input of calcareous fly ash emitted from the power plants in the study area[1]. Moreover, the correlation of the elemental profiles with the ^{210}Pb data (Chapter 2) confirms the link between the sudden increase in concentration of trace elements in the Wabamun sediment profiles and

[1] The existence of fly ash in the sediments from WAB1 and WAB2 is confirmed by SEM analyses (Chapter 5).

commencement of the Wabamun coal-fired power plant in year 1956 in the lake's watershed (Figures 3.1-3.2). The concentrations of trace elements reach their maximum levels at a depth (~10-12 cm) coinciding with the historical peak emission in the 1970 caused by the simultaneous operation of the Wabamun and Sundance power plants in the study area (Figures 3.1-3.2).

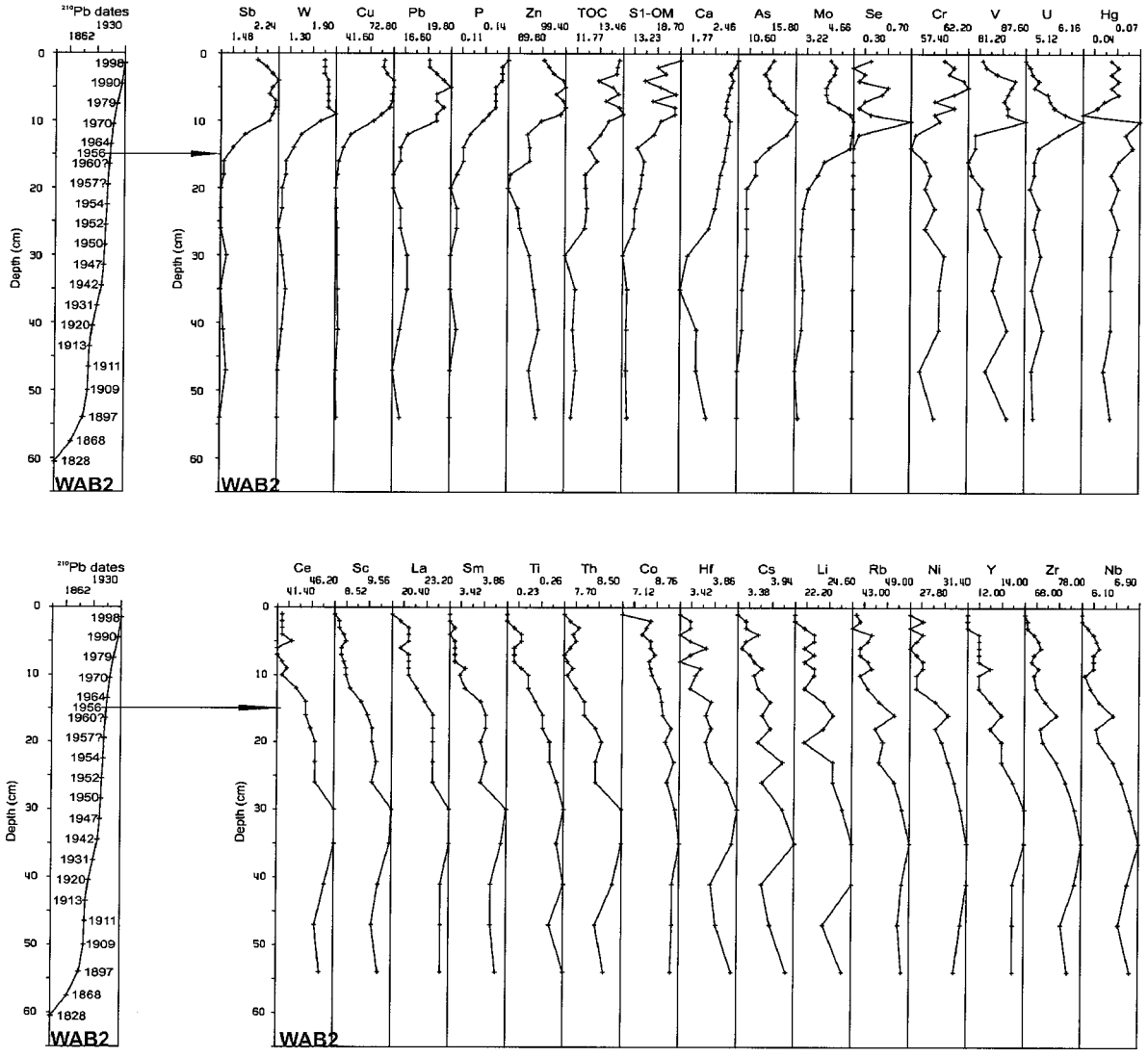

Figure 3.2. The temporal distribution of elements and organic matter throughout the WAB2 sediment profile as related to the ^{210}Pb-dates of the sediments.

Table 3.9. The Spearman correlation matrix for the elements and organic content of the sediments in WAB1 core.

	As	Ca	Cd	Co	Cr	Cu	Fe	Hg	Mn	Mo	Ni	P	Pb	Sb	Se	U	V	W	Zn	Zr	S	TOC	S1
Al																							
As	***																						
Ca	**0.6**	***																					
Cd		*-0.7*	***																				
Co	*-0.6*	*-0.8*		***																			
Cr	**0.4**		*-0.5*		***																		
Cu	**0.9**	**0.6**		*-0.6*	**0.5**	***																	
Fe	*-0.7*	*-0.9*	**0.6**	**0.8**		*-0.7*	***																
Hg	**0.7**	**0.7**	*-0.5*	*-0.6*	**0.4**	**0.9**	*-0.8*	***															
Mn	*-0.5*			**0.5**		*-0.4*	**0.5**	*-0.4*	***														
Mo	**0.9**	**0.7**		*-0.7*	**0.4**	**0.9**	*-0.8*	**0.8**	*-0.5*	***													
Ni	*-0.7*	*-0.8*	**0.5**	**0.9**		*-0.7*	**1.0**	*-0.8*	**0.5**	*-0.8*	***												
P	**0.7**	**0.9**	*-0.5*	*-0.8*		**0.8**	*-1.0*	**0.8**	*-0.5*	**0.8**	*-1.0*	***											
Pb	**0.9**	**0.6**		*-0.6*	**0.4**	**0.9**	*-0.7*	**0.8**	*-0.5*	**0.9**	*-0.6*	**0.7**	***										
Sb	**1.0**	**0.6**		*-0.6*	**0.5**	**0.9**	*-0.7*	**0.8**	*-0.4*	**1.0**	*-0.7*	**0.8**	**0.9**	***									
Se	**0.8**	**0.7**	*-0.5*	*-0.5*	**0.7**	**0.9**	*-0.7*	**0.8**		**0.9**	*-0.6*	**0.7**	**0.8**	**0.9**	***								
U	**0.7**				**0.6**	**0.7**		**0.5**		**0.7**			**0.6**	**0.7**	**0.6**	***							
V	**0.4**				**0.9**	**0.5**				**0.4**			**0.5**	**0.5**	**0.7**	**0.7**	***						
W	**0.7**	**0.7**	*-0.4*	*-0.5*	**0.5**	**0.7**	*-0.7*	**0.8**		**0.7**	*-0.7*	**0.8**	**0.8**	**0.8**	**0.8**	**0.5**	**0.4**	***					
Zn	**0.8**	**0.6**		*-0.5*	**0.5**	**0.7**	*-0.7*	**0.7**		**0.8**	*-0.6*	**0.7**	**0.8**	**0.8**	**0.8**	**0.6**	**0.4**	**0.7**	***				
Zr	*-0.5*	*-0.7*		**0.9**		*-0.4*	**0.8**	*-0.6*	**0.7**	*-0.5*	**0.9**	*-0.8*	*-0.4*	*-0.5*			**0.4**	*-0.4*		***			
S	*-0.8*	*-0.6*		**0.5**	*-0.5*	*-0.7*	**0.7**	*-0.6*	**0.4**	*-0.8*	**0.6**	*-0.7*	*-0.7*	*-0.8*	*-0.8*	*-0.6*	*-0.4*	*-0.7*	*-0.8*		***		
TOC				*-0.5*			*-0.4*		*-0.5*		*-0.5*	**0.4**	**0.4**				*-0.4*			*-0.6*		***	
S1	**0.6**	**0.6**		*-0.6*		**0.5**	*-0.7*	**0.6**		**0.5**	*-0.7*	**0.7**	**0.6**	**0.6**	**0.5**			**0.7**	**0.5**	*-0.6*	*-0.5*	**0.7**	***

* Only correlation coefficients significant at 95% confidence limit ($p<0.05$ at 0.39; n=24) are shown.
** Negative correlations are shown in *Italic*.

Table 3.10. The Spearman correlation matrix for the elements and organic content of the sediments in WAB2 core.

	As	Ca	Cd	Co	Cr	Cu	Fe	Hg	Mn	Mo	Ni	P	Pb	Sb	Se	U	V	W	Zn	Zr	S	OC	S1
Al																							
As	***																						
Ca	**0.7**	***																					
Cd			***																				
Co	*-0.8*	*-0.9*		***																			
Cr		**0.4**		*-0.5*	***																		
Cu	**0.7**	**0.8**		*-0.8*	**0.7**	***																	
Fe	*-0.7*	*-0.9*		**0.9**	*-0.5*	*-0.8*	***																
Hg								***															
Mn	**0.6**	**0.8**		*-0.9*	**0.7**	**0.8**	*-0.8*		***														
Mo	**0.9**	**0.8**		*-0.7*		**0.6**	*-0.6*		**0.6**	***													
Ni	*-0.8*	*-0.9*		**0.8**		*-0.7*	**0.9**		*-0.7*	*-0.7*	***												
P	**0.7**	**0.9**		*-0.9*	**0.6**	**0.9**	*-0.9*		**0.9**	**0.7**	*-0.8*	***											
Pb	**0.7**	**0.7**		*-0.8*	**0.7**	**0.9**	*-0.8*		**0.7**	**0.6**	*-0.7*	**0.8**	***										
Sb	**0.8**	**0.7**		*-0.8*	**0.6**	**0.9**	*-0.8*		**0.7**	**0.6**	*-0.7*	**0.8**	**0.9**	***									
Se	**0.8**	**0.7**		*-0.8*	**0.5**	**0.8**	*-0.7*		**0.6**	**0.6**	*-0.8*	**0.7**	**0.8**	**0.8**	***								
U	**0.5**													**0.4**	**0.4**	***							
V					**0.7**	**0.5**							**0.6**	**0.5**	**0.6**	**0.5**	***						
W	**0.8**	**0.7**		*-0.8*	**0.6**	**0.9**	*-0.8*		**0.7**	**0.8**	*-0.8*	**0.8**	**0.9**	**0.9**	**0.8**		**0.4**	***					
Zn	**0.6**	**0.6**		*-0.7*	**0.7**	**0.9**	*-0.7*		**0.7**	**0.4**	*-0.5*	**0.7**	**0.9**	**0.8**	**0.7**		**0.7**	**0.8**	***				
Zr	*-0.8*	*-0.9*	**0.4**	**0.9**	*-0.4*	*-0.7*	**0.9**		*-0.8*	*-0.8*	**0.9**	*-0.9*	*-0.6*	*-0.8*	*-0.6*			*-0.7*	*-0.5*	***			
S		*-0.7*		**0.7**	*-0.7*	*-0.8*	**0.8**		*-0.8*		**0.6**	*-0.7*	*-0.7*	*-0.7*	*-0.6*		*-0.6*	*-0.6*	*-0.8*	**0.5**	***		
OC	**0.9**	**0.8**		*-0.9*	**0.4**	**0.8**	*-0.8*		**0.8**	**0.8**	*-0.9*	**0.8**	**0.7**	**0.7**	**0.8**			**0.9**	**0.7**	*-0.8*	*-0.5*	***	
S1	**0.8**	**0.8**		*-0.9*	**0.4**	**0.7**	*-0.9*		**0.7**	**0.8**	*-0.9*	**0.8**	**0.7**	**0.7**	**0.8**			**0.8**	**0.6**	*-0.8*	*-0.5*	**1.0**	***

* Only correlation coefficients significant at 95% confidence limit ($p<0.05$ at 0.40; n=22) are shown.
** Negative correlations are shown in *Italic*.

Subsequently, the elemental contents tend to return to low concentrations towards the sediment-water-interface (SWI) (Figures 3.1-3.2), possibly due to the more recent decreases in emissions of the power plants or the dissolution of elements near SWI. Elemental output by the power plants has gradually declined in recent years due to the introduction of emission control systems.

3.4.1.2. Early diagenesis processes

Without taking the elemental mobility and porewater-sediment interactions into account, the variations of elements throughout the sediments can be well explained by the emission history of the coal-fired power plants in the study area. However, the study of porewater suggests that complex geochemical processes may also have a role in the observed elemental distributions in the studied sediment profiles. The results of the porewater analyses indicate the increased concentrations of dissolved As, Sb, Cu, Mo, Pb, and Zn at deeper sections of WAB1 and WAB2 porewater profiles (Figures 3.3-3.4). This suggests that the diagenetic dissolution/diffusion of these elements may have occurred at depth, thus acting as a conveyor of elements to the upper part of the sediment profile. This can partly contribute to the elevated concentrations of trace elements near the surface sediments (Figures 3.3-3.4), which are often attributed solely to the activities of power plants in this region.

The strong positive correlation between trace elements, Ca and organic matter (OM) in sediments from Wabamun Lake (Tables 3.9-3.10) suggest that the Ca-OM fraction, combined together, play a major role as substrate for trace elements and nutrient (P) in

Wabamun Lake. The cycle of metals in Wabamun Lake may also involve other geochemical processes such as Fe/Mn redox and sulphides fraction. The strong correlation between Mn and trace metals seen in the sediment profiles (especially WAB2 core) is in contrast with Fe and S which show little correlation with metals in the Wabamun Lake sediment cores (Tables 3.9-3.10). This can be explained by the fact that there is little reactive iron and sulphur available in such eutrophic, alkaline lakes to allow any significant effect by these geochemical fractions (Prepas et al., 2001; Riley and Prepas, 1984). The strong positive correlation between the temporal distribution of Fe and S with that of lithophilc Zr (Tables 3.9-3.10) suggests the dominance of non-reactive Fe and S with geogenic sources in Wabamun Lake sediments.

The effects of Ca and OM fractions in the distribution of metals in Wabamun Lake sediments are described as follows:

3.4.1.2.1. The effect of organic matter in the distribution of trace elements

The significant correlation between temporal distribution of metals and labile organic matter (S1-OM) in the Wabamun Lake sediments (Tables 3.9-3.10) suggest that organic matter plays an important role in the distribution of metals throughout the sediment profile (Chapters 7-8). The contributing metals in biological structures are transported from the water column to the bottom sediments with the deposition of phytoplankton (Hamilton-Tayler et al., 1984; Sigg, 1986; Sigg et al., 1987; Morfett et al., 1988; Gerringa, 1990; Balistrieri et al., 1992; Lee and Fisher, 1992). After deposition, these metals are subsequently

released into the water during the anaerobic degradation of organic matter (which contains these metals) (Morfett et al., 1988; Gerringa, 1990; Sigg, 1986). The freshwater sediments from Wabamun Lake have high organic carbon contents (13.2-16.6%) (Table 3.1-3.2). As a result, O_2 is rapidly consumed in the surface layer in freshwater sediments and hence anoxic conditions dominate the geochemical processes in such sediments (Jørgensen, 1983; Carignan and Nriagu, 1985; Schwedhelm et al., 1988; Vuynovich, 1989; Williams, 1992) (Appendix B). The degradation of labile organic matter is most intensive in the deeper sediments, as seen by the rapid reduction of labile organic matter with depth in both WAB1 and WAB2 sediment profiles (Figures 3.1-3.2; Chapter 7).

Degradation of organic matter in the deeper part of the sediment profile may result in an increased release of organic colloids (e.g. humic substances) into the porewater profile (Orem et al., 1986; Chin and Gschwend, 1991; Vuynovich, 1989). The coexistence of organic ligands (e.g. humic substances) and metal ions in porewater solutions often results in the formation of highly soluble organic complexes (Elderfield, 1981; Boulegue et al., 1982; Gerringa, 1990; Forstner and Wittmann, 1979; Park and Huang, 1989). This formation of metal-organic-complexes in the porewater column may result in the mobilization of trace elements during early diagenesis (Elderfield, 1981; van den Berg and Dharrnvanij, 1984; Douglas et al., 1986). The elements released from the bottom sediment layer diffuse into the porewater and may potentially move upward following their concentration gradients (Figures 3.3-3.4) (Song and Müller, 1999).

Figure 3.3. The distribution of trace metals and calcium between sediments and porewater throughout the WAB1 core.

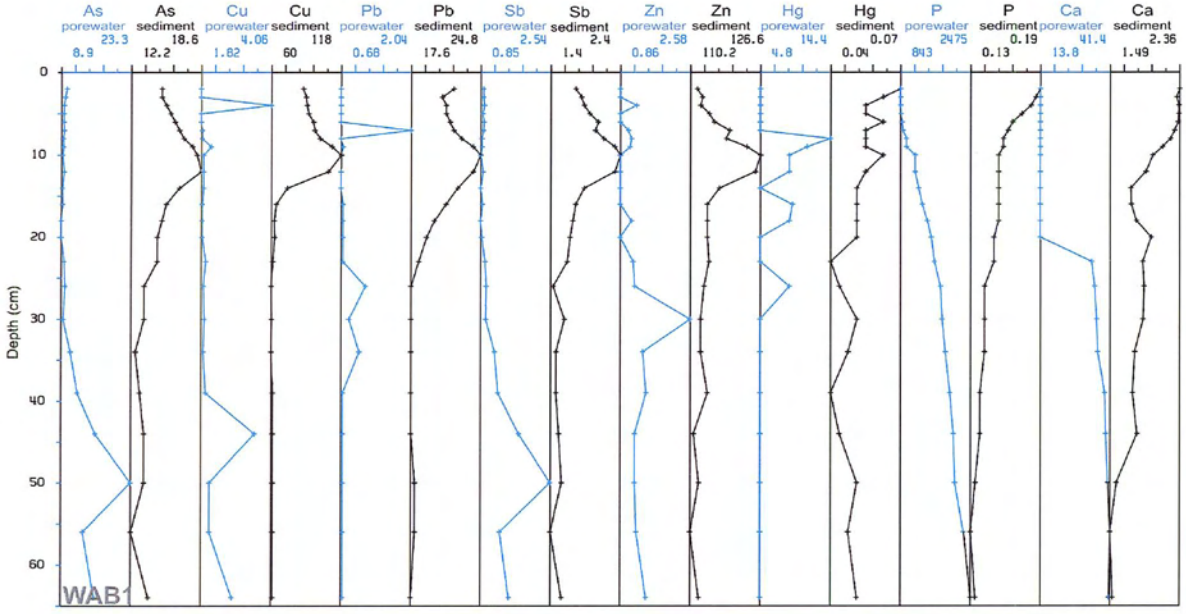

Figure 3.4. The distribution of trace metals and calcium between sediments and porewater throughout the WAB2 core.

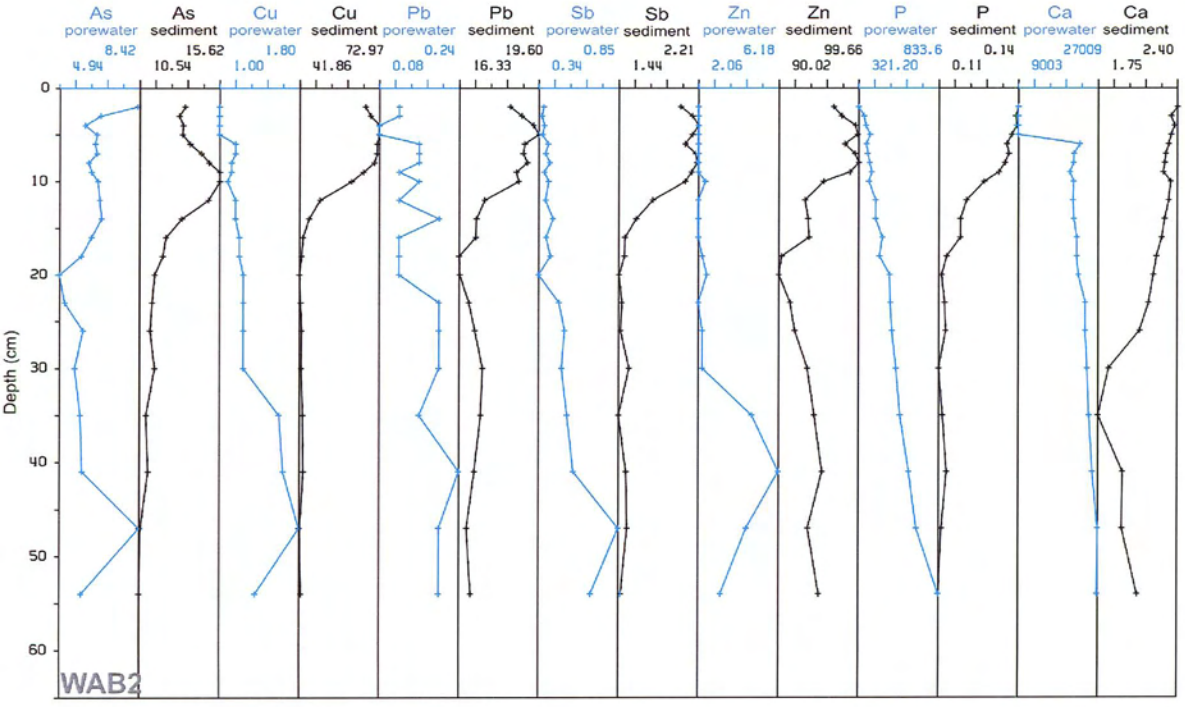

The dissolved metals released from organic degradation may become re-adsorbed on sediment particles at the upper sediment layer through various processes such as re-adsorption on freshly deposited organic matter, co-precipitation with Fe/Mn oxides and Ca-precipitation. This leads to the enrichment of elements in the upper part of the sediment profile and consequently the depletion of elements in deeper porewater (Figures 3.3-3.4).

3.4.1.2.2. Effect of Ca-minerals in distribution of trace elements

The significant positive correlations between Ca and trace metals (As, Cu, Cr, Hg, Mo, Pb, Sb, Se, and Zn) in Wabamun Lake sediment (Tables 3.9-3.10) are partly due to their association in power plant fly ash, but also may be due to diagenetic processes within the sediment column. Calcium in the form of lime (CaO, $CaCO_3$, $Ca(OH)_2$) is known to be an important substrate for trace elements, specifically in a hard water lake with a neutral pH such as Wabamun Lake (Chapter 3.4.5; Cowan et al., 1991; Tipping, 1993; Marinsky et al., 1999; Lyth et al., 2003; Sholkowitz, 1976; Sholkowitz and Copland, 1981.

The effects of calcium dissolution /precipitation may also be interrelated with the effects of organic matter diagenesis in the cycling of trace elements in sediments and porewater. The mineralization of organic matter releases CO_2 and NH_3 into porewater (mainly due to methanogenesis bacteria; Appnedix B). This process can change the precipitation/dissolution and adsorption/desorption equilibrium of Ca between sediments and porewater (Song and Müller, 1999; Kim et al., 2001):

$$CaCO_3 + CO_2 + H_2O \rightarrow CaHCO_3^+ + HCO_3^-$$

$$Ca^{2+}\text{-Clay} + NH_3 + CO_2 + H_2O \rightarrow NH_4^+\text{-Clay} + Me^+ + HCO_3^-$$

The dissolution of Ca in deeper sediment results in the release of trace elements attached to Ca-minerals into the porewater (Figures 3.3-3.4). The dissolved metals may migrate upward in the column and immobilize again due to re-precipitation of calcium minerals in the upper section of the sediment profiles (Figures 3.3-3.4) (Chapter 3.4.5; Cowan et al., 1991; Tipping, 1993; Marinsky et al., 1999; Lyth et al., 2003, Sigg, 1986; Sigg et al., 1987). Precipitation of Ca is confirmed by SEM/EDX analyses of surficial sediments from Wabamun Lake (Chapter 5.2.2.1). Any changes in physicochemical conditions (e.g. Eh-pH) of the sediments causing alteration of the equilibrium of precipitation/dissolution may lead to a redistribution of trace elements between the sediments and the porewater (Kersten et al., 1985; Wallmann, 1990; Gambrell et al., 1991; Calmano et al., 1992).

The addition of carbonates through the emission of calcareous fly ash into Wabamun Lake may serve as liming treatment for precipitation of sparingly soluble trace metal compounds and dissolved nutrients (Chapter 3.4.5) (Vanderploeg et al., 1987; Koschel, 1997; Otsuki and Wetzel, 1972; Koschel et al., 1983; Murphy et al., 1983; Cowan et al. 1991; Tipping, 1993; Marinsky et al. 1999; Prepas et al., 2001; Lyth et al., 2003).

Appendix A provides a detailed breakdown of each metal as related to their temporal distributions found in the porewater and sediments of Wabamun Lake.

3.4.2. Trace elements in sediments and porewater from Isle Lake

The depth profile of metals in the sediment from Isle Lake shows three distinct groups. The first group of metals consists of Pb and Hg, with profiles similar to those in Wabamun and LSA lakes, showing typical surface enrichment (Figures 3.5). The increase in concentration of these elements occurs below the depth corresponding to onset of coal-fired power generating in the Wabamun area (depth 14 cm = 1956) (Figures 3.5).

The depth profile of Pb and Hg in the Isle Lake sediment cores show significant positive correlation to the temporal distributions of labile organic matter (S1-OM) and calcium-associated elements (Ba, and Sr) (Figures 3.5; Tables 3.11). This indicates that the temporal distributions of Pb and Hg in sediments are likely to be controlled by combining effects of processes such as precipitation-dissolution of calcium compounds and metal-organic-complex reactions. Carbonates are known to be substrates for lead in lake sediment (Todorović et al., 2001).

Figure 3.5. The temporal distribution of elements and organic matter throughout the ISLE sediment profile as related to the ^{210}Pb-dates of the sediments.

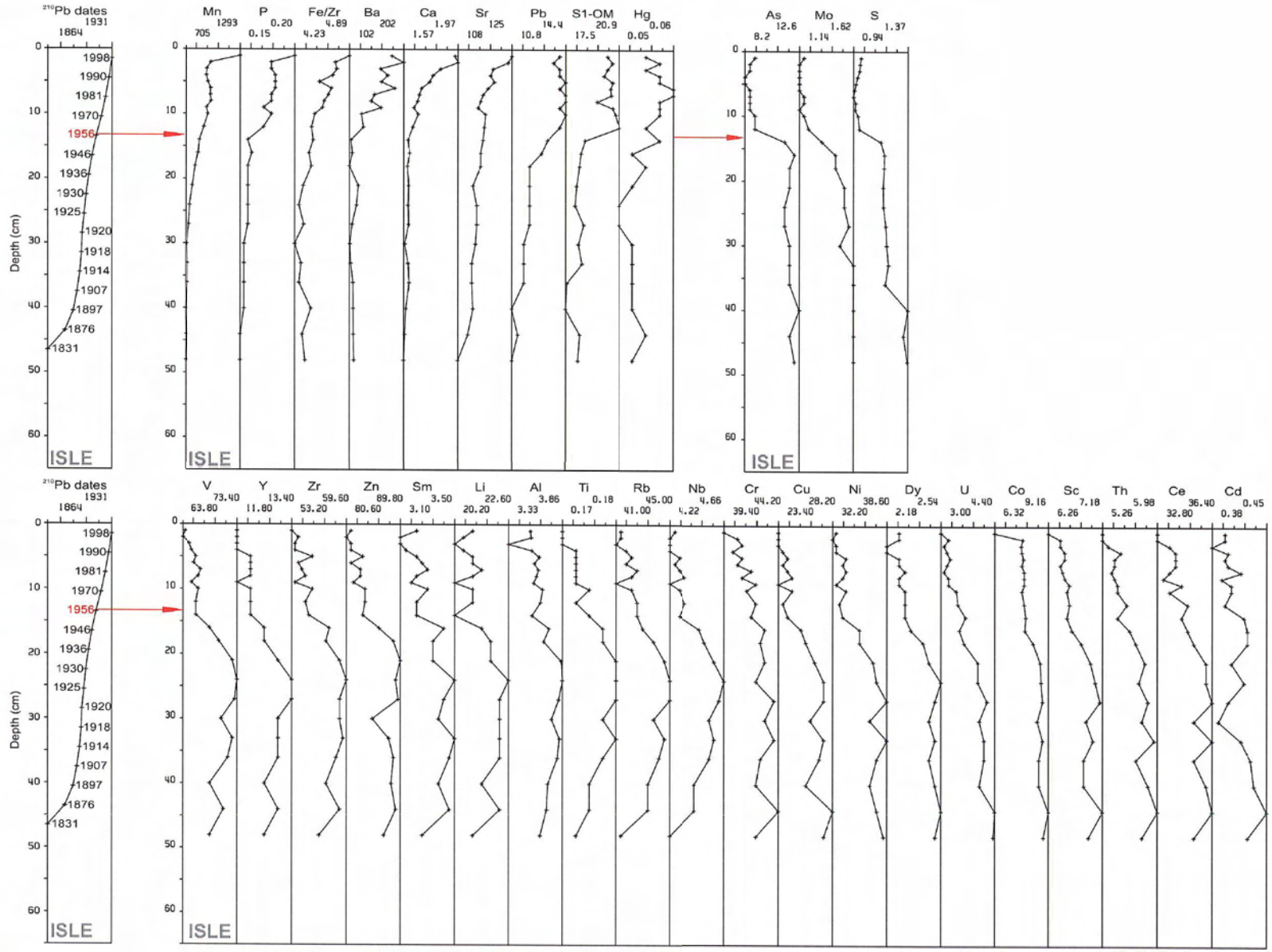
210Pb dates
1864
1931
1998
1990
1981
1970
1956
1946
1936
1930
1925
1920
1918
1914
1907
1897
1876
1831
Depth (cm)
ISLE
Mn
P
Fe/Zr
Ba
Ca
Sr
Pb
S1-OM
Hg
As
Mo
S
V
Y
Zr
Zn
Sm
Li
Al
Ti
Rb
Nb
Cr
Cu
Ni
Dy
U
Co
Sc
Th
Ce
Cd

Table 3.11. The Spearman correlation matrix for the elements and organic content of the sediments in ISLE core.

	Al	As	Ca	Cd	Co	Cr	Cs	Cu	Fe	Hg	K	Li	Mn	Mo	Ni	P	Pb	Rb	Sb	Sc	Sr	Th	Ti	U	V	W	Y	Zn	Zr	S	C	TOC	S1
Al	***																																
As	**0.6**	***																															
Ca	*-0.7*	*-0.8*	***																														
Cd	**0.5**	**0.7**	*-0.6*	***																													
Co	**0.8**	**0.7**	*-0.9*	**0.6**	***																												
Cr	**0.8**	**0.7**	*-0.8*	**0.5**	**0.8**	***																											
Cs	**1.0**	**0.6**	*-0.7*	**0.5**	**0.8**	**0.8**	***																										
Cu	**0.8**	**0.7**	*-0.8*	**0.6**	**0.9**	**0.8**	**0.9**	***																									
Fe									***																								
Hg	*-0.8*	*-0.7*	**0.6**		*-0.7*	*-0.7*	*-0.8*	*-0.7*		***																								
K	**0.6**					**0.5**	**0.6**			*-0.4*	***																							
Li	**0.9**	**0.6**	*-0.6*	**0.4**	**0.7**	**0.7**	**0.9**	**0.9**	**0.4**	*-0.7*	**0.5**	***																					
Mn	*-0.7*	*-0.8*	**0.9**	*-0.6*	*-0.9*	*-0.8*	*-0.7*	*-0.8*		**0.8**		*-0.7*	***																				
Mo	**0.8**	**0.8**	*-0.8*	**0.6**	**0.9**	**0.7**	**0.8**	**0.9**		*-0.8*		**0.8**	*-0.9*	***																			
Ni	**0.9**	**0.6**	*-0.8*	**0.6**	**0.9**	**0.8**	**0.9**	**1.0**		*-0.7*	**0.4**	**0.9**	*-0.8*	**0.9**	***																		
P	*-0.7*	*-0.8*	**0.9**	*-0.6*	*-0.9*	*-0.8*	*-0.7*	*-0.8*		**0.7**		*-0.6*	**0.9**	*-0.9*	*-0.8*	***																		
Pb	*-0.6*	*-0.8*	**0.8**	*-0.5*	*-0.8*	*-0.7*	*-0.6*	*-0.7*		**0.8**		*-0.6*	**0.9**	*-0.8*	*-0.7*	**0.9**	***																
Rb	**0.9**	**0.6**	*-0.6*	**0.4**	**0.7**	**0.7**	**0.9**	**0.7**		*-0.7*	**0.7**	**0.8**	*-0.6*	**0.8**	**0.8**	*-0.6*	*-0.5*	***															
Sb	**0.6**	**0.6**	*-0.7*	**0.4**	**0.7**	**0.7**	**0.6**	**0.7**		*-0.6*		**0.5**	*-0.7*	**0.6**	**0.6**	*-0.8*	*-0.6*	**0.5**	***														
Sc	**0.9**	**0.7**	*-0.8*	**0.6**	**0.9**	**0.9**	**0.8**	**0.9**		*-0.8*	**0.4**	**0.8**	*-0.9*	**0.8**	**0.9**	*-0.9*	*-0.8*	**0.8**	**0.8**	***													
Sr	*-0.7*	*-0.7*	**0.9**	*-0.6*	*-0.9*	*-0.8*	*-0.7*	*-0.9*		**0.6**		*-0.7*	**0.9**	*-0.8*	*-0.8*	**0.9**	**0.8**	*-0.6*	*-0.7*	*-0.9*	***												
Th	**0.8**	**0.7**	*-0.8*	**0.6**	**0.9**	**0.9**	**0.8**	**0.8**		*-0.8*		**0.7**	*-0.9*	**0.8**	**0.9**	*-0.9*	*-0.8*	**0.7**	**0.7**	**1.0**	*-0.9*	***											
Ti	**1.0**	**0.7**	*-0.7*	**0.5**	**0.8**	**0.8**	**0.9**	**0.9**		*-0.8*	**0.7**	**0.9**	*-0.7*	**0.8**	**0.9**	*-0.7*	*-0.6*	**0.9**	**0.7**	**0.9**	*-0.7*	**0.8**	***										
U	**0.8**	**0.7**	*-0.9*	**0.6**	**0.9**	**0.8**	**0.8**	**0.9**		*-0.8*		**0.7**	*-0.9*	**0.9**	**0.9**	*-0.9*	*-0.8*	**0.7**	**0.7**	**0.9**	*-0.9*	**0.9**	**0.8**	***									
V	**0.9**	**0.6**	*-0.8*	**0.5**	**0.9**	**0.8**	**1.0**	**0.9**		*-0.8*	**0.6**	**0.9**	*-0.7*	**0.8**	**0.9**	*-0.7*	*-0.6*	**0.9**	**0.7**	**0.9**	*-0.8*	**0.8**	**1.0**	**0.8**	***								
W	**0.6**					**0.5**	**0.6**	**0.4**			**0.6**	**0.5**			**0.4**			**0.5**		**0.4**			**0.6**		**0.6**	***							
Y	**0.9**	**0.6**	*-0.8*	**0.6**	**0.9**	**0.8**	**0.9**	**0.9**		*-0.8*	**0.6**	**0.9**	*-0.8*	**0.8**	**0.9**	*-0.7*	*-0.7*	**0.9**	**0.6**	**0.9**	*-0.8*	**0.9**	**1.0**	**0.9**	**1.0**	**0.5**	***						
Zn	**0.9**	**0.7**	*-0.8*	**0.6**	**0.9**	**0.8**	**0.9**	**0.9**		*-0.8*	**0.5**	**0.8**	*-0.8*	**0.9**	**0.9**	*-0.8*	*-0.7*	**0.8**	**0.7**	**0.9**	*-0.8*	**0.9**	**0.9**	**0.9**	**0.9**		**0.9**	***					
Zr	**0.9**	**0.6**	*-0.8*	**0.5**	**0.9**	**0.8**	**0.9**	**0.9**		*-0.8*	**0.6**	**0.9**	*-0.8*	**0.8**	**0.9**	*-0.8*	*-0.7*	**0.9**	**0.7**	**0.9**	*-0.7*	**0.8**	**1.0**	**0.9**	**0.9**	**0.5**	**1.0**	**0.9**	***				
S	**0.6**	**0.9**	*-0.8*	**0.5**	**0.8**	**0.7**	**0.6**	**0.7**		*-0.8*		**0.6**	*-0.9*	**0.9**	**0.7**	*-0.9*	*-0.9*	**0.5**	**0.6**	**0.7**	*-0.7*	**0.8**	**0.6**	**0.8**	**0.6**		**0.7**	**0.7**	**0.7**	***			
C											*-0.4*																				***		
TOC										*-0.5*		**0.4**								**0.4**												***	
S1	*-0.6*	*-0.8*	**0.7**	*-0.6*	*-0.7*	*-0.6*	*-0.7*	*-0.7*		**0.7**		*-0.7*	**0.8**	*-0.8*	*-0.7*	**0.7**	**0.8**	*-0.6*	*-0.5*	*-0.7*	**0.7**	*-0.7*	*-0.7*	*-0.7*	*-0.7*		*-0.7*	*-0.7*	*-0.7*	*-0.8*			***

* Only correlation coefficients significant at 95% confidence limit ($p<0.05$ at 0.39; n=23) are shown.

** Negative correlations are shown in *Italic*.

The depth profiles of dissolved Pb in the Isle Lake porewater shows enrichment in the bottom part of the profile, possibly due to the dissolution process (Figures 3.6). An increase in the concentrations of dissolved metals in the deeper section of porewater profile is likely due to the dissolution of carbonates (Figures 3.6). The concentrations of dissolved Pb tend to decrease towards the upper section of the porewater profile (Figures 3.6). This suggests that the dissolved Pb is gradually being fixed towards the upper section of the profile. The decreasing concentration of Pb near SWI could also be related to the reduced input from external sources such as the local power plant emission or even global reduction of leaded fuel.

The effects of redox-sensitive Fe/Mn may also mask the effects of the Ca-OM fraction on the distribution of metals. This is evident by a similar depth profile for metals and Fe/Mn in the ISLE sediment column (Figures 3.5; Tables 3.11). The close association of Hg with organic matter and Fe/Mn oxides is also well documented in relevant literature (El Bilali et al., 2002 and references therein). The mobility of metals, particularly in the upper sections of the porewater profile (Figure 3.6), is likely due to the reduction of Mn oxides resulting in the release of the metals (e.g., Co) into the porewater (Francis and Dodeg, 1990).

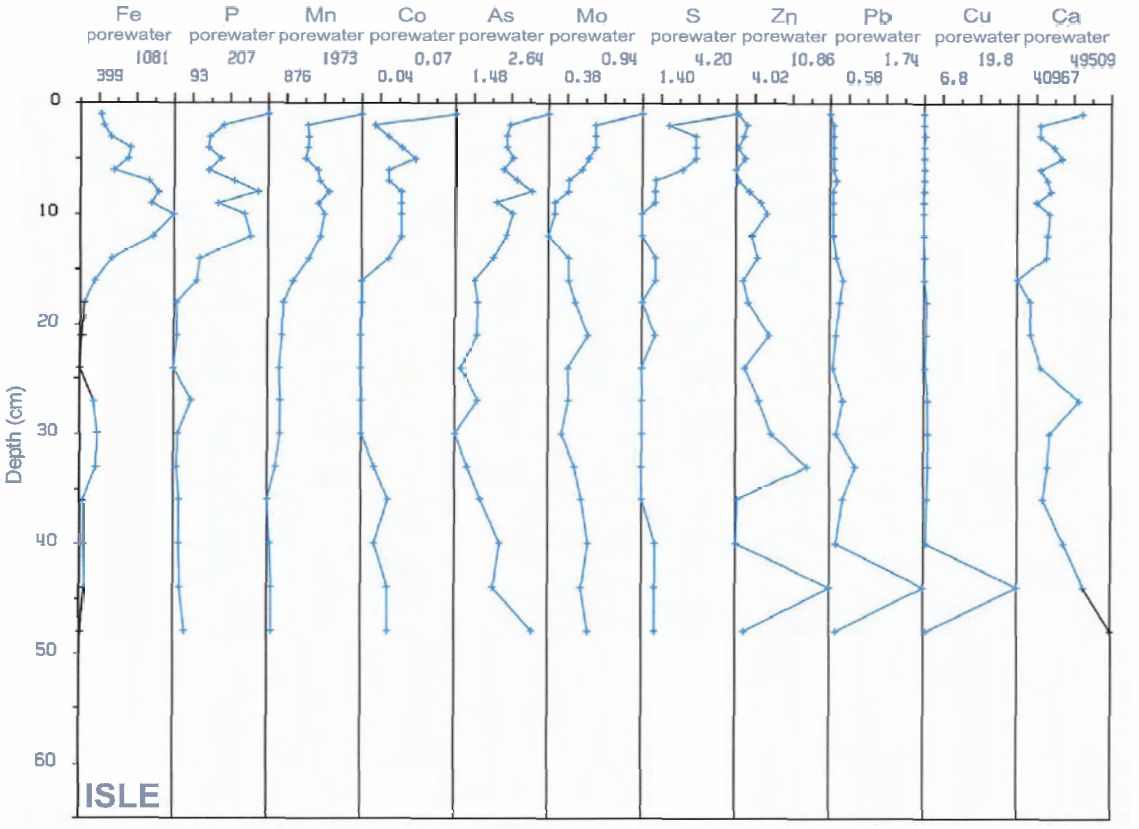

Figure 3.6. The temporal distribution of dissolved trace metals and other major elements throughout the ISLE porewater profile.

The second group of metals consists of As and Mo, both of which have depth profiles significantly similar to that of the total sulphur in the Isle Lake sediment core (Figures 3.5; Tables 3.11). Dissolved As and Mo are possibly precipitated as metal-sulfides at the sulphate reduction zone where HS^- is more available (Chapter 3.4.7 and Appendix B) (Moore et al., 1988). This is supported by strong similarities between the depth profiles of As, Mo, and total S in both sediment and porewater profiles (Figures 3.5-3.6; Table 3.11).

The third group of metals includes Zn, Cu, Cd, Ni, Cr, and Co, which follow the same patterns as lithophilic elements (e.g., Sc, Th, Rb, Al, Ti, Rare Earth Elements (REEs))

(Figures 3.5; Table 3.11). This suggests that the input of these metals into the bottom sediments from Isle Lake is mainly controlled by geogenic sources.

3.4.3. Trace elements in sediments and porewater from Lac Ste. Anne

The concentrations of metals throughout the sediment profile from LSA are shown in Figure 3.7. Lead and Hg show surface enrichments in their depth profiles. The depth in which the concentrations of these metals increase does not correspond well to the onset of coal-fired generating activities in the region as marked by ^{210}Pb data. There is a significant positive correlation between the depth profiles of Pb with that of Ca (and associated elements e.g., Sr) (Figure 3.7 and Table 3.12). This indicates that carbonates are substrates for lead in the LSA sediment core (Todorović et al., 2001). Lead found in association with carbonate minerals is more stable in solid compounds and less likely to be mobilized by biological activity (Todorović et al., 2001). Additionally, the temporal distribution of Hg shows significant positive correlation to Mn and organic matter (TOC and S1-OM) (Table 3.12 and Figure 3.7). This suggest that diagenesis of organic matter combined with the redox reactions involving Mn oxide may control temporal distribution of Hg in the LSA sediment core.

Figure 3.7. The temporal distribution of elements and organic matter throughout the LSA sediment profile as related to the ^{210}Pb-dates of the sediments.

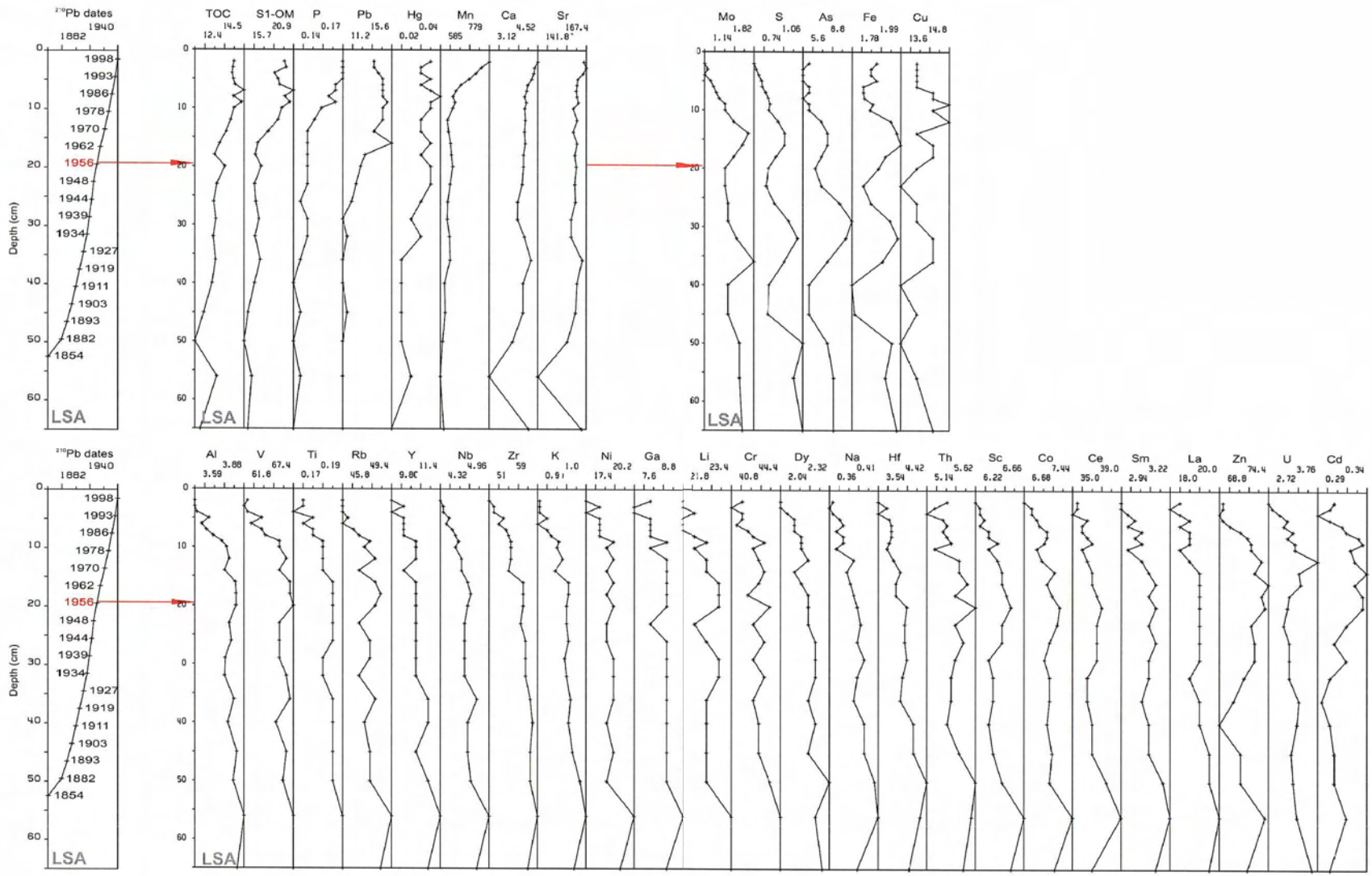
210Pb dates
1882
1940
1998
1993
1986
1978
1970
1962
1956
1948
1944
1939
1934
1927
1919
1911
1903
1893
1882
1854
Depth (cm)
LSA
TOC
S1-OM
P
Pb
Hg
Mn
Ca
Sr
Mo
S
As
Fe
Cu
Al
V
Ti
Rb
Y
Nb
Zr
K
Ni
Ga
Li
Cr
Dy
Na
Hf
Th
Sc
Co
Ce
Sm
La
Zn
U
Cd

Table 3.12. The Spearman correlation matrix for the elements and organic content of the sediments in LSA core.

	Al	As	Ca	Cd	Co	Cr	Cs	Cu	Fe	Hg	K	Li	Mn	Mo	Na	Ni	P	Pb	Rb	Sb	Sc	Sr	Th	Ti	U	V	W	Y	Zn	Zr	S	C	TOC	S1
Al	***																																	
As	0.6	***																																
Ca	*-0.6*	*-0.6*	***																															
Cd				***																														
Co	0.8	0.6	*-0.6*		***																													
Cr	0.7	0.7	*-0.6*		0.7	***																												
Cs	0.7	0.8	*-0.5*		0.6	0.7	***																											
Cu							0.4	***																										
Fe		0.7				0.4	0.6		***																									
Hg	*-0.5*	*-0.5*		0.5						***																								
K	0.9	0.7	*-0.6*		0.7	0.7	0.7			*-0.6*	***																							
Li	0.7	0.8	*-0.5*		0.6	0.7	0.9	0.4	0.6	*-0.5*	0.7	***																						
Mn	*-0.8*	*-0.7*	0.7		*-0.6*	*-0.7*	*-0.7*			0.7	*-0.8*	*-0.7*	***																					
Mo	0.7	0.8	*-0.5*		0.7	0.7	0.7		0.6	*-0.6*	0.8	0.7	*-0.8*	***																				
Na	0.8	0.7	*-0.8*		0.7	0.7	0.6			*-0.6*	0.9	0.6	*-0.9*	0.7	***																			
Ni	0.8	0.7	*-0.4*		0.6	0.8	0.8	0.4	0.5	*-0.5*	0.8	0.9	*-0.7*	0.8	0.7	***																			
P	*-0.8*	*-0.7*	0.7		*-0.7*	*-0.7*	*-0.5*			0.8	*-0.9*	*-0.6*	0.9	*-0.8*	*-0.9*	*-0.6*	***																			
Pb	*-0.5*	*-0.5*	0.4	0.5	*-0.5*	*-0.4*		0.4		0.8	*-0.7*	*-0.4*	0.7	*-0.5*	*-0.7*	*-0.4*	0.8	***																	
Rb	0.9	0.6	*-0.5*		0.6	0.7	0.8		0.5	*-0.4*	0.8	0.9	*-0.7*	0.7	0.6	0.8	*-0.6*		***																
Sb				0.7				0.4		0.4										***														
Sc	0.8	0.7	*-0.6*	0.4	0.9	0.8	0.7		0.5		0.8	0.7	*-0.6*	0.7	0.6	0.7	*-0.6*		0.8	0.4	***														
Sr	*-0.4*	*-0.6*	0.9		*-0.5*	*-0.4*	*-0.5*				*-0.4*	*-0.4*	0.6	*-0.4*	*-0.6*		0.5				*-0.5*	***													
Th	0.8	0.8	*-0.6*		0.8	0.8	0.6		0.5		0.8	0.7	*-0.7*	0.7	0.7	0.7	*-0.7*	*-0.4*	0.7		0.9	*-0.5*	***												
Ti	1.0	0.7	*-0.6*		0.8	0.7	0.7			*-0.5*	0.9	0.7	*-0.8*	0.7	0.8	0.8	*-0.8*	*-0.6*	0.9		0.8	*-0.4*	0.8	***											
U	0.5	0.5				0.6	0.6	0.5	0.4	*-0.4*	0.6	0.6	*-0.7*	0.8		0.6	*-0.5*		0.7		0.5		0.5	0.5	***										
V	0.9	0.7	*-0.5*		0.8	0.7	0.8	0.4	0.6	*-0.4*	0.8	0.9	*-0.7*	0.8	0.7	0.9	*-0.7*	*-0.4*	0.9		0.9	*-0.4*	0.8	0.9	0.6	***									
W	0.4	0.4							0.5	*-0.5*		0.5		0.6		0.6			0.4		0.4		0.5	0.4	0.5	0.5	***							
Y	0.9	0.7	*-0.6*		0.7	0.7	0.6			*-0.6*	1.0	0.8	*-0.8*	0.8	0.9	0.8	*-0.9*	*-0.7*	0.8		0.7	*-0.4*	0.7	0.9	0.6	0.9	0.4	***						
Zn	0.6	0.6	*-0.5*	0.8	0.6	0.5	0.7		0.5		0.4	0.6		0.5		0.5			0.7	0.5	0.8	*-0.5*	0.7	0.5	0.4	0.7		0.4	***					
Zr	0.8	0.7	*-0.7*		0.7	0.7	0.6			*-0.7*	0.9	0.7	*-0.9*	0.7	0.9	0.8	*-0.9*	*-0.7*	0.7		0.6	*-0.5*	0.6	0.9	0.5	0.7	0.4	0.9		***				
S	0.6	0.9	*-0.5*		0.6	0.7	0.8		0.7	*-0.6*	0.7	0.8	*-0.8*	0.9	0.7	0.8	*-0.7*	*-0.5*	0.7		0.7	*-0.6*	0.7	0.7	0.7	0.7	0.5	0.8	0.5	0.7	***			
C	*-0.8*	*-0.7*	0.6		*-0.6*	*-0.6*	*-0.5*			0.8	*-0.8*	*-0.6*	0.8	*-0.6*	*-0.9*	*-0.6*	0.9	0.8	*-0.7*		*-0.6*	0.4	*-0.7*	*-0.8*		*-0.6*		*-0.8*		*-0.8*	*-0.6*	***		
TOC	*-0.7*	*-0.7*	0.6		*-0.6*	*-0.5*	*-0.5*			0.8	*-0.8*	*-0.6*	0.8	*-0.7*	*-0.8*	*-0.5*	0.9	0.8	*-0.5*		*-0.5*		*-0.6*	*-0.7*		*-0.6*		*-0.8*		*-0.8*	*-0.6*	0.9	***	
S1	*-0.8*	*-0.6*	0.6		*-0.7*	*-0.6*	*-0.5*			0.7	*-0.9*	*-0.6*	0.8	*-0.7*	*-0.9*	*-0.6*	0.9	0.8	*-0.6*		*-0.6*	0.5	*-0.7*	*-0.8*		*-0.6*		*-0.8*		*-0.8*	*-0.6*	0.9	0.9	***

* Only correlation coefficients significant at 95% confidence limit ($p<0.05$ at 0.39; n=24) are shown.

** Negative correlations are shown in *Italic*.

The depth profiles of metals such as As, Mo, Fe, and to some extent Cu, appear to be significantly similar to that of sulphur in the LSA sediment core (Figure 3.7; Table 3.12). This pattern is characterized by periodic episodes of high and low concentrations throughout the sediment profile (Figure 3.7). Under anaerobic conditions, the dissolved trace elements may react with S(-II) produced by sulfate reducing bacteria (Appendix B). This leads to the formation of insoluble metal-sulfide and hence precipitation of metals into the sediments.

Metals such as Zn, Cd, Ni, Co, and Cr show vertical patterns similar to those of geogenic elements (lithophilic elements;), as indicated by their significant positive correlations (Figure 3.7; Table 3.12).

The porewater profile in the LSA core shows a gradual increase in concentrations of dissolved As, Mo, and to a lesser extent Cu, with increasing depth (Figure 3.8). The concentration of dissolved Hg is only detectable (12-28 ppt) in the upper section of LSA porewater profile (above depth 31 cm) (Table 3.8; Figure 3.8). The depth profile of dissolved Hg shows some resemblance to that of Mn (Figure 3.8) suggesting the redox sensitive reactions involving manganese oxide may control the distribution of Hg in LSA sediments. It appears that the distributions of metals in sediment and porewater profiles from LSA are controlled by a combination of various geochemical processes as discussed in the following text.

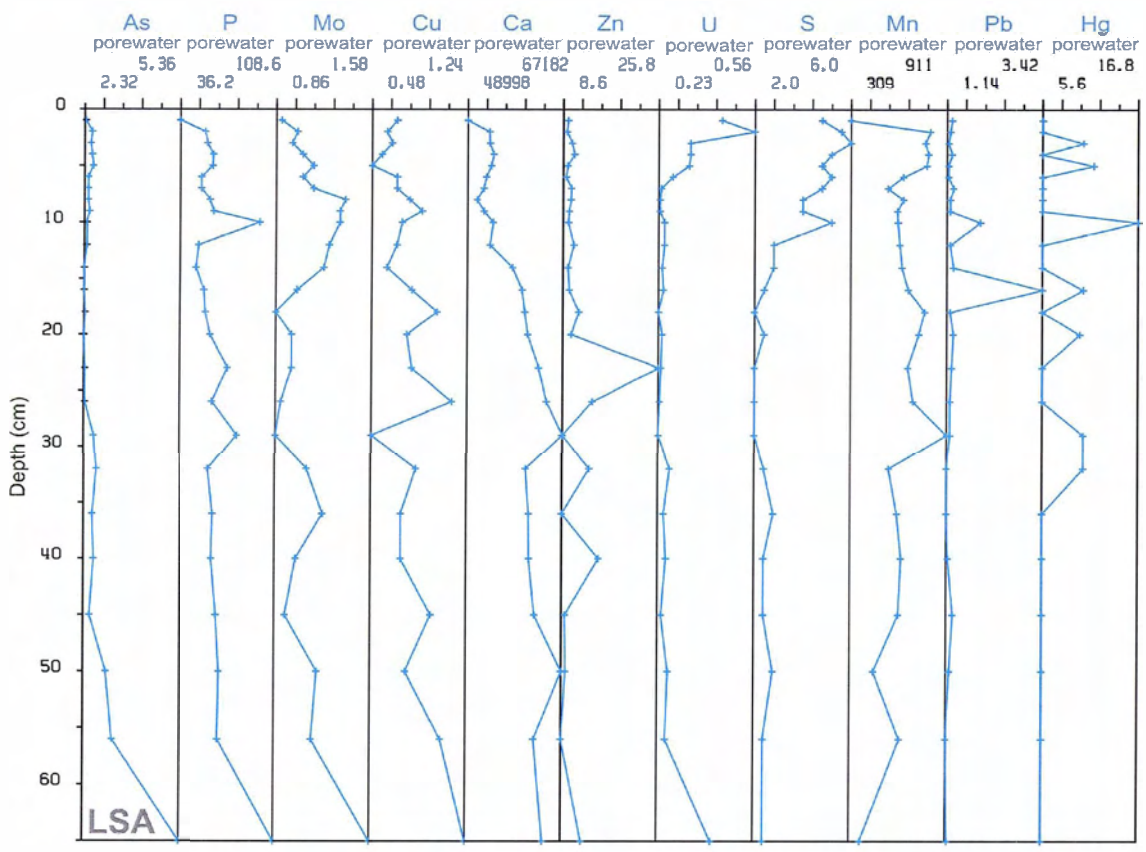

Figure 3.8. The temporal distribution of dissolved trace metals and other major elements throughout the LSA porewater profile.

3.4.4. Relationships between elements (elemental fractions) in sediments

The results of the multi-elemental analyses for the sediments were served to investigate the inter-relationships between the measured elements and various geochemical fractions. In order to define the types of association of elements, the elemental content of the sediments were correlated with the contents of various geochemical fractions' indicators such as major elements or organic matter. The grouping of elements was done by calculating the pair linear correlation coefficient between elements, and then constructing a hierarchical dendrogram

(Labonté and Goodarzi, 1985). The resulting dendrograms for Wabamun Lake, Isle Lake, and Lac Ste. Anne are shown in Figures 3.9a-d.

Based on the temporal distribution patterns, the elements in all studied sediment cores are classified into two main groups as follows:

3.4.4.1. Geogenic group

This group of elements mostly has lithophilic affinity and includes REEs, Zr, Th, Cs, Hf, Ti, Rb, Li, Sc, Co, Ni, and Y (Figures 3.9a-d). These elements show a similar temporal pattern throughout each of the sediment cores as characterized by the overall increase in concentration with increasing depth (Figures 3.1; 3.2; 3.5; 3.7).

The depth profiles of geogenic elements are inversely proportional to organic matter (S1-OM) especially in WAB1, WAB2, and LSA sediment cores (Figures 3.1; 3.2; 3.5; 3.7). This suggests that the increasing concentrations of lithophilic elements at deeper parts of the sediment cores are likely due to the decomposition of organic matter in these parts of the sediment profiles, as evident by the decreasing organic matter concentration with depth. The decomposition of organic matter in the sediment results in a larger inorganic portion and an apparent increase in the concentrations of geogenic elements (Figures 3.1; 3.2; 3.5; 3.7).

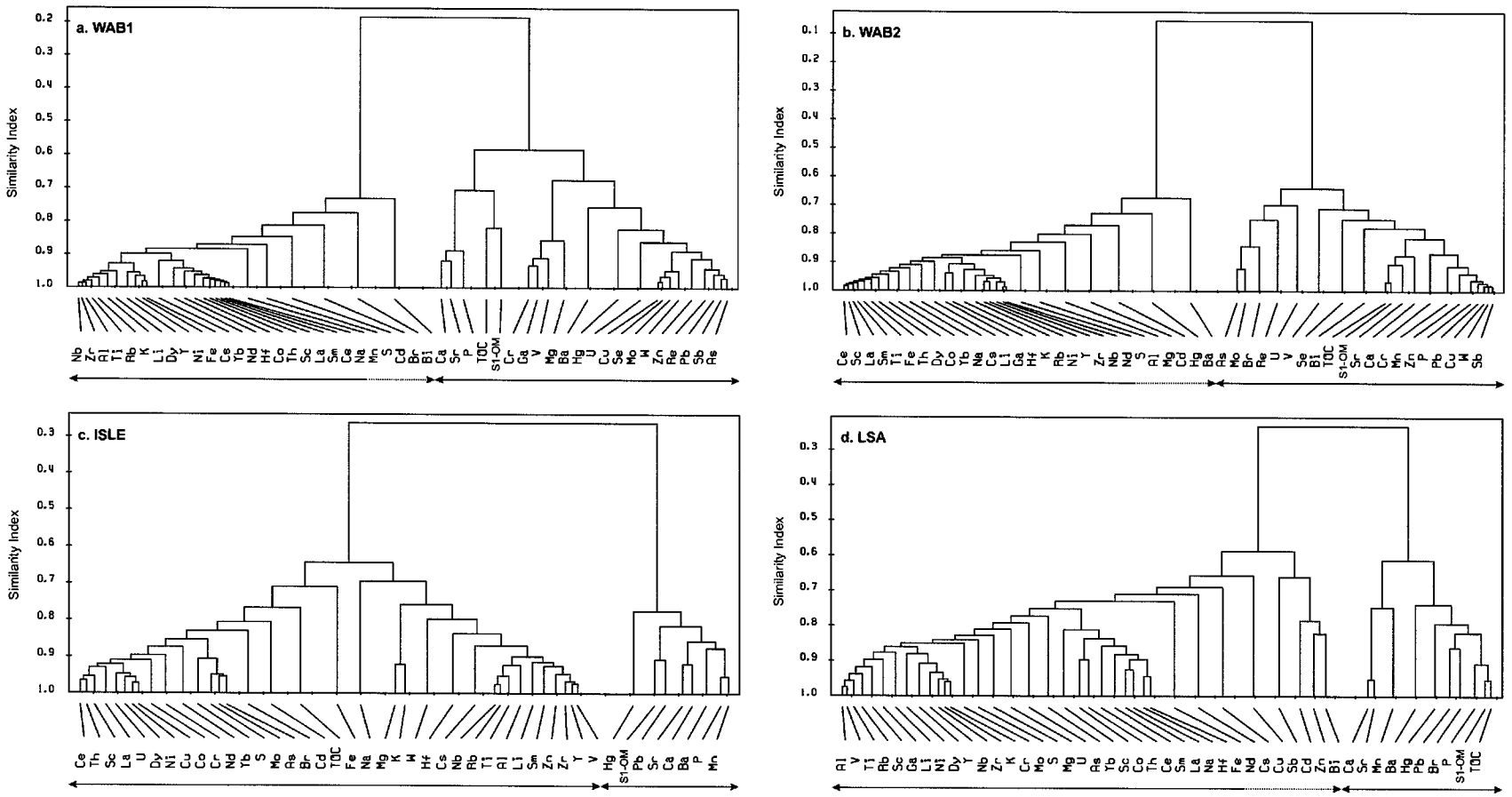

Figure 3.9.a-d. The grouping of elements based on the hierarchical dendrograms for the major, minor, trace elements, and organic content of the sediments from (a) WAB1 core, (b) WAB2 core, (c) ISLE core, and (d) LSA core.

The variation of lithophilic elements throughout the sediment profiles (Figures 3.1; 3.2; 3.5; 3.7) can also be related to factors such as fluctuation of clastic input of lithophilic elements from the drainage basins into the lake (e.g., flooding; Sanei et al, 2000; 2001), and dilution by other inorganic geochemical fractions such as carbonates and redox Fe/Mn.

3.4.4.2. Non-geogenic group

The second group of elements is associated with organic matter (S1 and/or TOC), calcium, and Mn in all studied sediment cores (Figures 3.9a-d). These elements are mainly originating from non-geogenic sources and their distribution in the sediments and porewater is likely controlled by biogeochemical reactions. In Wabamun sediment cores, this group of elements includes metals (Sb, As, Pb, Zn, Hg, Cu, Cr), carbonate-associated elements (Ba, Sr), phosphorus, and manganese (Figures 3.9a-b), which are characterized by their surface enrichment followed by decreasing concentrations with increasing depth (Figures 3.1; 3.2; 3.5; 3.7). In Isle Lake and Lac Ste. Anne sediments, only Pb, Hg, Ba, Sr, and P show affinity to this group and in contrast to Wabamun Lake, other metals are associated with geogenic elements, as shown by their dendograms (Figures 3.9c-d).

It is suggested that a combination of various biogeochemical processes may control the distribution of these elements and nutrients in sediment and porewater from the studied lakes. In this chapter, these biogeochemical processes are discussed as related to the observed elemental pattern in the studied sediments and the interrelationship between the elements and various geochemical fractions.

3.4.5. Effects of Calcium-Organic matter fraction (Ca-OM) in biogeochemistry of trace elements

The depth profiles of elements in the sediment cores from WAB1, WAB2, ISLE, and LSA are divided based on their similarities with respect to organic matter (labile S1-OM) and the carbonate fraction (Ca). This is demonstrated by the calculation of Spearman correlation coefficients between all elements, Ca, and the S1-OM (labile organic matter, see Chapter 8 for more details). The calculated correlation coefficients were plotted in a scattered graph (Figures 3.10a-d). The results for Wabamun sediment cores (WAB1 and WAB2) show the metals (Pb, Zn, Cu, Hg, As, Sb, Mo, Cr), P, W, U, V, and carbonate associated elements (Sr, Mg, and Ba) have a positive correlation to Ca and labile organic compounds (carbonate-organic fraction) (Figures 3.10a-d). In contrast, geogenic elements (Al, Cs, Zr, Ti, REEs), along with Fe, Na, Ni, S, Co, and Cd, show a negative correlation to the organic-carbonate fraction (Figures 3.10a-d).

Sediment cores from ISLE and LSA include a significantly lower number of elements in the carbonate-organic fraction as compared to the Wabamun cores (Figures 3.10a-d). Mercury, Pb, P, Mn, Ba, and Sr are positively correlated with the carbonate-organic fraction in ISLE and LSA sediments (Figures 3.10c-d). Other metals (Sb, Cr, Zn, As, Mo, Ni, and Co) show negative correlations with organic-carbonates fractions (Figures 3.10a-d).

The effect of calcium on the processes of metal retention is an important factor in especially the flocculation of metal containing particles (Lyth et al., 2003). Lyth et al., 2003 found that the addition of calcium increased the particle bound amount of metals (arsenic, copper and lead). The cycle of calcium is interrelated with the diagenesis of organic matter in biogeochemistry of trace elements in sediments and porewater. Sholkowitz (1976) and Sholkowitz and Copland (1981) showed that the increased salinity (especially Ca^{2+}) increases the trace metal removal by flocculation of trace metal-DOM (dissolved organic matter) complexes. Calcium may bind to DOM and hence prevent the formation of dissolved organic colloids, resulting instead in a formation of larger calcium induced particles, which readily precipitate (Lyth et al., 2003). Evidence of Ca-OM deposits was found in SEM/EDX images of the surficial sediments from Wabamun Lake (Chapter 5.2.2). Calcium may also compete with other metals for binding sites on solid surfaces and DOM (Cowan et al. 1991; Tipping, 1993; Marinsky et al. 1999; Lyth et al., 2003).

Deposition of Ca-rich fly ash in the studied lakes, in particular Wabamun Lake, may be beneficial partly because of the effect it has on raising the pH levels. Furthermore, the higher input of calcium in Wabamun Lake as compared to Isle Lake and Lac Ste. Anne may increase the scavenging of trace metals and nutrients (Lyth et al., 2003; Prepas et al., 2001). This effect is evident as more trace metals are correlated with the carbonate-organic fraction in Wabamun Lake than the other two studied lakes (Figures 3.10a-d).

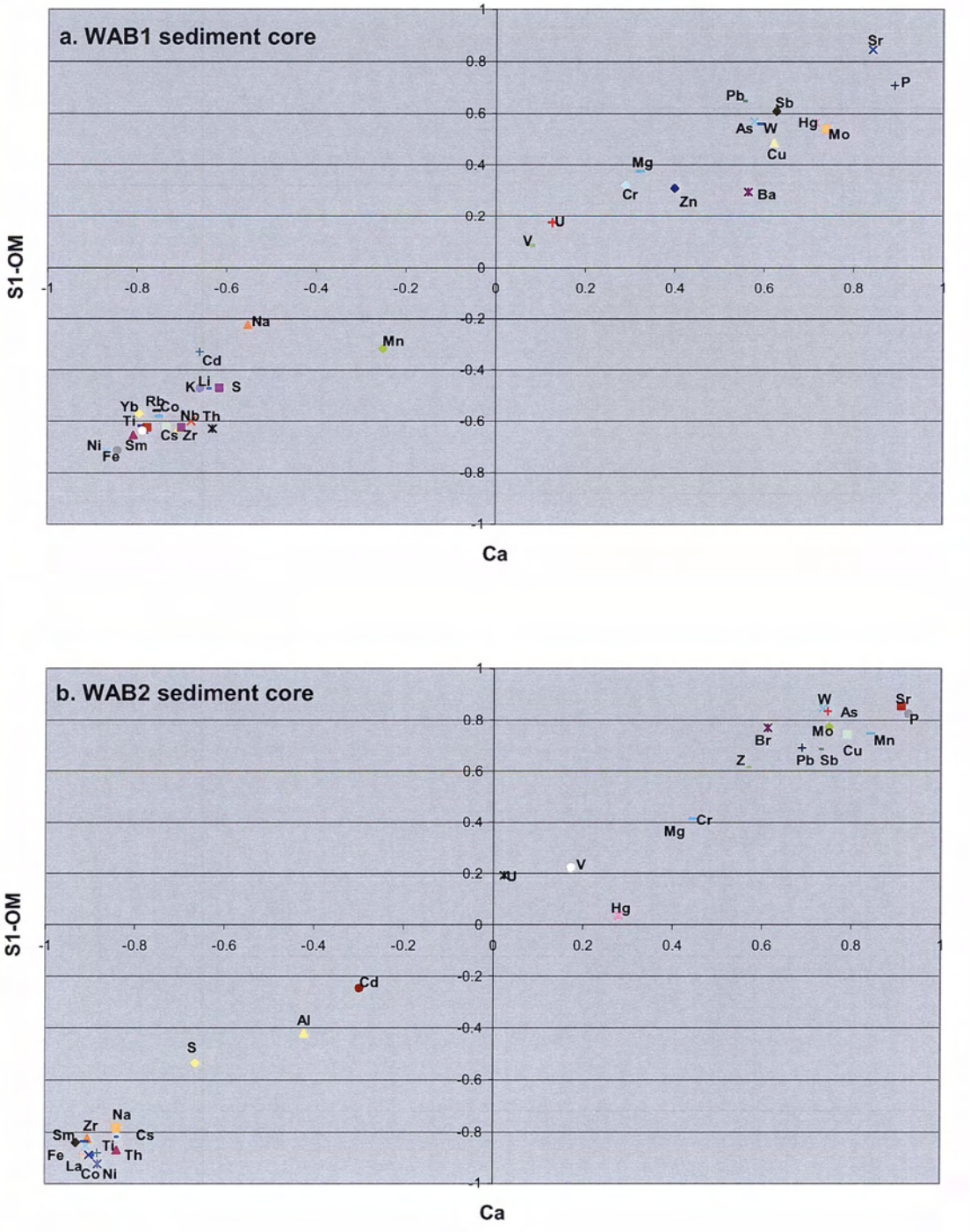

Figure 3.10.a-b. The calculated correlation coefficients (Spearman) of elements with respect to Ca and S1-OM (labile organic matter) in the sediments from (a) WAB1 core and (b) WAB2 core.

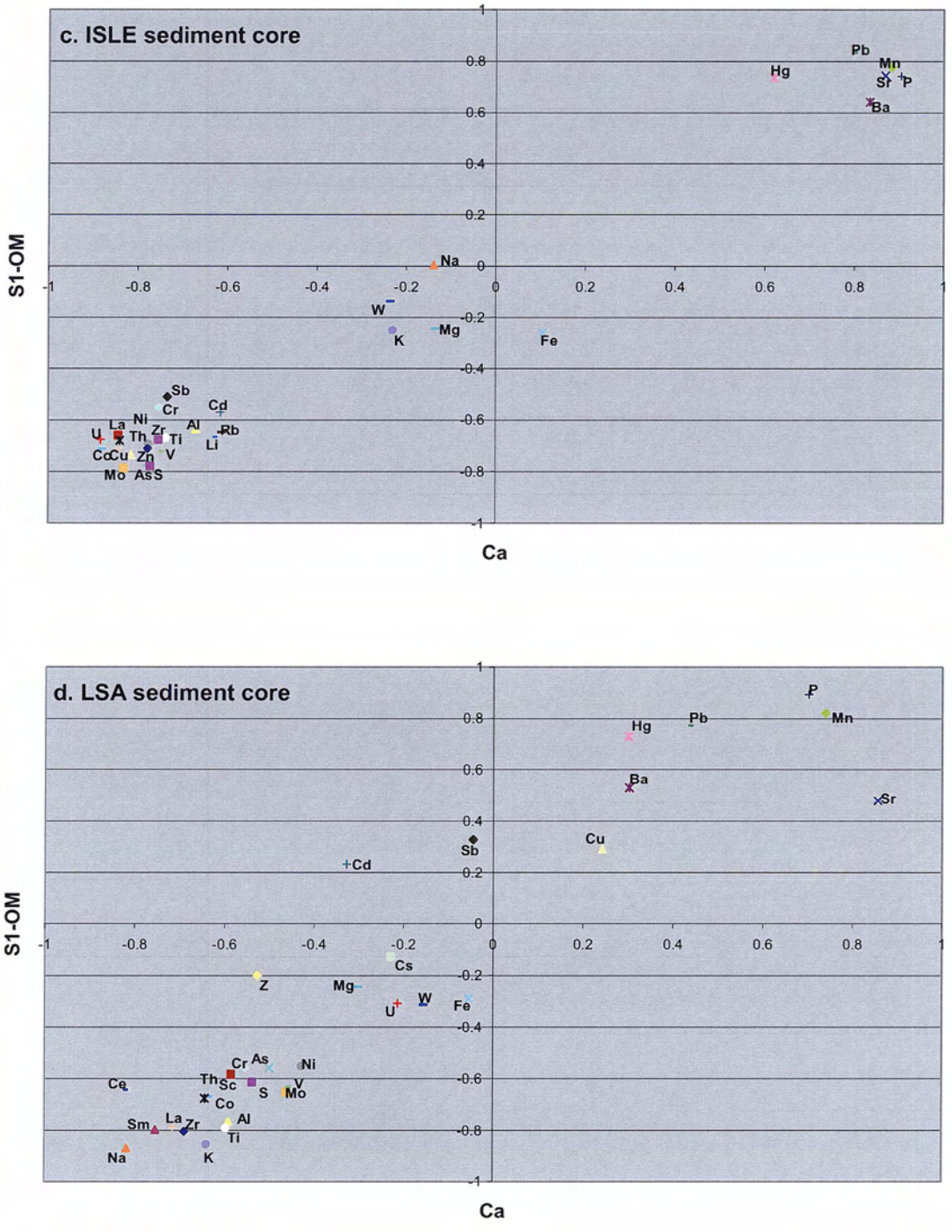

Figure 3.10.c-d. The calculated correlation coefficients (Spearman) of elements with respect to Ca and S1-OM (labile organic matter) in the sediments from (a) ISLE core and (b) LSA core.

3.4.5.1. Biogeochemical cycle of calcium in sediments and porewater

The concentrations of calcium (Ca) in each sediment profile from Wabamun Lake, Isle Lake, and Lac Ste. Anne show surficial enrichment followed by a decrease in concentration with increasing depth in the sediment core (Figure 3.11a-d). This pattern is mirrored with the dissolved Ca content of the porewater profiles from Wabamun Lake, Lac Ste. Anne, and to some extent, Isle Lake, which show increasing concentration with increasing depth (Figure 3.11a-d).

The sources of calcium into lake sediments in the study area are classified into three major groups:

- Calcium may enter the lake geogenically due to the erosion of calcium rich glacial tills covering the entire watershed in the study area (Mitchell and Prepas 1990, Kim et al., 2001).

- Calcium may be deposited in the form of calcareous fly ash into the lakes and subsequently their bottom sediments. Fly ash originating from coal combustion in Wabamun and Sundance plants are excellent sources of calcium, particularly for Wabamun Lake, which is located in their proximity.

- Calcium may also be biologically sequestered from the overlying water and deposited in surface sediment following senescence of the organisms.

- In highly productive and alkaline lakes in Central Alberta, calcium carbonate ($CaCO_3$) may precipitate as marl. This is due to high photosynthesis, which removes CO_2 from the water column and shift the following equilibrium towards production of $CaCO_3$ (Brunskill, 1969, Rosen et al., 1995):

  $Ca^{2+} + 2HCO_3^- \rightarrow CaCO_3 \downarrow + H_2O + CO_2$

  Precipitation of amorphous $CaCO_3$ is evident in SEM/EDX images of surficial sediments from Wabamun Lake (Chapter 5.2.2.1)

All the above sources may jointly contribute to the input of Ca-compounds in the studied alkaline lakes in central Alberta. However, the inverse relationship between the depth profiles of dissolved Ca in porewater and the Ca content of the studied sediments (Figure 3.11a-d), suggests that the precipitation/dissolution processes may ultimately determine the temporal distribution of Ca-compounds in the sediment profiles. The strong positive correlation between the depth profiles of Ca and labile organic matter (S1), in all studied sediment cores, suggests the possible link between geochemical cycle carbonates in the sediments and organic matter (Tables 3.9-3.12). The mineralization of organic matter in the deeper part of the sediment profile may change the chemical equilibrium (e.g., precipitation/dissolution) of carbonates between the sediments and porewater. Decomposition of organic matter by anaerobic bacteria changes the chemical equilibrium of Ca and results in the dissolution of calcium at the deeper parts of sediment profile (Figure 3.11a-d) (Chapter 3.4.1.2.2; Matisoff et al., 1981; Song and Müller, 1999). This is evident as for example; concentrations of dissolved Ca in the Wabamun Lake porewater profiles (mean

WAB1: 38.6 mg/L; WAB2: 35.7 mg/L) were substantially greater than lake-water concentrations (22 mg/L; Golder Associates, 2002) (Table 3.5-3.6). The dissolved calcium may re-precipitate as calcite ($CaCO_3$) in the upper section of sediment profile (Figure 3.11a-d) (Sigg, 1986; Sigg et al., 1987). This process constitutes a "carbon pump" that has significant implications with respect to the cycling of other elements (Dean and Schwalb, 2002).

3.4.6. Geochemical cycle of phosphorus in the sediments and porewater

The vertical distributions of phosphorus in the sediment cores from Wabamun Lake, Isle Lake, and Lac Ste. Anne follow similar patterns to that of Ca, characterized by decreasing concentration with increasing depth through the sediment profiles (Figure 3.11a-d). The highest concentration of P in the sediment profiles for all three lakes was observed near the sediment-water interface (Figure 3.11a-d). The surface enrichment of P in sediments of Wabamun Lake, Isle Lake and Lac Ste. Anne (Figure 3.11a-d) may suggest an increasing input of nutrient over the past several decades, concurrent with land-clearing and human settlement in the watershed (e.g., sewage effluent from residential and agricultural/farming activities in the lakes' watershed) (Allan et al., 1980; Reynoldson 1981; Mitchell and Prepas, 1990; Hall et al., 1999; Manning et al., 1999). Although the terrestrial input (geogenic and/or anthropogenic sources) may partly contribute towards an increase in P content of the surficial sediments in the studied lakes, the detailed examination of elemental data in the sediments and porewater suggests various geochemical processes may control the current distribution of P in this area.

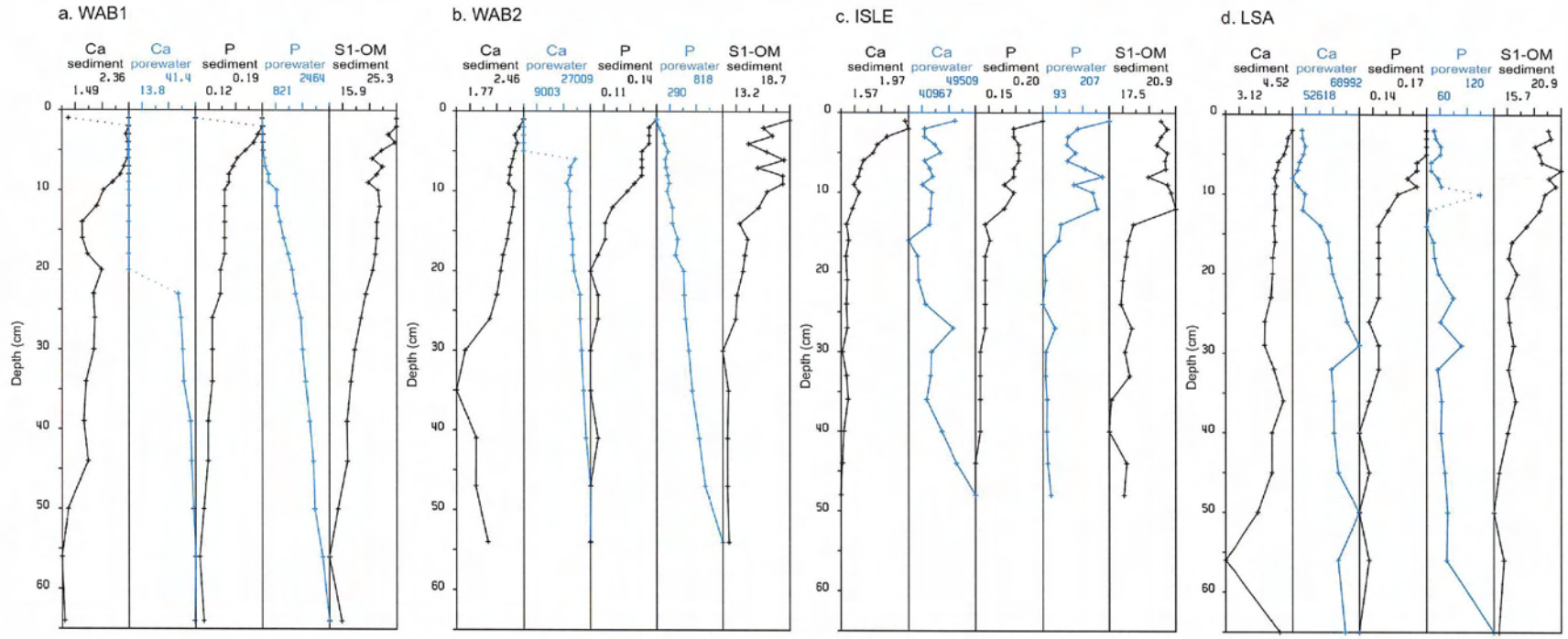

Figure 3.11.a-d. The distribution of Ca, P, and labile organic matter (S1-OM) between the sediments and porewater profiles from (a) WAB1 core, (b) WAB2 core, (c) ISLE core, and (d) LSA core.

The depth profiles of dissolved P in porewater from both Wabamun Lake and Lac Ste. Anne cores mirror those of the sediments (Figure 3.11a; 3.11b; 3.11d). The total dissolved P in Wabamun Lake and Lac Ste. Anne porewater profiles decreases towards the upper part of the core until it reaches the minimum amount at the SWI (3.11a; 3.11b; 3.11d). In contrast, the porewater profile from Isle Lake shows an enrichment of dissolved P near SWI followed by a decreasing trend with increasing depth (Figure 3.11c).

In general, the temporal distributions of P in cores from Wabamun Lake and Lac Ste. Anne illustrate the release of P into the porewater at deeper portions of the sediment columns, as well as the enrichment of P minerals in the surface sediments (Figures 3.11a; 3.11b; 3.11d). It appears that dissolved P in the upper sections of the Wabamun Lake and Lac Ste. Anne cores tends to precipitate into the sediment providing a cap that prevents the release of P into the porewater and subsequently the hypolimnion (Figures 3.11a; 3.11b; 3.11d). Therefore, the sediment appears to act as a sink rather than a source for phosphorus in Wabamun Lake and Lac Ste. Anne. These findings are contrary to the results for Isle Lake, which show a relative enrichment of dissolved P near the SWI (Figure 3.11c) suggesting a possible release of P from the sediments into the hypolimnion of the lake (Mitchell, 1984; Riley and Prepas, 1984; Boström et al., 1982).

Distribution of phosphorus (PO_4^{3-}) between surface sediments and porewater in freshwater lakes are typically controlled by processes such as oxidation-reduction of Fe and Mn (redox sensitive), the decomposition of organic matter, and precipitation/dissolution of calcium-compounds (Mortimer, 1941; 1942; Lijklema, 1976; Cooke, 1993; Böers et al.,

1994; Froelich et al., 1979; Pettersson, 1986; Dahmke et al., 1991; Sundby et al., 1992; Otsuki and Wetzel, 1972; Koschel et al., 1983; Stabel, 1986). The possible role of these processes as related to the observed distribution of phosphorus in the studied lake sediments are discussed as follows:

3.4.6.1. Cycle of phosphorus and organic matter decomposition

Phosphorus availability regulates phytoplankton biomass and eutrophication in many freshwater lakes in central Alberta and world-wide (Dillon and Rigler, 1974; Prepas and Trew, 1983; Schindler, 1977; Moss, 1985; Prepas, 1983; Prepas and Trimbee, 1988; Golterman, 1977). The significant correlation between labile organic compounds (S1-OM) and P contents in sediment profiles from Wabamun Lake, Isle Lake, and Lac Ste. Anne supports the association of P and organic matter in the recent sediments (Tables 3.9-3.12; Figure 3.11a-d). The rapid decomposition of organic matter in anoxic sediments may lead to a strong release of organically-bound phosphorus into the porewater (Song and Müller, 1999). The S1-OM is considered very labile and, immediately after deposition, it begins selectively decomposing during the early diagenesis processes (Chapter 7). Consequently, the decomposition of OM in sediments results in the release of organically-bound P from sediments deeper into the porewater (Figure 3.11a-d). This observation is consistent with a number of other studies on aquatic recent sediments (e.g., Krom and Berner, 1981; Balzer, 1989; Sundby et al., 1992).

3.4.6.2. Cycle of phosphorus and precipitation/dissolution of calcium

The strong correlation between P and Ca profiles (Tables 3.9-3.12) in all studied sediment cores indicates that the precipitation/dissolution of Ca-minerals may also play an important role in controlling phosphorus concentrations in the sediments of the studied lakes. The association of Ca and P in sediments and water is documented by Penn et al. (2000), Ishikawa and Ichikuni, 1981; Prepas et al., 2001; Reedyk et al., 2001 who studied the relationship between Ca (CaO, $CaCO_3$, $Ca(OH)_2$), P and pH. Calcium solubility is inversely proportional to pH. In summer when water temperatures and pH increase (from photosynthetic activity), calcite often precipitates from the water column naturally (Otsuki and Wetzel, 1972; Koschel et al., 1983; Stabel, 1986). The effect of calcium minerals on phosphorus biogeochemistry can be explained via apatite formation (Prepas et al., 2001; Nriagu and Dell, 1974; Emerson, 1976; Aller, 1980a; Nembrini et al., 1982; Holdren and Armstrong, 1986; Koschel, 1997):

$5\ Ca^{2+} + 3\ PO_4^{3-} + OH^- \rightarrow Ca_5(PO_4)_3(OH)$ (hydroxylapatite)

Calcium may adsorb dissolved P at surficial sediments thus preventing the release of phosphate into the overlying water. This process appears to act as a trap for dissolved phosphates in the surface layer of sediments from Wabamun Lake and Lac Ste. Anne (Figures 3.11a; 3.11b; 3.11d). Phosphorus bound with Ca^{2+} in the sediments is often stable and redox-insensitive (Cooke, 1993). Only sudden changes in pH may affect the solubility of Ca-minerals and cause release of PO_4^{3-} into the overlying water. However, the occurrence of

any significant changes in pH is highly unlikely due to high buffer capacity of the alkaline lakes in the study area (Song and Müller, 1999).

After the deposition of P-bearing materials in the sediments, phosphorus (PO_4^{3-}) is again released in the porewater as burial depth increases (Figures 3.11a; 3.11b; 3.11d). This is due to dissolution of Ca associated with organic matter decomposition, which controls the release of P from sediments (Song and Müller, 1999; Driscoll et al., 1993; Danen-Louwerse at al., 1995; Kim et al., 2001; Prepas et al., 2001; Reedyk et al., 2001). The changes in solubility of Ca-minerals in the sediment column may act as a conveyer, releasing P from sediment into porewater at depth and re-precipitating P at sediment-water-interface (Figures 3.11a; 3.11b; 3.11d).

Deposition of calcium-rich fly ash in the lakes in Wabamun area (especially Wabamun Lake) may encourage the capturing and immobilizing of dissolved phosphorus and other trace elements in the hypolimnion and porewater (Chapter 3). In surface waters of eutrophic lakes in western Canada with high pH and alkalinity, the addition of lime (CaO, $CaCO_3$, $Ca(OH)_2$) is known to help reduce high P concentrations in water (Prepas et al., 2001; Reedyk et al., 2001; Murphy et al., 1988; Prepas et al., 1990; Babin et al., 1994).

3.4.6.3. Cycle of phosphorus and oxidation/reduction of Fe/Mn (redox sensitive)

At the water-sediment interface samples where oxygen is present, Fe/Mn oxides may play an important role in the adsorption of phosphorus and prevent release of P from the

sediments (Mortimer, 1941, 1942; Lijklema, 1976; Cooke, 1993; Böers et al., 1994). The redox effect of Fe/Mn on phosphorus biogeochemistry can be explained by the formation of phosphorus minerals vivianite and reddingite controlling phosphate concentrations in porewater (Nriagu and Dell, 1974; Emerson, 1976; Suess, 1979; Elderfield et al., 1981; Postma, 1981).

$3\ Fe^{2+} + 2\ PO_4^{3-} + 8\ H_2O \rightarrow 4\ Fe_3(PO_4)_2\ 8H_2O$ (vivianite)

$3\ Mn^{2+} + 2\ PO_4^{3-} + 3\ H_2O \rightarrow Mn_3(PO_4)_2\ 3H_2O$ (reddingite)

The redox effect of Mn is evident in the porewater profile of Isle Lake, which shows an accumulation of total dissolved P and Mn, simultaneously (Figure 3.12). This is due to the release of inorganic P into porewater associated with the reduction of Mn oxides. Additionally, the depth profiles of P in surface sediments and porewater from Isle Lake show strong similarity to those of Fe (after being normalized to Zr to correct for effects of non reactive geogenic Fe) (Figure 3.12; Table 3.11). This indicates that, in addition to the geochemical effect of Ca processes, diagenesis and the mobility of phosphorus (PO_4^{3-}) in Isle Lake sediment may be significantly controlled by the oxidation and reduction of iron. In other word, the effects of redox Fe/Mn may mask the effects of calcium dissolution/precipitation (Driscoll et al., 1993; Kamp-Nielsen, 1974). The redox effect of Fe results in the release of P into the anoxic sediment and the capture of P in the oxic surface layer (Krom and Berner, 1981). Therefore, surface enrichment of Fe and P in the ISLE sediment core (Figure 3.12) may be partly caused by the formation of minerals such as vivianite under oxic conditions. This is confirmed by SEM/EDX images in Isle Lake

sediments showing abundant distribution of Fe-P minerals within the upper section of the sediment core (Chapter 5).

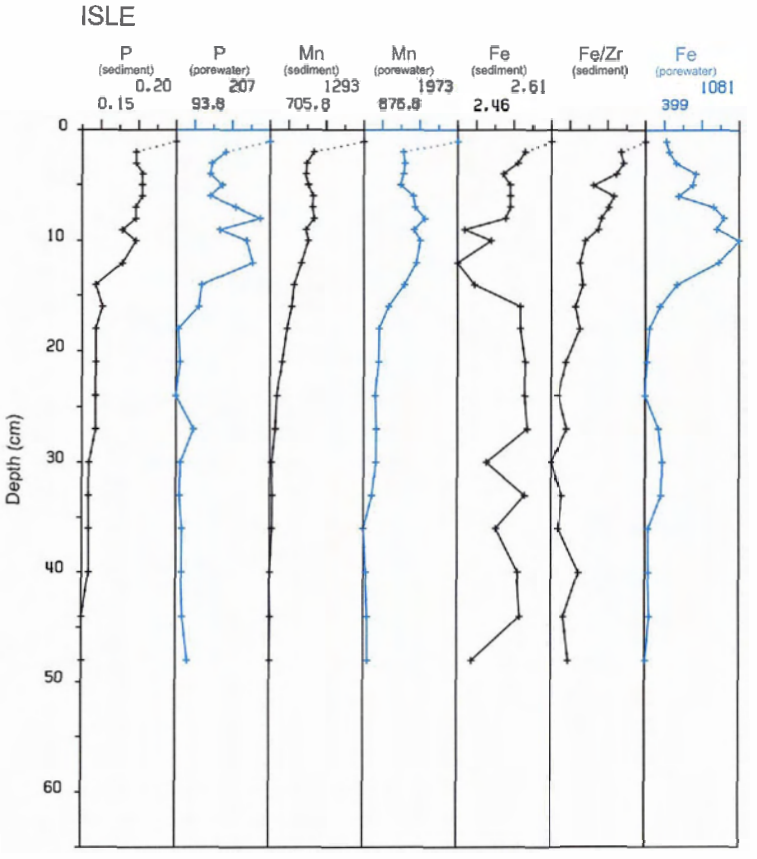

Figure 3.12. The redox-sensitive cycle of nutrient as shown by distribution of P, Fe, and Mn in the sediment and porewater profiles in ISLE profile.

In contrast to Isle Lake, lack of positive correlation between temporal variation of Fe and P in Wabamun Lake and Lac Ste. Anne sediments (Tables 3.9; 3.10; 3.12) suggest that redox-sensetive Fe reactions may not significantly affect the nutrient distribution in these lakes. Moreover, there is no SEM/EDX evidence of vivianite minerals found in the Wabamun Lake and Lac Ste. Anne sediments (Chapter 5). Number of studies reported that the surficial sediments from Lakes in western Canada have little reactive iron (nongeogenic)

and presumably phosphorus biogeochemistry is not controlled by iron reactions (Riley and Prepas, 1984; Prepas et al., 2001; Kim et al., 2001).

In summary, the result of this study indicates that distribution of P in the sediment and porewater of the studied lakes is predominantly controlled by the Ca-OM fraction. However, the redox effect of Fe/Mn may mask the dissolution/precipitation of Ca (Driscoll et al., 1993; Kamp-Nielsen, 1974). This is more evident in the sediment of Isle Lake, which shows evidences of vivianite formation.

3.4.7. The effect of iron-sulphur fraction on biogeochemistry of trace elements

The WAB1 depth profile of dissolved sulphur shows a rapid downward decline in concentration from the SWI to the depth of 10 cm where it reaches its lowest level for the rest of the profile (Figure 3.13). The total sulphur content of sediment in the WAB1 core follows the same trend for the top 10 cm (Figure 3.13). However, below 10 cm, total S begins to increase downward throughout the core until it reaches its maximum level (2.1 %) at the depth of 20 cm (Figure 3.13; Table 3.1).

The total concentration of dissolved S in the WAB2 porewater profile is enriched near the SWI, and then decreases for the rest of the profile (Figure 3.13). The total concentration of S in the WAB2 sediment profile shows an inverse pattern. The S content of the sediment of the WAB2 core remains low in the upper section of the profile followed by a rapid gain at

10 cm (Figure 3.13). The total S profile below 12 cm remains high and relatively constant throughout the rest of the profile (Figure 3.13).

Isle Lake shows a similar temporal distribution of sulphur in its sediment and porewater profiles as compared to the WAB2 core (Figure 3.13). The surface enrichment of dissolved S in the ISLE core is mirrored by a depletion of sulphur in the top 12 cm of the sediment profile (Figure 3.13). Similar to the WAB2 core, the total S content of the sediment in the ISLE core remains high below 12 cm, with little variation for the rest of the profile (Figure 3.13).

The dissolved S in the LSA porewater gradually decreases from the SWI until it reaches its lowest level at 16 cm (Figure 3.13). In contrast, the total S in the sediments shows the minimum concentration at the SWI, and a gradual increase in concentration with increasing depth (Figure 3.13). The highest gain in total S occurs at 16 cm, followed by periodical episodes of increases and decreases of total S for the rest of the sediment profile.

The upper sections of the sediment profiles in Wabamun Lake, Isle, Lake, and Lac Ste. Anne are likely representations of the SO_4^{2-} reduction zone (Figure 3.13). This zone is characterized by an exponential decrease of dissolved S (SO_4^{2-}) in the porewater (Figure 3.13).

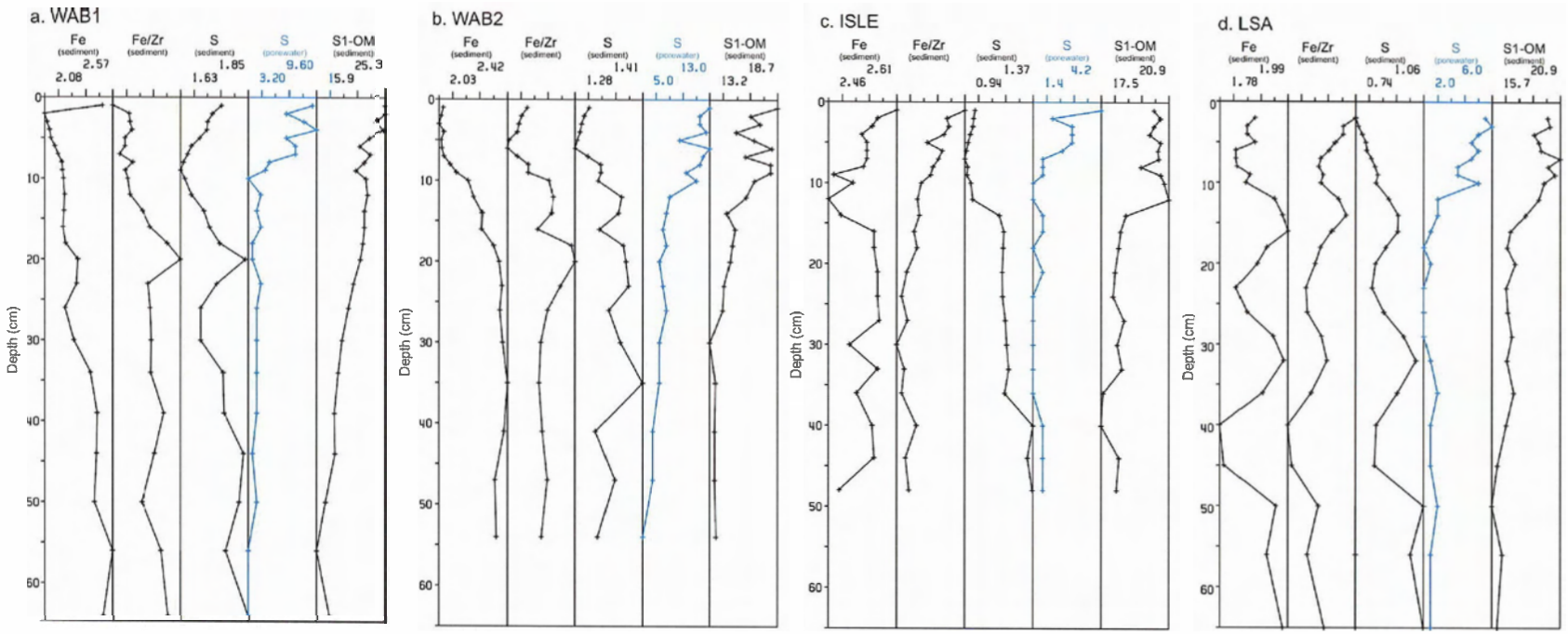

Figure 3.13. The geochemical cycle of Sulphur as shown by by distribution of Fe and S in the sediment and porewater profiles from (a) WAB1 core, (b) WAB2 core, (c) ISLE core, and (d) LSA core.

There is a very similar trend between the depth profiles of S and Fe for porewater and sediments from all four studied cores, suggesting a strong association between these two elements (Figure 3.13). This is likely due to the formation of Fe-S precipitates in the sediment at depths where reducing conditions prevail. Generally, SO_4^{2-} reduction during the mineralization of organic matter leads to production of HS^- in the sediments. The HS^- produced by the reduction of SO_4^{2-} rapidly precipitates dissolved Fe^{2+} in the form of FeS nH_2O (amorphous) or makinawite (FeS), which are both further converted into pyrite (Carignan and Lean, 1991).

$$Fe^{2+} + HS^- + nH_2O \rightarrow FeS\ nH_2O + H^+$$

$$Fe^{2+} + HS \rightarrow FeS\ (makinawite) + H^+$$

The formation of iron monosulfide is confirmed by the black color of the sediment cores in the study area.

Often, the similarity between the Fe and S profiles increase after data are normalized with respect to Zr content (Figure 3.13). Normalization to Zr corrects for geogenic input of Fe, which does not readily contribute to the biogenically induced reactions. The bulk concentration of Fe is bound with ferromagnesian minerals, which is not chemically reactive in porewater. Riley and Prepas, (1984) stated that lakes on the Boreal Plain of western Canada typically contain very little reactive Fe. Thus, the geogenic input of Fe-rich minerals into the lake may mask the sulphide-associated iron formed by bacterial sulphate reduction (Appendix B).

3.4.8. The effect of Fe-Mn fraction on biogeochemistry of trace elements

The depth profiles of Mn in sediment cores from Wabamun Lake, Isle Lake, and Lac Ste. Anne show surface enrichment followed by decreasing concentration with increasing depth (Figure 3.14). Similarly, the vertical distributions of dissolved Mn, after normalization to Zr (to remove geogenic input), show enrichment of Mn below the SWI with rapid downward decrease throughout all studied porewater profiles (WAB1, WAB2, ISLE, LSA) (Figure 3.14).

The processes of a redox controlled diagenetic cycle of Fe/Mn are well studied (Berner, 1980; Elderfield and Hepworth, 1975; Farmer and Lovell, 1986; Farmer, 1991). The upward increase of Mn in the studied porewater profiles is attributed to the dissolution of Mn under reducing conditions (e.g., Gobeil et al., 1987; Shaw et al., 1990). The rapid decline of Mn in the uppermost portion of the sediment profile (Figure 3.14) occurs because aerobic bacterial utilization of O_2 is sufficiently rapid to produce localized anaerobic microenvironments and cause MnO_2 dissolution immediately below the SWI (e.g., Gobeil et al., 1987).

Dissolution of Mn oxides/oxyhydrixides is bacterially catalyzed and leads to increased levels of more mobile reduced Mn (Mn^{2+}) in interstitial waters:

$$(CH_2O)_{113}(NH_3)_{15}(H_3PO_4) + 248.5\ MnO_2 + 497\ H^+ \rightarrow 248.5\ Mn^{2+} + 113\ CO_2 + 7.5\ N_2 + H_3PO_4 + 384\ H_2O$$

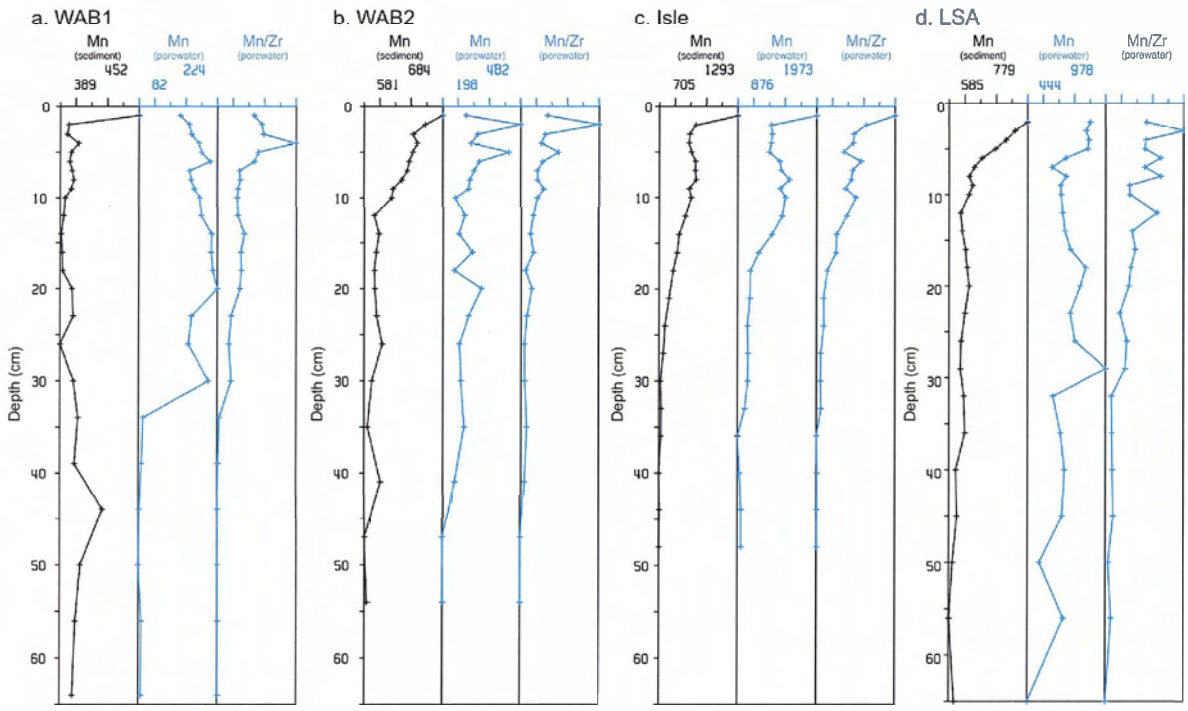

Figure 3.14.a-d. The temporal distribution of Mn in sediments, total dissolved Mn in porewater, and dissolved Mn after normalization to Zr (correction for mineral matrix) in the sediment and porewater profiles from (a) WAB1 core, (b) WAB2 core, (c) ISLE core, and (d) LSA core.

Dissolved Mn in the porewater diffuses towards the surface sediment layer due to concentration gradients (Figure 3.14), unless conditions conducive to precipitation are encountered (Farmer and Lovell, 1986). During the high turbation season, in which the hypolimnion is oxygenated, Mn^{2+} is reoxidized and immobilized in the surface oxic layer following the reaction (Aller, 1980b; Pedersen and Price, 1982; Dahmke et al., 1991):

$$Mn^{2+} + O_2 \rightarrow MnO_2 \downarrow$$

The concentration of Mn in the sediments may also be controlled by the dissolution/precipitation of minerals (Matsunaga et al., 1993):

$Mn^{2+} + CO_3^{2-} \rightarrow MnCO_3 \downarrow$ (rhodochrosite)

This may explain the similarities between the temporal variations of both Mn and Ca in the sediment profiles from the study area.

Redox cycling of Fe and Mn in many marine and freshwater sediments often results in a similar temporal distribution of these elements throughout sediment and porewater profiles (Froelich et al., 1979; Carignan and Nriagu, 1985; Eck and Smits, 1986; Carignan and Lean, 1991). However, Wabamun Lake sediment profiles show a poor correlation between Fe and Mn sediments (Tables 3.9-3.10). The correction for geogenic input, that involves normalizing Fe and Mn values to Zr, did not improve the correlation. This lack of correlation between Fe and Mn in the Wabamun sediments confirms that iron participates mainly in biogenically induced Fe-S reactions rather than redox sensitive Fe/Mn reactions (Chapter 3.4.7).

3.5. CONCLUSIONS

This study investigates temporal distribution of trace elements in the sediment cores from Wabamun Lake, Isle Lake, and Lac Ste. Anne in central Alberta as related to activities of the coal-fired power plants in the study region. A multi-elemental analysis of the recent sediments and their porewater in conjunction with organic matter was used to investigate the sources, quantity, and processes involved in the distribution of trace elements in the recent sediments.

The relative enrichment of trace elements (As, Sb, U, V, Cr, Cu, Mo, Pb, Se, Hg, and Zn) in the younger sediment layers of Wabamun Lake can be partly due to the emissions from the coal-fired power plants in the study area (as suggested by isotope dating data). However, the study of porewater suggests that diagenetic dissolution/diffusion of some trace elements may have occurred at depth, acting as a conveyor of elements to the upper part of the sediment profile. This can also contribute to the elevated concentrations of trace elements near the surface sediments, which are often attributed solely to the activities of power plants in this region.

This study indicates that a combination of various biogeochemical processes may control the temporal distribution of elements and nutrients in sediment and porewater from the lakes in the study area. However, due to the alkalinity and eutrophic conditions of the studied lakes, and in particular Wabamun Lake, the Ca-OM fraction plays the most important role as substrate for trace elements and nutrients (e.g., P). Degradation of organic matter in the deeper part of the sediment profile may result in the formation of highly soluble metal-organic complexes, which is responsible for the mobilization of trace elements during early diagenesis. The organic decomposition in deeper sediments may also cause dissolution of Ca-compounds and release of trace elements attached to Ca-minerals into the porewater. The dissolved metals may migrate upward in the column and immobilize again due to re-precipitation of calcium minerals in the upper section of the sediment profiles.

The addition of calcium through aerial deposition of Ca-rich fly ash in the studied lakes, in particular Wabamun Lake, may serve as liming treatment for precipitation of soluble trace metal compounds and dissolved nutrients. The higher input of calcareous fly ash in Wabamun Lake as compared to Isle Lake and Lac Ste. Anne may cause higher scavenging of trace metals in this lake than the other two studied lakes.

The temporal distribution of lithophilic elements in the studied sediments is determined by the degree of dilution by organic matter in the sediment profiles. The variation of lithophilic elements throughout the sediment profiles can also be related to factors such as fluctuation of detrital material from the watershed and dilution by other inorganic geochemical fractions such as carbonates and redox Fe/Mn.

CHAPTER 4: SPATIAL DISTRIBUTION OF MERCURY AND OTHER TRACE ELEMENTS IN LAKE SEDIMENTS DURING THE POST-COAL UTILIZATION PERIOD IN THE WABAMUN AREA, ALBERTA, CANADA

4.1. INTRODUCTION

The spatial distribution of mercury (Hg) and other elements of environmental concern (Cu, Pb, Zn, and Sb) in post industrial sediments (after 1956) were investigated in nine sediment cores from the following 8 lakes located in central Alberta: Lac La Nonne (LLN), Lessard Lake (LSD), Chip Lake (CHIP), Brock Lake (BCK), Isle Lake (ISLE), Jackfish Lake (JFL), Lac St Anne (LSA), Sandy Lake (SND), and Wabamun Lake (WAB). Each lake is located within various emission ranges from the region's four power plants, namely the Wabamaun, Sundance, Keephills, and Genesee stations (Figure 4.1).

Using isotope ^{210}Pb dating information, the 1956 horizon in all the retrieved cores was identified as a marker indicating the commencement of coal utilization in the Wabamun region (Chapter 2.1.3). Then, the average concentrations of Hg and other trace elements were calculated in the sediment layers deposited above the 1956 horizon (Table 4.1). This approach is used to study the spatial distribution of Hg and other trace elements in the lake sediments deposited after the coal-utilization era.

Where the statistical analyses were applied, Chip Lake was excluded from the data set, as it belongs to a different drainage basin from the rest of the studied lakes (Chapter 1.6).

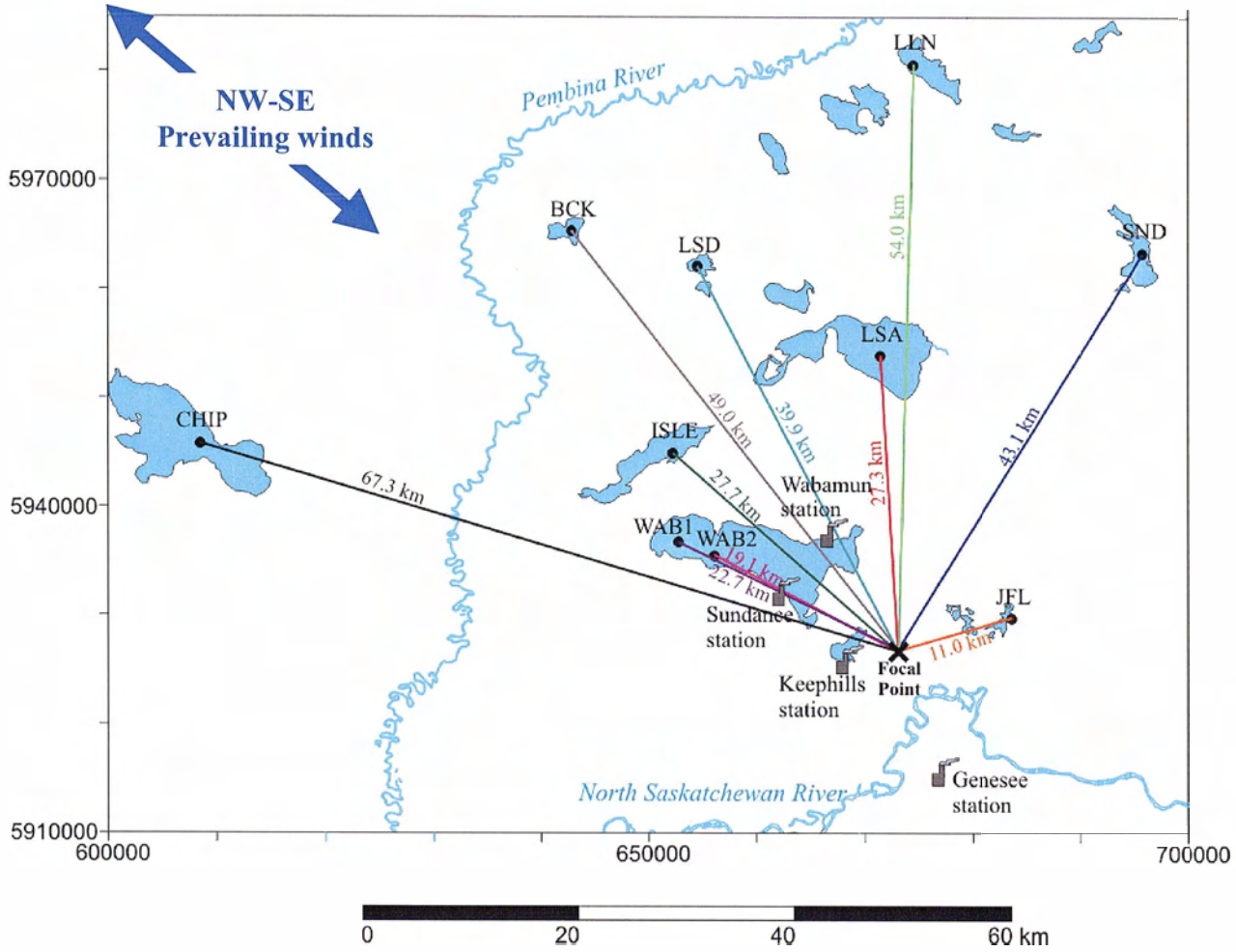

Figure 4.1. Radial distance of the studied sediment cores from the focal point of region's four power plants (the Keephills, and Genesee stations).

Table 4.1. The average concentration of elements in post-industrial sediments (sediments younger than 1956) from the various lakes (sediment cores) in central Alberta.

Sediment	Distance*	Al	As	Ba	Ca	Cd	Ce	Co	Cr	Cs	Cu	Dy	Eu	Fe	Ga	Gd	Hf	Hg	K	La	Li	Lu	Mg	Mn
cores	(km)	%	ppm	ppm	%	ppm	ppm	ppm	ppm	ppm	ppm	ppm	ppm	%	ppm	ppm	ppm	ppm	%	ppm	ppm	ppm	%	ppm
BCK	49.0	3.25	5.7	259	1.33	0.48	31	10.2	41.00	2.8	23	2.2	0.62	2.01	8	2.0	1.7	0.09	0.80	16.8	21	0.18	0.41	315
CHIP	67.3	6.29	6.2	592	1.00	0.35	48	11.1	64.00	4.3	25	2.9	0.83	3.22	15	2.8	2.4	0.11	1.57	25.5	36	0.20	0.91	386
ISLE	27.7	3.70	8.3	474	1.47	0.36	34	9.6	35.40	2.3	23	1.7	0.44	2.34	8	1.7	1.7	0.09	0.89	17.2	21	0.10	0.58	1045
JFL	11.0	3.92	5.3	269	2.32	0.34	37	9.3	46.86	2.3	18	2.1	0.60	2.10	10	1.9	2.1	0.06	1.10	18.3	23	0.17	0.60	708
LSA	27.3	3.85	8.5	488	5.85	0.34	36	6.5	40.43	2.7	18	2.2	0.60	2.05	9	2.4	1.8	0.05	0.92	19.7	23	0.17	0.69	1057
LSD	39.9	2.21	4.7	256	1.19	0.28	20	4.7	23.25	1.5	12	1.3	0.33	1.03	5	1.3	1.0	0.10	0.60	10.5	15	0.10	0.39	209
LLN	54.0	3.70	6.8	276	1.36	0.30	33	8.7	45.20	2.7	27	1.8	0.54	2.19	9	1.9	1.7	0.08	0.89	18.0	25	0.10	0.57	928
SND	43.1	3.68	7.7	496	3.78	0.32	32	8.9	41.00	2.5	26	1.7	0.40	2.32	9	1.8	1.6	0.09	0.83	16.4	19	0.13	0.68	1076
WAB1	22.7	4.75	14.0	383	2.69	0.43	35	7.2	48.00	3.1	89	2.1	0.60	2.13	13	2.4	2.0	0.09	0.68	17.8	17	0.18	0.57	390
WAB2	19.1	5.30	9.7	475	2.35	0.33	41	9.3	49.13	3.3	54	2.4	0.65	2.18	14	2.4	2.6	0.08	0.95	21.8	23	0.20	0.69	604

Table 4.1: Continued

Sediment	Distance*	Mo	Na	Nb	Nd	Ni	P	Pb	Rb	S	Sb	Sc	Sm	Sr	Th	Ti	U	V	W	Y	Yb	Zn	Zr	S1	TOC
cores	(km)	ppm	%	ppm	ppm	ppm	%	ppm	ppm	%	ppm	ppm	ppm	ppm	ppm	%	ppm	ppm	ppm	ppm	ppm	ppm	ppm		%
BCK	49.0	2.1	0.19	4.6	14	37	0.185	13.4	44	1.7	0.6	5.4	3.0	81	5.2	0.15	3.7	71.5	0.50	12.1	1.1	116	50	21.0	23.6
CHIP	67.3	0.8	0.39	7.8	21	36	0.125	17.6	83	0.2	0.6	9.4	4.3	124	8.9	0.27	2.4	116.5	0.88	15.7	1.5	569	75	4.8	11.2
ISLE	27.7	1.3	0.38	4.5	12	35	0.228	18.3	39	0.8	0.6	5.1	2.4	114	5.6	0.14	3.0	57.0	0.56	11.7	0.9	74	47	16.6	18.8
JFL	11.0	1.5	0.58	5.9	13	22	0.099	22.0	45	1.3	0.7	5.8	2.7	170	5.7	0.21	3.4	59.7	0.81	12.1	1.1	84	57	7.7	8.3
LSA	27.3	1.4	0.41	5.5	15	21	0.291	18.3	50	0.6	0.6	5.9	3.2	188	5.8	0.18	3.0	67.6	0.56	11.4	1.3	79	58	14.5	13.2
LSD	39.9	1.4	0.22	3.1	8	15	0.196	14.2	29	0.8	0.5	3.2	1.8	71	3.4	0.10	1.4	38.3	0.20	6.3	0.6	64	31	29.9	26.5
LLN	54.0	3.0	0.30	4.8	13	27	0.187	23.3	44	1.9	0.7	6.1	2.5	90	5.7	0.16	3.2	67.4	0.48	11.0	1.2	86	48	19.5	18.0
SND	43.1	1.8	0.72	4.7	11	26	0.182	21.5	37	1.0	0.7	5.9	2.4	187	6.0	0.17	2.5	55.6	0.47	10.6	1.0	75	47	23.0	17.9
WAB1	22.7	17.8	0.42	5.6	13	30	0.151	25.2	41	1.6	2.0	6.6	2.9	133	6.7	0.18	6.3	77.0	1.84	11.3	1.2	113	55	20.0	17.1
WAB2	19.1	4.3	0.49	6.8	16	30	0.135	18.9	43	1.3	1.6	7.5	3.2	155	8.1	0.21	4.8	78.5	1.59	13.1	1.3	90	71	11.8	12.3

* Radial distance between the sediment core and the focal point of the power plants in the study area (Figure 4.1).

LLN: Lac La Nonne, LSD: Lessard Lake, CHIP: Chip Lake, BCK: Brock Lake, ISLE: Isle Lake, JFL: Jackfish Lake, LSA: Lac St Anne, SND: Sandy Lake, WAB: Wabamun Lake

4.2. RESULTS AND DISCUSSION

4.2.1. Spatial distribution of elements in post-1956 sediments

The spatial distributions of the various elements are plotted for the post-1956 sediments from the lakes in the study area (Figures 4.2-18). The spatial patterns of Al, Ti, and W and appear to show a strong relationship to distance from the focal point of the four power plants in the study region (Figures 4.2; 4.15; 4.17). This relationship is characterized by elevated concentrations at proximal sites (WAB1, WAB2, and JFL), which rapidly decrease with distance from the power plants. The elements Al, W, and Ti belong to the lithophilic group of elements, which enrich in silicaceous fly ash (Goodarzi, 1996).

Cores WAB1 and WAB2, located near both the Wabamun and Sundance power plants, show some of the highest concentrations of As, Cu, Mo, Pb, Sb, Se, Th and U in top sediments throughout the entire study area (Figures 4.3; 4.7; 4.9; 4.11; 4.12; 4.13; 4.14; 4.16). These elements are typically affiliated with coal-utilizing activities (Chapter 3.4.1) and their enrichment in the Wabamun sediments are possibly due to proximity of these sediment cores to Wabamun and Sundance power plants. Interestingly, the relative enrichment of these elements does not occur in the other lakes, which are also located in close proximity to the power plants (e.g., JFL; Figures 4.1) suggesting that the influence of the power plants on the lake sediments in the study region may have been limited to Wabamun Lake and does not extend to a wider geographic region.

The elements Cd, Co, Cr, Hg, Ni, and Zn are randomly distributed throughout the study region with no apparent enrichment near the coal-fired power plants (Figures 4.4; 4.5; 4.6; 4.8; 4.10; 4.18). Typically, in a region strongly influenced by an industrial point source, the distribution of emitted elements forms a so-called "bulls-eye" pattern in the environment around the point source (e.g. smelter; see Telmer et al., 2004., Goodarzi et al., 2003). This "bulls-eye" distribution pattern is defined by a high central concentration of elements near the point source that rapidly decays, with increasing distance from the point source, to near background levels. However, such a pattern was not found for Hg in the studied area (Figures 4.8). The lack of relationship between spatial distribution of heavy metals (Hg, Zn, Cr, etc.) and distance from the power plants suggests an absence of widespread influence by the power plants in the geographical scale as defined by the study area. This result contradicts a previous study on the Wabamun region lake sediments, which claims a direct relationship between the spatial distribution of trace elements and emissions from the power plants (Donahue, 2002). However, Donahue (2002) based his conclusion on a limited number of lakes in the study area by comparison between the relative enrichment of Hg (and other trace elements) in Wabamun Lake sediments and three other lakes (Isle Lake, Lac Ste. Anne, and Pigeon Lake) further away from the power plants in Wabamun region.

Figure 4.2. The spatial distributions of Aluminum (Al) in post-1956 sediments from the lakes in the study area.

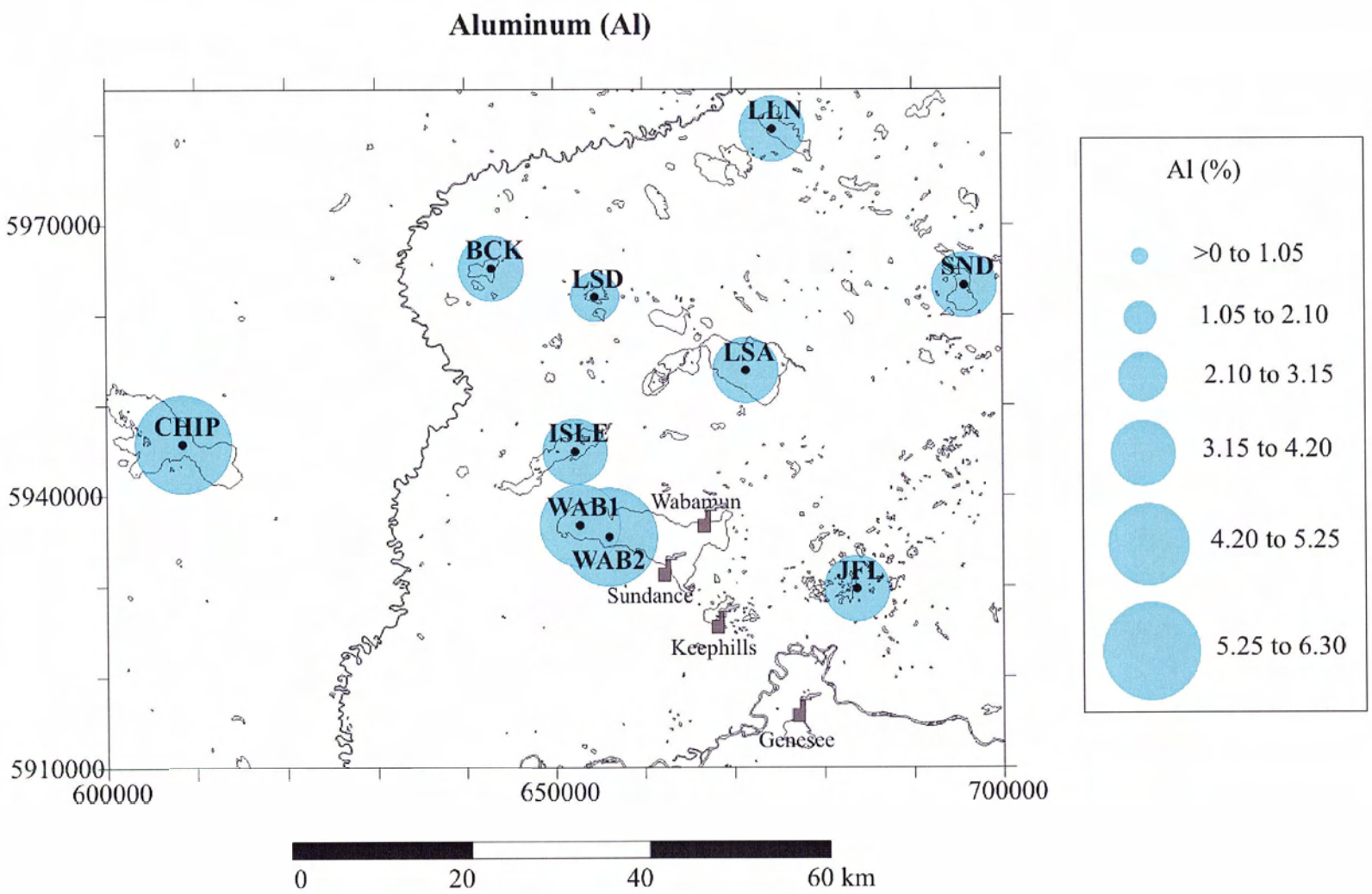

Figure 4.3. The spatial distributions of Arsenic (As) in post-1956 sediments from the lakes in the study area.

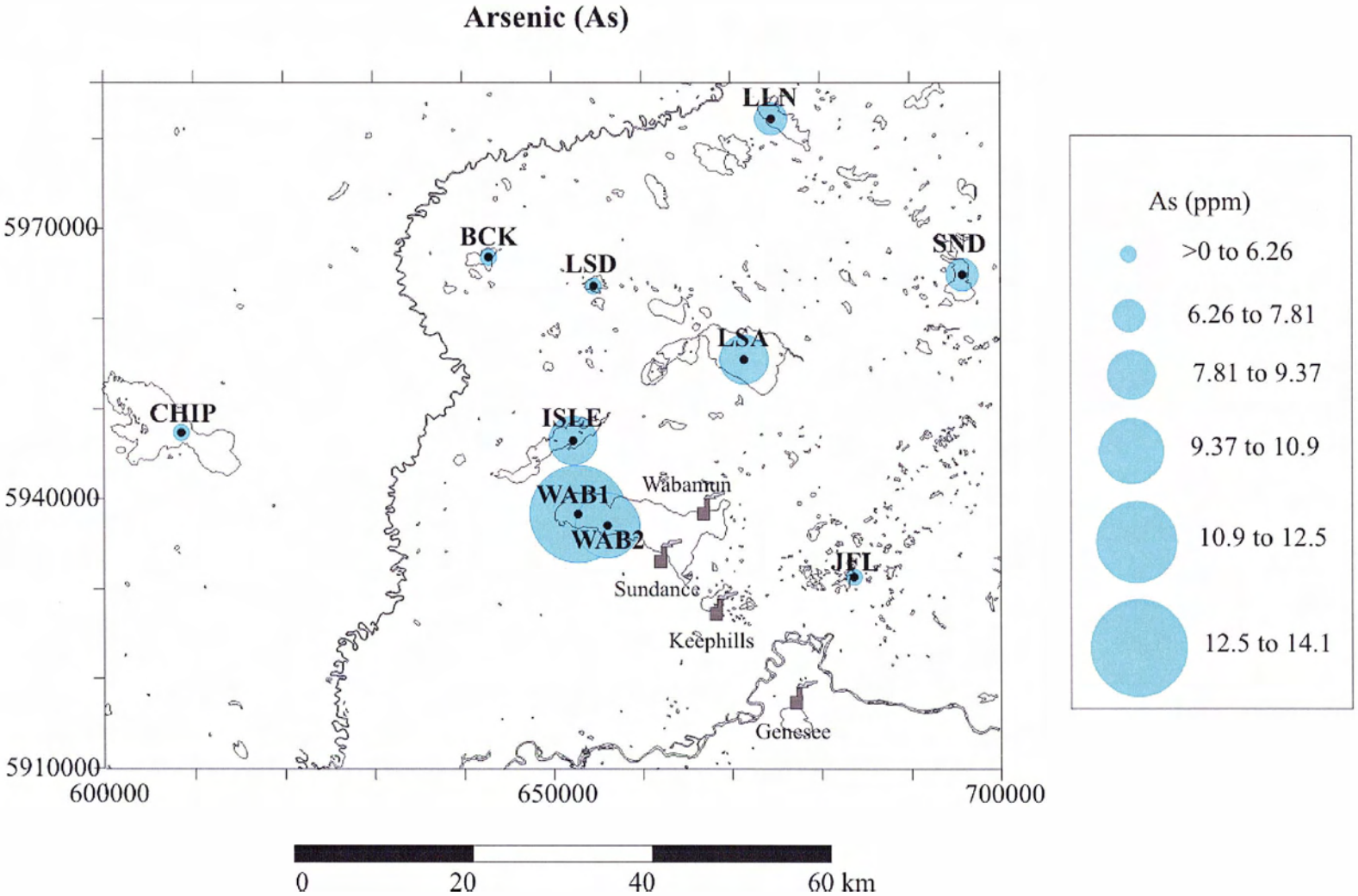

Figure 4.4. The spatial distributions of Cadmium (Cd) in post-1956 sediments from the lakes in the study area.

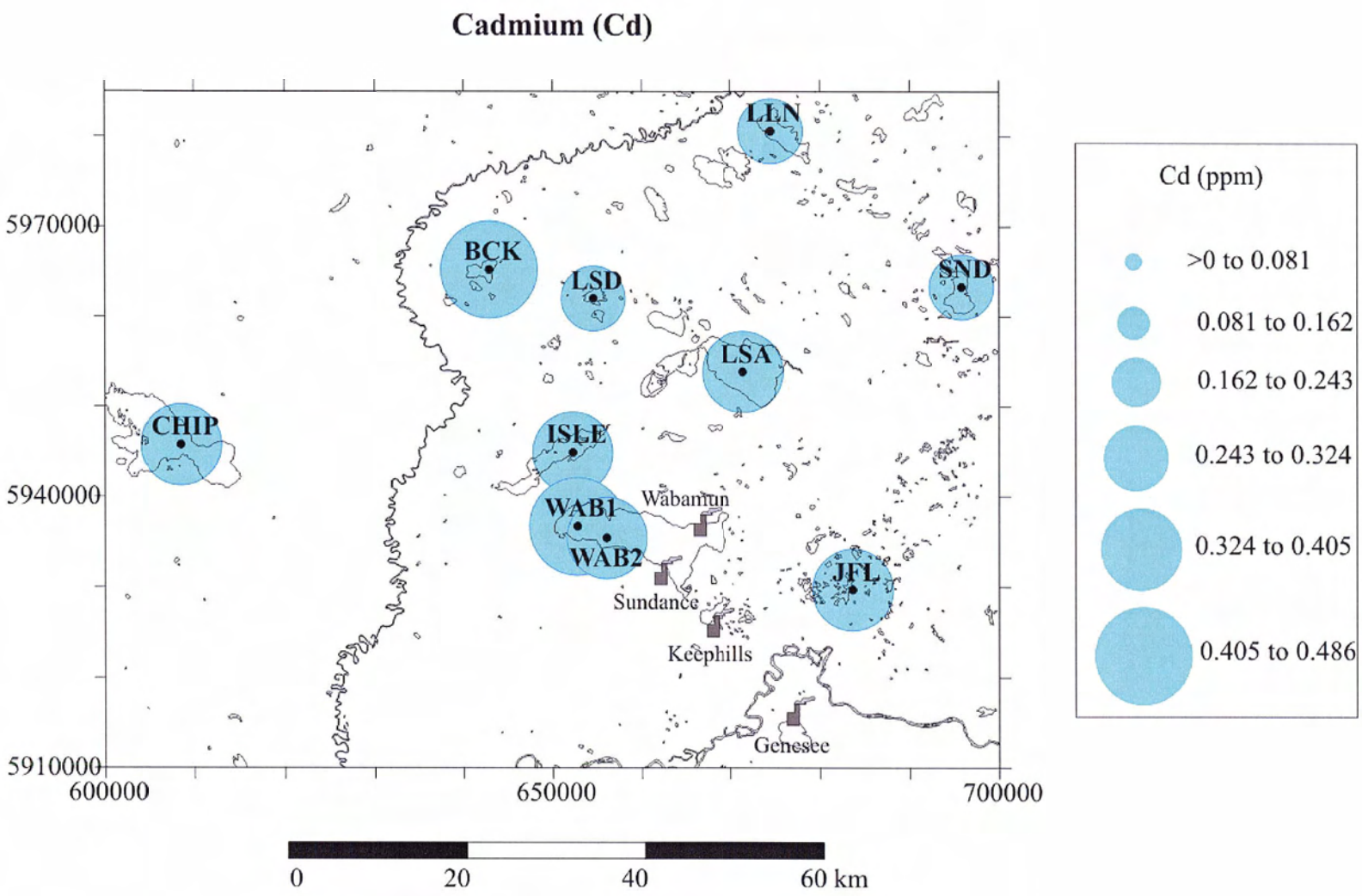

Figure 4.5. The spatial distributions of Cobalt (Co) in post-1956 sediments from the lakes in the study area.

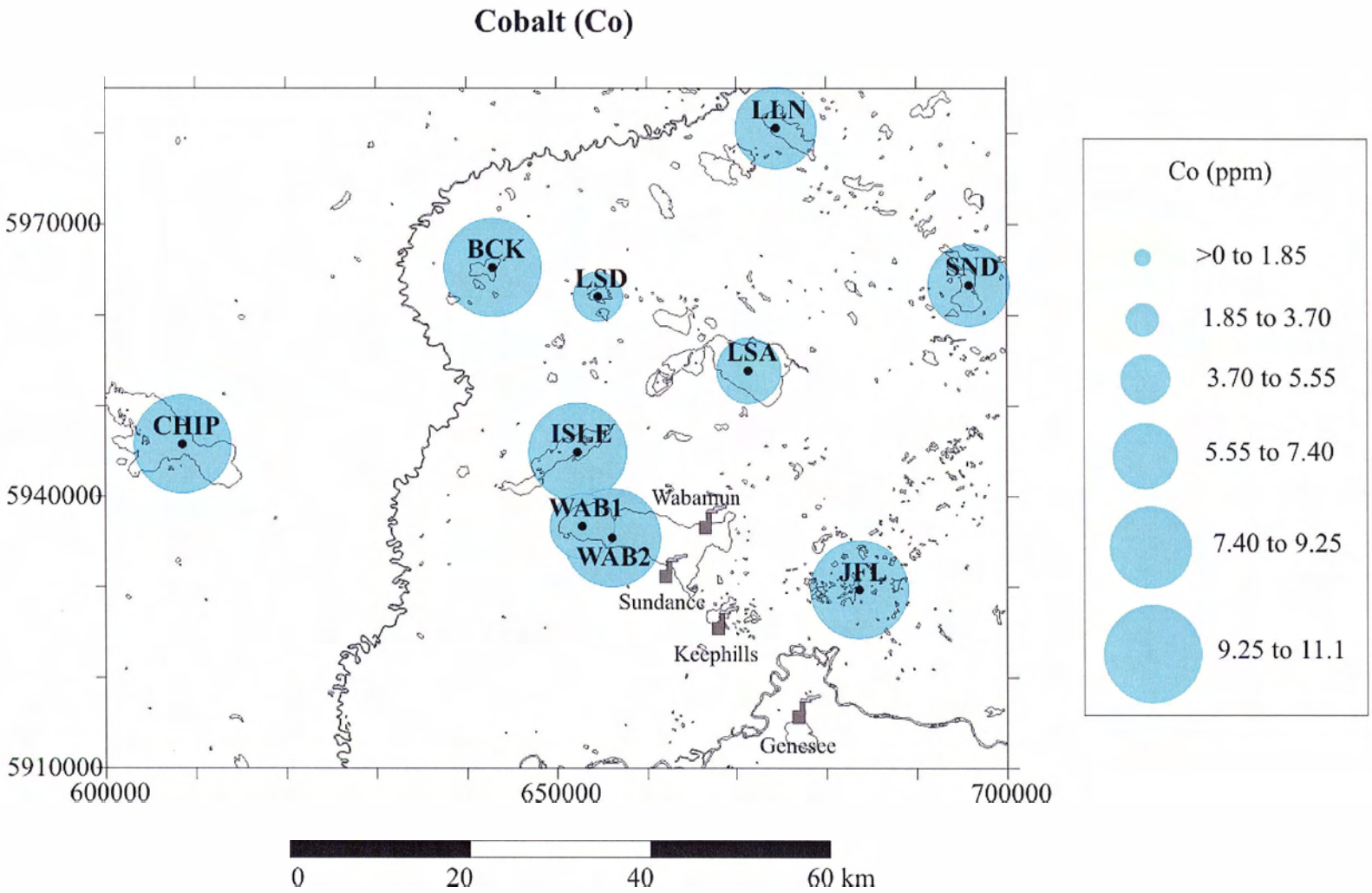

Figure 4.6. The spatial distributions of Chromium (Cr) in post-1956 sediments from the lakes in the study area.

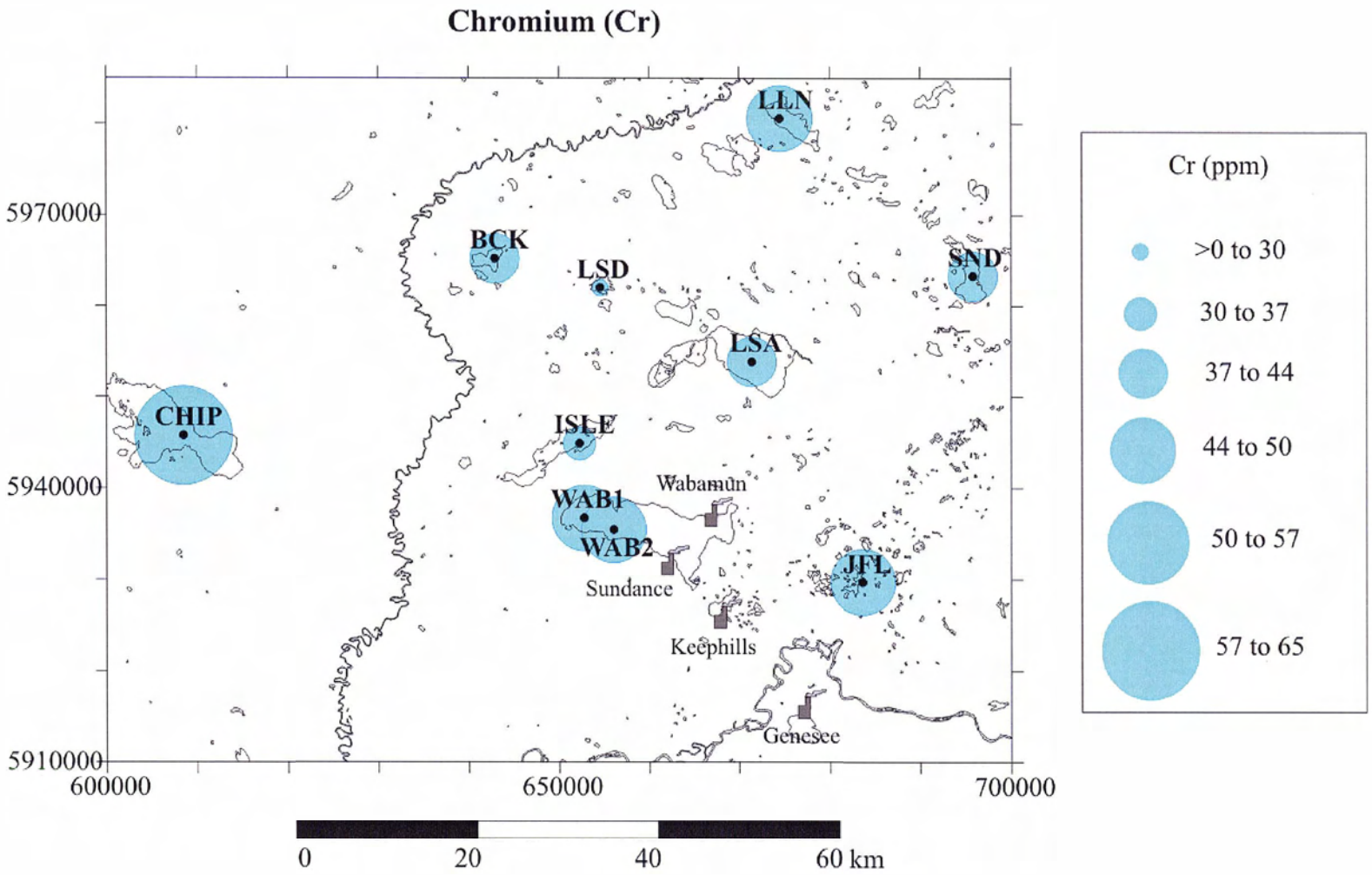

Figure 4.7. The spatial distributions of Copper (Cu) in post-1956 sediments from the lakes in the study area.

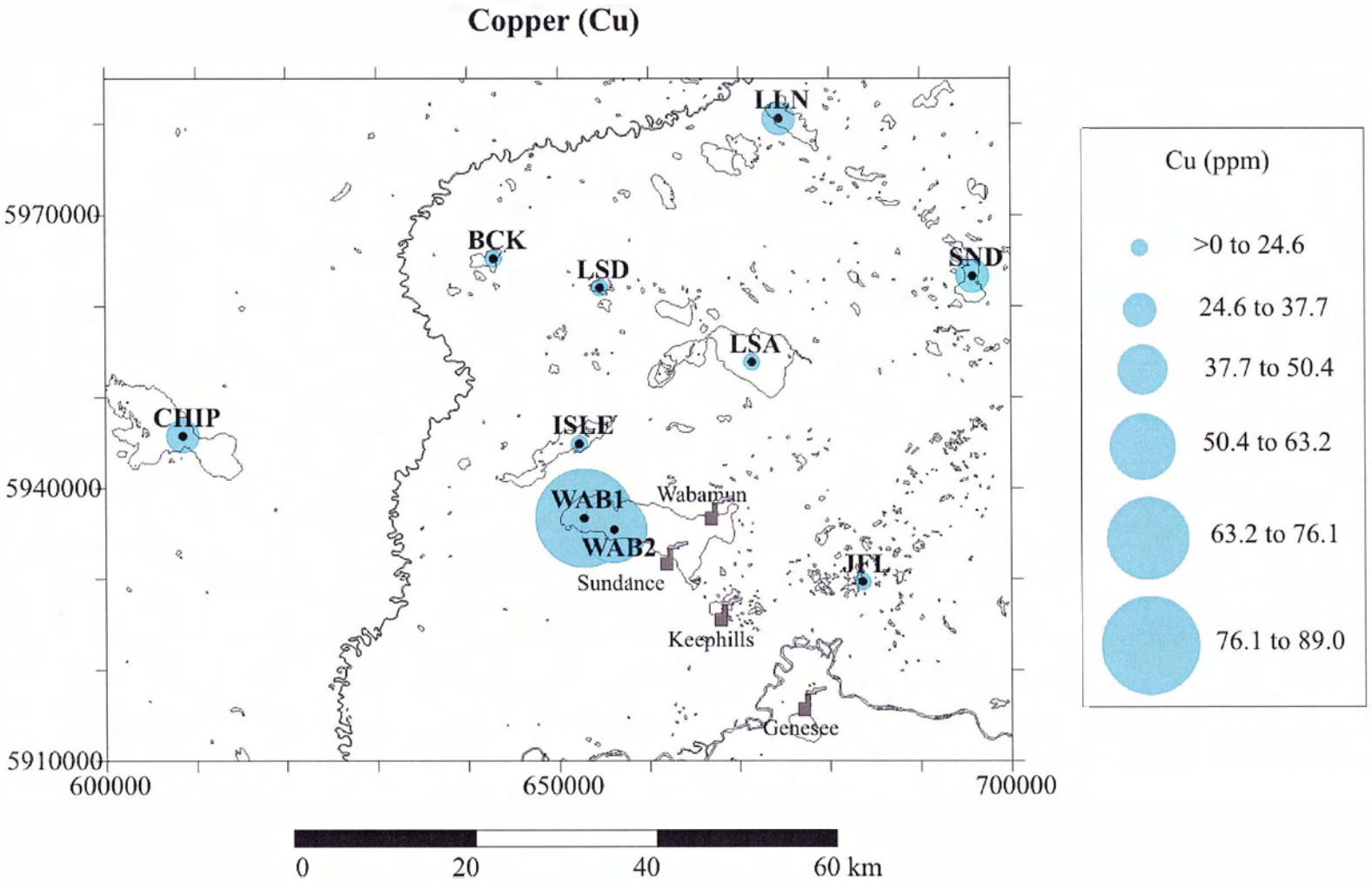

Figure 4.8. The spatial distributions of Mercury (Hg) in post-1956 sediments from the lakes in the study area.

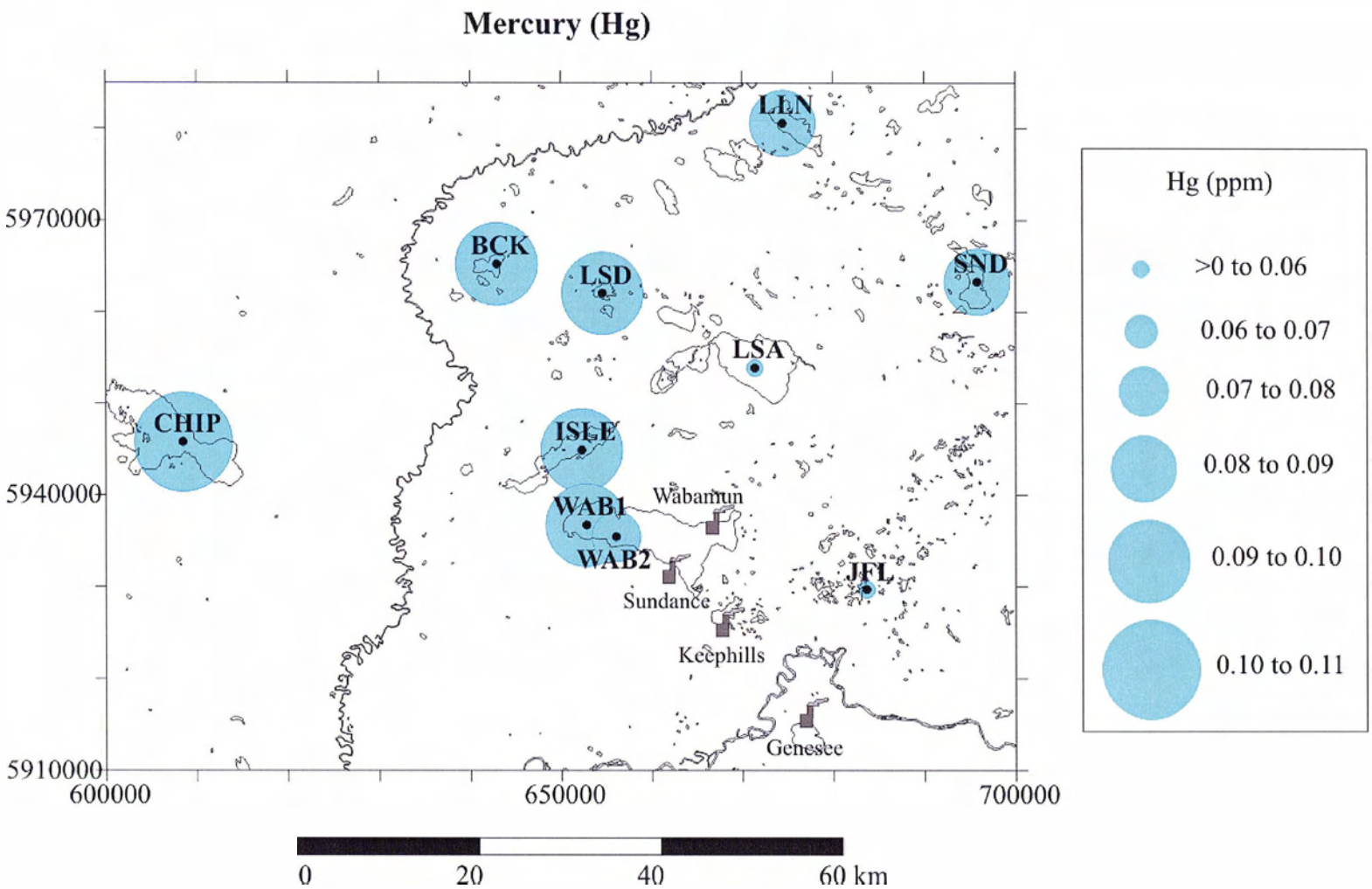

Figure 4.9. The spatial distributions of Molybdenum (Mo) in post-1956 sediments from the lakes in the study area.

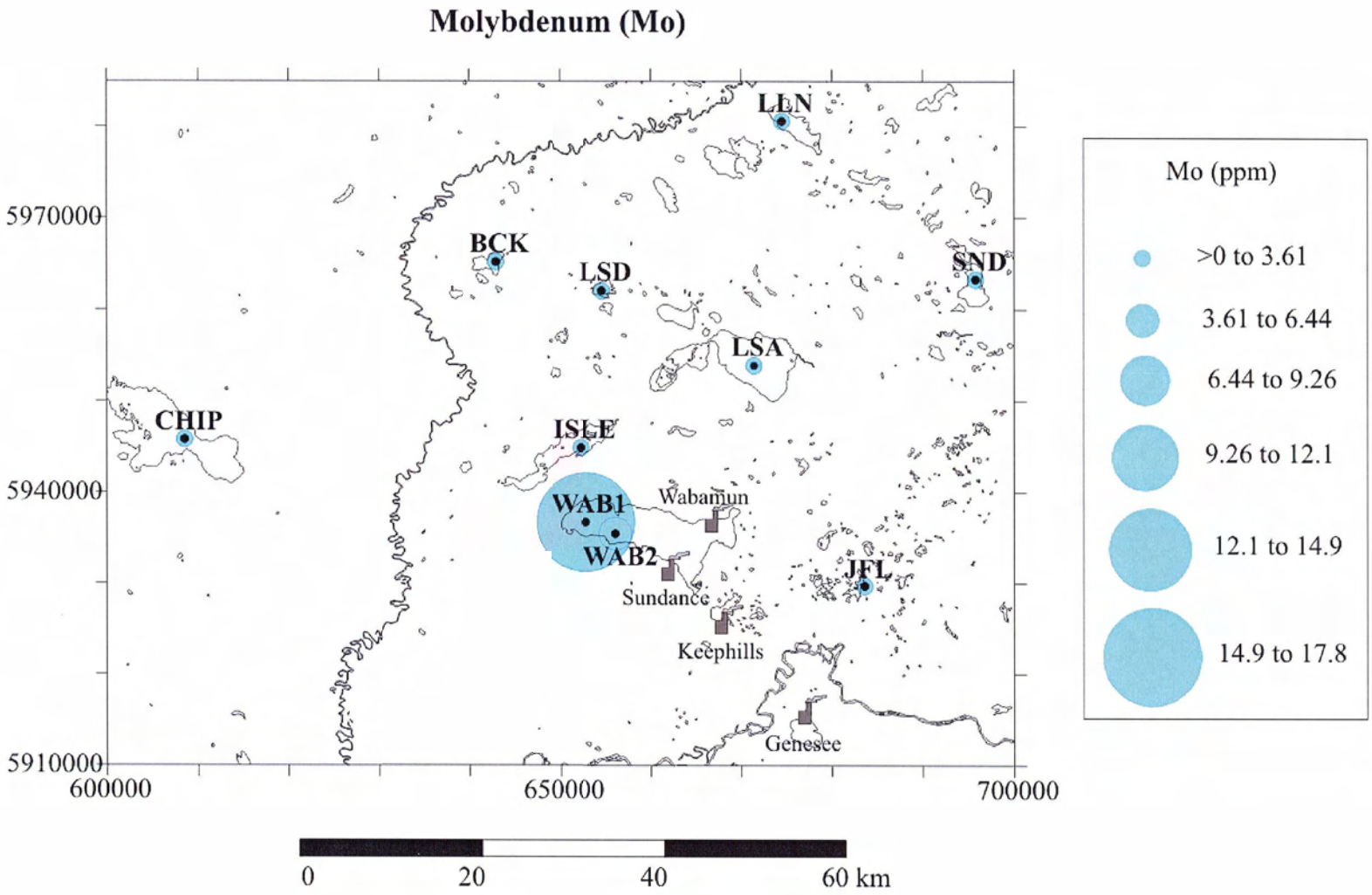

Figure 4.10. The spatial distributions of Nickel (Ni) in post-1956 sediments from the lakes in the study area.

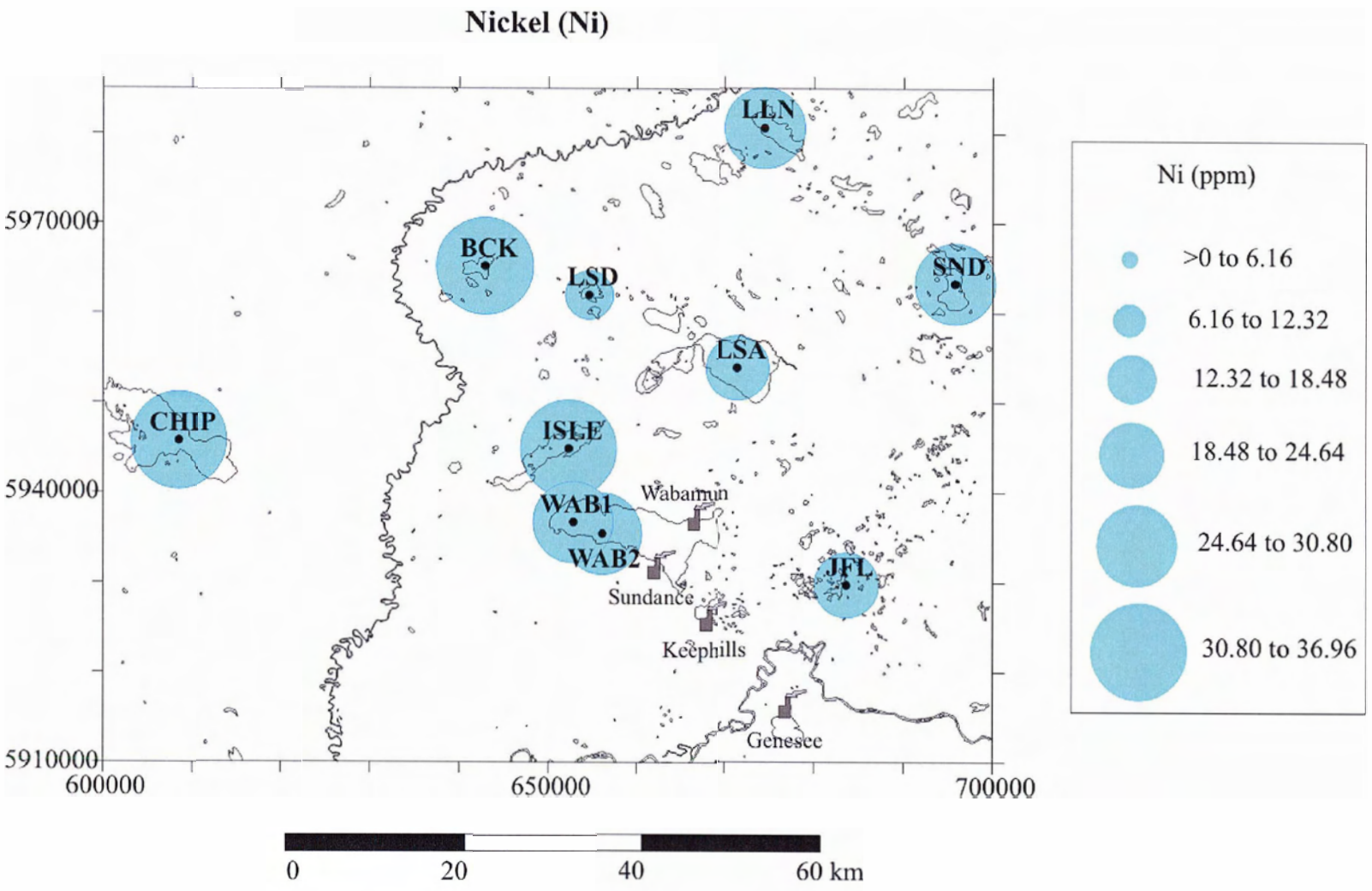

Figure 4.11. The spatial distributions of Lead (Pb) in post-1956 sediments from the lakes in the study area.

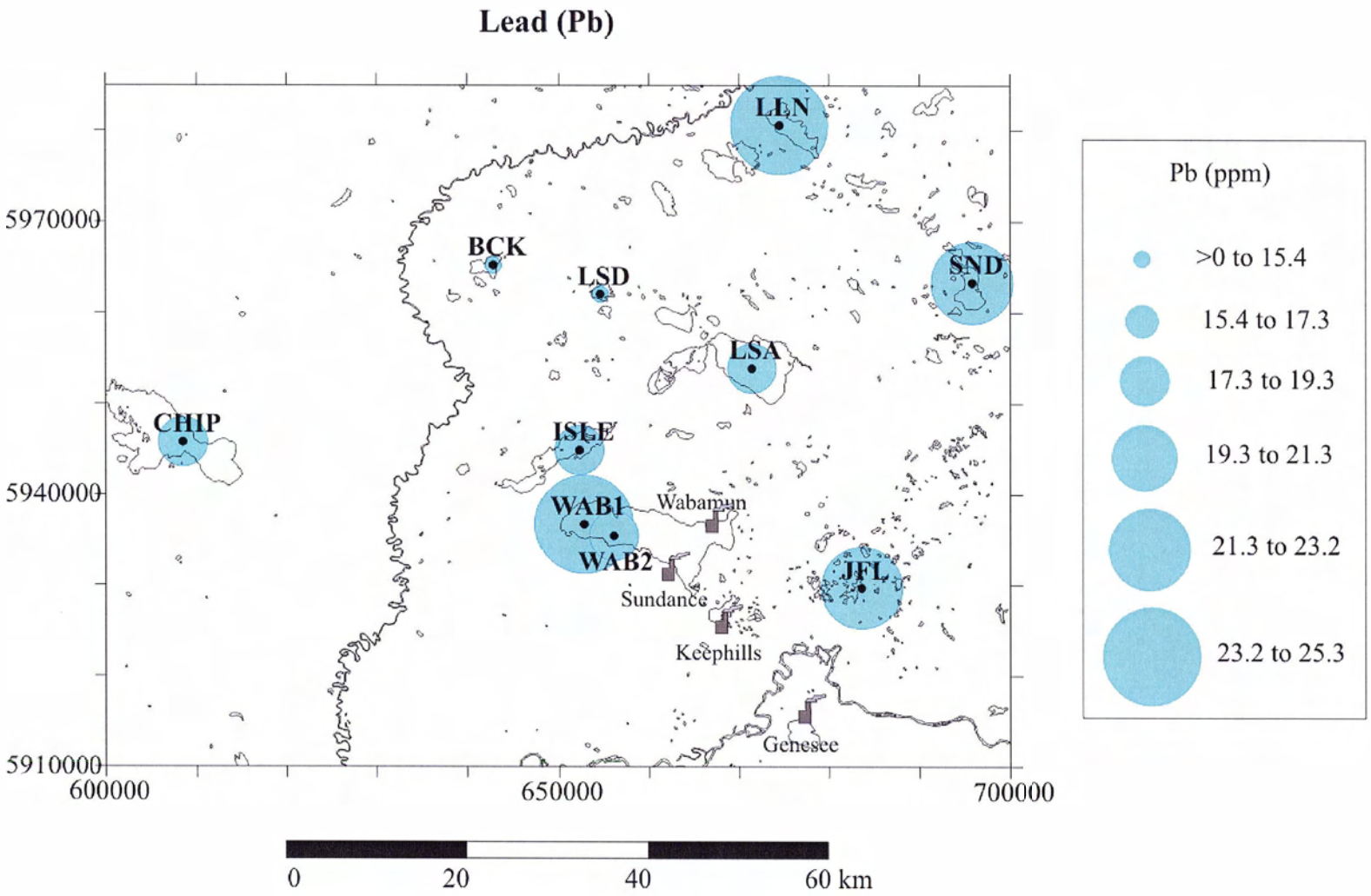

Figure 4.12. The spatial distributions of Antimony (Sb) in post-1956 sediments from the lakes in the study area.

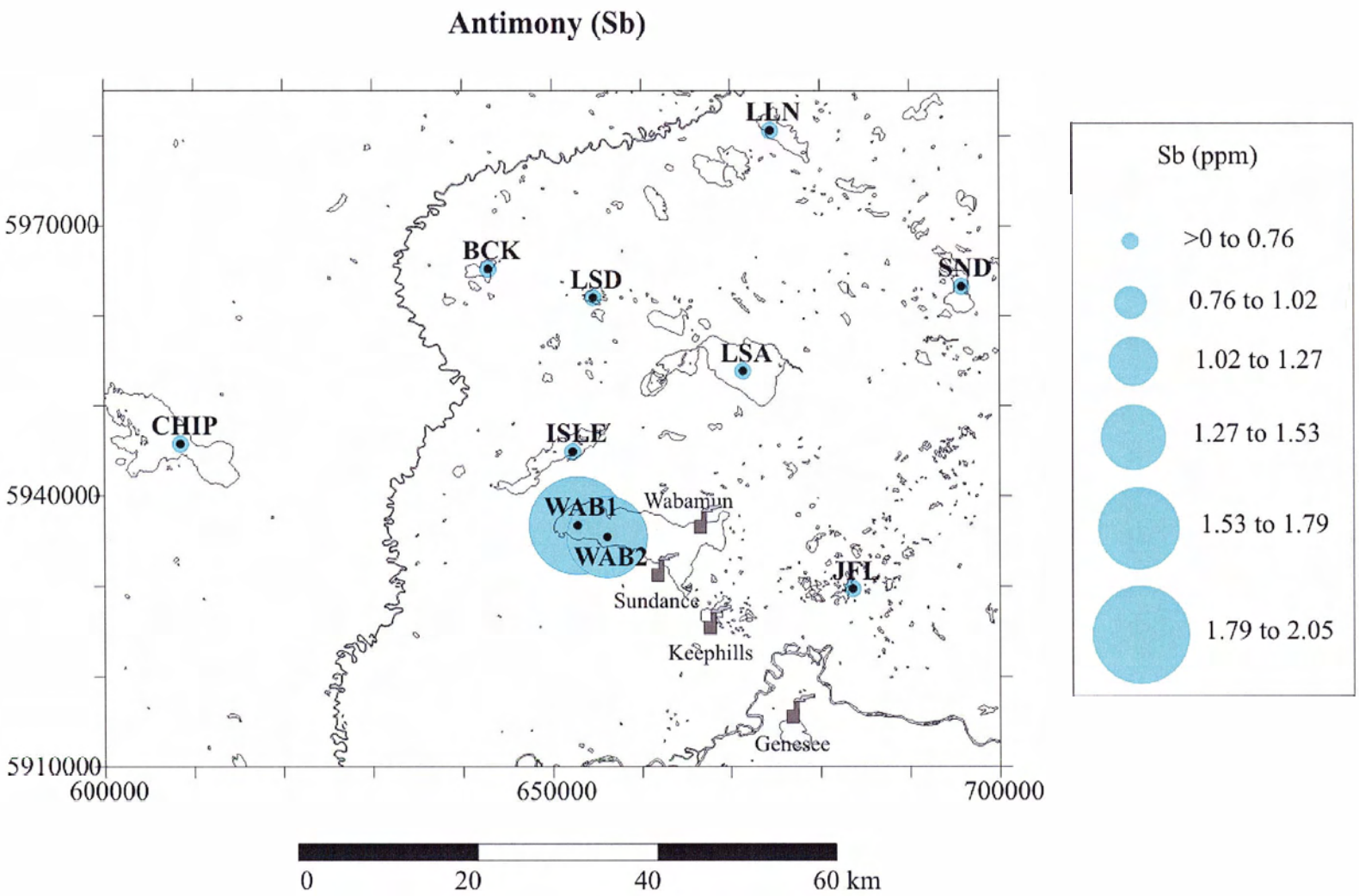

Figure 4.13. The spatial distributions of Selenium (Se) in post-1956 sediments from the lakes in the study area.

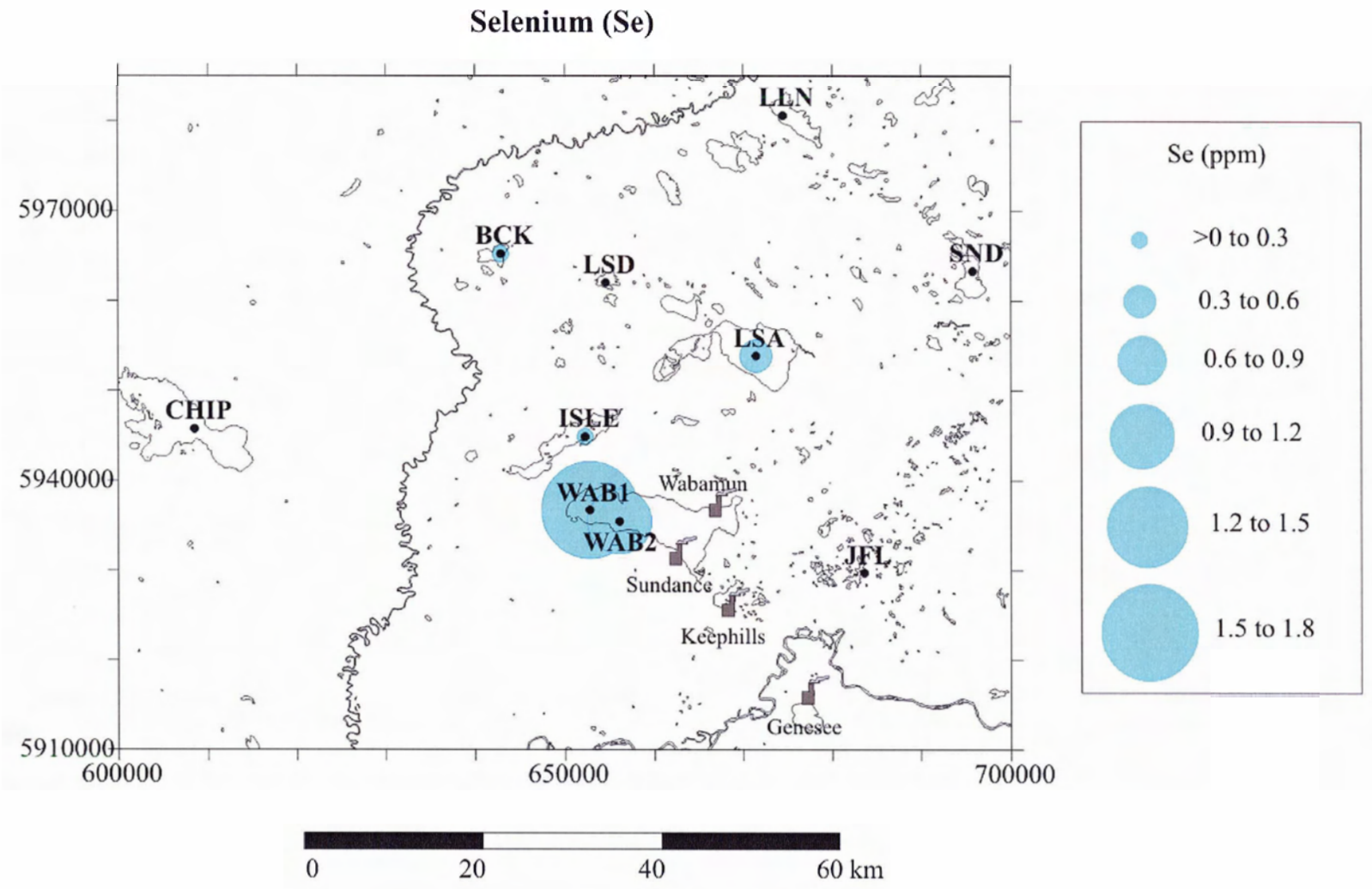

Figure 4.14. The spatial distributions of Thorium (Th) in post-1956 sediments from the lakes in the study area.

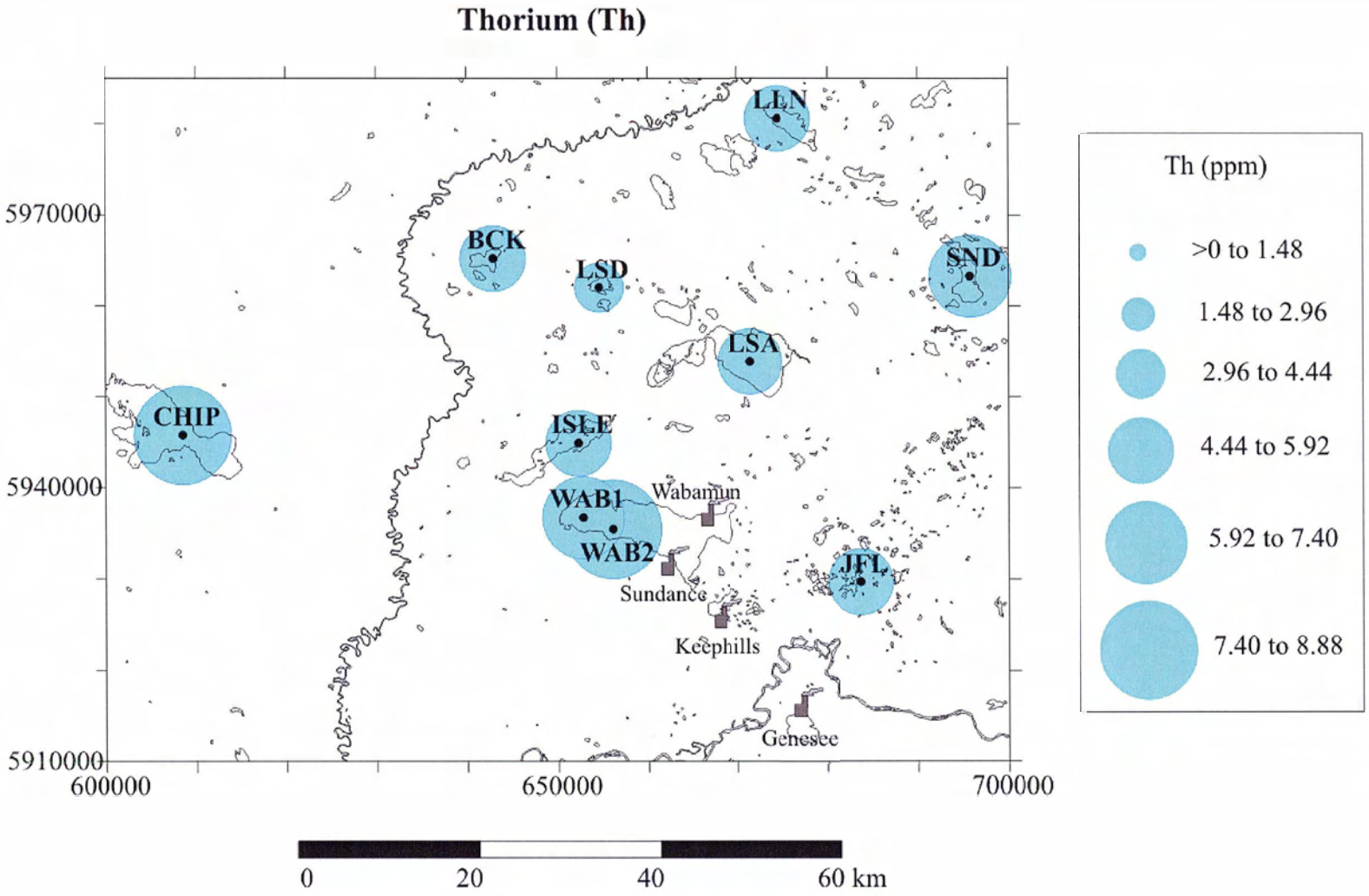

Figure 4.15. The spatial distributions of Titanium (Ti) in post-1956 sediments from the lakes in the study area.

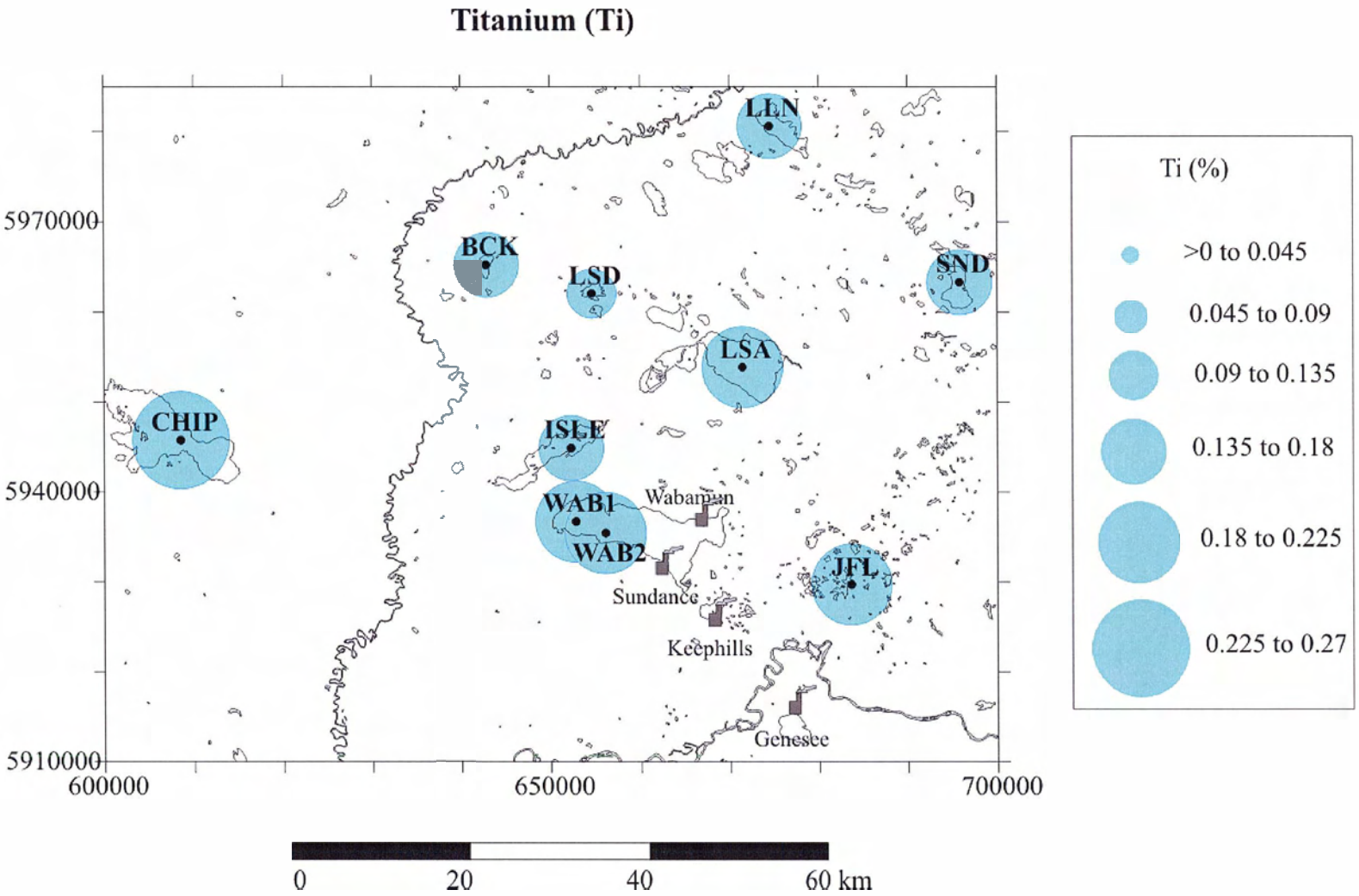

Figure 4.16. The spatial distributions of Uranium (U) in post-1956 sediments from the lakes in the study area.

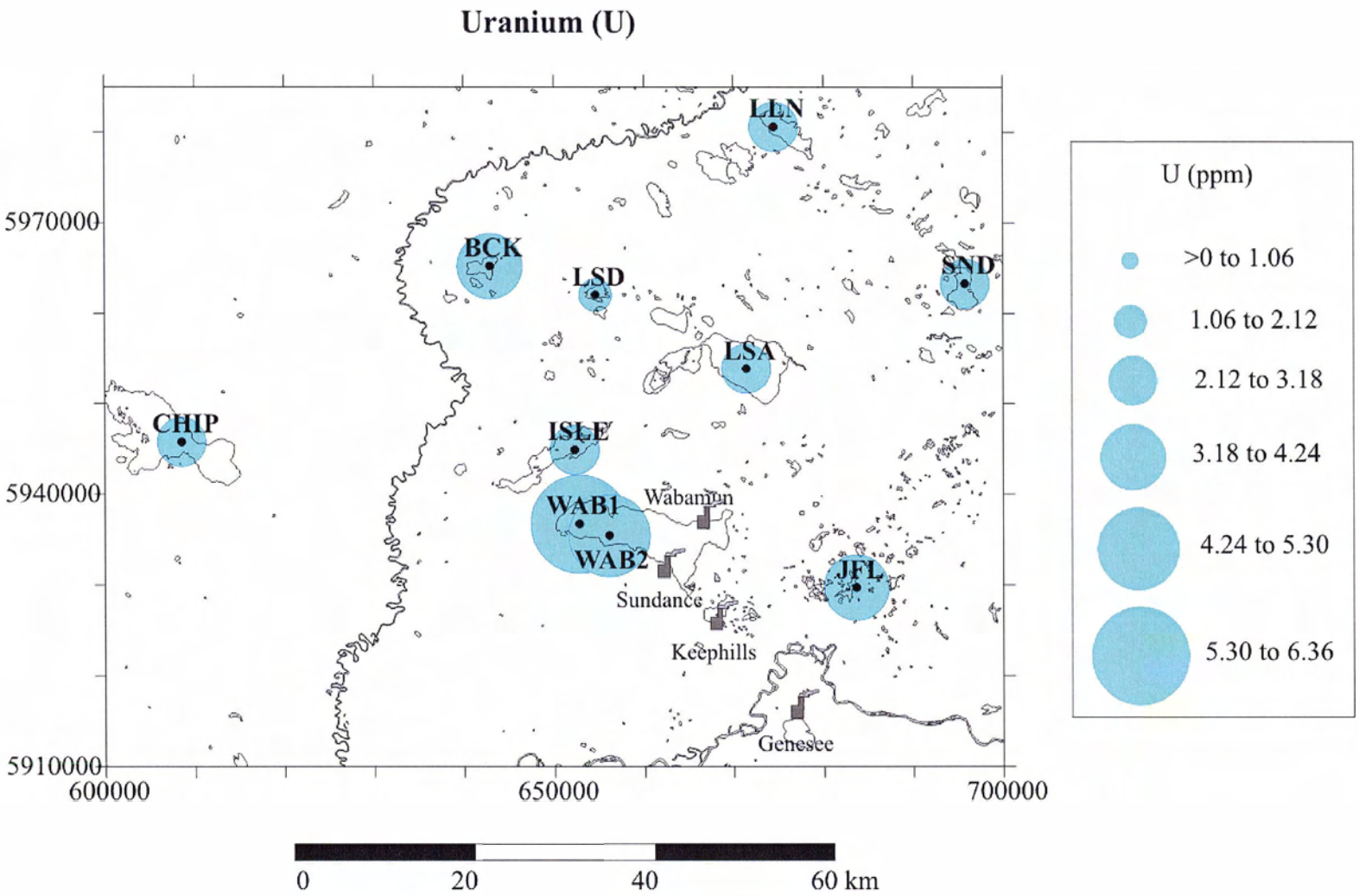

Figure 4.17. The spatial distributions of Tungsten (W) in post-1956 sediments from the lakes in the study area.

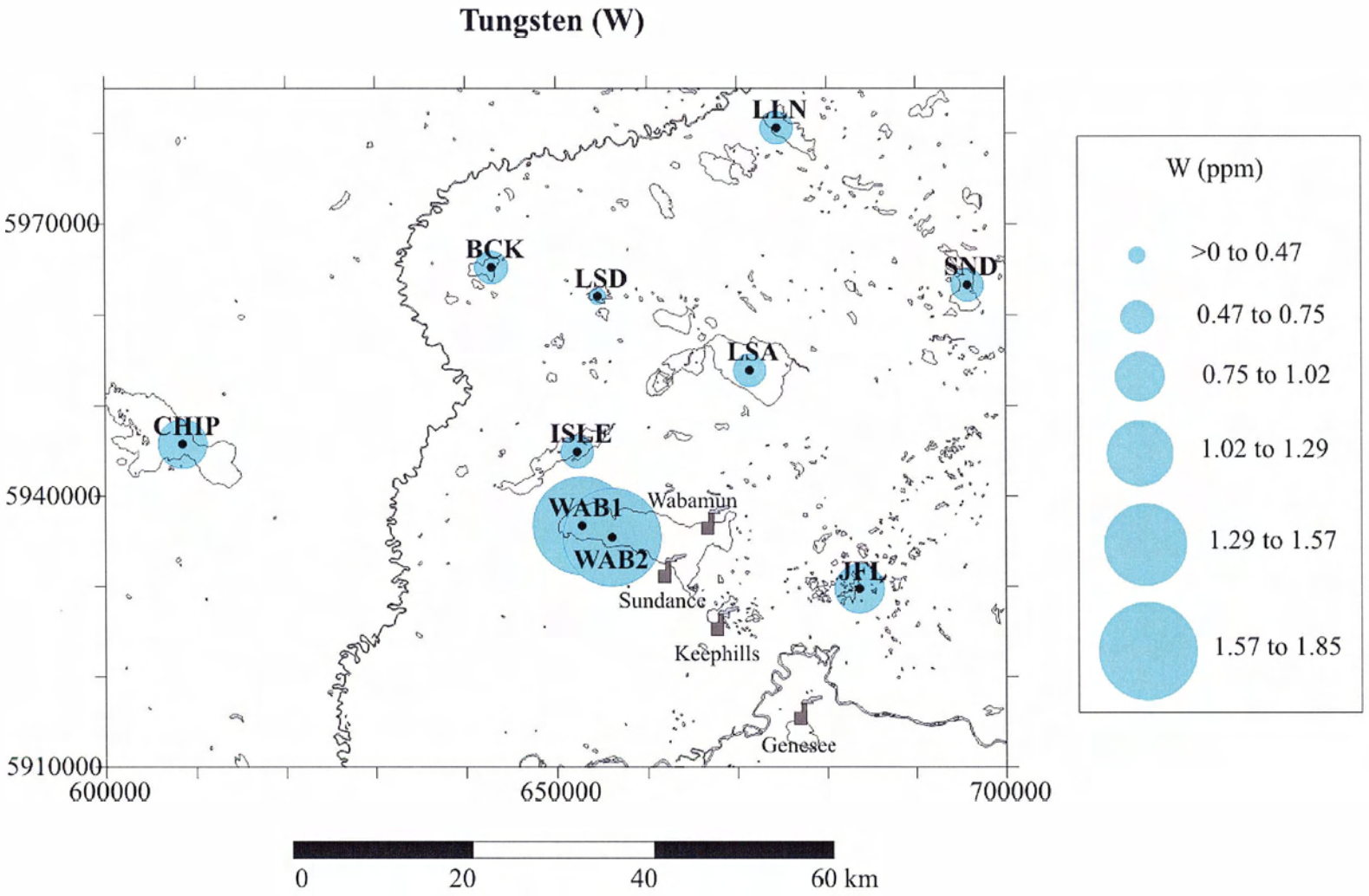

Figure 4.18. The spatial distributions of Zinc (Zn) in post-1956 sediments from the lakes in the study area.

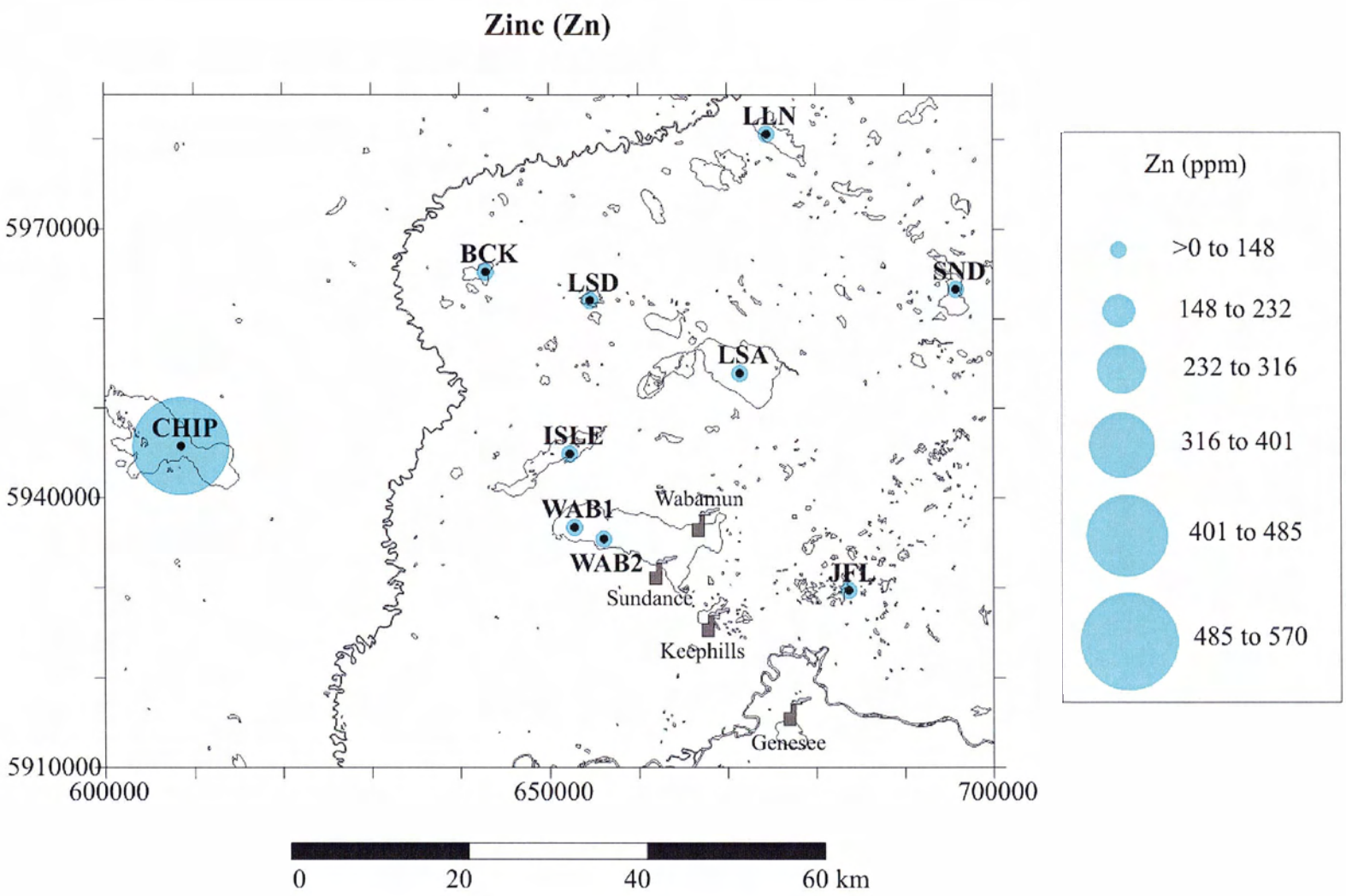

4.2.2. Relationship between the distribution of elements in post-1956 sediments and the power plants

The relationship between the distribution of elements in post-1956 sediments from the studied lakes and emissions from the power plants in the region was studied using a non-parametric Spearman rank correlation method. The correlation was calculated between the elemental data for sediments and the radial distance of the sampling cores from the focal point of power plants in the Wabamun area. The use of a non-parametric correlation is required because of the large range and degree of skew of the data. This method has been successfully used by Telmer et al., (2004) to find links between the emissions from a point source and the distribution of elements in sampling media collected in the study area.

This method is particularly useful when there is no visible indication of influence by an anthropogenic point source. In general, the higher concentrations of elements in proximity to a point source and a rapid decrease in concentrations with increasing distance from the source is often indicative of a link between the emission from the point source and the distribution of elements in their surrounding environment. Therefore, the elevated concentrations of elements in the top sediments cannot be confidently attributed to the emissions from power plants unless there is a measurable decrease in the concentrations in sediments located further from the emission sources, as compared to those that are closer.

Figure 4.19 shows the results of Spearman correlation coefficients between elements in post-1956 sediments from eight lakes in the Wabamun region and radial distance from the

focal point of power plants. Chip Lake (CHIP) is excluded from analyses since it has a different drainage basin from the rest of the studied lakes. All the correlation coefficients are arranged numerically from the lowest (negative correlation coefficient) to the highest (positive correlation coefficient) (Figure 4.19). The results show generally three types of elements in regards to their correlations, which are grouped as follows:

Group I: Elements with a significant negative correlation coefficient (at $p<0.05$ for $n=9$) to the radial distance are related to the impact by the power plants in the region (Ce, Al, W, Hf, Ti, Nb, Ga, and Zr; Figure 4.19). The premise is that the deposition of these elements around the power plants is characterized by a decrease in loading with increasing distance from the power plants' focal point. These elements are known to be enriched in the siliceous structure of fly ash, so the emissions from the power plants in the region may control the distribution of these lithophilic elements in the surficial lake sediments in the study area.

Group II: Elements with random distribution patterns with respect to their radial distance from the power plants are generally identified by statistically insignificant positive or negative correlations (at $p<0.05$ for $n=9$; Figure 4.19). This pattern is attributed to a mix of behaviors, which can be explained by competing inputs from the power plant and natural sources (Telmer, 2004). Alternatively, the obscure relationship indicates that post-depositional diagenetic processes affect the distribution of these elements in the sediments. Elements such as Sb, Cr, Ca, As, Pb, and Ba show a statistically insignificant negative correlation to the radial distances from the power plants (Figure 4.19).

Figure 4.19. Correlation coefficients between concentration of post-1956 sediments and the core's radial distance from the powerplants' focal point (the correlation coefficients are arranged from min of -1 to max of +1; $p<0.05$ at 0.595, n=9).

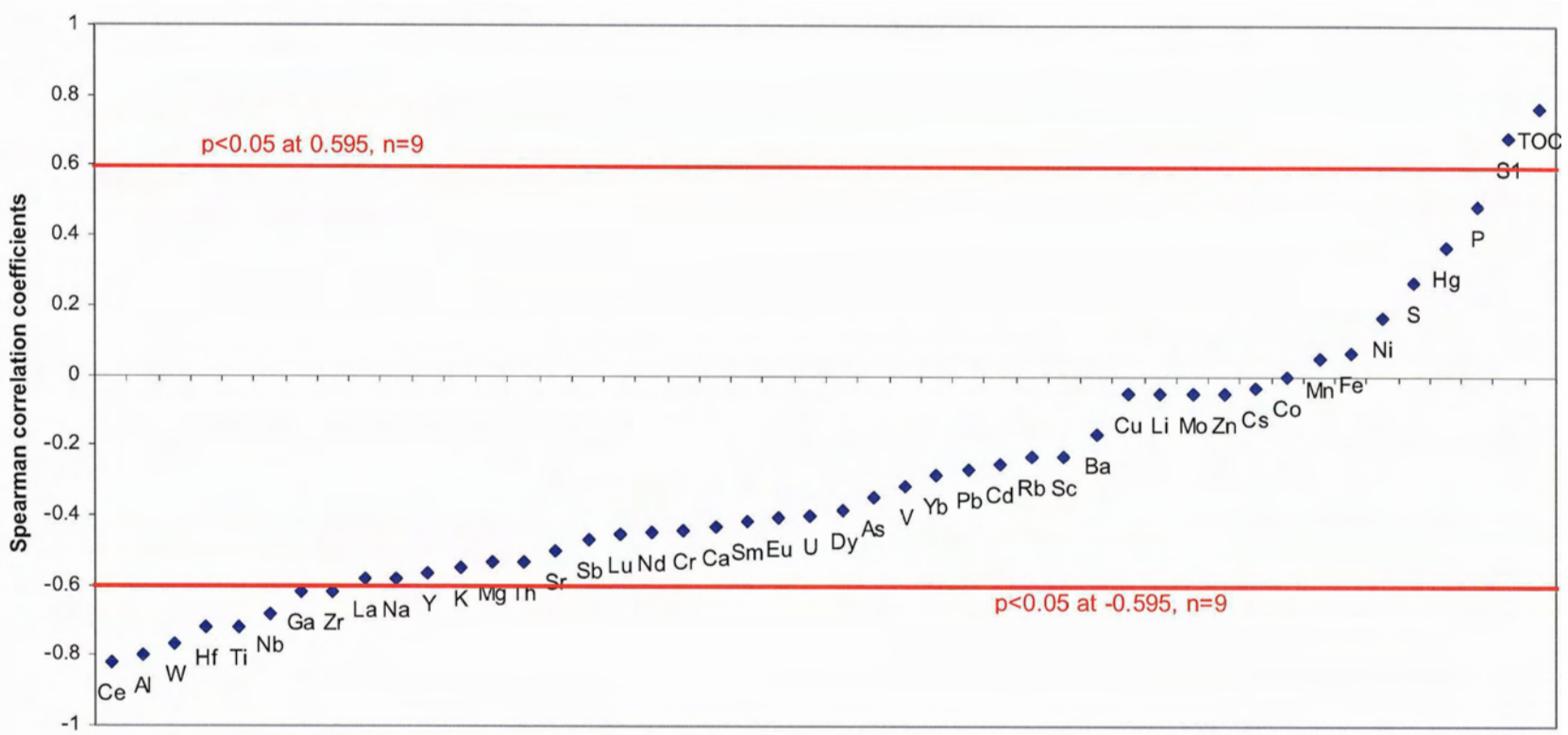

This is supported by SEM/EDX results, which indicate that fly ash particles are rare as compared to the inorganic and organic particles present in the sediments (Chapter 5). The spatial distribution of Hg in top sediments shows an insignificant positive correlation, indicating an insignificant relationship to the power plants (Figure 4.19). The lack of relationship may indicate that the emitted species of Hg (dominantly gaseous Hg (0); Goodarzi, 2004) does not readily precipitate within the study area – it is transported great distances – and so a "bulls-eye" is not developed.

4.2.3. Examining the TOC-normalization approach

The interpretation of elemental data is often complemented with various normalization methods. The normalizing approach corrects the elemental data for interference caused by diluting factor(s) (organic matter, carbonates, silicates) (Håkanson and Jansson, 1983, Horowitz 1991; Sanei et al., 2001). The level of dilution of trace elements may differ from lake to lake depending on their depositional environments and geochemical systems. Hence, it is very important to identify the dilution level of trace elements before applying the normalization technique.

In a study on the recent sediments from Wabamun region (Donahue, 2002), the TOC-normalization method was applied to correct for dilution of Hg and other trace elements in the lake sediments. Although TOC-normalizing is a useful method for identifying the distribution of inorganically induced elements (e.g., geogenic elements; Sanei et al., 2001),

the use of such a method for correcting Hg data requires careful examination to identify whether or not organic matter dilutes Hg in the sediment.

The Spearman rank correlation analysis between spatial distributions of Hg in top sediments of the study area versus that of organic matter (OM) shows a significant positive correlation (0.767; n=9), in particular for very labile S1-compounds (0.8; n=9). This is in agreement with the results of temporal variation for Hg in the sediment profiles from Wabamun Lake, which show a strong positive correlation to OM throughout the studied sediment cores (Chapter 7). These results indicate that both spatial and temporal distributions of Hg in the recent sediments are associated and controlled by organic matter. In other words, organic matter acts as a "concentrator" of Hg rather than a "diluter". In this case, the TOC-normalization approach for correcting the distribution of Hg in sediments (e.g., Donahue, 2002) may also eliminate the variation of Hg and cannot be applied.

4.3. CONCLUSIONS

This chapter focuses on the spatial distribution of Hg and other elements in the recent lake sediments representing the post-coal utilization era (post-1956) in the Wabamun region. The spatial distribution of Hg and most elements of environmental concern (e.g., Sb, As, Cu, Cd, Pb, Zn) in post-1956 deposited sediments do not show a so-called "bulls-eye" pattern around any of the power plants. The lack of such a pattern in the more recent sections of the lake sediment profiles suggests either an insignificant impact from the power plants in the study area or possible redistribution of elements throughout the sediment columns.

The link between distributions of trace elements in the lake sediments around the emission sources was investigated using a non-parametric correlation between the spatial distribution of elements in post-1956 deposited sediments and the radial distances of the cores from the power plants in the Wabamun region.

A significant negative correlation was found for elements Ce, Al, W, Hf, Ti, Nb, Ga, and Zr, which typically enrich in the siliceous structure of fly ash. The negative correlation is caused by a decrease in deposition loading of the given element with increasing distance from the power plants. Often this is a good indication of a possible link with emissions from the power plant.

Spatial dispersion patterns of Hg in post-1956 sediments obtained from 8 lakes in the study area do not show any clear relationship to the radial distance from the power plants, indicating the absence of significant influence by power plants in the study area, with respect to Hg. This obscure relationship indicates that various geochemical processes may form the current spatial distribution of Hg in the sediments. These processes, in conjunction with the natural input of Hg into the sediments, determine the overall temporal and spatial distribution of Hg.

Similarly, the other trace elements such as As, Cd, Cu, Pb, and Zn demonstrate insignificant correlation coefficients to the radial distances from the power plants. This

indicates that inputs of these elements in lakes are from mixed sources, both natural and anthropogenic, or their distribution is affected by the post-depositional diagenesis processes.

The result of this study indicates that organic matter is temporally and spatially associated with Hg in the sediment. Therefore, organic matter acts as a "concentrator" for Hg, so normalizing to TOC also eliminates the variation of Hg.

CHAPTER 5: THE MINERALOGY AND MORPHOLOGY OF RECENT SEDIMENT FROM VARIOUS LAKES IN THE WABAMUN AREA OF ALBERTA, CANADA

5.1. INTRODUCTION

The mineralogy and morphology of the sediment particles from Wabamun Lake, Isle Lake, and Lac Ste. Anne were studied using SEM/EDX analyses (Chapter 1.7.3.3). The study was conducted on selected samples representing temporal variations of trace elements throughout the studied sediment profiles. The results of such analyses for sediment cores WAB1, WAB2, ISLE, and LSA are outlined in this chapter.

5.2. RESULTS AND DISCUSSION

5.2.1. Characterization of the sediments from Wabamun Lake (core WAB1)

The characterization of sediments throughout the WAB1 core is chronologically divided into two sections: (1) post-coal-utilization period and (2) pre-coal-utilization period (Figure 3.1).

5.2.1.1. Post-coal-utilization period

Sediment-Water interface (depth 1cm)

The sediment sample obtained from SWI (depth 1cm) is geochemically characterized by a sharp increase in concentration of all lithophilic elements (e.g., REEs, Zr, Al, Th, etc.) as well as Fe, Mn, and S (Figure 3.1). However, the majority of trace metals (e.g., Cu, Hg, Mo, As, Pb, and Sb), Ca-associated elements (Ca and Sr), and P show a rapid decline at this

depth (Figure 3.1). The mineralogy and morphology of the sediments at the sediment-water interface (depth 1cm) in the WAB1 core is characterized by an abundant presence of spherical particles of fly ash (Figure 5.1). These particles have, for the most part, diameters of less than 2.5 µm (PM2.5) (Figure 5.1).

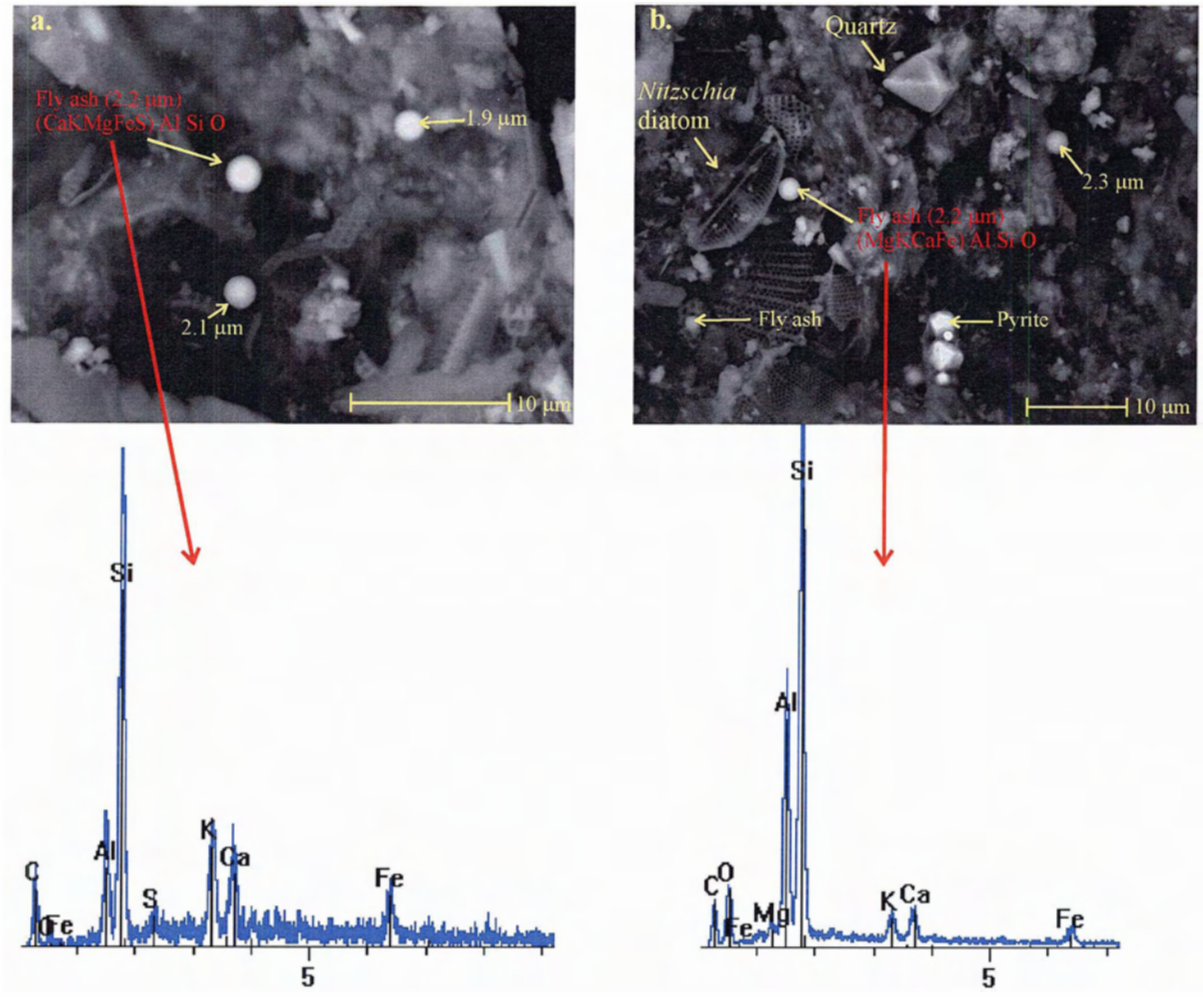

Figure 5.1. The morphology and chemical composition of the WAB1 sediment core at depth 1 cm using back-scattered SEM/EDX. (a) The ferrocalsialic particles of fly ash. (b) Spherical particles of fly ash; a prismatic crystal of quartz, and silicaseous stucture of *Nitzschia* diatom.

This is possibly the result of particle emission control measures adopted by the power plants (e.g., ESP technology), which capture most large particles of PM10, PM>10. The chemical compositions of the fly ash particles consist predominantly of Si-Al, which is accompanied by other major elements such as Ca, Mg, Fe, Ti, K, and S (Figure 5.1). Goodarzi (1996) has classified the stack-emitted fly ash from the Wabamun region powerplants into the ferrocalsialic group, based on their variations in major oxides. The ferrocalsialic fly ash in the Wabamun region is dominated by SiO_2, Al_2O_3, CaO, and, to a lesser extent, Fe_2O_3 (Goodarzi, 1996). The crystalline particles of pyrite and fine, angular fragments of aluminosilicate minerals (clay) as well as quartz are the examples of geogenic particles in this sediment sample (Figure 5.1). Various organic structures such as aquatic plant cell walls and diatom frustules can be seen in the sediment core (Figure 5.1).

2 to 4 cm Interval

The composite sediment sample from the interval of 2 to 4 cm is geochemically characterized by a decrease in concentration of lithophilic elements, while TOC, S and P concentrations remaining high (Figure 3.1). At this interval, there is a period of high concentration for elements Mo, W, Cu, Se, Hg, and Ca (Figure 3.1), which are typically enriched in fly ash. The SEM/EDX results confirm that the sediment at this part of the profile contains an appreciable amount of fine fly ash particles (<3.5 μm) (Figure 5.2). The siliceous fly ash with significant amounts of Al and Ca are often seen trapped within net structures of aquatic plants (Figure 5.2). Furthermore, there is evidence of Ca precipitates in this sediment layer (Figure 5.2), which is attributed to biogeochemical formation of marl (Chapter 3.4.5.1).

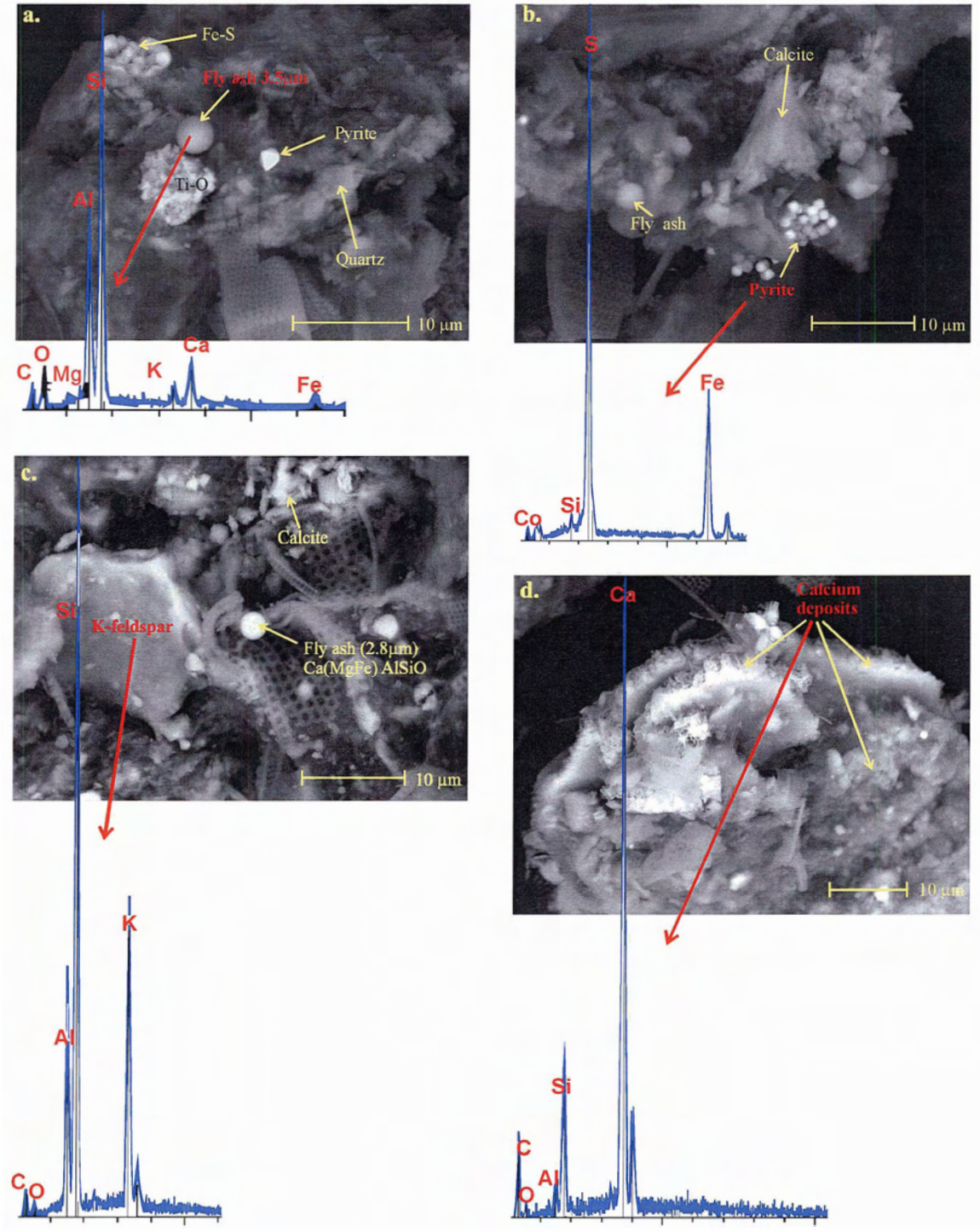

Figure 5.2. The morphology and chemical composition of the WAB1 sediment composite of depth intervals 2-4 cm using back-scattered SEM/EDX. (a) ferrocalsialic particle of fly. (b) agglomerate of framboidal pyrite. (c) angular particle of geocgenic K-Feldspar. (d) calcium deposits.

This Ca deposits show an amorphous structure (Figure 5.2), which can be distinguished from the angular, crystalline calcite derived from geogenic source. The crystalline form of pyrite is abundant throughout the entire sample. These crystals of pyrite are frequently observed agglomerated, and are thus referred to as framboidal pyrite (Figure 5.2). The framboidal pyrite is the result of bacterial activity in the sediment at this depth. Ca-rich minerals, clays, and quartz are abundant in this interval of the studied sediment sample.

9 to 10 cm Interval

The sediment interval between 9 cm and 10 cm represents a period of elevated concentration of most trace metals including those enriched in fly ash (Figure 3.1). This interval also coincides with the historically high emissions in 1970 caused by the simultaneous operations of the Wabamun and Sundance stations (Figure 3.1; Chapter 3.4.1.1). The SEM/EDX analyses of these sediment layers show the presence of larger particles of silicaceous-calcareous (ferrocalsialic) fly ash (up to 8.3 μm) often trapped within organic structures (Figure 5.3). The larger particle size in the fly ash deposited at this depth possibly represents the period in which no particulate control devices (Electrostatic Static Precipitators (ESPs) and filter baghouses) were applied by the power plants and hence larger particles of fly ash were able to be emitted. An abundant amount of framboidal pyrite is present within the cavities of organic matter and host minerals (Figure 5.3). The relatively higher occurrence of framboidal pyrite at this interval as compared to the previous samples may suggest the peak activities of sulfate reducing bacteria and subsequent reactions between the resulting HS^- and Fe^{2+} at this depth (Chapter 3.4.7).

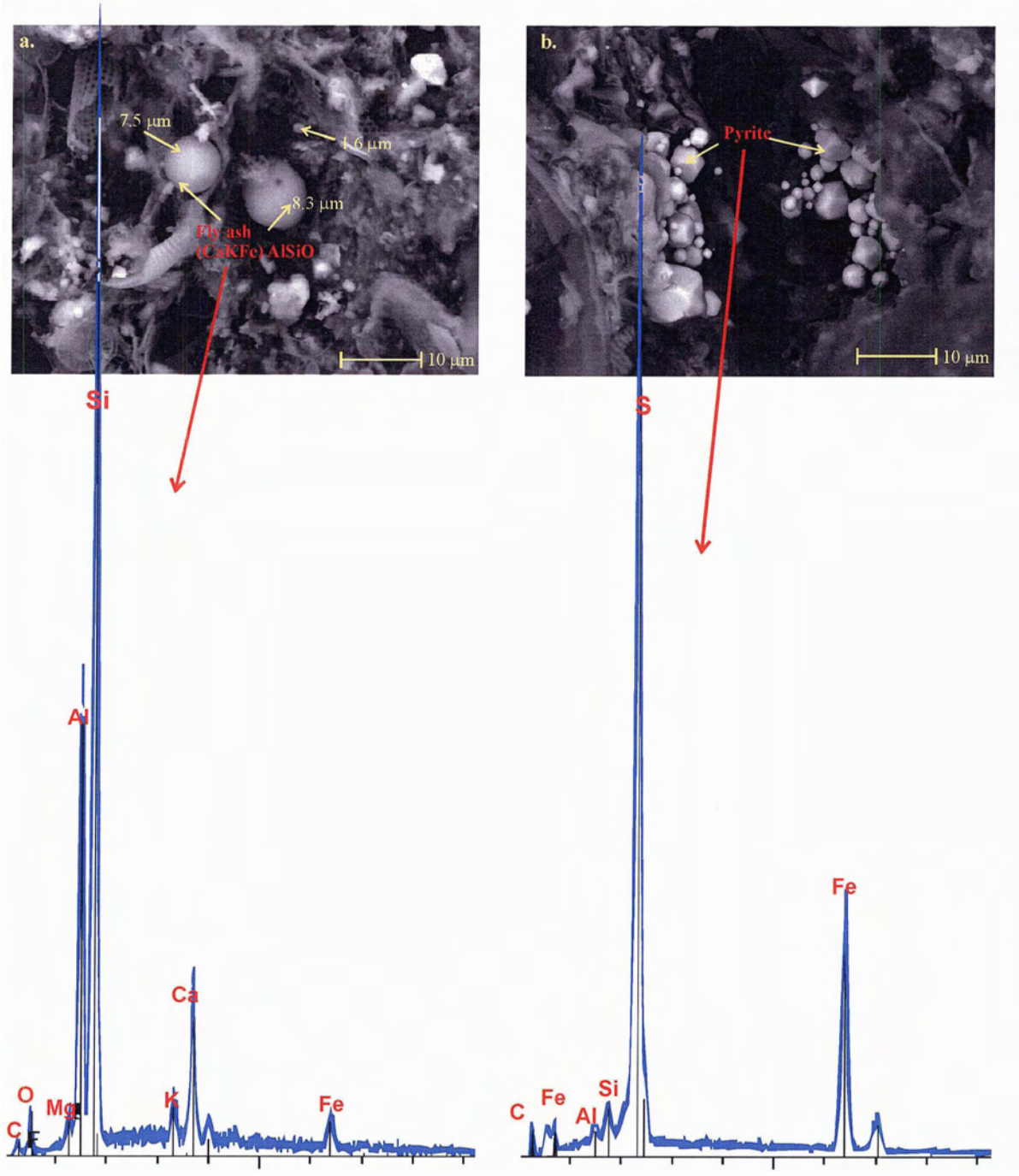

Figure 5.3. The morphology and mineralogy (back-scattered SEM/EDX) of the sediment sample from intervals 9-10 cm in WAB1 core, corresponding to the peak power plant emission period in 1970 in the region. (a) Large (PM10) spherical particles of fly ash. (b) framboidal pyrite formed in the cavity of mineral matrix and organic matter.

5.2.1.2. Pre-coal utilization period

The sediment layer at a depth of 20 cm reflects a rapid increase in concentrations of total sulphur (Figure 3.19). This is evident by a dominating presence of crystalline, framboidal pyrite (Figure 5.4). There is no evidence of fly ash particles in this sediment interval (Figure 5.4). This is expected, as a depth of 20 cm in the WAB1 core marks the era prior to the commencement of coal-fired power plants in the study area (before 1956) (Figure 3.1; Chapter 3.4.1.1). A lack of power plant fly ash at this depth coincides with reduced concentrations of trace elements and heavy metals associated with coal utilization (Cr, V, Ba, Mo, W, Cu, Se, W, Hg, U, Zn, As, Pb, and Sb) (Figure 3.1).

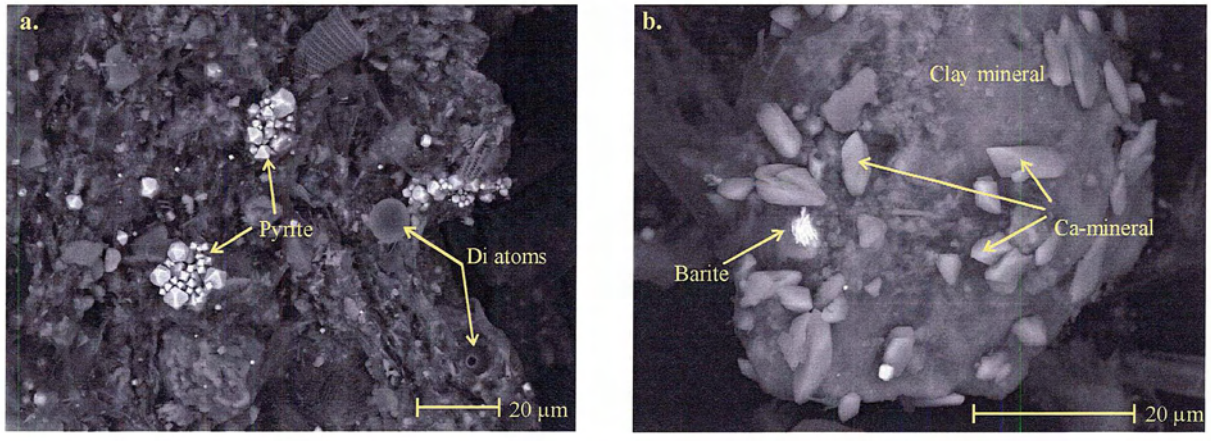

Figure 5.4. The morphology and mineralogy (back-scattered SEM/EDX) of the WAB1 sediment sample from depth 20 cm representing pre-1956 period. (a) A view of the sediment matrix showing abundance of framboidal pyrite and various organic fragments such as Cyclotella diatom. (b) Angular geogenic fragments of $CaCO_3$ and barite mineral in clay matrix.

The sediment layer at a depth of 56 cm is characterized by high concentrations of lithophilic elements (Figure 3.1). The SEM/EDX results show that the sample is dominated by aluminosilicate minerals, which are enriched in lithophilic elements (Figure 5.5). Increases in both Fe and S contents in this sediment layer (Figure 3.19) can be explained by the presence of framboidal pyrite. This sediment interval also includes gypsum, quartz, and siliceous diatom frustules (Figure 5.5).

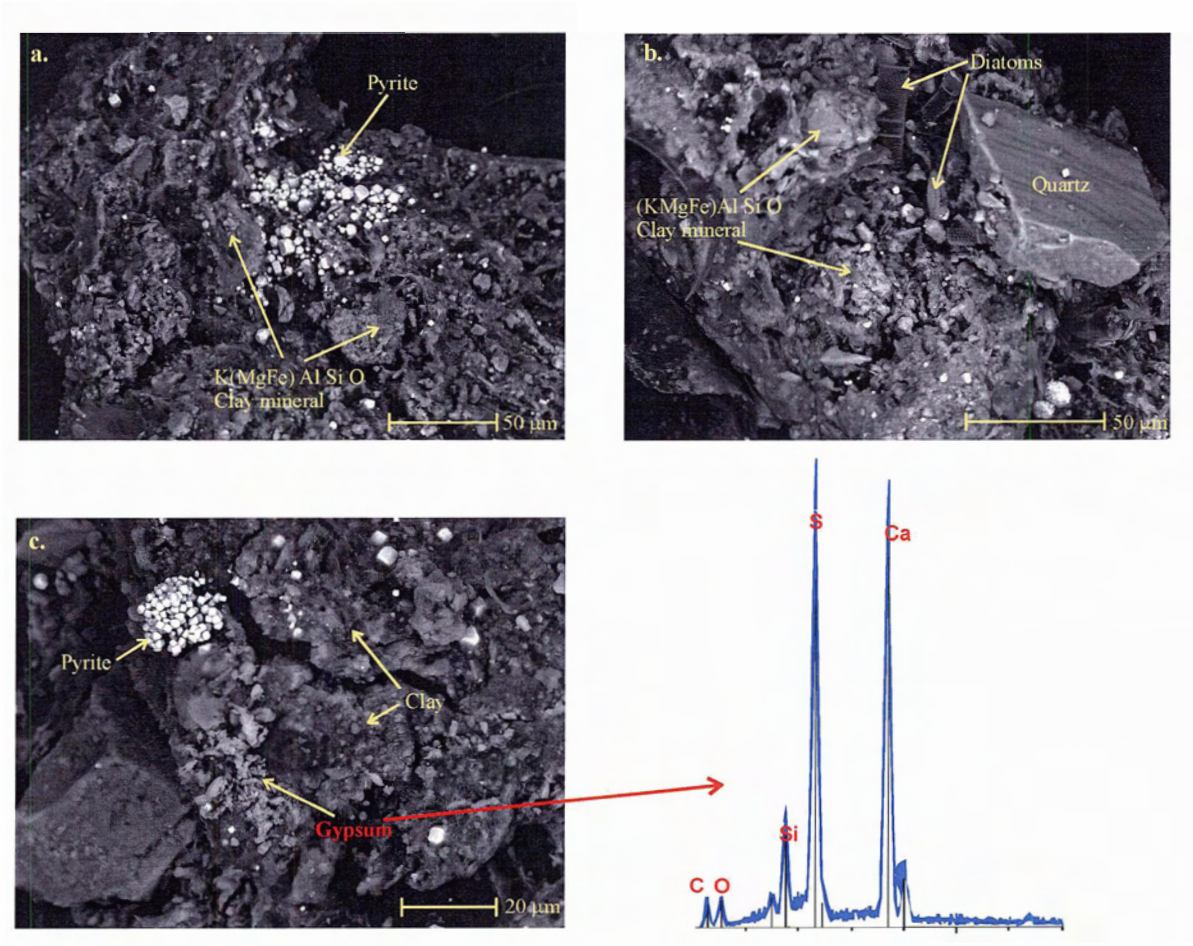

Figure 5.5. The SEM/EDX images of the pre-1956 sediment samples (depth of 56cm) from WAB1 core. (a) Framboidal pyrite formed due to bacterial activities, within the clay mineral matrix. (b) Large angular geogenic quartz and the silicaseous Nitzschia diatom frustule with their glasslike cell walls. (c) Clay mineral matrix containing quartz, mica, pyrite, and gypsum.

5.2.2. Characterization of the sediments from Wabamun Lake (core WAB2)

Sediments from the WAB2 core have very similar mineralogy and morphology as compared to the WAB1 core. The characterization of sediments from the top to the bottom sections of the WAB2 core is as follows:

4 cm to 10 cm interval

A composite sample from sediment intervals at a depth of 4 cm to 6 cm and a sediment layer from a depth of 10cm were selected for SEM/EDX analyses. These sediment intervals reflect the periods of high concentrations of elements associated with fly ash (Figure 3.2; Chapter 3.4.1.1). The SEM images confirm an abundant presence of fly ash particles at these intervals (Figure 5.6), suggesting the effects of emissions from coal-fired power plants on the Wabamun Lake. There are also appreciable amounts of crystalline framboidal pyrite and angular fragments of clay minerals, feldspars, and other aluminosilicates present in these samples (Figure 5.6). The presence of amorphous organic matter deposits in association with Ca (Figure 5.6) is strong evidence for Ca-OM fraction, which is responsible for distribution of trace elements and nutrient (P) in the recent sediment in Wabamun Lake (Chapter 3.4.5).

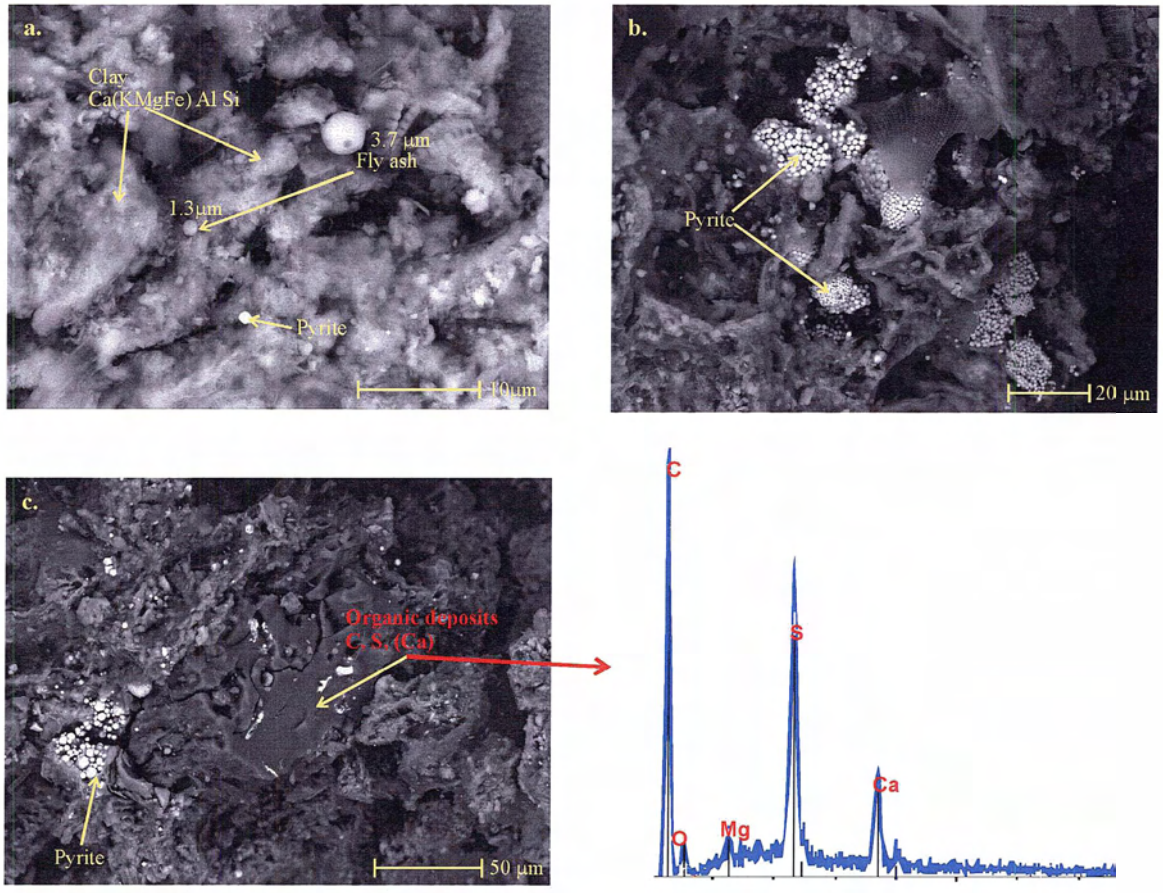

Figure 5.6. The morphology and mineralogy (back-scattered SEM/EDX) of the post-1956 sediments (intervals of 4 cm -10 cm) from WAB2 core. (a) Spherical particles of fly ash (PM>2.5). (b) Agglomerates of framboidal pyrite. (c) The organic deposits enriched in Ca.

16 cm interval

Sediment interval at the depth of 16 cm is characterized by a sudden increase in concentrations of lithophilic elements from geogenic sources and a rapid decline in concentrations of trace metals (Figure 3.2). The SEM/EDX analysis of the sample indicates that the sediment layer is enriched in angular fragments of aluminosilicates (Figure 5.7). There are inclusions of framboidal pyrite formed in the cavities (Figure 5.7). The remnants of living organisms are abundant, often showing perfectly structured cell walls (Figure 5.7).

This indicates the degree of immaturity of the sediment organic matter, which is still in the early stages of the diagenesis process (Chapter 7-8).

According to ^{210}Pb data, the 16 cm interval in the WAB2 profile represents the post-1956 period, which coincides with the onset of the Wabamun power plant (Figure 3.2). However, there is no evidence of fly ash particles found in SEM analysis of this interval (Figure 5.7). Similarly, the elemental data indicate this interval has the lowest concentrations of fly ash-associated elements (Figure 3.2; Chapter 3.4.1.1). This confirms the possible error in determining the 1956 horizon in the WAB2 core, which was discussed in Chapter 2.1.3. It is likely that the 1956 horizon for WAB2 occurs at approximately the same depth as the WAB1 core (depth 15 cm) (Chapter 2.1.3) as suggested by absence of fly ash in underlying sediments (Figure 5.7).

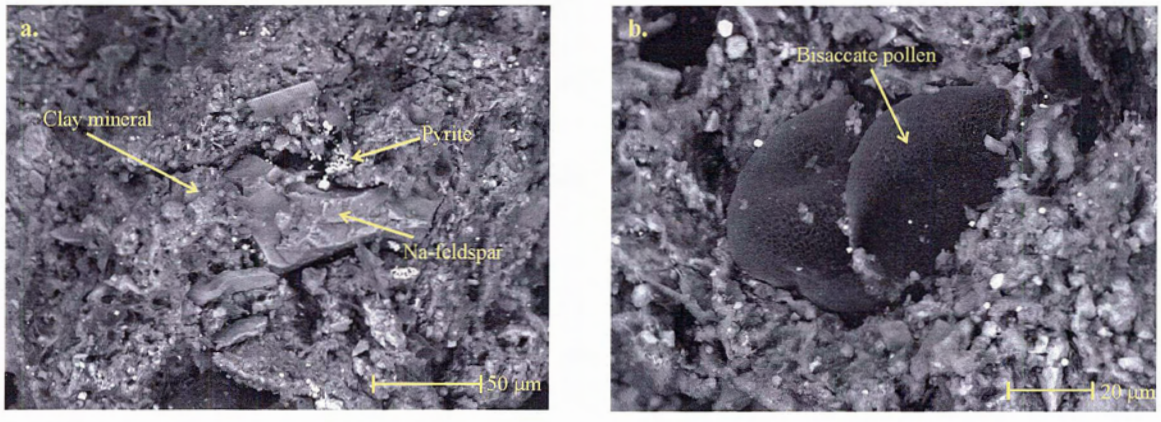

Figure 5.7. The morphology and mineralogy (back-scattered SEM/EDX) of the pre-1956 sediments (depth 16 cm) in WAB2 core. (a) Various geogenic particles. (b) A bisaccate pollen grain.

5.2.3. Characterization of the sediments from Isle Lake (core ISLE)

5.2.3.1. Post-coal utilization period (1-7 cm)

The sediment intervals representing the post-1956 coal utilization era in Isle Lake sediment core (depths 1, 6, and 7 cm) are characterized by the occurrence of spherical fly ash (Figure 5.8). These fly ash particles are likely deposited in the lake by the prevailing winds carrying stack emissions from the power plants in the study region (Figure 5.8). The chemical composition of these fly ash particles are very similar to those found in Wabamun Lake sediments, consisting of Si, Al, and O with the inclusion of Ca, K, and Fe as well (Figure 5.8). In comparison with the Wabamun Lake sediments, Isle Lake sediments show significantly less fly ash particles, as observed by SEM (Figure 5.8). This is due to further distance of Isle Lake from the power plants, as compared to Wabamun Lake (Figure 4.1).

The majority of the inorganic particles consist of Fe, Mn, and Ca (Figure 5.8) indicating the dominant role of these elements as geochemical substrate for trace elements in Isle Lake sediments. The formation of Fe-Mn-P minerals in the uppermost sediment in Isle Lake is indicative of redox-sensitive processes, controlling the distributions of nutrient (P) and trace elements at the surficial sediments in ISLE core (Figure 5.8; Chapter 3.4.6.3). This is in agreement with elemental data showing an abrupt increase in the concentrations of both Fe and Mn at the uppermost sediment sample (Figure 3.18; Chapter 3.4.6.3). Iron (Fe) and Mn are precipitated on the surface of the sediment particles due to oxic conditions in the sediment-water interface (Chapter 3.4.6.3).

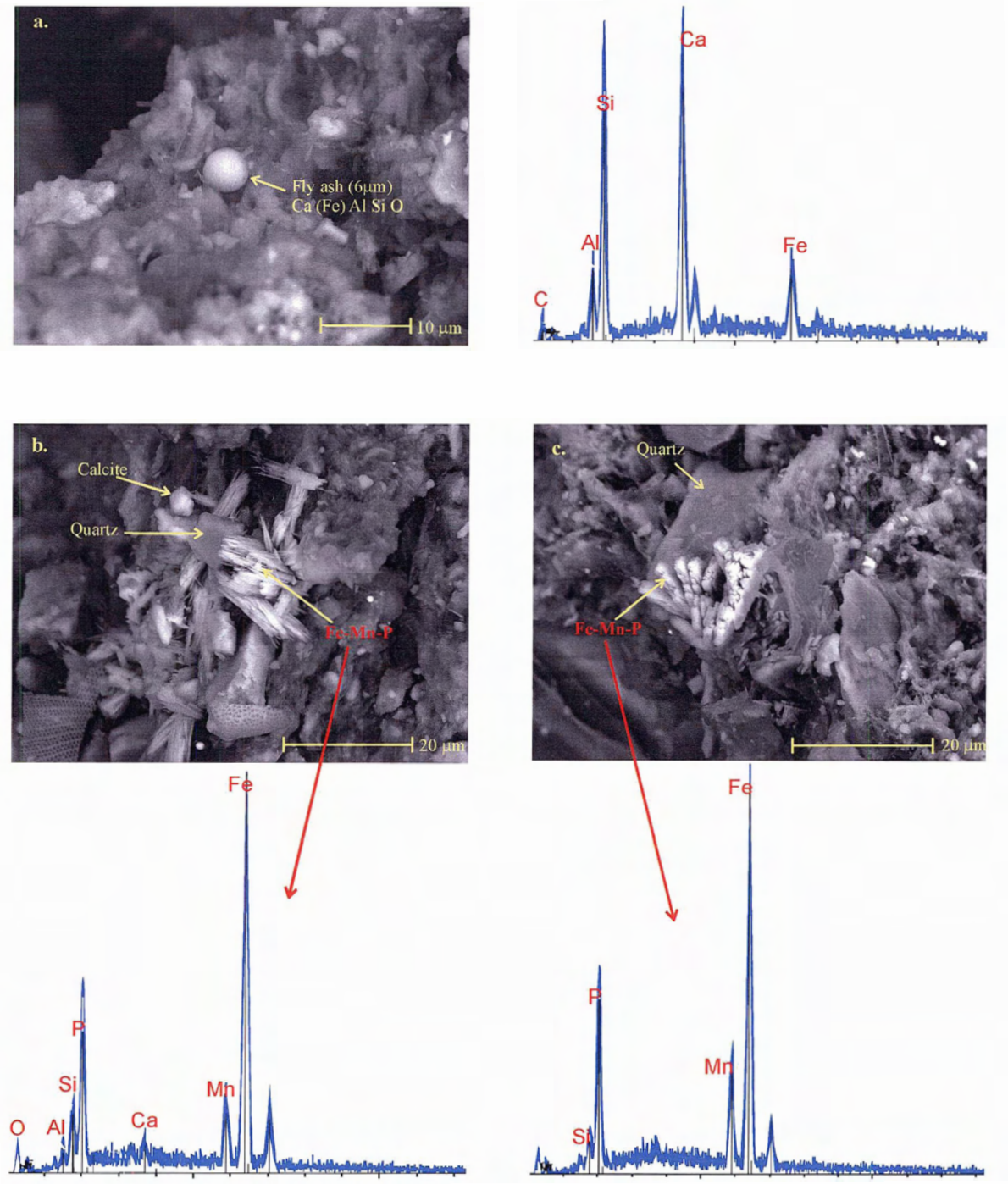

Figure 5.8. The morphology and chemical composition of the post-1956 sediments in Isle Lake using back-scattered SEM/EDX. (a) Spherical fly ash; (b) and (c) The formation of Fe-Mn-P minerals.

5.2.3.2. Pre-coal utilization period Interval (15-16cm)

The sediment obtained from the pre-1956 interval (15 and 16 cm composite) is marked by the absence of any fly ash particles and the relatively higher amounts of spherical agglomerates of framboidal pyrite (Figure 5.9). The geogenic particles in this interval consist of angular fragments of K and Na-feldspars, clay minerals, and quartz (Figure 5.9). Framboidal pyrite is abundant throughout all of the sediment samples from Isle Lake. They often form a spherical agglomerate of small crystalline pyrite minerals (Figure 5.9).

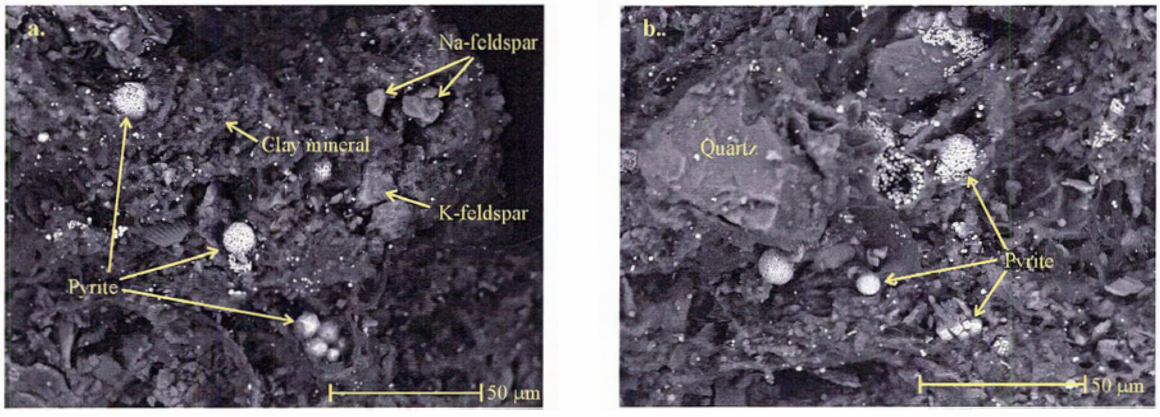

Figure 5.9. The morphology and chemical composition of the pre-1956 sediments in Isle Lake using back-scattered SEM/EDX. (a) Various geogenic minerals; (b) The agglomerates of framboidal pyrite.

5.2.4. Characterization of the sediments from Lac Ste. Anne (core LSA)

In contrast to Wabamun and Isle Lake sediments, the post-1956 sediments from the LSA core (intervals 1-19 cm) do not present any evidence of fly ash particles (Figure 5.10). This is due to further radial distance between Lac Ste. Anne and the power plants in the study

area (Figure 4.1). Furthermore, Lac Ste. Anne is not located downwind the power plants, considering the NW-SE direction of prevailing wind in the region (Figure 4.1).

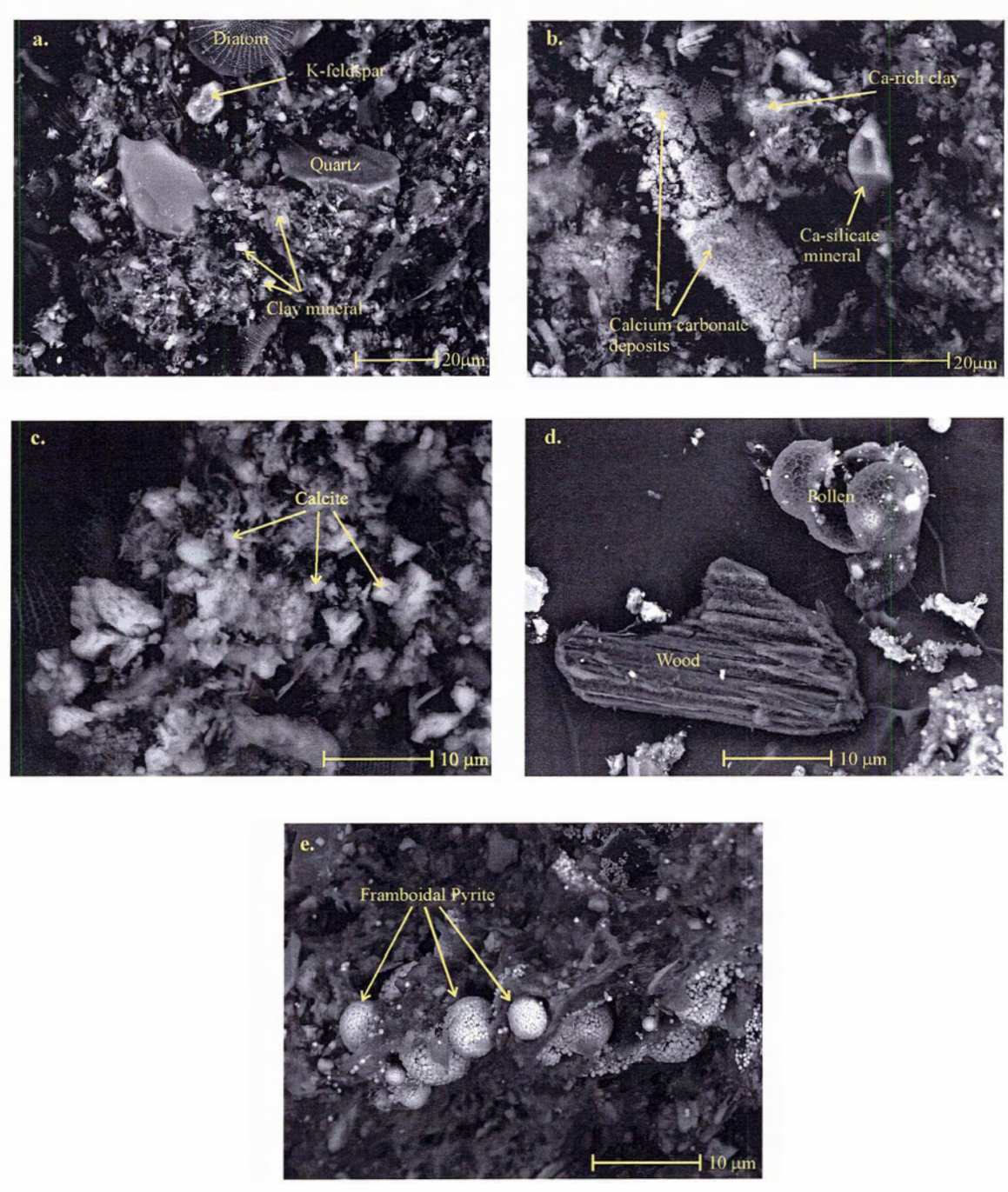

Figure 5.10. The morphology and chemical composition of the sediments throughout Lac Ste. Anne sediment core using back-scattered SEM/EDX.

Overall, the sediment intervals from LSA core consist of various geogenic minerals characterized by angular fragmented minerals such as K/Na-feldspar, quartz, clay, and other alumino-silicates minerals (Figure 5.10). Carbonates are present in both angular crystalline and amorphous forms (Figure 5.10). The angular particles of Ca-minerals indicate the geogenic source, while the amorphous form often represents the authigenic formation of Ca minerals in the sediment layers (Figure 5.10). The organic matter in the LSA sediment intervals consists of the glass-like cell walls of *Cyclotella* diatoms, as well as woody fragments, pollen, and various silicified organic structures (Figure 5.10). Framboidal pyrite is abundant throughout the LSA sediment profile (Figure 5.10), due to widespread bacterial actions. Similar to the other sediment cores, the framboidal pyrite often occurs in spherical agglomerates, which consist of large numbers of small crystalline minerals of pyrite (Figure 5.10).

5.3. CONCLUSIONS

The mineralogy and morphology of the post-industrial sediments from Wabamun Lake is characterized by an abundant presence of spherical particles of fly ash (Figure 5.1). The size of fly ash particles tend to decrease (PM2.5) towards more recent part of the sediment profile indicating the effect of particle emission control measures adopted by the power plants (e.g., ESP technology), which filters the emission of larger particles. There is no evidence of fly ash particles in the sediments deposited prior to the commencement of coal-fired power plants in Wabamun Lake (before 1956).

The fly ash particles can also be found in the post-industrial sediments of Isle Lake. However, our study on the sediment samples of Lac Ste. Anne shows no evidence of fly ash deposition possibly due to unfavorable wind direction from the power plants.

There is evidence of authigenic deposition of lime in the surficial sediments of especially Wabamun Lake and Lac Ste. Anne. These Ca deposits show an amorphous structure, which can be distinguished from the angular, crystalline calcite derived from geogenic sources. The presence of organic matter deposits in association with Ca is also strong evidence for the Ca-OM fraction, which is responsible for distribution of trace elements and nutrients (P) in the recent sediment from the study area.

In Isle Lake sediments, the majority of the inorganic particles consist of Fe, Mn, and Ca, indicating the dominant role of these elements as geochemical substrate for trace elements. The formation of Fe-Mn-P minerals in the uppermost sediment in Isle Lake is indicative of redox-sensitive processes, controlling the distributions of nutrient (P) and trace elements at the surficial sediments of Isle Lake.

The great abundance of framboidal pyrite in the studied sediments corresponds to the maximum concentration of Fe and S in the sediment profiles. The abundance of these pyrite minerals confirms the geochemical affinity of Fe and S in the sediment.

CHAPTER 6: TEMPORAL DISTRIBUTIONS OF RARE EARTH ELEMENTS IN THE SEDIMENTS AND POREWATER FROM LAKES IN CENTRAL ALBERTA, CANADA

6.1. INTRODUCTION

Rare Earth Elements (REEs) (Lanthanide group) consist of a series of fifteen chemically similar elements with atomic numbers ranging from 57 (lanthanum) to 71 (lutetium). Rare Earth Elements are available in the entire geosphere as trace metals and have become important geochemical tracers during the last few decades. They are widely used to study the geochemical behavior of surface and ground waters and their interactions with surrounding rocks/sediments (e.g. Elderfield et al., 1990; Smedley, 1991; Hall et al., 1995; Johannesson et al., 2000). This is because the trivalent REEs are transported through the environment as a group. However, a systematic decrease in ionic radii leads to systematic differences in the chemical properties of REEs, resulting in a fractionation of these elements during reaction and transport in the natural environment (Henderson, 1984).

This chapter is dedicated to the geochemistry of the REEs and their distribution and mobility in the porewater and sediment profiles from Wabamun Lake, Lac Ste. Anne, and Isle Lake in central Alberta.

6.2. RESULTS AND DISCUSSION

6.2.1. Temporal distributions of REEs

The bulk concentrations of REEs in sediment and pore water samples from Wabamun Lake, Lac Ste. Anne, and Isle Lake are shown in Tables 6.1a-d and 6.2a-d. Some of the REEs levels were below the detection limit in the solution phase Tables 6.2a-d. The depth profile of

Table 6.1.a. The total concentration of rare earth elements (REEs) and Y in the sediments from the WAB1 core (Wabamun Lake).

Sediment	La		Ce		Pr	Nd		Sm		Eu		Gd	Tb		Dy	Ho	Er	Tm	Yb		Lu		Y
intervals	NAA*	IMS	NAA*	IMS	IMS	NAA*	IMS	NAA*	IMS	NAA*	IMS	IMS	NAA*	IMS	IMS	IMS	IMS	IMS	NAA*	IMS	NAA*	IMS	IMS
(cm)	ppm	ppm	ppm	ppm	ppm	ppm	ppm	ppm	ppm	ppm	ppm	ppm	ppm	ppm	ppm	ppm	ppm	ppm	ppm	ppm	ppm	ppm	ppm
Wab1-01	28	25	54	44	5.3	21	20	4.5	4.2	0.98	0.80	3.1	0.57	0.60	3.2	0.60	2.1	0.30	1.9	1.9	0.31	0.30	15
Wab1-02	16	15	30	28	3.2	12	12	2.5	2.7	0.52	0.50	2.0	0.37	0.30	1.8	0.40	1.2	0.10	1.0	1.1	0.18	0.10	9
Wab1-03	16	15	32	27	3.3	11	12	2.6	2.5	0.54	0.50	2.0	0.43	0.40	2.0	0.40	1.2	0.20	1.1	1.0	0.18	0.10	9
Wab1-04	17	16	32	29	3.5	11	13	2.7	2.8	0.55	0.50	2.1	0.28	0.40	2.1	0.40	1.3	0.20	1.1	1.2	0.18	0.20	9
Wab1-05	16	17	30	30	3.5	11	13	2.6	2.7	0.53	0.50	2.0	0.36	0.40	2.1	0.40	1.4	0.10	1.2	1.1	0.18	0.20	10
Wab1-06	17	17	32	30	3.6	13	13	2.7	2.8	0.53	0.60	2.0	0.52	0.40	2.1	0.40	1.3	0.20	1.1	1.3	0.17	0.20	10
Wab1-07	18	17	34	31	3.8	12	14	2.8	3.0	0.54	0.60	2.2	0.28	0.40	2.2	0.40	1.4	0.20	1.3	1.2	0.19	0.20	10
Wab1-08	18	18	33	31	3.8	13	14	2.8	2.9	0.59	0.60	2.3	0.37	0.40	2.3	0.50	1.5	0.20	1.2	1.2	0.21	0.20	10
Wab1-09	18	19	34	34	3.9	14	14	2.9	3.2	0.53	0.60	2.3	*<0.24*	0.40	2.4	0.50	1.4	0.20	1.3	1.4	0.21	0.20	11
Wab1-10	18	19	36	34	4.2	14	15	3.0	3.4	0.56	0.60	2.3	0.33	0.50	2.4	0.50	1.5	0.20	1.1	1.4	0.21	0.20	11
Wab1-12	18	18	34	32	3.8	14	14	2.8	3.2	0.64	0.60	2.3	0.39	0.40	2.3	0.40	1.4	0.20	1.4	1.2	0.22	0.20	11
Wab1-14	18	17	35	32	3.8	15	14	2.9	3.0	0.59	0.60	2.2	0.24	0.40	2.3	0.50	1.5	0.20	1.2	1.4	0.21	0.20	11
Wab1-16	17	17	33	30	3.7	14	14	2.8	3.0	0.70	0.60	2.2	0.27	0.40	2.3	0.50	1.5	0.20	1.3	1.3	0.20	0.20	11
Wab1-18	18	17	33	31	3.6	12	14	2.9	3.1	0.63	0.60	2.4	0.38	0.40	2.4	0.40	1.4	0.20	1.3	1.3	0.20	0.20	11
Wab1-20	17	17	33	31	3.7	14	15	2.9	3.3	0.64	0.60	2.5	0.23	0.50	2.3	0.50	1.4	0.20	1.3	1.4	0.18	0.20	11
Wab1-23	18	18	35	33	4.0	15	15	3.1	3.2	0.64	0.60	2.5	0.45	0.50	2.4	0.50	1.6	0.20	1.3	1.5	0.23	0.20	12
Wab1-26	19	18	36	32	3.7	15	14	3.0	3.1	0.60	0.60	2.3	0.57	0.50	2.5	0.50	1.5	0.20	1.3	1.3	0.22	0.20	11
Wab1-30	20	19	40	34	4.1	16	16	3.3	3.4	0.64	0.70	2.6	0.37	0.50	2.6	0.50	1.7	0.20	1.6	1.5	0.24	0.20	12
Wab1-34	21	20	41	37	4.5	16	16	3.4	3.8	0.68	0.80	2.6	*<0.25*	0.50	2.7	0.50	1.7	0.20	1.5	1.6	0.22	0.20	13
Wab1-39	21	21	42	38	4.6	17	17	3.5	3.8	0.68	0.70	2.8	0.33	0.50	2.7	0.60	1.9	0.20	1.5	1.6	0.24	0.20	13
Wab1-44	22	21	43	38	4.6	16	18	3.6	3.7	0.76	0.80	2.6	0.47	0.60	2.8	0.60	1.7	0.20	1.5	1.6	0.25	0.20	14
Wab1-50	23	21	44	38	4.6	17	18	3.8	3.7	0.77	0.80	2.9	0.41	0.60	2.8	0.60	1.9	0.20	1.6	1.7	0.27	0.20	14
Wab1-56	19	22	39	40	4.8	14	18	3.2	4.1	0.59	0.80	2.7	0.43	0.60	3.0	0.60	1.8	0.20	1.4	1.8	0.21	0.20	14
Wab1-64	23	21	42	38	4.7	17	18	3.7	3.9	0.85	0.80	2.8	0.44	0.60	2.7	0.60	1.8	0.20	1.7	1.7	0.26	0.20	13
Min	16	15	30	27	3.2	11	12	2.5	2.5	0.52	0.50	2.0	*ND*	0.30	1.8	0.40	1.2	0.10	1.0	1.0	0.17	0.10	9
Median	18	18	34	32	3.8	14	14	2.9	3.2	0.62	0.60	2.3	0.38	0.45	2.4	0.50	1.5	0.20	1.3	1.4	0.21	0.20	11
Max	28	25	54	44	5.3	21	20	4.5	4.2	0.98	0.80	3.1	0.57	0.60	3.2	0.60	2.1	0.30	1.9	1.9	0.31	0.30	15
Mean	19	19	36	33	4.0	14	15	3.1	3.3	0.64	0.64	2.4	0.39	0.47	2.4	0.49	1.5	0.20	1.3	1.4	0.21	0.20	11

"<" denotes values below detection limits ND: Not detected IMS: Inductively Coupled Plasma-Mass Spectrometry NAA: Instrumental Neutron Activation Analysis * : Preferred method

Table 6.1.b. The total concentration of rare earth elements (REEs) and Y in the sediments from the WAB2 core (Wabamun Lake).

Sediment	La		Ce		Pr	Nd		Sm		Eu		Gd	Tb		Dy	Ho	Er	Tm	Yb		Lu		Y
intervals	NAA*	IMS	NAA*	IMS	IMS	NAA*	IMS	NAA*	IMS	NAA*	IMS	IMS	NAA*	IMS	IMS	IMS	IMS	IMS	NAA*	IMS	NAA*	IMS	IMS
(cm)	ppm	ppm	ppm	ppm	ppm	ppm	ppm	ppm	ppm	ppm	ppm	ppm	ppm	ppm	ppm	ppm	ppm	ppm	ppm	ppm	ppm	ppm	ppm
Wab2-01	19	19	40	33	3.9	14	15	3.2	3.1	0.64	0.60	2.2	*<0.43*	0.50	2.3	0.50	1.5	0.20	1.2	1.3	0.18	0.20	11
Wab2-02	20	19	40	33	4.0	13	14	3.2	3.1	0.69	0.60	2.4	0.49	0.50	2.3	0.50	1.5	0.20	1.4	1.4	0.25	0.20	11
Wab2-03	21	19	40	34	4.0	14	15	3.3	3.1	0.62	0.60	2.4	0.49	0.50	2.4	0.50	1.6	0.20	1.3	1.4	0.21	0.20	11
Wab2-04	21	20	40	37	4.3	16	16	3.2	3.6	0.66	0.60	2.4	0.55	0.50	2.4	0.50	1.7	0.20	1.4	1.4	0.24	0.20	12
Wab2-05	21	20	42	36	4.4	16	16	3.3	3.4	0.72	0.70	2.4	0.48	0.50	2.3	0.50	1.6	0.20	1.5	1.3	0.25	0.20	12
Wab2-06	20	20	39	35	4.2	16	16	3.3	3.4	0.64	0.70	2.6	0.29	0.50	2.4	0.50	1.6	0.20	1.4	1.5	0.21	0.20	12
Wab2-07	21	20	39	35	4.2	16	16	3.3	3.4	0.60	0.70	2.5	0.46	0.50	2.3	0.50	1.6	0.20	1.4	1.5	0.22	0.20	12
Wab2-08	21	20	40	36	4.3	15	16	3.3	3.4	0.68	0.70	2.7	0.53	0.50	2.5	0.50	1.6	0.20	1.3	1.3	0.22	0.20	12
Wab2-09	21	20	41	36	4.4	15	16	3.5	3.4	0.66	0.70	2.6	0.44	0.50	2.5	0.50	1.7	0.20	1.5	1.5	0.22	0.20	13
Wab2-10	21	20	40	37	4.2	16	16	3.4	3.2	0.72	0.70	2.6	0.51	0.50	2.6	0.50	1.6	0.20	1.5	1.6	0.24	0.20	12
Wab2-12	22	20	43	38	4.4	15	17	3.5	3.5	0.80	0.70	2.6	0.35	0.50	2.4	0.50	1.6	0.20	1.6	1.5	0.25	0.20	12
Wab2-14	23	22	45	41	4.8	16	19	3.8	3.7	0.85	0.70	2.9	0.53	0.60	2.6	0.60	1.8	0.20	1.7	1.6	0.29	0.20	13
Wab2-16	24	24	45	44	5.1	17	20	3.9	4.1	0.78	0.80	3.2	0.41	0.60	3.1	0.60	1.9	0.20	1.8	1.7	0.27	0.20	14
Wab2-18	24	21	46	40	4.7	19	19	3.9	3.6	0.83	0.70	2.9	0.39	0.50	2.8	0.50	1.7	0.20	1.6	1.5	0.26	0.20	13
Wab2-20	24	21	47	40	4.7	18	18	3.8	3.8	0.80	0.80	2.8	0.52	0.50	2.6	0.60	1.8	0.20	1.7	1.5	0.29	0.20	14
Wab2-23	24	24	47	44	5.0	17	20	3.9	4.0	0.82	0.90	3.1	0.55	0.60	3.1	0.60	1.9	0.20	1.7	1.7	0.27	0.20	14
Wab2-26	24	23	47	43	5.0	15	20	3.8	4.1	0.85	0.80	3.1	0.38	0.60	3.0	0.60	1.9	0.20	1.6	1.8	0.30	0.20	15
Wab2-30	26	25	51	47	5.4	21	22	4.3	4.3	0.87	0.80	3.4	0.43	0.60	3.2	0.60	1.9	0.20	1.8	1.9	0.30	0.20	16
Wab2-35	26	25	51	48	5.5	19	22	4.2	4.4	0.80	0.90	3.4	0.38	0.60	3.1	0.60	1.9	0.30	1.7	1.8	0.31	0.30	16
Wab2-41	25	24	49	45	5.3	18	20	4.0	4.1	0.88	0.80	3.0	0.48	0.60	3.1	0.70	2.2	0.30	1.9	1.9	0.29	0.30	15
Wab2-47	25	23	47	44	5.1	18	20	4.0	4.0	0.88	0.80	3.1	0.60	0.60	3.0	0.60	1.9	0.20	1.8	1.9	0.28	0.20	15
Wab2-54	25	23	48	45	5.3	19	21	4.1	4.4	0.95	0.90	3.1	*<0.28*	0.60	3.1	0.60	1.9	0.20	1.7	1.9	0.29	0.20	15
Min	19	19	39	33	3.9	13	14	3.2	3.1	0.60	0.60	2.2	*ND*	0.50	2.3	0.50	1.5	0.20	1.2	1.3	0.18	0.20	11
Median	23	21	44	39	4.6	16	17	3.7	3.6	0.79	0.70	2.8	0.48	0.50	2.6	0.50	1.7	0.20	1.6	1.5	0.25	0.20	13
Max	26	25	51	48	5.5	21	22	4.3	4.4	0.95	0.90	3.4	0.60	0.60	3.2	0.70	2.2	0.30	1.9	1.9	0.31	0.30	16
Mean	23	21	44	40	4.6	17	18	3.6	3.7	0.76	0.74	2.8	0.46	0.54	2.7	0.55	1.7	0.21	1.6	1.6	0.26	0.21	13

"<" denotes values below detection limits ND: Not detected IMS: Inductively Coupled Plasma-Mass Spectrometry NAA: Instrumental Neutron Activation Analysis * : Preferred method

Table 6.1.c. The total concentration of rare earth elements (REEs) and Y in the sediments from the ISLE core (Isle Lake).

Sediment intervals	La		Ce		Pr	Nd		Sm		Eu		Gd	Tb		Dy	Ho	Er	Tm	Yb		Lu		Y
	NAA*	IMS	NAA*	IMS	IMS	NAA*	IMS	NAA*	IMS	NAA*	IMS	IMS	NAA*	IMS	IMS	IMS	IMS	IMS	NAA*	IMS	NAA*	IMS	IMS
(cm)	ppm	ppm	ppm	ppm	ppm	ppm	ppm	ppm	ppm	ppm	ppm	ppm	ppm	ppm	ppm	ppm	ppm	ppm	ppm	ppm	ppm	ppm	ppm
ISLE-01	18	16	31	31	3.6	11	15	3.0	3.2	0.55	0.60	2.5	*<0.49*	0.40	2.2	0.40	1.5	0.20	1.5	1.2	0.22	0.20	11
ISLE-02	17	16	31	30	3.5	14	14	3.0	2.9	0.63	0.60	2.3	0.47	0.40	2.2	0.40	1.4	0.20	1.4	1.4	0.24	0.20	11
ISLE-03	18	16	33	30	3.5	14	15	3.0	2.9	0.57	0.60	2.2	0.50	0.40	2.0	0.40	1.3	0.20	1.3	1.4	0.22	0.20	11
ISLE-04	17	15	34	30	3.6	13	14	3.0	3.0	0.57	0.60	2.4	0.43	0.40	2.0	0.40	1.4	0.20	1.3	1.3	0.24	0.20	11
ISLE-05	18	17	34	31	3.7	15	14	3.0	3.2	0.73	0.70	2.6	*<0.27*	0.50	2.2	0.50	1.6	0.20	1.4	1.3	0.21	0.20	12
ISLE-06	17	17	34	32	3.9	12	16	3.0	3.3	0.67	0.70	2.5	0.54	0.50	2.2	0.50	1.5	0.20	1.4	1.4	0.21	0.20	12
ISLE-07	18	17	33	33	3.8	15	16	3.0	3.4	0.77	0.70	2.4	0.31	0.50	2.3	0.50	1.5	0.20	1.3	1.3	0.20	0.20	12
ISLE-08	18	17	32	32	3.7	12	15	3.0	3.2	0.68	0.70	2.7	*<0.25*	0.50	2.2	0.50	1.5	0.20	1.4	1.4	0.21	0.20	12
ISLE-09	18	16	35	30	3.5	15	14	3.1	3.1	0.73	0.60	2.3	0.65	0.40	2.2	0.50	1.4	0.20	1.3	1.2	0.22	0.20	11
ISLE-10	18	17	33	32	3.8	15	15	3.1	3.4	0.59	0.70	2.4	0.37	0.40	2.3	0.50	1.5	0.20	1.3	1.3	0.23	0.20	12
ISLE-12	19	17	36	33	3.9	13	15	3.2	3.2	0.70	0.70	2.6	0.35	0.40	2.3	0.40	1.4	0.20	1.4	1.3	0.25	0.20	12
ISLE-14	19	17	35	32	3.9	15	15	3.2	3.2	0.69	0.70	2.5	0.38	0.50	2.3	0.50	1.4	0.20	1.4	1.4	0.24	0.20	12
ISLE-16	20	17	36	35	4.2	14	17	3.3	3.7	0.84	0.70	2.7	0.30	0.50	2.4	0.50	1.6	0.20	1.6	1.5	0.26	0.20	13
ISLE-18	19	18	37	34	4.2	15	16	3.3	3.5	0.75	0.70	2.8	0.51	0.50	2.6	0.50	1.5	0.20	1.5	1.5	0.23	0.20	13
ISLE-21	21	19	39	36	4.3	18	18	3.6	3.5	0.86	0.70	2.8	0.55	0.50	2.7	0.50	1.6	0.20	1.6	1.6	0.26	0.20	14
ISLE-24	20	19	39	37	4.5	21	18	3.6	3.9	0.76	0.80	2.9	0.43	0.50	2.9	0.60	1.8	0.20	1.6	1.7	0.27	0.20	15
ISLE-27	21	18	40	37	4.3	17	18	3.6	3.7	0.83	0.80	2.9	0.45	0.50	2.8	0.60	1.7	0.20	1.5	1.6	0.31	0.20	15
ISLE-30	20	18	37	36	4.3	16	17	3.4	3.6	0.82	0.70	3.0	0.46	0.50	2.7	0.50	1.6	0.20	1.6	1.6	0.27	0.20	14
ISLE-33	21	19	40	36	4.3	17	18	3.6	3.9	0.72	0.80	3.1	0.62	0.50	2.8	0.60	1.8	0.20	1.6	1.8	0.23	0.20	14
ISLE-36	20	18	37	36	4.3	15	18	3.5	3.8	0.81	0.80	2.9	0.42	0.50	2.7	0.50	1.8	0.20	1.5	1.6	0.23	0.20	14
ISLE-40	21	18	39	33	4.4	15	16	3.6	3.6	0.76	0.80	3.0	0.39	0.50	2.8	0.50	1.7	0.20	1.6	1.5	0.26	0.20	13
ISLE-44	21	18	40	35	4.4	18	18	3.8	3.8	0.86	0.80	3.1	0.49	0.60	2.9	0.60	1.9	0.20	1.8	1.7	0.28	0.20	14
ISLE-48	20	16	37	30	3.9	16	16	3.5	3.3	0.74	0.70	2.7	0.57	0.50	2.8	0.50	1.7	0.20	1.7	1.5	0.28	0.20	13
Min	17	15	31	30	3.5	11	14	3.0	2.9	0.55	0.60	2.2	*ND*	0.40	2.0	0.40	1.3	0.20	1.3	1.2	0.20	0.20	11
Median	19	17	36	33	3.9	15	16	3.2	3.4	0.73	0.70	2.7	0.46	0.50	2.3	0.50	1.5	0.20	1.5	1.4	0.24	0.20	12
Max	21	19	40	37	4.5	21	18	3.8	3.9	0.86	0.80	3.1	0.65	0.60	2.9	0.60	1.9	0.20	1.8	1.8	0.31	0.20	15
Mean	19	17	36	33	4.0	15	16	3.3	3.4	0.72	0.70	2.7	0.46	0.47	2.5	0.50	1.6	0.20	1.5	1.5	0.24	0.20	13

"<" denotes values below detection limits ND: Not detected IMS: Inductively Coupled Plasma-Mass Spectrometry NAA: Instrumental Neutron Activation Analysis * : Preferred method

Table 6.1.d. The total concentration of rare earth elements (REEs) and Y in the sediments from the LSA core (Lac Ste. Anne).

Sediment	La		Ce		Pr	Nd		Sm		Eu		Gd	Tb		Dy	Ho	Er	Tm	Yb		Lu		Y
intervals	NAA*	IMS	NAA*	IMS	IMS	NAA*	IMS	NAA*	IMS	NAA*	IMS	IMS	NAA*	IMS	IMS	IMS	IMS	IMS	NAA*	IMS	NAA*	IMS	IMS
(cm)	ppm	ppm	ppm	ppm	ppm	ppm	ppm	ppm	ppm	ppm	ppm	ppm	ppm	ppm	ppm	ppm	ppm	ppm	ppm	ppm	ppm	ppm	ppm
LSA-01	18	*I.S.*	34	*I.S.*	*I.S.*	11	*I.S.*	2.8	*I.S.*	0.64	*I.S.*	*I.S.*	0.44	*I.S.*	3.2	*I.S.*	*I.S.*	*I.S.*	1.2	*I.S.*	0.20	*I.S.*	*I.S.*
LSA-02	18	17	34	30	3.6	15	14	2.8	2.9	0.58	0.50	2.1	0.38	0.40	1.9	0.40	1.3	0.20	1.3	1.2	0.21	0.10	9
LSA-03	17	17	34	32	3.9	14	15	2.8	2.8	0.60	0.60	2.2	0.44	0.40	1.9	0.40	1.4	0.20	1.3	1.3	0.20	0.20	10
LSA-04	18	17	33	30	3.7	13	14	2.9	2.9	0.66	0.50	2.1	0.29	0.40	2.0	0.40	1.4	0.20	1.4	1.2	0.22	0.20	9
LSA-05	19	17	36	31	3.9	14	15	3.0	3.0	0.71	0.60	2.3	0.37	0.40	2.1	0.40	1.4	0.20	1.3	1.4	0.21	0.20	10
LSA-06	18	17	35	31	3.7	13	14	2.9	3.0	0.61	0.60	2.1	0.26	0.40	2.1	0.40	1.4	0.20	1.4	1.2	0.24	0.20	10
LSA-07	19	18	35	32	4.0	14	15	3.1	2.9	0.58	0.60	2.2	0.41	0.40	2.1	0.40	1.3	0.20	1.4	1.2	0.19	0.20	10
LSA-08	19	18	36	33	3.9	12	15	3.0	3.0	0.60	0.60	2.4	0.52	0.40	2.2	0.40	1.3	0.20	1.3	1.4	0.22	0.20	10
LSA-09	19	19	37	33	4.1	15	16	3.1	3.1	0.62	0.60	2.3	0.39	0.50	2.2	0.40	1.5	0.20	1.5	1.5	0.23	0.20	11
LSA-10	18	18	35	34	4.1	15	16	2.9	3.2	0.60	0.60	2.1	0.41	0.40	2.2	0.40	1.4	0.20	1.3	1.3	0.25	0.20	11
LSA-12	19	19	36	37	4.5	13	17	3.1	3.4	0.61	0.60	2.4	0.42	0.40	2.3	0.40	1.5	0.20	1.5	1.3	0.25	0.20	11
LSA-14	20	18	37	33	4.1	15	16	3.2	3.2	0.77	0.60	2.4	0.52	0.40	2.1	0.40	1.4	0.20	1.4	1.2	0.20	0.20	10
LSA-16	20	19	37	35	4.1	15	17	3.3	3.5	0.67	0.70	2.4	0.58	0.40	2.2	0.40	1.5	0.20	1.4	1.5	0.23	0.20	11
LSA-18	20	19	38	36	4.3	14	17	3.2	3.4	0.74	0.70	2.5	0.42	0.50	2.3	0.50	1.6	0.20	1.4	1.5	0.24	0.20	11
LSA-20	20	20	39	37	4.3	16	17	3.3	3.4	0.76	0.60	2.5	0.48	0.50	2.3	0.50	1.5	0.20	1.5	1.4	0.29	0.20	11
LSA-23	20	20	38	36	4.3	17	16	3.2	3.3	0.75	0.70	2.3	0.48	0.40	2.3	0.50	1.5	0.20	1.4	1.4	0.22	0.20	11
LSA-26	20	20	38	37	4.3	16	17	3.3	3.5	0.70	0.70	2.6	0.43	0.50	2.4	0.50	1.5	0.20	1.5	1.5	0.30	0.20	11
LSA-29	20	19	38	36	4.2	16	16	3.2	3.3	0.72	0.60	2.4	0.32	0.40	2.4	0.50	1.5	0.20	1.5	1.4	0.28	0.20	11
LSA-32	19	19	36	36	4.2	16	16	3.2	3.4	0.69	0.70	2.4	0.31	0.50	2.4	0.40	1.4	0.20	1.4	1.5	0.23	0.20	11
LSA-36	20	19	36	36	4.2	15	17	3.1	3.4	0.64	0.70	2.5	0.34	0.40	2.3	0.40	1.5	0.20	1.3	1.5	0.20	0.20	12
LSA-40	20	19	37	36	4.2	12	16	3.2	3.2	0.65	0.60	2.5	*<0.25*	0.50	2.4	0.50	1.5	0.20	1.5	1.4	0.28	0.20	12
LSA-45	21	20	37	38	4.3	14	17	3.2	3.3	0.80	0.60	2.5	0.44	0.40	2.3	0.50	1.6	0.20	1.5	1.4	0.24	0.20	11
LSA-50	21	20	40	38	4.6	14	18	3.4	3.6	0.72	0.70	2.7	0.49	0.50	2.6	0.50	1.5	0.20	1.6	1.5	0.25	0.20	12
LSA-56	22	21	43	40	4.6	16	18	3.5	3.7	0.83	0.80	2.7	0.33	0.50	2.4	0.50	1.6	0.20	1.6	1.4	0.25	0.20	13
LSA-65	21	20	37	38	4.5	16	18	3.3	3.9	0.72	0.70	2.6	*<0.26*	0.50	2.5	0.50	1.5	0.20	1.5	1.4	0.28	0.20	12
Min	17	*ND*	33	*ND*	*ND*	11	*ND*	2.8	*ND*	0.58	*ND*	*ND*	*ND*	*ND*	1.9	*ND*	*ND*	*ND*	1.2	*ND*	0.19	*ND*	*ND*
Median	20	19	37	36	4.2	15	16	3.2	3.3	0.67	0.60	2.4	0.42	0.40	2.3	0.40	1.5	0.20	1.4	1.4	0.23	0.20	11
Max	22	21	43	40	4.6	17	18	3.5	3.9	0.83	0.80	2.7	0.58	0.50	3.2	0.50	1.6	0.20	1.6	1.5	0.30	0.20	13
Mean	19	19	37	35	4.2	14	16	3.1	3.3	0.68	0.63	2.4	0.41	0.44	2.3	0.44	1.5	0.20	1.4	1.4	0.24	0.20	11

<: below detection limits ND: Not detected I.S.: Insufficient sample IMS: Inductively Coupled Plasma-Mass Spectrometry NAA: Neutron Activation Analysis * : Preferred method

Table 6.2.a. The total concentration of dissolved rare earth elements (REEs) and Y in the porewater from the WAB1 core (Wabamun Lake).

Sediment	La	Ce	Pr	Nd	Sm	Eu	Gd	Tb	Dy	Er	Tm	Yb	Lu	Y
depths (cm)	ppb	ppb	ppb	ppb	ppb	ppb	ppb	ppb	ppb	ppb	ppb	ppb	ppb	ppb
Wab1-01	< .01	0.01	< .01	0.01	< .02	< .01	0.01	< .01	< .01	< .01	< .01	< .01	< .01	0.02
Wab1-02	< .01	0.01	< .01	0.01	< .02	0.01	< .01	< .01	< .01	< .01	< .01	< .01	< .01	0.02
Wab1-03	< .01	0.01	< .01	0.01	< .02	< .01	< .01	< .01	< .01	< .01	< .01	< .01	< .01	0.02
Wab1-04	0.01	0.02	< .01	0.01	< .02	0.01	0.01	< .01	< .01	< .01	< .01	< .01	< .01	0.03
Wab1-05	< .01	0.02	< .01	0.01	< .02	0.01	< .01	< .01	< .01	< .01	< .01	< .01	< .01	0.03
Wab1-06	0.01	0.02	< .01	0.01	< .02	< .01	< .01	< .01	< .01	< .01	< .01	< .01	< .01	0.04
Wab1-07	0.01	0.02	< .01	0.02	< .02	< .01	< .01	< .01	< .01	< .01	< .01	< .01	< .01	0.03
Wab1-08	0.02	0.04	< .01	0.02	< .02	0.01	0.01	< .01	0.01	< .01	< .01	0.01	< .01	0.04
Wab1-09	0.02	0.05	0.01	0.02	< .02	< .01	0.01	< .01	< .01	< .01	< .01	< .01	< .01	0.05
Wab1-10	0.02	0.05	0.01	0.02	< .02	0.01	0.01	< .01	0.01	< .01	< .01	< .01	< .01	0.06
Wab1-12	0.02	0.04	0.01	0.02	< .02	0.01	0.01	< .01	0.01	< .01	< .01	< .01	< .01	0.05
Wab1-14	0.03	0.05	0.01	0.02	< .02	0.01	0.01	< .01	0.01	< .01	< .01	< .01	< .01	0.05
Wab1-16	0.03	0.05	0.01	0.02	< .02	0.01	0.01	< .01	0.01	< .01	< .01	0.01	< .01	0.06
Wab1-18	0.03	0.05	0.01	0.03	< .02	0.01	0.01	< .01	0.01	0.01	< .01	0.01	< .01	0.05
Wab1-20	0.03	0.05	0.01	0.02	< .02	0.01	0.01	< .01	0.01	< .01	< .01	0.01	< .01	0.08
Wab1-23	0.03	0.06	0.01	0.03	< .02	< .01	0.02	< .01	0.01	0.01	< .01	< .01	< .01	0.08
Wab1-26	0.03	0.05	0.01	0.03	< .02	< .01	0.02	< .01	0.01	0.01	< .01	0.01	< .01	0.08
Wab1-30	0.04	0.08	0.01	0.05	< .02	0.01	0.02	< .01	0.01	0.01	< .01	0.01	< .01	0.10
Wab1-34	0.04	0.08	0.01	0.04	< .02	< .01	0.01	< .01	0.01	0.01	< .01	0.01	< .01	0.10
Wab1-39	0.05	0.09	0.01	0.05	< .02	0.01	0.02	< .01	0.02	0.01	< .01	0.01	< .01	0.11
Wab1-44	0.06	0.11	0.01	0.05	0.02	0.01	0.02	< .01	0.02	0.01	< .01	0.01	< .01	0.13
Wab1-50	0.07	0.12	0.02	0.06	0.02	0.01	0.02	< .01	0.02	0.01	< .01	0.01	< .01	0.17
Wab1-56	0.07	0.13	0.02	0.07	< .02	0.01	0.03	< .01	0.02	0.01	< .01	0.01	< .01	0.15
Wab1-64	0.06	0.10	0.02	0.06	< .02	0.01	0.03	< .01	0.02	0.01	< .01	0.01	< .01	0.16
Min	*ND*	0.01	*ND*	0.01	*ND*	*ND*	*ND*	*ND*	*ND*	*ND*	*ND*	*ND*	*ND*	0.02
Median	0.03	0.05	0.01	0.02	0.02	0.01	0.01	*ND*	0.01	0.01	*ND*	0.01	*ND*	0.06
Max	0.07	0.13	0.02	0.07	0.02	0.01	0.03	*ND*	0.02	0.01	*ND*	0.01	*ND*	0.17
Mean	0.03	0.05	0.01	0.03	0.02	0.01	0.02	*ND*	0.01	0.01	*ND*	0.01	*ND*	0.07

"<" denotes values below detection limits ND: Not detected

Table 6.2.b. The total concentration of dissolved rare earth elements (REEs) and Y in the porewater from the WAB2 core (Wabamun Lake).

Sediment	La	Ce	Pr	Nd	Sm	Eu	Gd	Tb	Dy	Er	Tm	Yb	Lu	Y
depths (cm)	ppb	ppb	ppb	ppb	ppb	ppb	ppb	ppb	ppb	ppb	ppb	ppb	ppb	ppb
Wab2-01	0.01	0.01	< .01	0.01	< .02	0.01	< .01	< .01	< .01	< .01	< .01	< .01	< .01	0.03
Wab2-02	0.01	0.02	< .01	0.01	< .02	< .01	< .01	< .01	< .01	< .01	< .01	< .01	< .01	0.03
Wab2-03	0.01	0.02	< .01	0.01	< .02	< .01	< .01	< .01	< .01	< .01	< .01	< .01	< .01	0.03
Wab2-04	0.01	0.02	< .01	0.01	< .02	< .01	0.01	< .01	< .01	< .01	< .01	< .01	< .01	0.03
Wab2-05	0.01	0.03	< .01	0.01	< .02	< .01	< .01	< .01	< .01	< .01	< .01	< .01	< .01	0.03
Wab2-06	0.01	0.03	< .01	0.01	< .02	< .01	< .01	< .01	< .01	< .01	< .01	< .01	< .01	0.02
Wab2-07	0.01	0.02	< .01	0.01	< .02	< .01	0.01	< .01	< .01	< .01	< .01	< .01	< .01	0.02
Wab2-08	< .01	0.02	< .01	0.01	< .02	< .01	< .01	< .01	< .01	< .01	< .01	< .01	< .01	0.02
Wab2-09	0.01	0.03	< .01	0.01	< .02	< .01	< .01	< .01	< .01	< .01	< .01	< .01	< .01	0.02
Wab2-10	0.02	0.03	< .01	0.02	< .02	< .01	0.01	< .01	< .01	< .01	< .01	< .01	< .01	0.03
Wab2-12	0.02	0.04	0.01	0.02	< .02	< .01	0.01	< .01	0.01	< .01	< .01	< .01	< .01	0.03
Wab2-14	0.03	0.06	0.01	0.04	< .02	< .01	0.01	< .01	0.01	0.01	< .01	< .01	< .01	0.04
Wab2-16	0.04	0.08	0.01	0.04	< .02	< .01	0.01	< .01	0.01	0.01	< .01	0.01	< .01	0.05
Wab2-18	0.04	0.08	0.01	0.04	< .02	< .01	0.01	< .01	0.01	0.01	< .01	< .01	< .01	0.05
Wab2-20	0.03	0.07	0.01	0.04	< .02	< .01	0.01	< .01	0.01	< .01	< .01	< .01	< .01	0.04
Wab2-23	0.05	0.10	0.01	0.05	< .02	< .01	0.02	< .01	0.01	0.01	< .01	0.01	< .01	0.07
Wab2-26	0.06	0.11	0.01	0.07	< .02	< .01	0.02	< .01	0.01	0.01	< .01	0.01	< .01	0.08
Wab2-30	0.07	0.13	0.02	0.08	0.02	< .01	0.02	< .01	0.01	0.01	< .01	0.01	< .01	0.09
Wab2-35	0.07	0.13	0.02	0.07	0.02	< .01	0.02	< .01	0.01	0.01	< .01	0.01	< .01	0.09
Wab2-41	0.09	0.17	0.02	0.11	0.02	< .01	0.02	< .01	0.02	0.01	< .01	0.01	< .01	0.11
Wab2-47	0.10	0.21	0.03	0.13	0.03	< .01	0.03	< .01	0.02	0.01	< .01	0.01	< .01	0.14
Wab2-54	0.11	0.19	0.02	0.12	0.02	< .01	0.03	< .01	0.02	0.01	< .01	0.01	< .01	0.13
Min	*ND*	0.01	*ND*	0.01	*ND*	*ND*	*ND*	*ND*	*ND*	*ND*	*ND*	*ND*	*ND*	0.02
Median	0.03	0.05	0.01	0.03	0.02	0.01	0.01	*ND*	0.01	0.01	*ND*	0.01	*ND*	0.04
Max	0.11	0.21	0.03	0.13	0.03	0.01	0.03	*ND*	0.02	0.01	*ND*	0.01	*ND*	0.14
Mean	0.04	0.07	0.02	0.04	0.02	0.01	0.02	*ND*	0.01	0.01	*ND*	0.01	*ND*	0.05

"<" denotes values below detection limits ND: Not detected

Table 6.2.c. The total concentration of dissolved rare earth elements (REEs) and Y in the porewater from the ISLE core (Isle Lake).

Sediment	La	Ce	Pr	Nd	Sm	Eu	Gd	Tb	Dy	Er	Tm	Yb	Lu	Y
depths (cm)	ppb	ppb	ppb	ppb	ppb	ppb	ppb	ppb	ppb	ppb	ppb	ppb	ppb	ppb
ISLE-01	0.01	0.01	< .01	0.01	< .02	< .01	0.01	< .01	< .01	< .01	< .01	< .01	< .01	0.02
ISLE-02	0.01	0.02	< .01	0.01	< .02	< .01	< .01	< .01	< .01	< .01	< .01	< .01	< .01	0.02
ISLE-03	0.01	0.03	< .01	0.02	< .02	< .01	0.01	< .01	< .01	< .01	< .01	< .01	< .01	0.02
ISLE-04	0.02	0.04	0.01	0.02	< .02	< .01	< .01	< .01	< .01	< .01	< .01	< .01	< .01	0.03
ISLE-05	0.02	0.04	0.01	0.03	< .02	< .01	0.01	< .01	< .01	< .01	< .01	< .01	< .01	0.04
ISLE-06	0.02	0.03	< .01	0.02	< .02	< .01	0.01	< .01	< .01	< .01	< .01	< .01	< .01	0.03
ISLE-07	0.02	0.05	0.01	0.03	< .02	< .01	0.01	< .01	0.01	< .01	< .01	< .01	< .01	0.04
ISLE-08	0.02	0.05	0.01	0.03	< .02	< .01	0.01	< .01	< .01	< .01	< .01	< .01	< .01	0.04
ISLE-09	0.03	0.05	0.01	0.04	< .02	0.01	0.01	< .01	0.01	< .01	< .01	< .01	< .01	0.04
ISLE-10	0.03	0.05	0.01	0.04	< .02	< .01	0.01	< .01	0.01	< .01	< .01	< .01	< .01	0.04
ISLE-12	0.03	0.05	0.01	0.04	< .02	< .01	0.01	< .01	0.01	< .01	< .01	< .01	< .01	0.05
ISLE-14	0.03	0.06	0.01	0.04	< .02	< .01	0.01	< .01	0.01	< .01	< .01	< .01	< .01	0.04
ISLE-16	0.03	0.05	0.01	0.04	< .02	< .01	0.02	< .01	0.01	< .01	< .01	0.01	< .01	0.05
ISLE-18	0.04	0.07	0.01	0.06	< .02	< .01	0.01	< .01	0.01	< .01	< .01	0.01	< .01	0.06
ISLE-21	0.05	0.09	0.01	0.08	< .02	< .01	0.01	< .01	0.01	0.01	< .01	0.01	< .01	0.07
ISLE-24	0.02	0.06	0.01	0.06	< .02	< .01	0.01	< .01	0.01	< .01	< .01	< .01	< .01	0.07
ISLE-27	0.04	0.08	0.02	0.07	< .02	< .01	0.02	< .01	0.01	0.01	< .01	0.01	< .01	0.06
ISLE-30	0.06	0.10	0.02	0.09	0.02	< .01	0.02	< .01	0.01	0.01	< .01	0.01	< .01	0.08
ISLE-33	0.06	0.10	0.02	0.10	0.02	< .01	0.02	< .01	0.01	0.01	< .01	0.01	< .01	0.08
ISLE-36	0.07	0.11	0.02	0.10	0.02	< .01	0.01	< .01	0.01	0.01	< .01	0.01	< .01	0.09
ISLE-40	0.07	0.11	0.02	0.10	0.02	< .01	0.01	< .01	0.01	0.01	< .01	0.01	< .01	0.09
ISLE-44	0.09	0.15	0.03	0.14	0.03	< .01	0.03	< .01	0.02	0.01	< .01	0.01	< .01	0.13
ISLE-48	0.10	0.16	0.03	0.16	0.03	< .01	0.03	< .01	0.02	0.01	< .01	0.01	< .01	0.13
Min	0.01	0.01	*ND*	0.01	*ND*	*ND*	*ND*	*ND*	*ND*	*ND*	*ND*	*ND*	*ND*	0.02
Median	0.03	0.05	0.01	0.04	0.02	0.01	0.01	*ND*	0.01	0.01	*ND*	0.01	*ND*	0.05
Max	0.10	0.16	0.03	0.16	0.03	0.01	0.03	*ND*	0.02	0.01	*ND*	0.01	*ND*	0.13
Mean	0.04	0.07	0.01	0.06	0.02	0.01	0.01	*ND*	0.01	0.01	*ND*	0.01	*ND*	0.06

"<" denotes values below detection limits ND: Not detected

Table 6.2.d. The total concentration of dissolved rare earth elements (REEs) and Y in the porewater from the LSA core (Lac Ste. Anne).

Sediment depths (cm)	La ppb	Ce ppb	Pr ppb	Nd ppb	Sm ppb	Eu ppb	Gd ppb	Tb ppb	Dy ppb	Er ppb	Tm ppb	Yb ppb	Lu ppb	Y ppb
LSA-01	< .01	< .01	< .01	< .01	< .02	< .01	< .01	< .01	< .01	< .01	< .01	< .01	< .01	0.01
LSA-02	< .01	0.01	< .01	0.01	< .02	< .01	< .01	< .01	< .01	< .01	< .01	< .01	< .01	0.01
LSA-03	< .01	0.01	< .01	0.01	< .02	< .01	< .01	< .01	< .01	< .01	< .01	< .01	< .01	0.01
LSA-04	< .01	0.01	< .01	0.01	< .02	< .01	< .01	< .01	< .01	< .01	< .01	< .01	< .01	0.01
LSA-05	0.01	0.01	< .01	0.01	< .02	< .01	< .01	< .01	< .01	< .01	< .01	< .01	< .01	0.01
LSA-06	0.01	0.01	< .01	0.01	< .02	< .01	< .01	< .01	< .01	< .01	< .01	< .01	< .01	0.01
LSA-07	< .01	0.01	< .01	0.01	< .02	< .01	< .01	< .01	< .01	< .01	< .01	< .01	< .01	0.01
LSA-08	0.01	0.02	< .01	0.01	< .02	< .01	< .01	< .01	< .01	< .01	< .01	< .01	< .01	0.01
LSA-09	0.01	0.02	< .01	0.01	< .02	< .01	0.01	< .01	< .01	< .01	< .01	< .01	< .01	0.01
LSA-10	0.01	0.02	< .01	0.01	< .02	< .01	< .01	< .01	< .01	< .01	< .01	< .01	< .01	0.01
LSA-12	0.01	0.02	< .01	0.02	< .02	< .01	0.01	< .01	< .01	< .01	< .01	< .01	< .01	0.01
LSA-14	0.01	0.02	< .01	0.02	< .02	< .01	< .01	< .01	< .01	< .01	< .01	0.01	< .01	0.01
LSA-16	0.02	0.03	< .01	0.02	< .02	< .01	< .01	< .01	< .01	< .01	< .01	< .01	< .01	0.02
LSA-18	0.02	0.03	0.01	0.02	< .02	< .01	0.01	< .01	< .01	< .01	< .01	< .01	< .01	0.02
LSA-20	0.02	0.04	0.01	0.04	< .02	< .01	0.01	< .01	< .01	< .01	< .01	< .01	< .01	0.02
LSA-23	0.03	0.05	0.01	0.04	< .02	< .01	0.01	< .01	< .01	< .01	< .01	0.01	< .01	0.03
LSA-26	0.03	0.06	0.01	0.05	< .02	< .01	0.01	< .01	< .01	< .01	< .01	0.01	< .01	0.03
LSA-29	0.02	0.05	0.01	0.04	< .02	< .01	0.01	< .01	< .01	< .01	< .01	< .01	< .01	0.02
LSA-32	< .01	0.01	< .01	0.01	< .02	< .01	< .01	< .01	< .01	< .01	< .01	< .01	< .01	0.01
LSA-36	< .01	0.02	< .01	0.02	< .02	< .01	< .01	< .01	< .01	< .01	< .01	< .01	< .01	0.02
LSA-40	< .01	0.02	< .01	0.02	< .02	< .01	< .01	< .01	< .01	< .01	< .01	< .01	< .01	0.02
LSA-45	< .01	0.02	< .01	0.01	< .02	< .01	< .01	< .01	< .01	< .01	< .01	< .01	< .01	0.02
LSA-50	< .01	0.02	< .01	0.03	< .02	< .01	< .01	< .01	< .01	< .01	< .01	< .01	< .01	0.01
LSA-56	< .01	0.03	< .01	0.01	< .02	< .01	< .01	< .01	< .01	< .01	< .01	< .01	< .01	0.04
LSA-65	< .01	0.05	< .01	0.03	< .02	< .01	< .01	< .01	< .01	< .01	< .01	< .01	< .01	0.04
Min	*ND*	*ND*	*ND*	*ND*	*ND*	*ND*	*ND*	*ND*	*ND*	*ND*	*ND*	*ND*	*ND*	0.01
Median	0.01	0.02	0.01	0.02	*ND*	*ND*	0.01	*ND*	*ND*	*ND*	*ND*	0.01	*ND*	0.01
Max	0.03	0.06	0.01	0.05	*ND*	*ND*	0.01	*ND*	*ND*	*ND*	*ND*	0.01	*ND*	0.04
Mean	0.02	0.02	0.01	0.02	*ND*	*ND*	0.01	*ND*	*ND*	*ND*	*ND*	0.01	*ND*	0.02

"<" denotes values below detection limits ND: Not detected

- REEs for all studied sediment cores show an increase in concentration with increasing depth (Figures 3.1; 3.2; 3.5; 3.7; Chapter 3.4.4.1). This pattern follows that of other lithophilic elements and occurs due to the lower diluting effect of organic matter with increasing depth because of bacterial degradation (Chapter 3.4.4.1). Furthermore, the variation of REEs throughout the sediment profiles can be related to fluctuation in input of detrital inorganic material in the sediments. This is in agreement with the results of Ingri et al., (2000), who determined a strong relationship between the REEs concentration, organic carbon, and lithophilic elements.

6.2.2. Distributions of Chondrite-normalized REEs

The cosmic abundance patterns of REEs as a function of their atomic numbers or the inverse of their ionic radii show a distinct "sawtooth pattern". This sawtooth pattern can be removed by normalization to the abundance of REEs in chondrites. The resulting REEs patterns obtained after normalization to chondrites often demonstrate the geochemical behavior of rare earth elements as indicated by relative enrichment or depletion of certain elements in the series. Hence, the concept of chondrite-normalized REE signature in various environmental media allows a better insight into geochemical processes (Henderson, 1984, Taylor and McClennan, 1988).

Figures 6.1a-d and 6.3a-d show the chondrite-normalized pattern of REEs for the sediments and pore water profiles of WAB1, WAB2, ISLE, and LSA cores.

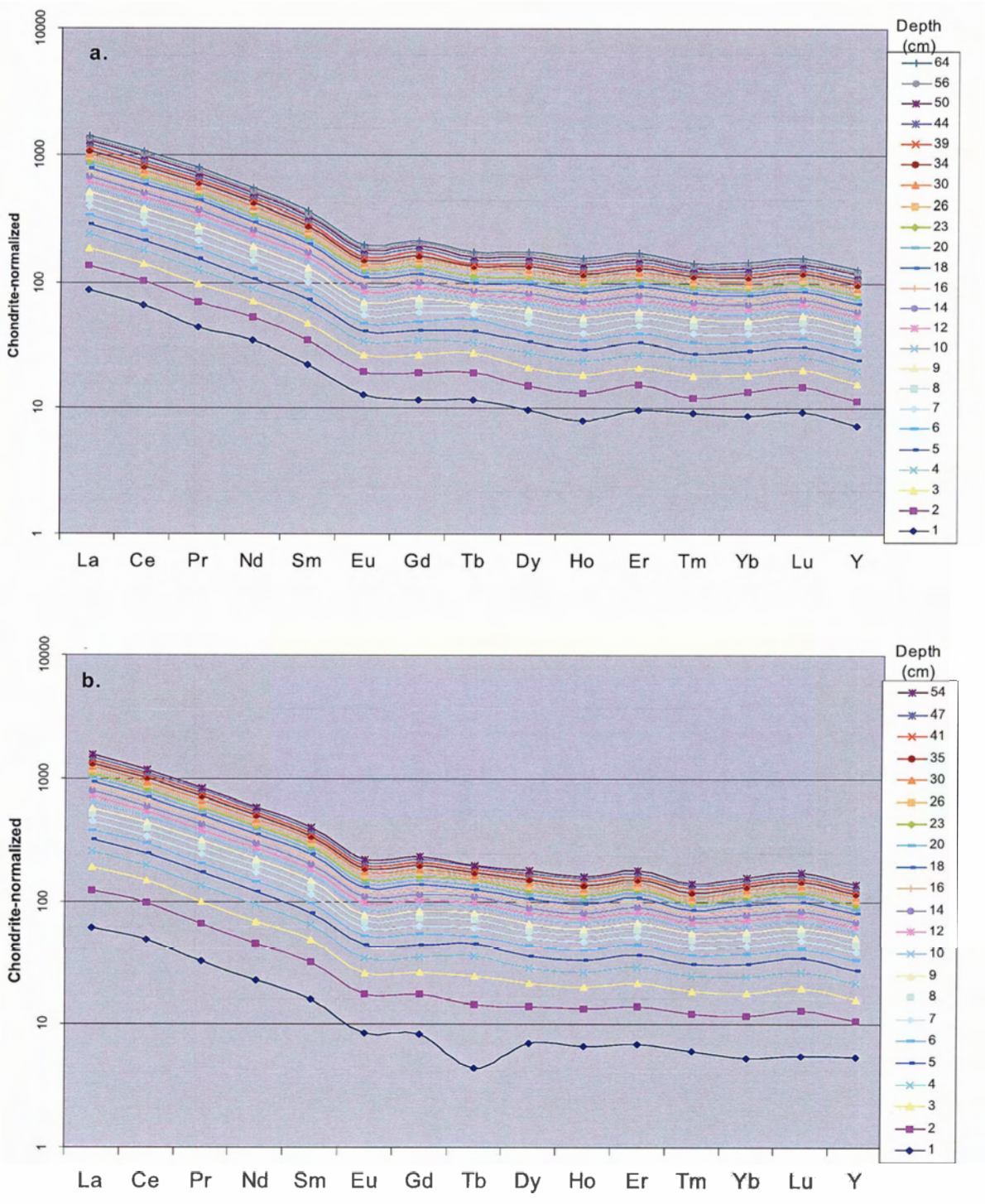

Figure 6.1.a-b. Chondrite-normalized pattern of rare earth elements (REEs) and Y in the sediment profiles from (a) WAB1 core and (b) WAB2 core (Wabamun Lake).

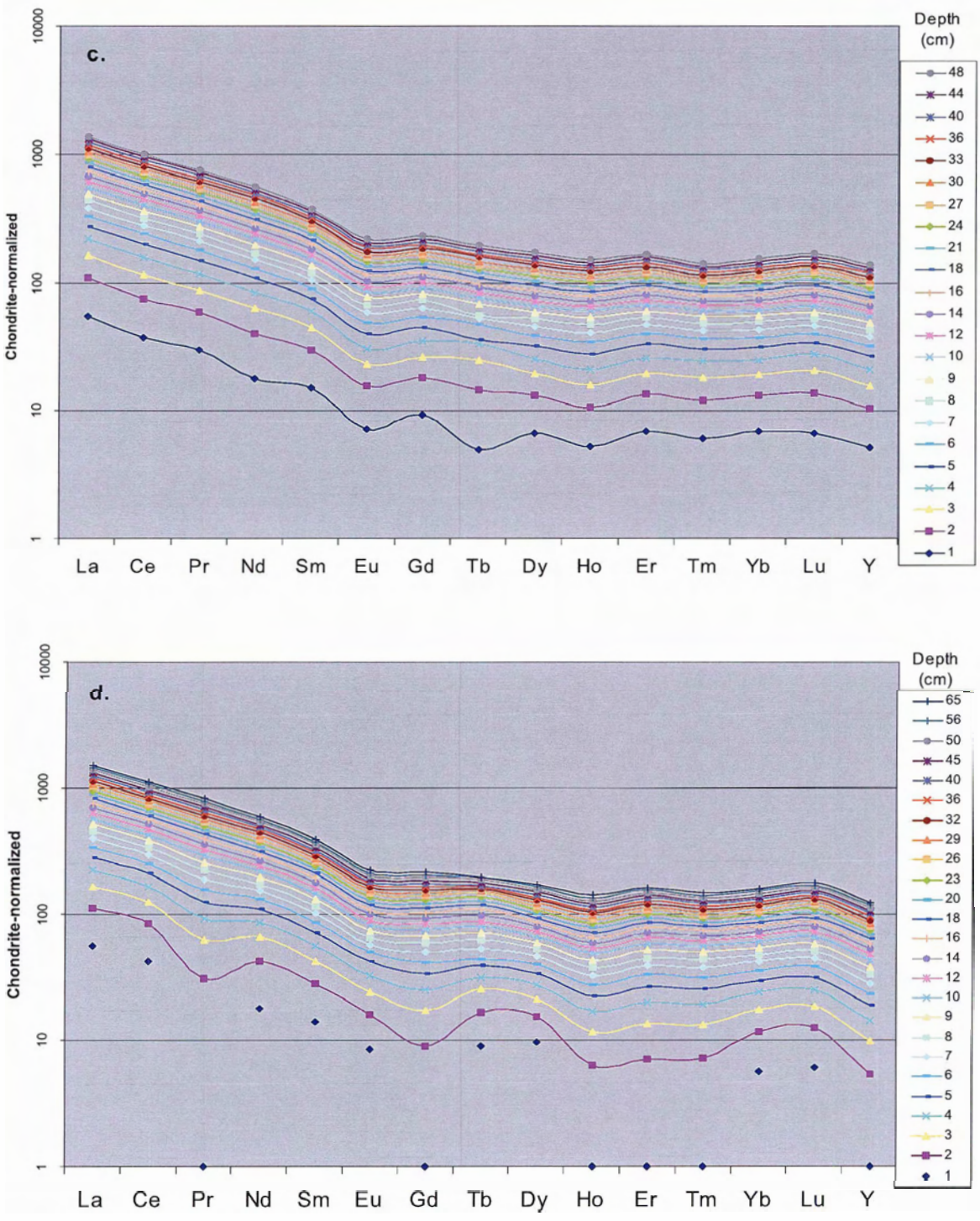

Figure 6.1.c-d. Chondrite-normalized pattern of rare earth elements (REEs) and Y in the sediment profiles from (c) Isle Lake (ISLE core) and (d) Lac Ste. Anne (LSA core).

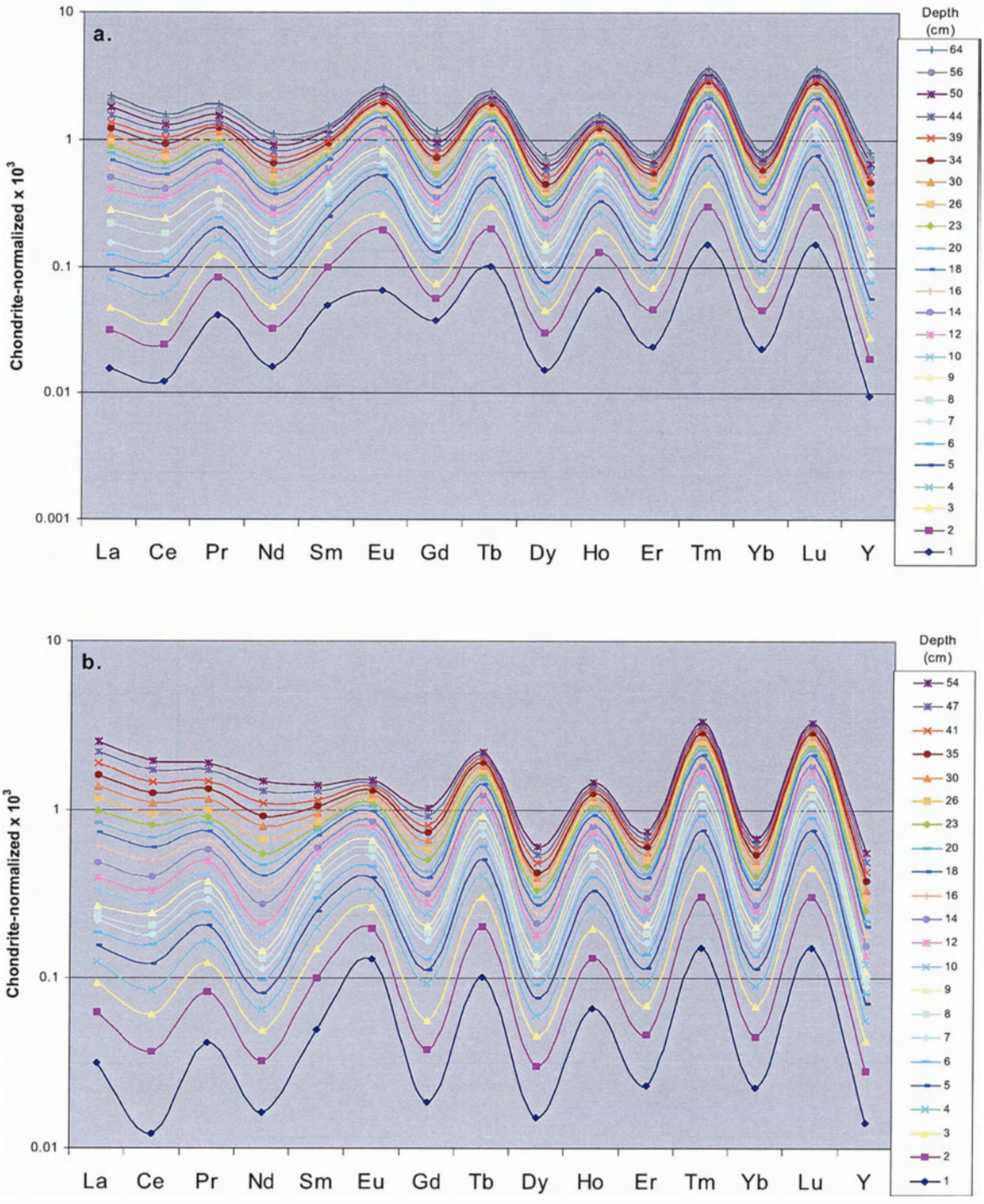

Figure 6.2.a-b. Chondrite-normalized pattern for dissolved rare earth elements (REEs) and Y in the porewater profiles from (a) WAB1 core and (b) WAB2 core (Wabamun Lake).

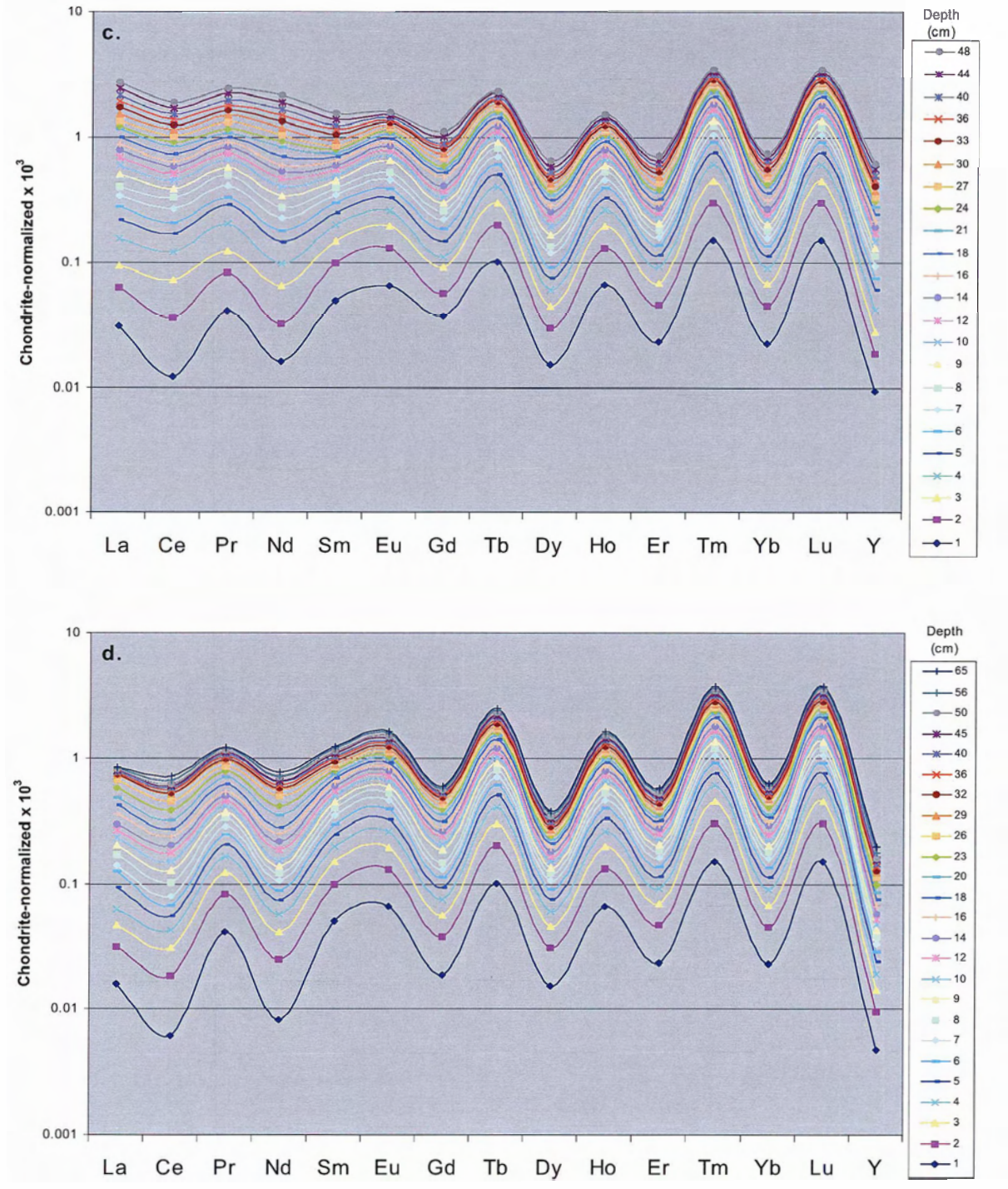

Figure 6.2.c-d. Chondrite-normalized pattern for dissolved rare earth elements (REEs) and Y in the porewater profiles from (c) Isle Lake (ISLE core) and (d) Lac Ste. Anne (LSA core).

The distributions of chondrite-normalized REEs in all studied sediment cores show a relative enrichment of Light Rare Earth Elements (LREEs) versus Heavy Rare Earth Elements (HREEs) with little variation throughout the sediment profiles (Figures 6.1a-d). This pattern is very similar to REEs patterns for upper earth crust and soil in Alberta, Canada (Goodarzi et al., Submitted c).

The chondrite-normalized REEs patterns for pore water profiles suffer from lack of detection for some REEs in solution phase, which appear as artificial (false) anomalies in REEs patterns (Tables 6.2a-d; Figures 6.2a-d). However, the overall results suggest fractionation of LREEs versus HREEs throughout the porewater profiles from all studied cores (Figures 6.2a-d).

6.2.2.1. Fractionation of LREEs relative to HREEs

The fractionation of elements within the REE group may reveal valuable information concerning the geochemical interaction between water and sediments. The comparison between LREEs and HREEs is often used to demonstrate the preferential solubility of these elements under given geochemical conditions. For this purpose, the chondrite-normalized ratio of Σ LREEs / Σ HREEs is calculated for all pore water samples throughout the studied sediment profiles. The resulting LREE/HREE ratios are plotted against depth for WAB1, WAB2, ISLE, and LSA profiles (Figures 6.3a-d).

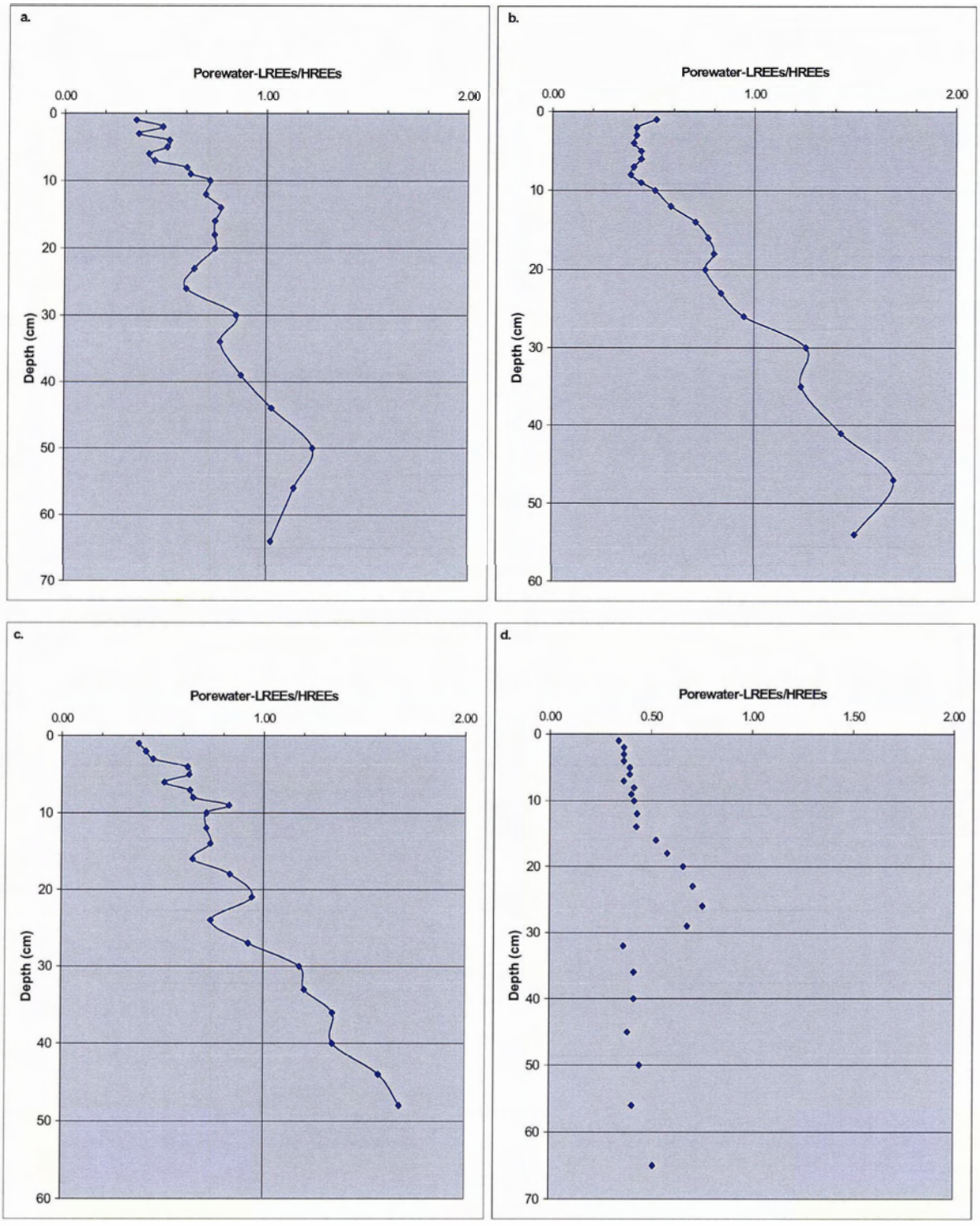

Figure 6.3.a-d. The chondrite-normalized ratios of LREEs/HREEs throughout the porewater profiles from (a) WAB1 core; (b) WAB1 core; (c) ISLE core, and (d) LSA core.

The results show a downward increasing trend in relative enrichment of LREEs versus HREEs throughout the porewater profiles from WAB1, WAB2, and ISLE cores (Figures 6.3a-c). The enrichment of HREEs in the upper parts of the pore water columns (Figures 6.3a-c) is likely due to increased solubility of HREEs and hence preferential release of these elements from sediment into pore water. This pattern is in accordance with Elderfield et al. (1990) who stated that the HREEs are preferentially released into solution during the diagenesis process, since they form stronger complexes with ligands in solution as compared to LREEs (also, Johanneson and Zhou, 1999). There is a strong tendency for REEs to form organic complexes in the presence of humic substances (Takahashi et al., 1999). This results in fractionation between HREEs and LREEs (Land et al., 1999; Ingri et al., 2000). The S1-compounds are very labile/reactive and more readily form organic complexes with elements (Chapter 7). The higher S1-compounds in the uppermost part of the sediment profiles (Chapter 7) form complexes with HREEs. The HREEs-organic complexes are more soluble and are released into the pore water. This preferential release of HREEs (relative to the other REEs) into the pore water causes a lower LREEs/HREEs ratio in the upper part of the porewater profiles (Figures 6.3a-c).

Relative depletion of LREEs versus HREEs in uppermost pore water samples (Figures 6.3a-c) is also attributed to precipitation of Fe-oxides and/or carbonates in near-surface sediment (Chapter 3). Release of ferrous iron into pore water is often associated with the release of scavenged trivalent metals, which was adsorbed on the surface of ferric iron in sediments. Some elements, such as La, are more readily scavenged by Fe-oxyhydroxide and hence tend to release in pore water at higher rates due to the reduction of ferric iron.

Precipitates of carbonate ligands under basic pH conditions are also known to sequester LREEs preferentially to HREEs (Dupré et al., 1996; Leybourne et al., 2000; Åström, 2001), resulting in negative LREEs anomalies in waters and positive LREEs anomalies in carbonate precipitates. Indeed, the variation of LREEs/HREEs ratios in pore water profile from Lac Ste. Anne (LSA core) is very similar to the temporal distribution of dissolved Ca in LSA core (Figure 3.11). This suggests the involvement of carbonates in fractionation of REEs in porewater from Lac Ste. Anne.

6.2.2.2. Fractionation of REEs relative to Yttrium (Y)

Bau (1999) indicated that scavenging of dissolved REEs and Y by Fe oxyhydroxides might result in significant modification of REE/Y distribution in the remaining solution (de Carlo et al., 1998; Bau, 1996, 1999; Bau and Dulski, 1999). The scavenging by Fe oxyhydroxides is more pronounced for Y, as compared to other REEs, thus causing a fractionation between Y and other REEs (Bau, 1999). The vertical variation of the ΣREEs/Y ratio throughout the pore water profiles from Wabamun Lake, Isle Lake, and Lac Ste. Anne are shown in Figures 6.4a-d. The results show the increasing trend of ΣREEs/Y ratios towards the upper sections of WAB1, WAB2, ISLE and in some extent, LSA porewater profiles (Figures 6.4a-d). The higher scavenging of Y by Fe oxyhydroxides result in preferential depletion of Y in porewater near the oxic surface sediment and hence decrease in the ΣREEs/Y ratio (Bau, 1999).

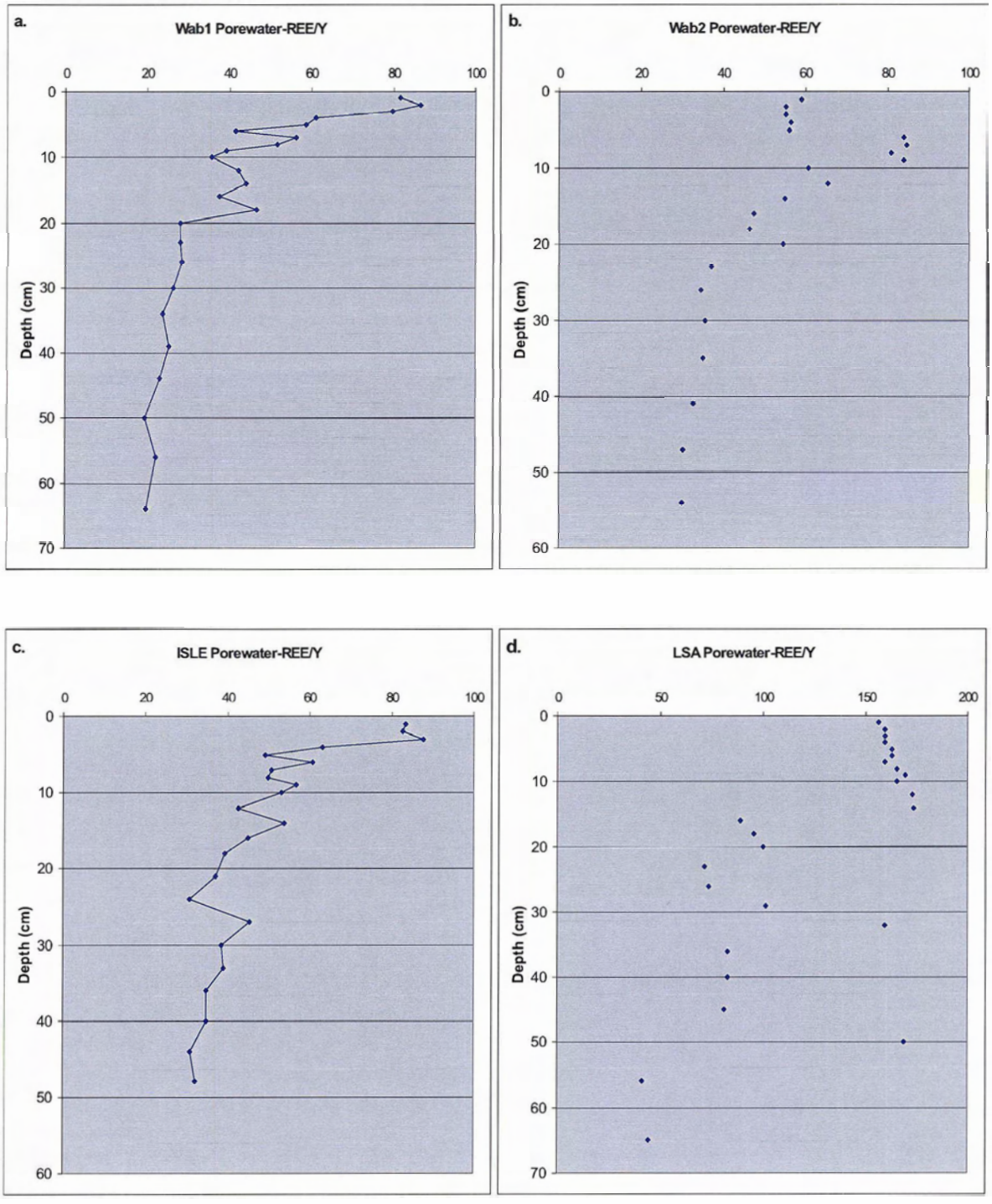

Figures 6.4.a-d. The variation of REEs with respect to Y throughout the porewater profiles from (a) WAB1 core; (b) WAB2 core; (c) ISLE core; and (d) LSA core.

6.2.2.3. Cerium Anomaly

Oxidation reactions of Ce^{3+} to Ce^{4+} occur in oxic water and result in the removal of Ce^{4+} by scavenging (Moffett, 1990; 1994a; 1994b). Therefore, Ce is expected to be relatively depleted in pore water and enriched in the oxic part of the sediment profile. The deviation of Ce from other trivalent REEs, with respect to geochemical behavior, is generally expressed as a Ce anomaly. The Ce anomaly can be evaluated relative to the trivalent neighbors (La and Pr) in the lanthanides series using the following equation (Taylor and McClennan, 1985):

$$Ce^{*} = \frac{(Ce)_N}{\sqrt{(La)_N (\mathrm{Pr})_N}}$$

The resulting Ce anomalies were then plotted for the pore water and sediment profiles from Wabamun Lake, Isle Lake, and Lac Ste. Anne (Figures 6.5a-d; 6.6a-d). The variation of Ce anomalies in all pore water profiles show a decreasing trend towards upper part of the porewater profiles (Figures 6.5a-c). This depletion of Ce in the pore water samples (Figures 6.5a-c) is possibly caused by the scavenging effect. The oxidation of Ce^{3+} to Ce^{4+} at the surface may cause co-precipitation of Ce along with Fe oxides from the pore water into the sediments.

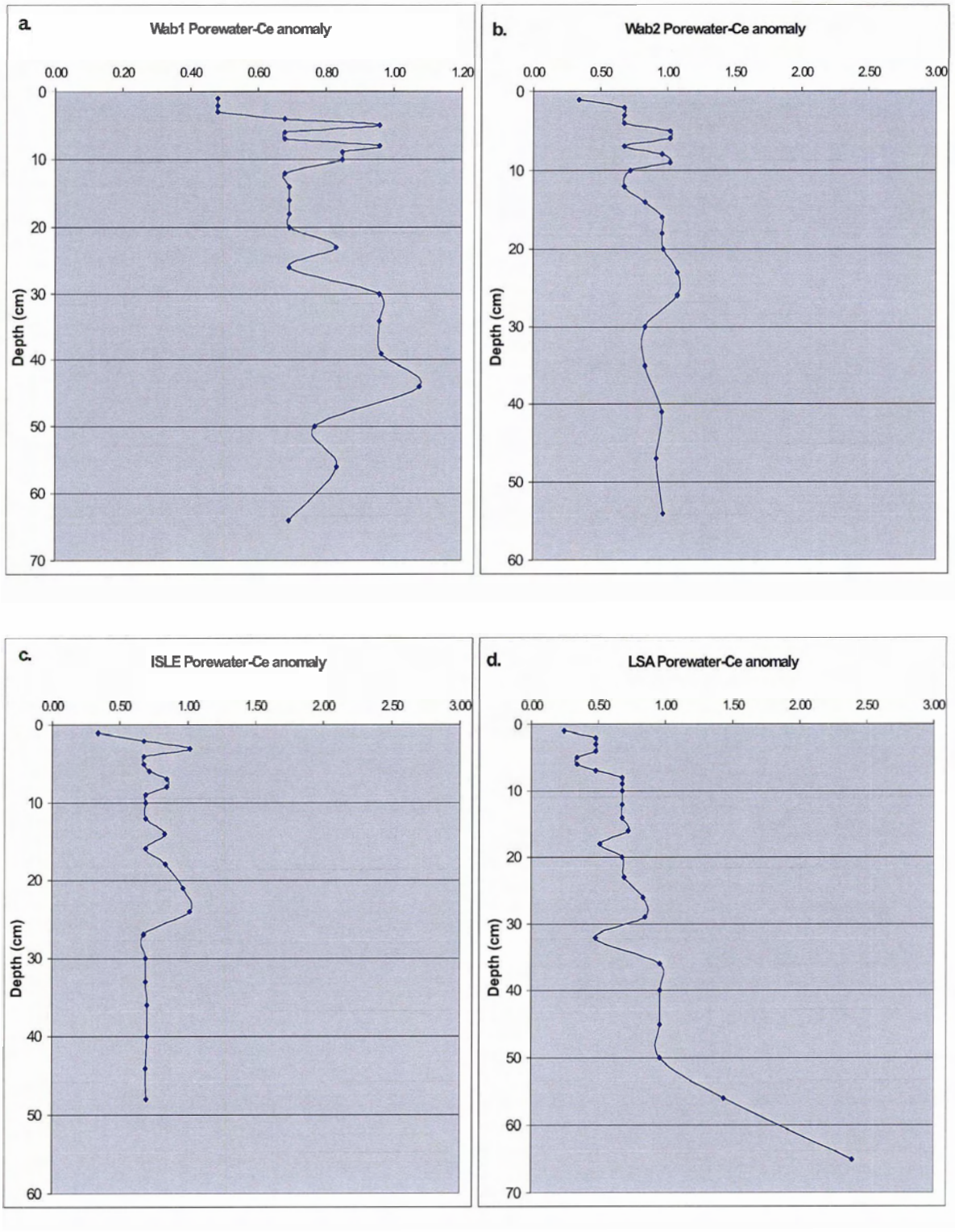

Figures 6.5.a-d. The variation of Ce-anomaly throughout the porewater profiles from (a) WAB1 core; (b) WAB2 core; (c) ISLE core; and (d) LSA core.

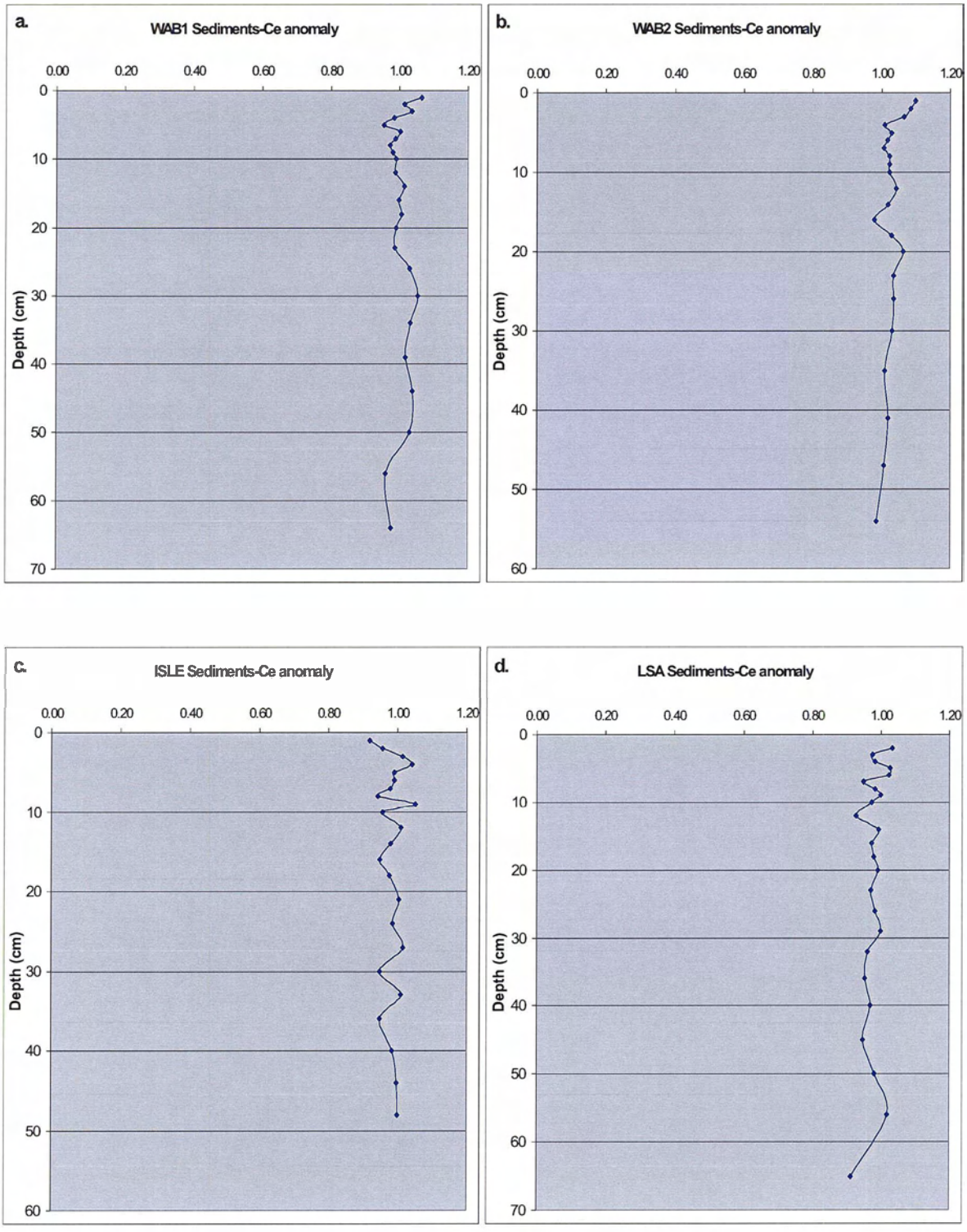

Figures 6.6.a-d. The variation of Ce-anomaly throughout the sediment profiles from (a) WAB1 core; (b) WAB2 core; (c) ISLE core; and (d) LSA core.

Temporal variations of Ce anomalies throughout the studied sediment profiles (WAB1, WAB 2, ISLE, LSA) are constant (Figures 6.6a-d). This is because REEs signatures from the earth's crust are carried in the sediments and are less likely to be affected by precipitation/mobilization caused by redox conditions. In other words, the dominant geogenic input of REEs into the sediments masks any redox variation of Ce caused by an interaction between sediment and pore water.

6.3. CONCLUSIONS

The distributions of chondrite-normalized REEs in all studied sediment cores show a relative enrichment of LREEs versus HREEs throughout the sediment profiles, very similar to REEs patterns for upper earth crust and soil in Alberta, Canada. In contrast, porewater samples show relative enrichment of HREEs to LREEs.

The relative enrichment of HREEs to LREEs increases towards the upper parts of pore water columns, due to preferential release of HREEs into solution during the diagenesis process. There is more labile organic matter (S1-OM) available in the uppermost part of the sediment profiles, which form more soluble complexes with HREEs. The scavenging effect of iron oxides and carbonate ligands are also known to sequester LREEs preferentially to HREEs, resulting in negative LREEs anomalies in porewater.

The scavenging of dissolved REEs and Y by Fe oxyhydroxides also result in significant modification of REE/Y distribution in the porewater column. The higher scavenging of Y by

Fe oxyhydroxides result in preferential depletion of Y in porewater near the oxic surface sediment and hence decrease in the ΣREEs/Y ratio.

The Ce anomalies in all pore water profiles show a decreasing trend towards the upper part of the porewater profiles, possibly due to co-precipitation of Ce^{4+} along with Fe oxides from the pore water into the sediments.

In contrast to porewater samples, the sediments show little fractionation of REEs throughout the vertical profiles. This is possibly due to high clastic input of REEs-enriched clay minerals in the sediment that mask the patterns caused by diagenetic processes.

CHAPTER 7: RELATIONSHIP BETWEEN TEMPORAL DISTRIBUTION OF ORGANIC MATTER AND METALS IN THE RECENT SEDIMENTS FROM LAKES IN THE WABAMUN AREA

7.1. INTRODUCTION

Organic matter (OM) is important in controlling trace element concentrations in suspended and bottom sediments, and in sediment-water interactions (Gibbs, 1973; Elderfield, 1981; van den Berg and Dharmvanij, 1984; Douglas et al., 1986; Orem et al., 1986; Chin and Gschwend, 1991). Therefore, the measurement of total organic carbon (TOC) is often regarded as an important parameter in defining and interpreting geochemical data, especially when dealing with trace elements (Horowitz, 1991, Sanei et al., 2001).

The capacity of organic matter to concentrate trace elements varies with the amount and type of organic matter (Swanson, et al., 1966; Saxby, 1969; Jonasson, 1977; Hirner, et al., 1990). Various chemical and physical factors including large surface area, high cation-exchange capacity, high negative surface charge, and physical trappings may determine the ability of organic matter to concentrate trace elements (Horowitz, 1991).

There are numerous studies describing the chemical relationship between OM and trace elements. These studies have focused primarily on the role of organic complexing materials such as humic substances in concentrating trace elements during the geochemical processes in the sediments (Kerndorff and Schnitzer, 1980; Elderfield, 1981; van den Berg and Dharmvanij, 1984; Davis, 1984; Douglas et al., 1986; Prapaipong et al., 1999).

From the physical perspective, aquatic organic matter in aquatic sediment exists as either surface coatings or separate organic particles/debris. The organic matter present in the

form of surface coatings provides a larger surface area since it is able to concentrate in the finer sediment size fractions. This leads to the accumulation of more trace elements (Horowitz, 1991). Hence, it is important to differentiate between surface coatings and particulate organic matter due to their different abilities in controlling trace element distributions in sediments (Horowitz, 1991).

In this study, the relationship between type of organic matter (as determined by Rock-Eval) and distribution of trace elements is studied for the sediment profiles from Wabamun Lake, Isle Lake, and Lac Ste. Anne. This study further investigates the petrological characteristics of different types of organic compounds as related to their capability to concentrate trace elements in sediment (Chapter 8).

7.2. METHODOLOGY

Type of organic compounds was determined based on thermal devolatilization of various organic compounds during programmed heating of the sediments using Rock-Eval® pyrolysis (Chapter 1.7.3.2). Besides measuring the total organic carbon (TOC %) in the sediments, the other parameters obtained from the Rock-Eval® method consists of S1, S2, Residual Carbon (RC) (Tables 7.1a-d). As explained in Chapter 1.7.3.2 and 8.2.1), S1 and S2 represent the quantity of free hydrocarbons in the sediment (S1 peak, mg hydrocarbons/g of sample) and the amount of hydrocarbons released by the thermal cracking of OM in the samples (S2; mg hydrocarbons/g of sample) (Tables 7.1a-d). The refractory portion of organic matter (e.g., charcoal, reworked-oxidized organic matter) is determined by RC (%) in

Rock-Eval analyses (Tables 7.1a-d). These organic matters are very resistant and cannot be further modified by bacterial activity in early diagenesis.

7.3. RESULTS AND DISCUSSION

7.3.1. Temporal variations of organic matter in sediments

Rock Eval® data for the studied sediment cores from Wabamun Lake, Isle Lake and Lac Ste. Anne are shown in (Tables 7.1a-d). The average Total Organic Carbon (TOC) content of the sediment in WAB1, WAB2, ISLE, and LSA cores were measured at 16.6, 13.2, 20.3, and 14.3 (wt. %), respectively (Tables 7.1a-d). The TOC content in the Wabamun Lake cores show much lower TOC values than those found by Hamilton and Reynoldson, (1981), who detected the highest percentage of organic matter (41 %) in sediments collected from the west end of the Wabamun Lake.

On average, Isle Lake showed the highest sediment TOC content (20.3%) as compared to Wabamun Lake and Lac Ste. Anne (Tables 7.1a-d). This is in agreement with the trophic status of the lake, since it is classified as a hyper-eutrophic lake, while Wabamun Lake and Lac Ste. Anne are eutrophic (Mitchell and Prepas, 1990).

Table 7.1.a-d. The variation of various organic compounds as measured by programmed heating of the sediments using Rock-Eval® pyrolysis for (a) WAB1 core, (b) WAB2 core, (c) ISLE, and (d) LSA core.

a. WAB1

Sediment depth (cm)	S1*	S2*	TOC %	RC %
Wab1-1	34.62	76.99	18.19	8.60
Wab1-2	34.66	76.65	18.06	8.48
Wab1-3	31.74	76.97	17.38	8.04
Wab1-4	34.08	75.69	17.93	8.53
Wab1-5	29.40	75.87	16.87	7.80
Wab1-6	26.07	74.72	16.18	7.52
Wab1-7	29.73	72.09	16.60	8.00
Wab1-8	27.68	71.34	16.36	7.82
Wab1-9	24.71	71.62	15.64	7.34
Wab1-10	28.19	76.82	17.20	8.15
Wab1-12	28.79	82.95	17.42	7.75
Wab1-14	27.73	87.30	18.25	8.30
Wab1-16	27.68	90.76	18.76	8.59
Wab1-18	27.20	91.17	18.74	8.57
Wab1-20	26.29	90.81	18.68	8.65
Wab1-23	23.93	89.80	17.59	7.84
Wab1-26	22.24	85.55	16.81	7.58
Wab1-30	20.04	82.95	16.19	7.37
Wab1-34	18.69	75.43	15.29	7.20
Wab1-39	17.36	74.65	15.04	7.14
Wab1-44	17.56	76.17	15.31	7.22
Wab1-50	14.25	71.78	14.35	6.95
Wab1-56	11.27	52.76	11.03	5.49
Wab1-64	15.61	73.01	14.57	6.95
Min	11.27	52.76	11.03	5.49
Median	26.75	76.41	16.84	7.81
Max	34.66	91.17	18.76	8.65
Mean	24.98	78.08	16.60	7.75

b. WAB2

Sediment depth (cm)	S1*	S2*	TOC %	RC %
Wab2-1	24.17	63.10	14.88	7.26
Wab2-2	18.79	60.43	14.73	7.91
Wab2-3	20.62	58.59	14.67	7.82
Wab2-4	15.75	55.86	13.34	7.09
Wab2-5	19.44	58.76	14.38	7.61
Wab2-6	23.06	61.55	14.82	7.50
Wab2-7	17.63	61.52	13.88	7.01
Wab2-8	22.79	64.54	14.89	7.37
Wab2-9	22.81	65.58	15.15	7.52
Wab2-10	19.50	66.01	14.10	6.73
Wab2-12	17.84	63.86	13.51	6.46
Wab2-14	13.95	59.20	12.66	6.31
Wab2-16	15.56	60.39	13.24	6.63
Wab2-18	15.02	57.76	12.38	6.07
Wab2-20	14.64	58.90	12.42	5.97
Wab2-23	13.39	57.00	12.50	6.34
Wab2-26	13.12	58.38	12.36	6.09
Wab2-30	10.50	50.80	10.92	5.48
Wab2-35	11.65	53.78	11.68	5.92
Wab2-41	11.46	56.38	11.51	5.69
Wab2-47	11.46	57.17	11.75	5.81
Wab2-54	11.74	55.95	11.41	5.59
Min	10.50	50.80	10.92	5.48
Median	15.66	58.83	13.29	6.55
Max	24.17	66.01	15.15	7.91
Mean	16.59	59.34	13.24	6.64

c. ISLE

Sediment depth (cm)	S1*	S2*	TOC %	RC %
ISLE-1	22.51	85.87	20.77	11.43
ISLE-2	23.34	85.25	20.35	11.01
ISLE-3	22.50	84.53	19.72	10.51
ISLE-4	21.97	84.71	19.96	10.79
ISLE-5	23.36	86.45	20.39	10.91
ISLE-6	23.03	88.91	20.58	10.94
ISLE-7	23.13	82.11	19.32	10.21
ISLE-8	20.88	85.84	18.94	9.79
ISLE-9	23.38	85.06	19.83	10.68
ISLE-10	23.82	84.30	20.10	10.72
ISLE-12	24.40	86.67	20.57	10.90
ISLE-14	18.96	84.70	19.17	10.55
ISLE-16	18.31	81.36	18.81	10.21
ISLE-18	18.05	86.75	19.79	10.72
ISLE-21	17.60	86.53	19.37	10.34
ISLE-24	17.36	93.23	21.15	11.62
ISLE-27	18.74	99.63	22.92	12.73
ISLE-30	17.88	92.37	21.60	12.11
ISLE-33	18.47	96.19	20.58	10.73
ISLE-36	16.12	93.69	20.20	10.69
ISLE-40	15.87	88.54	19.60	10.58
ISLE-44	18.09	98.14	21.47	11.44
ISLE-48	17.77	96.17	20.94	11.07
Min	15.87	81.36	18.81	9.79
Median	18.96	86.53	20.20	10.73
Max	24.40	99.63	22.92	12.73
Mean	20.24	88.57	20.27	10.90

d. LSA

Sediment depth (cm)	S1*	S2*	TOC %
LSA-1	IS	IS	IS
LSA-2	23.81	64.41	15.52
LSA-3	24.28	64.37	15.41
LSA-4	21.14	61.56	15.32
LSA-5	22.10	63.78	15.45
LSA-6	22.53	64.60	15.63
LSA-7	26.24	71.64	16.59
LSA-8	23.92	67.62	15.46
LSA-9	25.26	70.05	16.33
LSA-10	23.10	67.07	15.52
LSA-12	22.09	65.15	15.17
LSA-14	19.50	64.52	14.70
LSA-16	16.66	62.81	14.00
LSA-18	16.03	62.58	13.46
LSA-20	17.60	64.19	14.55
LSA-23	15.83	61.25	13.70
LSA-26	16.15	57.42	13.36
LSA-29	16.98	62.93	13.59
LSA-32	15.96	63.61	13.32
LSA-36	17.33	65.29	13.56
LSA-40	15.82	62.80	13.20
LSA-45	14.12	56.88	12.32
LSA-50	13.06	53.09	11.38
LSA-56	15.06	65.47	13.68
LSA-65	14.07	55.95	11.94
Min	0.00	0.00	0.00
Median	17.47	63.99	14.28
Max	26.24	71.64	16.59

*mg hydrocarbons/g of sediment

IS: insufficient sample

The temporal variations of TOC throughout the WAB1, WAB2, and LSA sediment profiles show an overall gradual decrease with oscillations through the top 24 cm of the sediment profile (Figures 7.1a-d). The fluctuation of TOC in the sediment profiles is related to a combination of factors including: (i) deposition of aquatic organic matter due to primary productivity (authochtonous); (ii) input of detrital organic matter from the lake's watershed (allochthonous); (iii) inorganic dilution; and (iv) degree of organic decomposition (due to the diagenesis process) (Tyson, 2001).

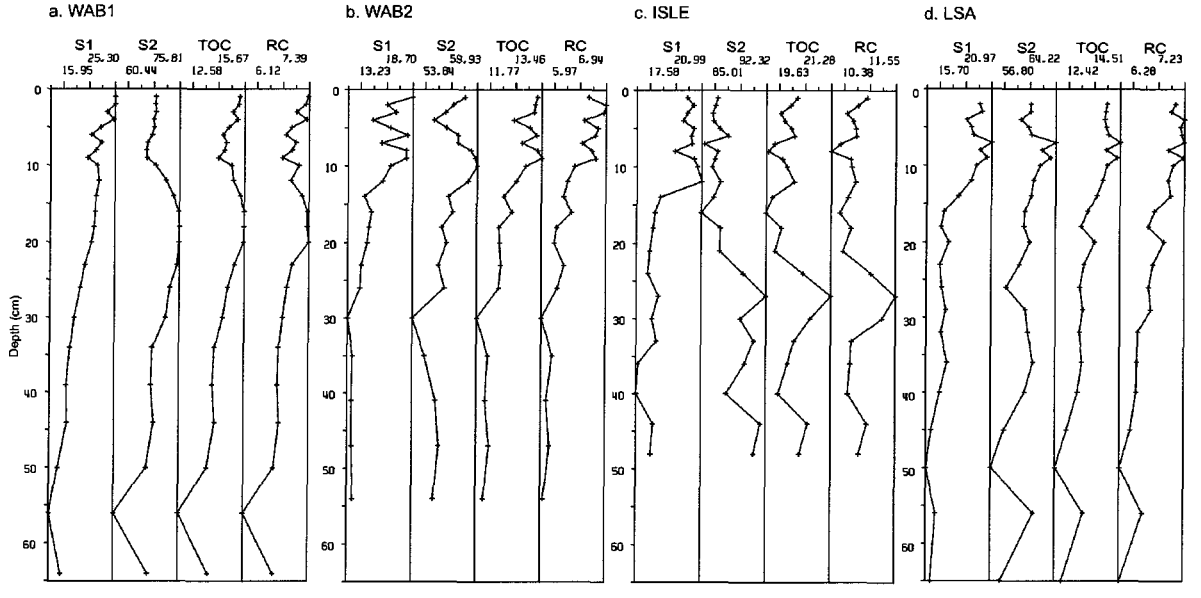

Figure 7.1.a-d. The temporal distribution of various types of organic compounds as determined by Rock-Eval® pyrolysis for (a) WAB1 core, (b) WAB2 core, (c) ISLE, and (d) LSA core.

The increasing trend of TOC towards the upper part of the WAB1, WAB2, and LSA sediment profiles is often interpreted as the result of a recent increase in primary productivity (Figures 7.1a-d). This is often attributed to anthropogenic activities in the watershed (e.g,

input of nutrients from agricultural and residential sewage/waste water; Chapter 3.4.6) (Nelson and Mitchell, 1988; Mitchell and Prepas, 1990; Crosby, 1994). Although increasing anthropogenic input of nutrients in the past century could be partly responsible for higher TOC in surficial sediments, the selective degradation of organic matter may also contribute to the observed temporal trend of OM from the studied sediment profiles.

A high input of organic matter in the surface sediment layer may result in a rapid depletion of O_2 and an accumulation of labile organic matter in the surface sediments. Temporal variations of labile S1-OM for all studied cores show more pronounced downward decreases throughout the sediment profiles as compared to those of TOC and other organic parameters (RC, S2) (Figures 7.1a-d). This is due to selective degradation of OM in which labile organic matter (e.g., S1-OM) tends to degrade more efficiently during diagenetic processes (Matsuda and Koyama, 1977a; 1977b; Meyers et al., 1984; Ishiwatari, 1985; Tyson 1995; Sanei et al., 2000; 2001). Selective degradation of the more labile OM in the uppermost sediments results in a decrease in TOC with increasing depth (Figures 7.1a-d).

In contrast to the sediment cores from Wabamun Lake and Lac Ste. Anne, the Isle Lake sediment profile shows no distinct decrease in TOC with depth (Figure 7.1.c). This suggests that the primary sedimentation of organic matter controls the contents of OM, rather than diagenetic processes. A high input of organic matter is reflected by the period of high TOC content beginning at a depth of 40 cm and continuing until a depth of 21 cm in the Isle Lake sediment profile (Figure 7.1c). The rapid increase in TOC content of the sediment coincides with the first settlement around Isle Lake in 1905 (Chapter 2.1.3), which was followed by

intense clear cutting of the forested lands for agriculture (Buckland-Nicks and Mitchell, 1990).

7.3.2. Interrelationships between trace elements and organic matter

Comparisons between temporal variations of TOC throughout the sediment cores and the concentrations of trace elements were carried out using a non-parametric, Spearman correlation (Tables 7.2a-d). The results of these analyses are as follows:

7.3.2.1. Wabamun Lake

The correlation coefficients between TOC and the concentrations of trace elements (Cu, Zn, and Sb) in the WAB1 core were, for the most part, below any significant value (Table 7.2a). However, the S1-OM shows significant correlation coefficients with trace elements throughout the sediment profile (Table 7.2a).

In the WAB2 sediment core, all trace elements show significant correlation with TOC (Table 7.2b). However, there is a higher correlation between S1 and trace elements than there is between S2 and trace elements (Table 7.2b). Furthermore, the significant correlation between residual carbon (RC) and trace elements in WAB2 is indicative of an affinity of trace elements to a portion of refractory organic matter (Table 7.2b). This is possibly due to the input of metal-rich, coal particles from the coal outcrops in the drainage basin and at the

bottom of the lake. The presence of coaly particles in Wabamun Lake sediment is confirmed by petrographic observation (Figure 7.2).

Table 7.2.a-d. The Spearman correlation coefficients between concentration of trace metals and various organic compounds (Rock-Eval parameters) for the sediments from (a) WAB1 core, (b) WAB2 core, (c) ISLE, and (d) LSA core.

a. WAB1

	Hg	Pb	Cu	Zn	Sb
S1	0.57	0.65	0.49	0.50	0.64
S2	-	-	-	-	-
TOC	-	0.41	-	-	-
RC	-	0.44	-	-	0.41

$p<0.05$ at 0.39; n=24

b. WAB2

	Hg	Pb	Cu	Zn	Sb
S1	-	0.69	0.74	0.61	0.71
S2	-	0.42	0.44	-	0.50
TOC	-	0.71	0.75	0.66	0.73
RC	-	0.75	0.81	0.69	0.72

$p<0.05$ at 0.40; n=22

c. ISLE

	Hg	Pb	Cu	Zn	Sb
S1	0.74	0.84	-0.74	-0.71	-0.47
S2	-0.64	-0.70	0.69	0.60	0.52
TOC	-0.45	-	-	-	-
RC	-	-	-	-	-

$p<0.05$ at 0.39; n=23

d. LSA

	Hg	Pb	Cu	Zn	Sb
S1	0.73	0.77	-	-	-
S2	0.49	0.54	0.53	-	-
TOC	0.79	0.83	-	-	-
RC	0.76	0.81	-	-	-

$p<0.05$ at 0.39; n=24

Only correlation coefficients significant at 95% confidence limit are shown.

7.3.2.2. Isle Lake

There is a poor correlation between trace elements and TOC in the Isle Lake sediment (Table 7.2c). Temporal variations of the S2-OM are negatively correlated with concentrations of Pb (Table 7.2c). This indicates that the S2-OM dilute the Pb in ISLE sediments. On the other hand, S1-OM shows significant positive correlation coefficients with

Pb (Table 7.2c), suggesting that Pb in ISLE sediment is mainly associated with labile S1-OM.

7.3.2.3. Lac Ste. Anne

The TOC content in the LSA sediment profile is not correlated to Cu, Zn, or Sb (Table 7.2d). In contrast, the distribution of Pb is significantly correlated with TOC (Table 7.2d). Similar to all other studied sediment cores, S1-OM shows higher correlation coefficients with Pb as compared to S2-OM (Table 7.2a-d). Significant correlation of Pb with residual carbon (RC) (Table 7.2d) may also suggest the detrital input of metal-rich coaly particles from the watershed into the lake (Figure 7.2).

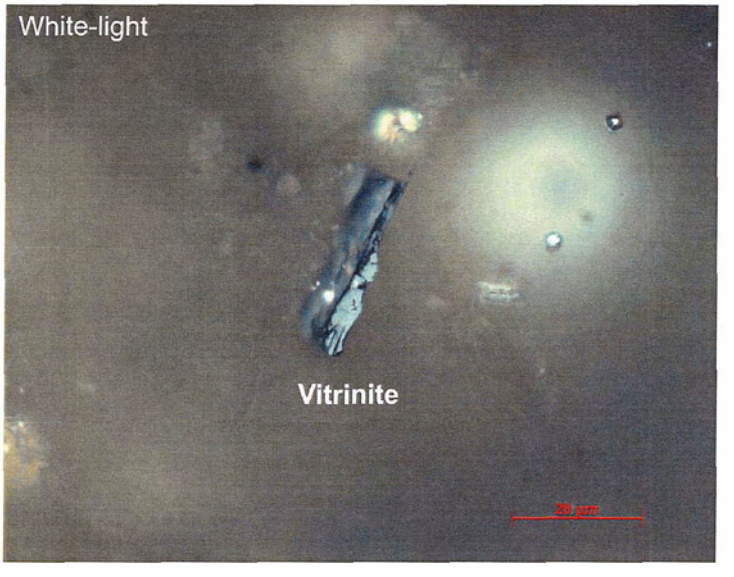

Figure 7.2. The white light microscopy (reflected light) of a typical sediment sample showing a low reflectance particle of coal maceral (vitrinite) originating from the surrounding outcrops in the study area. (for details on methodology see Chapter 1.7.3.4 and 8.2.2).

7.3.3. Relationship between Hg and organic matter

The relationship between Hg and organic compounds in Wabamun Lake is shown as a regression plot (Figure 7.3a-c). The results indicate a lack of good correlation between Hg and TOC and S2-OM (Figure 7.3b-c). However, a significant correlation between Hg and S1-OM (Figure 7.3a) suggests that distribution of Hg in Wabamun Lake sediment is mainly controlled by labile S1-OM. Vertical distribution of Hg in Isle Lake sediment core is also inversely correlated with S2 and TOC contents (Figure 7.4b-c). However, a significant positive correlation between S1-compounds and Hg (Figure 7.4a) suggests a strong affinity between Hg and very labile S1-OM in the sediment. These results imply that S2-OM and TOC are dilutents of Hg while S1-OM are considered "concentrators" of Hg in the ISLE sediment core. The LSA sediment demonstrates the strong affinity between Hg and TOC (Figure 7.5c). The linear relationship between Hg and organic compounds (Figure 7.5c) suggests that organic matter is a concentrator of Hg in LSA sediments.

7.3.4. Petrological characteristics of OM as related to the concentration capacity of metals

The results of this study indicate that labile organic compounds detected as S1-compounds in Rock-Eval® pyrolysis play a key role in concentrating the trace elements in the sediments. In most cases, the significant positive correlation between TOC and Hg (and other trace elements) arises from the portion of organic matter related to S1-OM rather than S2-OM.

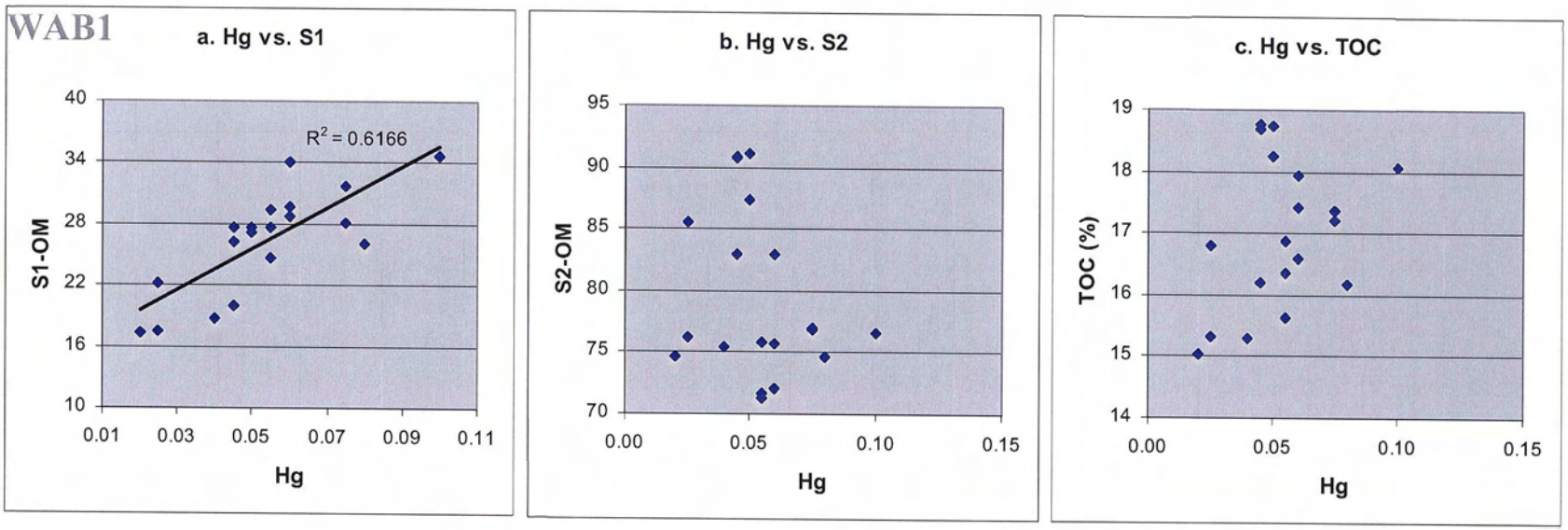

Figure 7.3.a-c. The regression plots of Hg versus S1-OM (a), S2-OM (b), and (c) TOC content of the sediments from the Wabamun Lake.

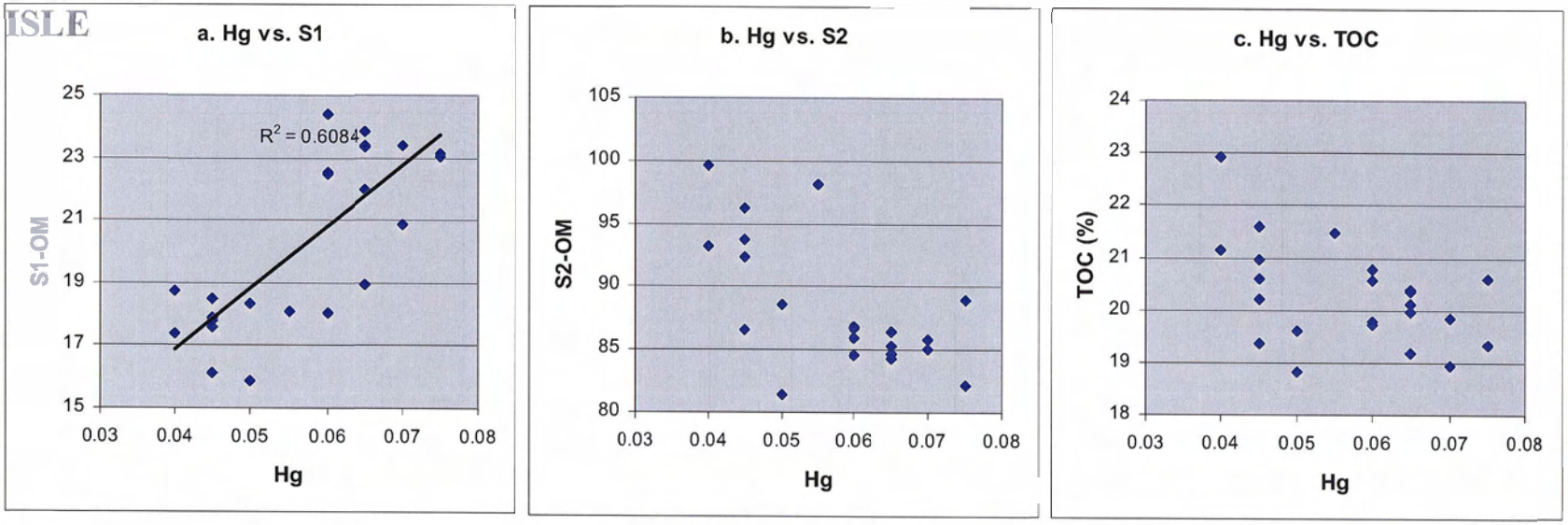

Figure 7.4.a-c. The regression plots of Hg versus S1-OM (a), S2-OM (b), and (c) TOC content of the sediments from the Isle Lake.

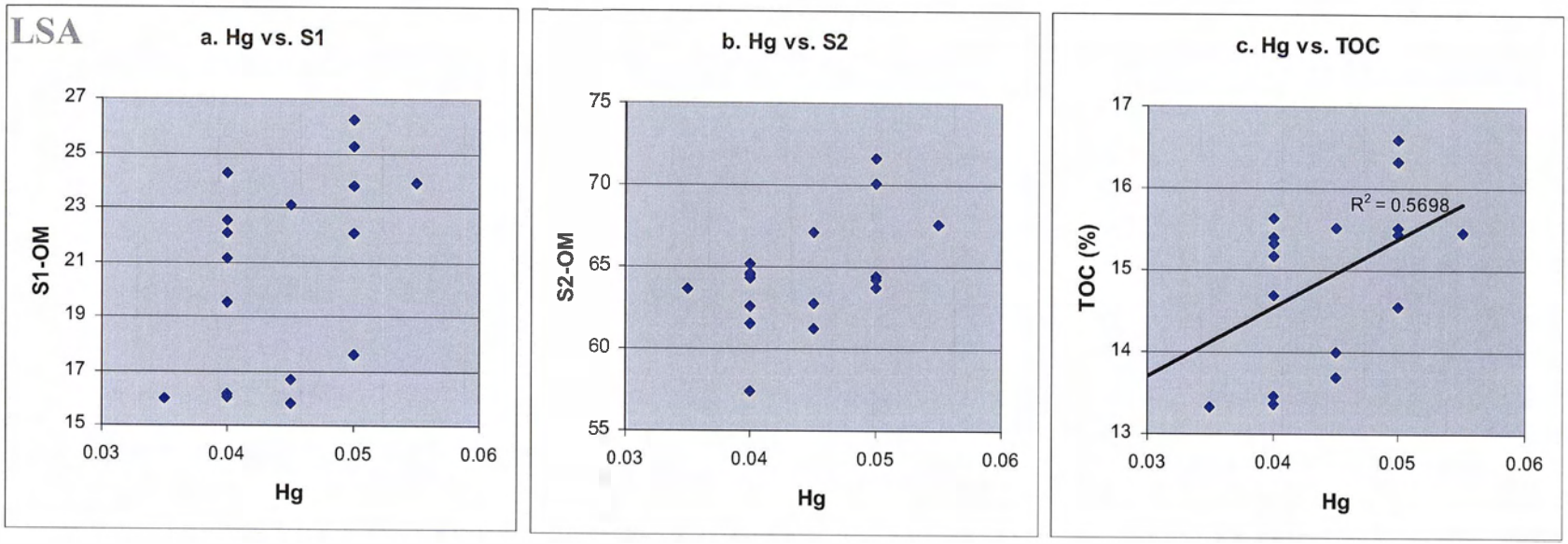

Figure 7.5.a-c. The regression plots of Hg versus S1-OM (a), S2-OM (b), and (c) TOC content of the sediments from the Lac Ste. Anne.

As mentioned in Chapter 8, S1-OM represent the most thermally labile, free hydrocarbons in sediments, while S2-OM correspond to the higher molecule, kerogen-derived hydrocarbons (such as algal cell walls). The S1-OM are petrographically characterized as "stain like" amorphous organic matter (AOM). This portion of organic matter tends to fill in granular imperfections or physical gaps in the sediments and provide surface coatings for various organic and inorganic particles (Chapter 8).

The organic coatings cement fine silt and clay-sized particles together, providing larger surface areas. It is known that surface area, sediment grain size, and geochemical substrates are interrelated with sediment trace element concentrations (Horowitz, 1991). Hence, the amorphous S1-OM provides larger surface areas, as they tend to concentrate in the finer size fractions. These physical characteristics of S1-OM provide sediment with the capacity to accumulate more trace elements. Additionally, the fluid characteristic of S1-OM accounts for the strong grain surface adsorption of organic matter, as well as the mobility of trace elements during early diagenesis in the recent sediments (Chapter 8).

The relationship between TOC and metals can be significantly reduced in sediments containing high proportions of allochthonous refractory organic matter (e.g., woody material and reworked OM). These high carbon particles have the greatest influence on TOC, but they are chemically non-reactive and the least capable of bonding with most metals.

7.3.5. Quantifying the surface coating organic matter

The petrological study of the sediment in Chapter 8 indicate that the quantity of organic carbon released during the pyrolysis stage of up to 300 °C, is likely a relative measure of amorphous organic matter (AOM), which also correspond to the amount of surface coating portion of organic matter. This thermally labile portion of organic matter primarily consists of volatile hydrocarbons known as S1-OM. As well, a minor fraction of oxygen-containing OM (S3a-OM) is released simultaneously with S1-OM (Chapter 1.7.3.2). Based on this information, a relative quantification of surface coating OM is proposed according to the following equation:

$$AOM\ \% = (S1 \times 0.083^{1}) + [(S3aCO \times 12/280^{2}) + (S3aCO_2 \times 12/440^{2})],$$

Where AOM is the concentration of amorphous organic matter, equivalent to surface coating OM; S1 represents the quantity of volatile hydrocarbons; and S3a is the quantity of labile oxygen-containing OM (Chapter 1.7.3.2).

Using this equation, the portion of surface coating OM can be differentiated from the quantity of particulate OM, which correspond to kerogen-derived OM released before 650°C (e.g., alginite, liptodetrinite) (Chapter 8).

---

[1] Empirical factor for measuring the amount of hydrocarbons using standards (Lafargue et al., 1998).
[2] Ratio of atomic weight of carbon to molecular weight corrected for the concentration factor.

The results of the calculation for the WAB1 sediment core indicate that the average portion of surface coating organic matter is 2.46% (Table 7.3). This value is relatively low as compared to mean TOC (16.6%; Table 7.3). The surface coating OM is at the highest level (3.40%) near sediment-water interface (SWI) due to presence of labile organic matter in this part of the sediment profile (Table 7.3).

Table 7.3. The estimated amount of amorphous organic matter (AOM), which is believed to form the substantial portion of surface coating organic matter in the sediments (WAB1 sediment core). For more details about the Rock-Eval parameters see Chapter 8.

Depth (cm)	S1	S2	S3CO	S3aCO	S3bCO	$S3CO_2$	$S3aCO_2$	$S3bCO_2$	TOC%	AOM%
Wab1-1	34.62	76.99	7.33	1.40	5.93	32.98	17.10	15.88	18.19	3.40
Wab1-2	34.66	76.65	7.79	1.20	6.59	29.48	14.90	14.58	18.06	3.33
Wab1-3	31.74	76.97	7.09	1.00	6.09	28.50	14.20	14.30	17.38	3.06
Wab1-4	34.08	75.69	6.50	1.30	5.20	30.17	15.10	15.07	17.93	3.30
Wab1-5	29.40	75.87	7.43	1.10	6.33	28.44	13.90	14.54	16.87	2.87
Wab1-6	26.07	74.72	6.59	0.90	5.69	27.12	13.30	13.82	16.18	2.57
Wab1-7	29.73	72.09	3.33	0.50	2.83	19.67	10.20	9.47	16.60	2.77
Wab1-8	27.68	71.34	7.27	1.10	6.17	27.90	12.90	15.00	16.36	2.70
Wab1-9	24.71	71.62	6.93	0.80	6.13	24.83	11.70	13.13	15.64	2.40
Wab1-10	28.19	76.82	7.63	1.10	6.53	27.10	12.60	14.50	17.20	2.73
Wab1-12	28.79	82.95	8.91	1.20	7.71	27.61	12.50	15.11	17.42	2.78
Wab1-14	27.73	87.30	9.07	1.30	7.77	30.05	13.60	16.45	18.25	2.73
Wab1-16	27.68	90.76	7.72	1.10	6.62	28.96	13.50	15.46	18.76	2.71
Wab1-18	27.20	91.17	7.76	1.10	6.66	28.76	13.60	15.16	18.74	2.68
Wab1-20	26.29	90.81	6.96	1.00	5.96	27.53	13.40	14.13	18.68	2.59
Wab1-23	23.93	89.80	6.94	1.00	5.94	25.90	12.40	13.50	17.59	2.37
Wab1-26	22.24	85.55	6.36	0.90	5.46	24.84	12.00	12.84	16.81	2.21
Wab1-30	20.04	82.95	6.17	0.90	5.27	23.60	11.30	12.30	16.19	2.01
Wab1-34	18.69	75.43	6.31	0.90	5.41	22.60	11.20	11.40	15.29	1.90
Wab1-39	17.36	74.65	5.93	0.80	5.13	22.75	10.80	11.95	15.04	1.77
Wab1-44	17.56	76.17	7.04	0.90	6.14	22.61	10.50	12.11	15.31	1.78
Wab1-50	14.25	71.78	5.79	0.80	4.99	21.29	10.30	10.99	14.35	1.50
Wab1-56	11.27	52.76	5.26	0.90	4.36	19.32	9.80	9.52	11.03	1.24
Wab1-64	15.61	73.01	6.10	1.00	5.10	22.25	10.80	11.45	14.57	1.63
Median	*26.75*	*76.41*	*6.95*	*1.00*	*5.95*	*27.11*	*12.55*	*13.98*	*16.84*	2.63
Mean	*24.98*	*78.08*	*6.84*	*1.01*	*5.83*	*26.01*	*12.57*	*13.44*	*16.60*	2.46

7.4. CONCLUSIONS

In this study, the relationships between temporal distribution of organic matter and concentrations of trace elements are investigated. The conclusions of this study are as follows:

- Higher TOC content in the surficial sediments is the combined effect of the recent increase in the primary productivity of the lake in the past century, as well as selective degradation of more reactive organic matter in early diagenesis.

- From this data, it can be concluded that the significant positive correlation between TOC and metals in recent sediments arises mainly from the portion of organic matter related to the thermally labile compounds released during pyrolysis at 300 $^{\circ}$C. The higher molecular, kerogen-derived hydrocarbons show consistently lesser correlation with trace elements.

- The strong affinity between temporal distribution of metals and thermally labile compounds is due to both the chemical reactivity and petrological characteristics of these amorphous compounds. They act as a stain by coating the outer part of fine sediment particles and concentrate in the finer sediment size fractions.

CHAPTER 8: PETROLOGICAL CHANGES OCCURRING IN ORGANIC MATTER FROM RECENT LACUSTRINE SEDIMENTS DURING THERMAL ALTERATION BY ROCK-EVAL PYROLYSIS

8.1. INTRODUCTION

There is increasing interest in quantitative and qualitative analyses of organic matter (OM) in recent sediments. This is due to the importance of OM with respect to chemical properties of sediments (Connan, 1987; Huc, 1988, Di-Giovanni et al, 1998). Temperature programmed Rock-Eval pyrolysis is widely used for characterizing sedimentary OM in petroleum geoscience (Sykes and Snowdon, 2002; Lafargue et al., 1998; Tissot and Welte, 1985). However, recent sediments, as compared to lithified sedimentary rocks, have received less attention with respect to the application of Rock-Eval pyrolysis.

There are some studies which attempted to chemically characterize the OM contributing to the peaks evolving during Rock-Eval pyrolysis of Recent marine sediments (e.g, Liebezeit and Wiesner, 1990) and soil (e.g., Di-Giovanni et al, 1998; Disnar et al, 2003). However, these studies did not extensively incorporate the petrographic characteristics of OM undergoing the thermal alteration stages of Rock-Eval pyrolysis.

The present study is designed to document petrological changes occurring in OM from Recent lacustrine sediments during Rock-Eval pyrolysis. This study focuses specifically on the organic compounds released in S1 and S2 peaks during pyrolysis, within the temperature range of 100 to 650 °C.

8.2. METHODOLOGY

The sediments used for this study were obtained from the various depth intervals of WAB1 core (Chapter 1.7.1). The unconsolidated sediment samples were separated from the pore-water, under a N_2 environment (Chapter 1.7.2). The sediments were then freeze-dried, ground to a flour-like consistency using a swing mill grinder and stored under nitrogen headspace in sealed containers (Chapter 1.7.1; 1.7.2). A portion of the freeze-dried sediment was then prepared for Rock Eval and organic petrology.

8.2.1. Rock-Eval Analyses

Rock-Eval 6® was used for quantitative and qualitative study of OM in the sediment samples from WAB1 core. This method consists of pyrolysis and oxidation ovens, both performing the temperature programmed heating of the sediments (20 mg) and standard samples (100 mg) at a heating rate of 25 °C per minute (Chapter 1.7.3.2).

In the oven, the pyrolysis stage occurs between 100 °C and 650 °C under an inert atmosphere (He). During the pyrolysis process, the quantity of free, 'volatile' hydrocarbons present in the sample (S1 peak, mg hydrocarbons/g of sample) and the amount of hydrocarbons released by the thermal cracking of OM (S2; mg hydrocarbons/g of sample) are detected by the Flame Ionization Detector (FID) (Figure 8.1a; Table 8.1). Simultaneously, the CO and CO_2 released during thermal cracking of oxygen-bearing organic compounds (S3; mg CO-CO_2/g of sample) are measured by online Infrared (IR) detectors

(Figures 8.1b-c; Table 8.1). The quantity of these oxygen-containing OM (S3) are presumably negligible as compared to the quantity of S1 and S2 hydrocarbons. The calculation of Rock-Eval data for WAB1 core (Table 8.1) indicates that S3 comprises only 1% of total organic carbon in the sediments. This is while S1 and S2 together account for the major portion of OM (7.9%) (for calculations, see Lafarge et al., 1998). Therefore, the petrographic changes occurring during pyrolysis between 100 and 650 °C are attributed to the release of S1- and S2-compounds.

Following the pyrolysis stage, the sample is automatically transferred to the oxidation oven where it is heated from 400 °C to 850 °C, incinerating all the residual organic carbon in the sample. At this step, the CO and CO_2 released during combustion of residual organic carbon (S4; mg CO-CO_2/g of sample) are measured by online Infrared (IR) detectors (Figure 8.1d). The quantity of all OM released during pyrolysis (pyrolysable carbon; 100 °C -650 °C) and oxidation (Residual carbon; 400 °C -850 °C) accounts for the total organic carbon (TOC; wt.%) in the sediment sample (Table 8.1).

8.2.2. Organic petrology

Organic petrography of the sediments was conducted using an incident light microscope system equipped with white and fluorescent light sources. The detailed methodology and sample preparation for organic petrology is discussed in Chapter 1.7.3.4.

Figure 8.1.a-d. Example pyrograms for a complete Rock-Eval 6® analysis of the recent sediments from Wabamun Lake core. (a) Evolution of hydrocarbon peaks (S1 and S2) during the pyrolysis stage (100-650 °C) as detected by a Flame Ionization Detector (FID); (b and c) Formation of S3CO and $S3CO_2$ peaks corresponding to the release of oxygen-bearing organic compounds (mg CO-CO_2/g of sample) during the pyrolysis stage; (d) Formation of S4CO and $S4CO_2$ peaks during the oxidation stage.

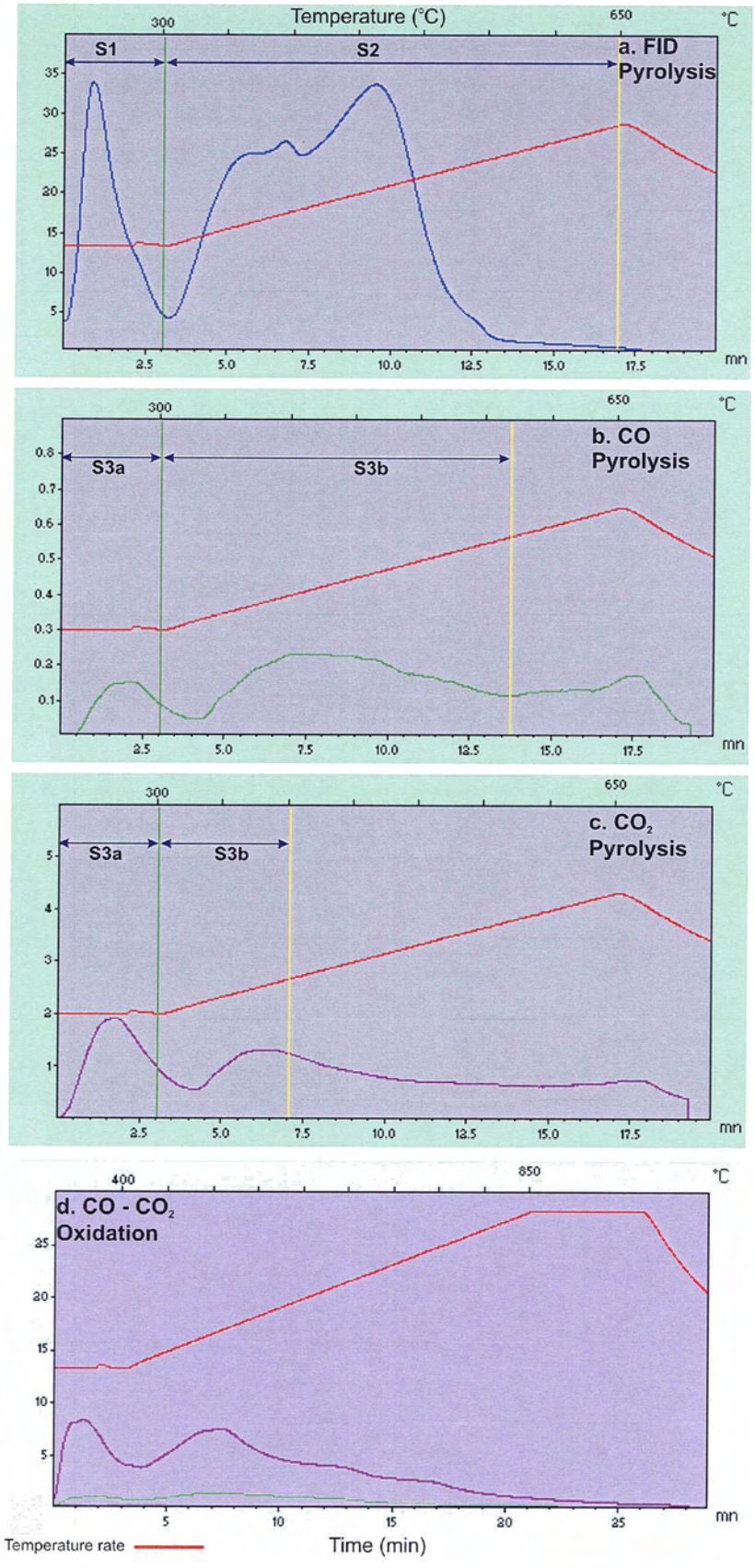
Temperature (°C)
300
650
°C
S1
S2
a. FID
Pyrolysis
mn
S3a
S3b
b. CO
Pyrolysis
c. CO2
Pyrolysis
400
850
d. CO - CO2
Oxidation
Temperature rate
Time (min)

Table 8.1. Rock-Eval 6® data for the sediments from WAB1 core in Wabamun Lake, Alberta, Canada.

Sediment depth (cm)	S1	S2	$S3CO_2$	$S3aCO_2$	$S3bCO_2$	S3CO	S3aCO	S3bCO	PC^1(%)	RC^2(%)	TOC (%)
	mg hydrocarbons/g		mg CO_2/g of sediemt			mg CO/g of sediemt			wt. %		
WAB1-01	34.62	76.99	32.98	17.10	15.88	7.33	1.40	5.93	9.59	8.60	18.19
WAB1-02	34.66	76.65	29.48	14.90	14.58	7.79	1.20	6.59	9.58	8.48	18.06
WAB1-03	31.74	76.97	28.50	14.20	14.30	7.09	1.00	6.09	9.34	8.04	17.38
WAB1-04	34.08	75.69	30.17	15.10	15.07	6.50	1.30	5.20	9.40	8.53	17.93
WAB1-05	29.40	75.87	28.44	13.90	14.54	7.43	1.10	6.33	9.07	7.80	16.87
WAB1-06	26.07	74.72	27.12	13.30	13.82	6.59	0.90	5.69	8.66	7.52	16.18
WAB1-07	29.73	72.09	19.67	10.20	9.47	3.33	0.50	2.83	8.60	8.00	16.60
WAB1-08	27.68	71.34	27.90	12.90	15.00	7.27	1.10	6.17	8.54	7.82	16.36
WAB1-09	24.71	71.62	24.83	11.70	13.13	6.93	0.80	6.13	8.30	7.34	15.64
WAB1-10	28.19	76.82	27.10	12.60	14.50	7.63	1.10	6.53	9.05	8.15	17.20
WAB1-12	28.79	82.95	27.61	12.50	15.11	8.91	1.20	7.71	9.67	7.75	17.42
WAB1-14	27.73	87.30	30.05	13.60	16.45	9.07	1.30	7.77	9.95	8.30	18.25
WAB1-16	27.68	90.76	28.96	13.50	15.46	7.72	1.10	6.62	10.17	8.59	18.76
WAB1-18	27.20	91.17	28.76	13.60	15.16	7.76	1.10	6.66	10.17	8.57	18.74
WAB1-20	26.29	90.81	27.53	13.40	14.13	6.96	1.00	5.96	10.03	8.65	18.68
WAB1-23	23.93	89.80	25.90	12.40	13.50	6.94	1.00	5.94	9.75	7.84	17.59
WAB1-26	22.24	85.55	24.84	12.00	12.84	6.36	0.90	5.46	9.23	7.58	16.81
WAB1-30	20.04	82.95	23.60	11.30	12.30	6.17	0.90	5.27	8.82	7.37	16.19
WAB1-34	18.69	75.43	22.60	11.20	11.40	6.31	0.90	5.41	8.09	7.20	15.29
WAB1-39	17.36	74.65	22.75	10.80	11.95	5.93	0.80	5.13	7.90	7.14	15.04
WAB1-44	17.56	76.17	22.61	10.50	12.11	7.04	0.90	6.14	8.09	7.22	15.31
WAB1-50	14.25	71.78	21.29	10.30	10.99	5.79	0.80	4.99	7.40	6.95	14.35
WAB1-56	11.27	52.76	19.32	9.80	9.52	5.26	0.90	4.36	5.54	5.49	11.03
WAB1-64	15.61	73.01	22.25	10.80	11.45	6.10	1.00	5.10	7.62	6.95	14.57
Median	*26.75*	*76.41*	*27.11*	*12.55*	*13.98*	*6.95*	*1.00*	*5.95*	*9.06*	*7.81*	*16.84*
Mean	*24.98*	*78.08*	*26.01*	*12.57*	*13.44*	*6.84*	*1.01*	*5.83*	*8.86*	*7.75*	*16.60*

[1] PC: Pyrolysable carbon [2] RC: Residual carbon

8.2.3. Experimental procedure

The following experimental procedures were used in this study:

a. The bulk sediment samples, before being thermally altered by Rock-Eval pyrolysis, were characterized by conventional white light and fluorescence microscopy (Chapter 1.7.3.4).

b. The samples were pyrolysed using Rock-Eval 6®. The starting temperature was set to 100 °C. The samples were heated (at the rate of 25 °C /min) until they reached 300 °C when the analyses were interrupted. At this temperature, the pyrogram showed that the S1 peak was fully evolved and the "volatile" were released from the samples (Figure 8.1a). Simultaneously, the portions of oxygen-containing organic compounds are released in S3aCO and $S3aCO_2$ peaks (Figures 8.1b-c). The heated samples were then subject to microscopic analyses (Chapter 1.7.3.4).

c. The sediment samples were pyrolysed up to 650 °C in the Rock-Eval6 pyrolysis oven. A bimodal S2 peak was fully evolved and pyrolysis products were released from the sample (Figure 8.1a). Simultaneously, the second portion of oxygen-containing organic compounds was released in S3bCO and $S3bCO_2$ peaks (Figures 8.1b-c). At this point, the analyses were interrupted and samples were taken out for pellet preparation and microscopic analyses (Chapter 1.7.3.4).

d. The sediment samples were then subject to the full-cycle run by Rock-Eval analyses. In this procedure the samples where heated in a pyrolysis oven, and then in an oxidation oven to a temperature of up to 850 °C (Figure 8.1d). The resulting samples were prepared into a pellet for microscopy (Chapter 1.7.3.4).

8.3. RESULTS AND DISCUSSIONS

The following describes the petrological characteristics of OM in the sediments before and after each step of thermal alteration by Rock-Eval pyrolysis, using white light and fluorescence microscopy:

8.3.1. Fresh sample (before pyrolysis)

Organic matter in the lacustrine sediments before pyrolysis consists of a mixture of intense fluorescing, very low reflecting to 'translucent' liptinitic materials (hereafter referred to as liptinite; Figures 8.2a-b), woody huminitic materials, vitrinitic materials, and inertinitic materials, hereafter referred to as huminite, vitrinite (from detrital coal particles), and inertinite, respectively.

The sediment samples before pyrolysis are notably enriched with 'stain-like', amorphous organic matter (AOM), including various pigments, presumably (and their by-products), and lipid-derived materials with strong yellow, green, and red fluorescence (Figures 8.2a-b). The particulate macerals (e.g., sporinite, alginite) are dispersed in the intensely fluorescing AOM matrix under the fluorescence light microscopy (Figures 8.2a-b).

The fluorescing liptinite OM within the Wabamun Lake sediment samples were classified into two major groups:

8.3.1.1. Particulate liptinite and liptodetrinites

This group consists of various particulate OM, often showing well defined structure with a range of fluorescing colors from blue to red (e.g., alginite, sporinite, and cutinite, and their broken debris; Figures 8.2a-b). Commonly the fluorescence colors of liptinites are

determined by type of 'soluble' AOM (e.g., pigments and lipid oils) with which they are stained (Figures 8.2a-b).

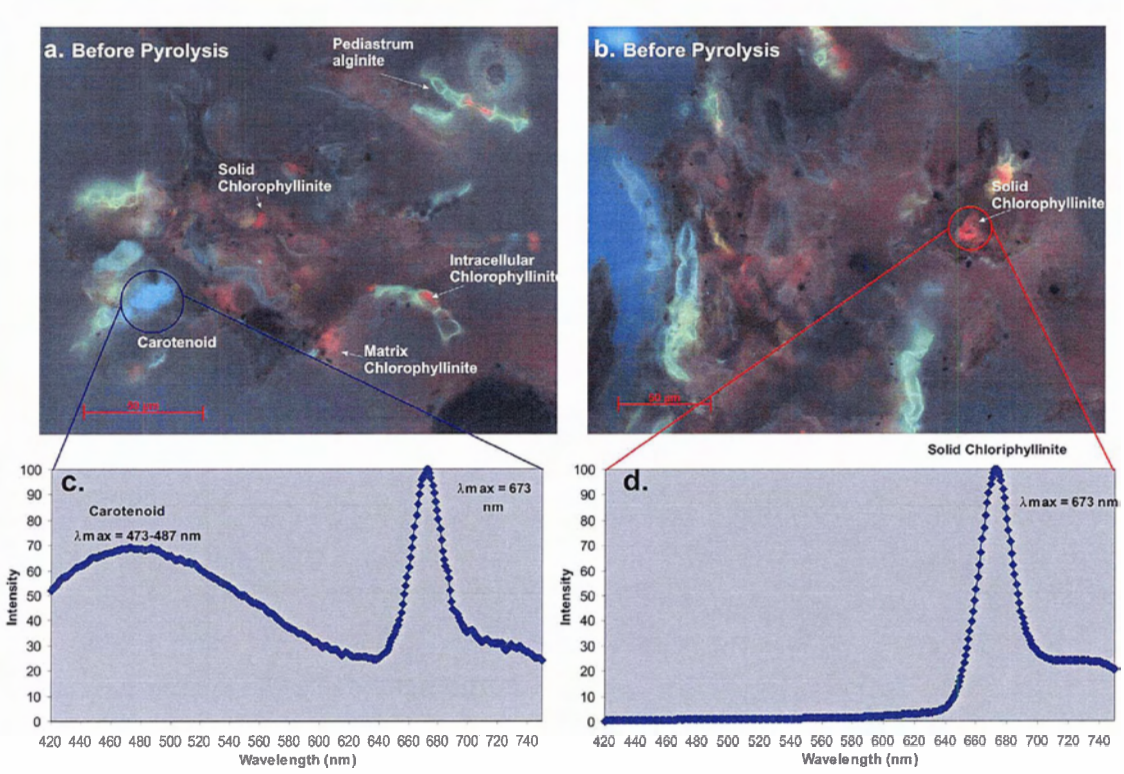

Figure 8.2.a-d. Dispersed organic matter in Wabamun Lake sediments, before pyrolysis: (a and b) Photomicrograph taken in oil immersion, UV conventional light source showing liptinitic particles in "stain-like" AOM matrix; (c) Visible light region fluorescence spectra corresponding to blue-fluorescing pigments (possibly carotinoids and their by-products); and (d) Red-fluorescing solid chlrophyllinite (possibly chlorophyll a, b, and their by-products).

The particulate liptinites are often very well preserved, showing perfect botanical structure such as cell walls, layering, and ornamentation (Figures 8.2a-b; 8.3a; 8.4a; 8.5a). The particulate liptinites consist primarily of: (i) *Pediastrum* alginite (Figure 8.3a) showing very bright greenish-yellow fluorescence with an average λ_{max} of 554 nm (Figure 8.3b), (ii) some sporinite (Figure 8.4a) with strong blue/green fluorescence with an average λ_{max} of 504 nm (Figure 8.4b), and (iii) blue fluorescing *Botryococcus* alginite (Figure 8.5a) with an

average λ_{max} of 502 nm (Figure 8.5b). Generally, all the fluorescence spectra measured for the particulate liptinites (alginite, sporinite, etc.), regardless of their apparent emission fluorescence color; Figures 8.3a; 8.4a; 8.5a), demonstrate a secondary peak around 673 nm (Figures 8.3b; 8.4b; 8.5b). This secondary peak corresponds to chlorophyll a standards (Stasiuk and Sanei, 2001), indicating the presence of amorphous chlorophyllinite within the particles and as surface coatings.

8.3.1.2. Amorphous organic matter (AOM)

These 'bitumen stain-like', amorphous liptinites are present in 'solid' or matrix form, which tend to fill in granular imperfections or physical gaps in the sediments and form surface coatings (i.e. chlorophyllinite adsorbed on to or 'staining' mineral matter; Figures 8.2a-b). The fluorescence colors of the amorphous liptinites are dominantly red, blue, and yellow (Figures 8.2a-b). Spectra of the red (λ_{max}=673 nm) and blue (λ_{max}=473-487) amorphous material in the studied samples (Figures 8.2c-d) correspond to those of chlorophyll a standards (Stasiuk and Sanei, 2001) and possibly a degraded carotenoid (standard λ_{max}= 445-450) , respectively. Occasionally, the amorphous pigments are seen concentrated in inter-particulate regions or entrapped inside the cell structure of *Pediastrum* and diatoms (Figures 8.2a; 8.3a). The red fluorescing chlorophyllinite immediately alters following exposure to the UV light such that the red fluorescing chlorophyllinite turned yellow (Stasiuk and Sanei, 2001).

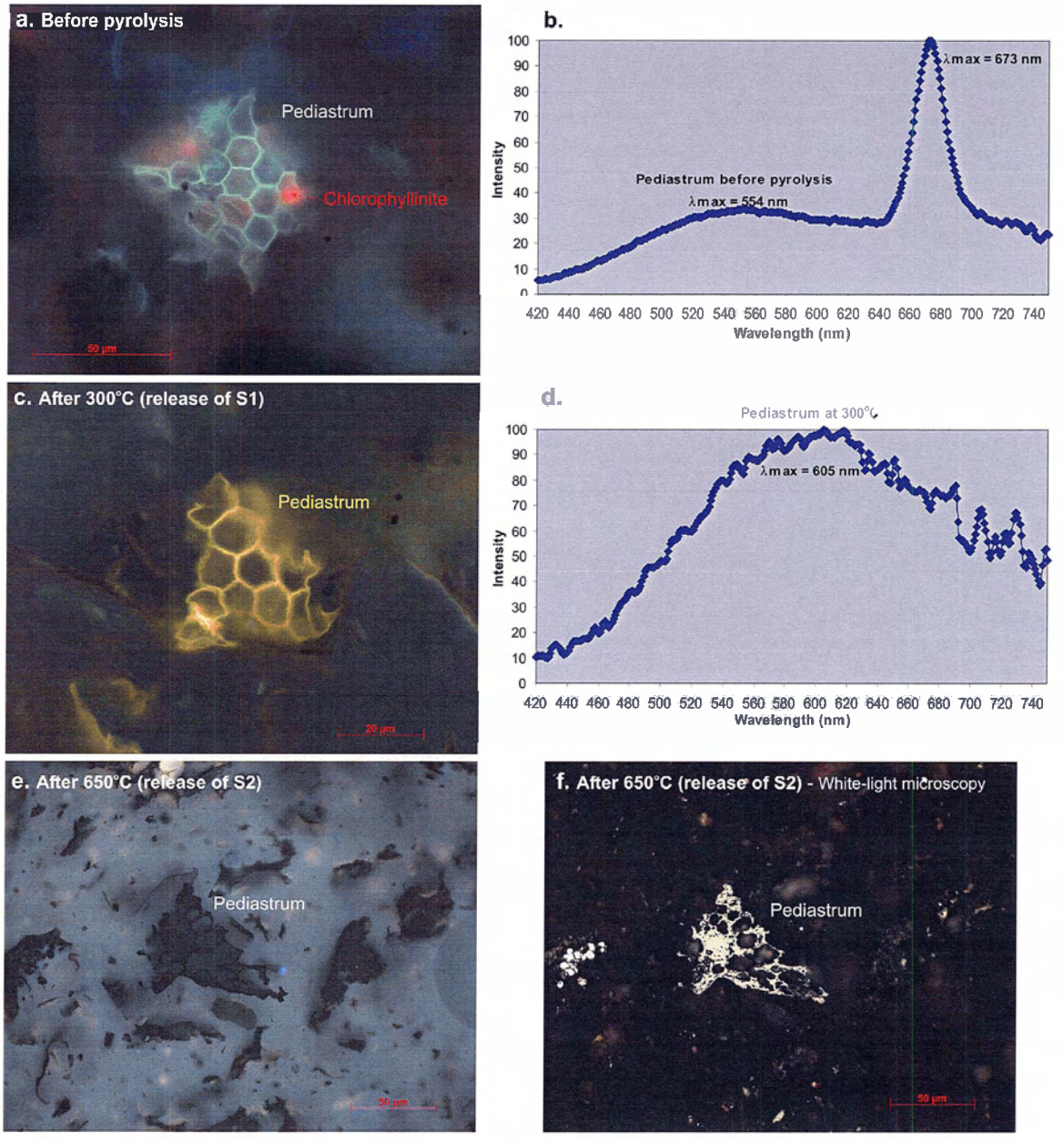

Figure 8.3.a-f. Fluorescence-light photomicrographs of a *Pediastrum* alginite (a, c, e, f) and its corresponding fluorescence spectra (b and d) during various stages of thermal alteration by Rock-Eval pyrolysis. (d) White-light photomicrographs of the *Pediastrum* alginite showing high reflectance due to thermal alteration.

The presence of a secondary peak (λ_{max} =673nm) in all spectra measured for various algal cell walls (before pyrolysis) corresponds to red fluorescing chlorophyllinite (Figures

8.2c; 8.3b; 8.4b; 8.5b), which is diffused into the sediment matrix thus providing surface coatings of the sediment particles.

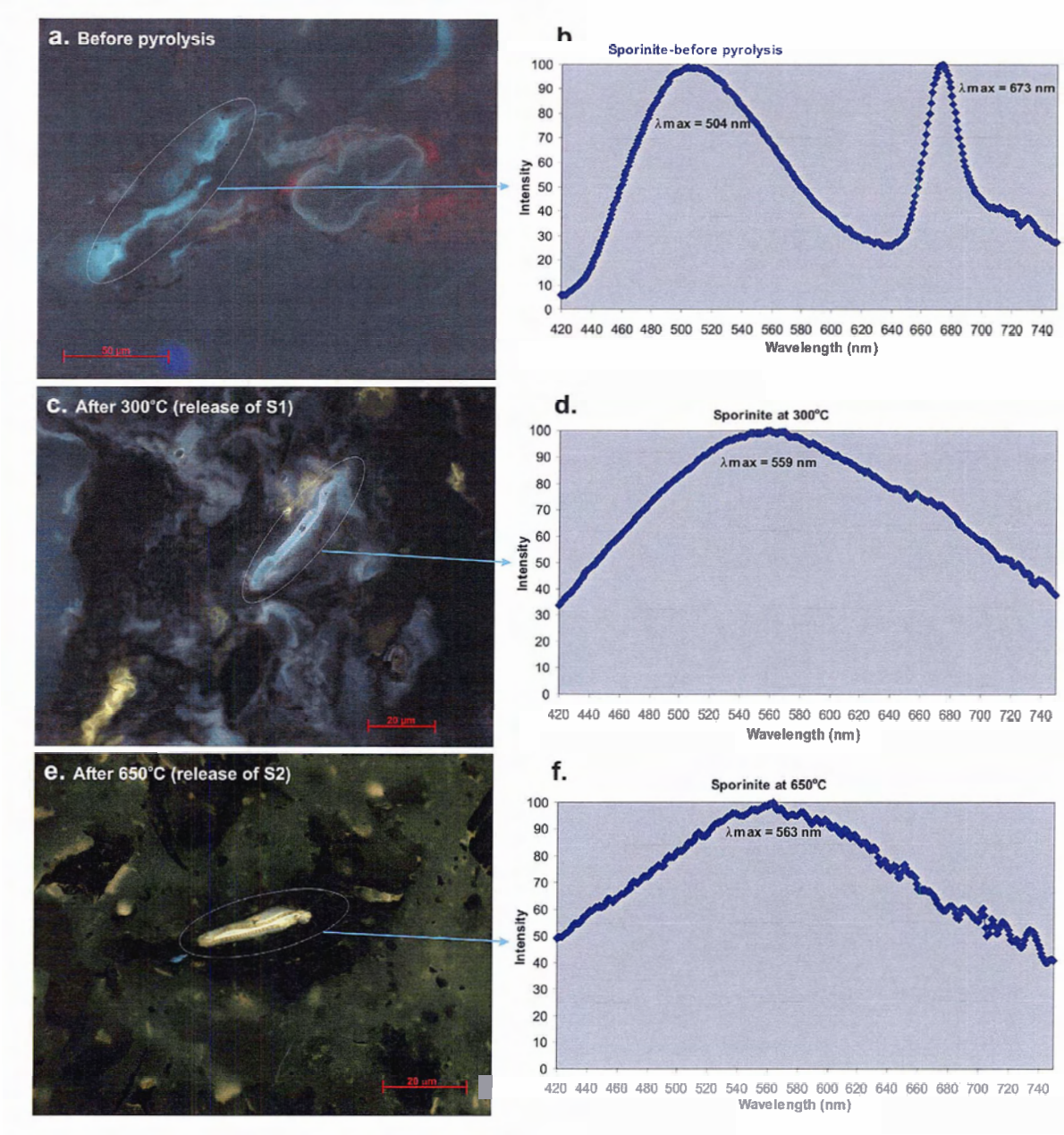

Figure 8.4.a-f. Fluorescence-light photomicrographs of a sporinite (a, c, e) and its corresponding fluorescence spectra (b, d, f) during various stages of thermal alteration by Rock-Eval pyrolysis.

8.3.2. Pyrolysis to 300 °C

The cell wall structure of the particulate liptinitic OM remains intact showing little morphological alteration after pyrolysis to 300°C (Figures 8.3c; 8.4c; and 8.5c). Fluorescence spectra for *Pediastrum* algae (λ_{max} =554 nm; Figures 8.3a-b) do however show a shift towards the red region of spectra (λ_{max}=605 nm; Figures 8.3c-d). Similarly, the fluorescence properties of sporinite shift to a higher wavelength (λ_{max} =554 nm; Figures 8.4c-d). *Botryococcus* alginite also show a dramatic change from blue (λ_{max} =502 nm; Figures 8.5a-b) to yellow fluorescence after this stage of pyrolysis (λ_{max}=588 nm; Figures 8.5c-d).

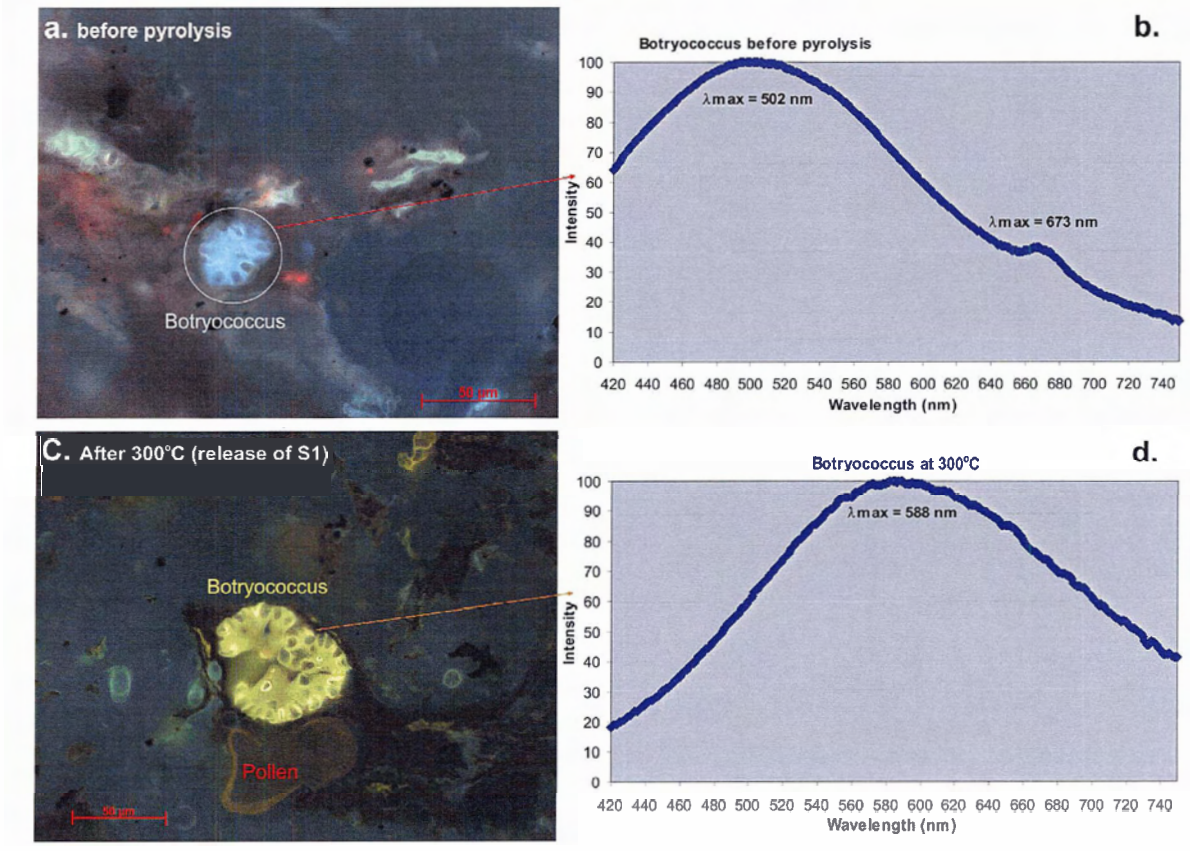

Figure 8.5: Fluorescence-light photomicrographs of a *Botryococcus* alginite (a, c) and its corresponding fluorescence spectra (b, d) during various stages of thermal alteration by Rock-Eval pyrolysis.

It appears that thermal alteration of the sediment causes almost all blue, red, and yellow fluorescing AOM to disappear (Figures 8.3c; 8.5c). This is also confirmed as the secondary chlorophyllinite peaks (λ_{max} =673 nm), usually associated with other spectra, are eliminated (Figures 8.3d; 8.4d; 8.5d).

There are two possible scenarios to explain what happened to the fluorescing AOM during this stage of pyrolysis. First, some of the more volatile compounds would be lost from the sediment during pyrolysis. These thermally labile materials are present as free hydrocarbons including free fatty acids, alcohols, ketones, etc, which form the S1 peak during Rock-Eval pyrolysis (Liebezeit and Wiesner, 1990). The removal of the S1-compound causes disaggregation of the sediment particles, which are likely 'cemented' by AOM. As a result, the agglomerates of particulate OM and mineral matter break down into their original, smaller, separate particles after pyrolysis at 300 °C. The micro-textural relationship between the thermally labile S1-compounds and the sediment grains/ particulate OM appears as a 'matrix' or coating. The close association between the S1-compounds and particulate OM in the sediments demonstrates the importance of surface absorption by labile OM onto sediment grains (Mayer 1993; Keil et al. 1994; Salmon et al., 2000). Furthermore, the fluid-like characteristics of the S1-compounds in the sediment are a good indication of the potential for early diagenetic geochemical processes involving OM such as mobility/fixation of trace elements in the recent sediments (Elderfield 1981; Douglas et al. 1986).

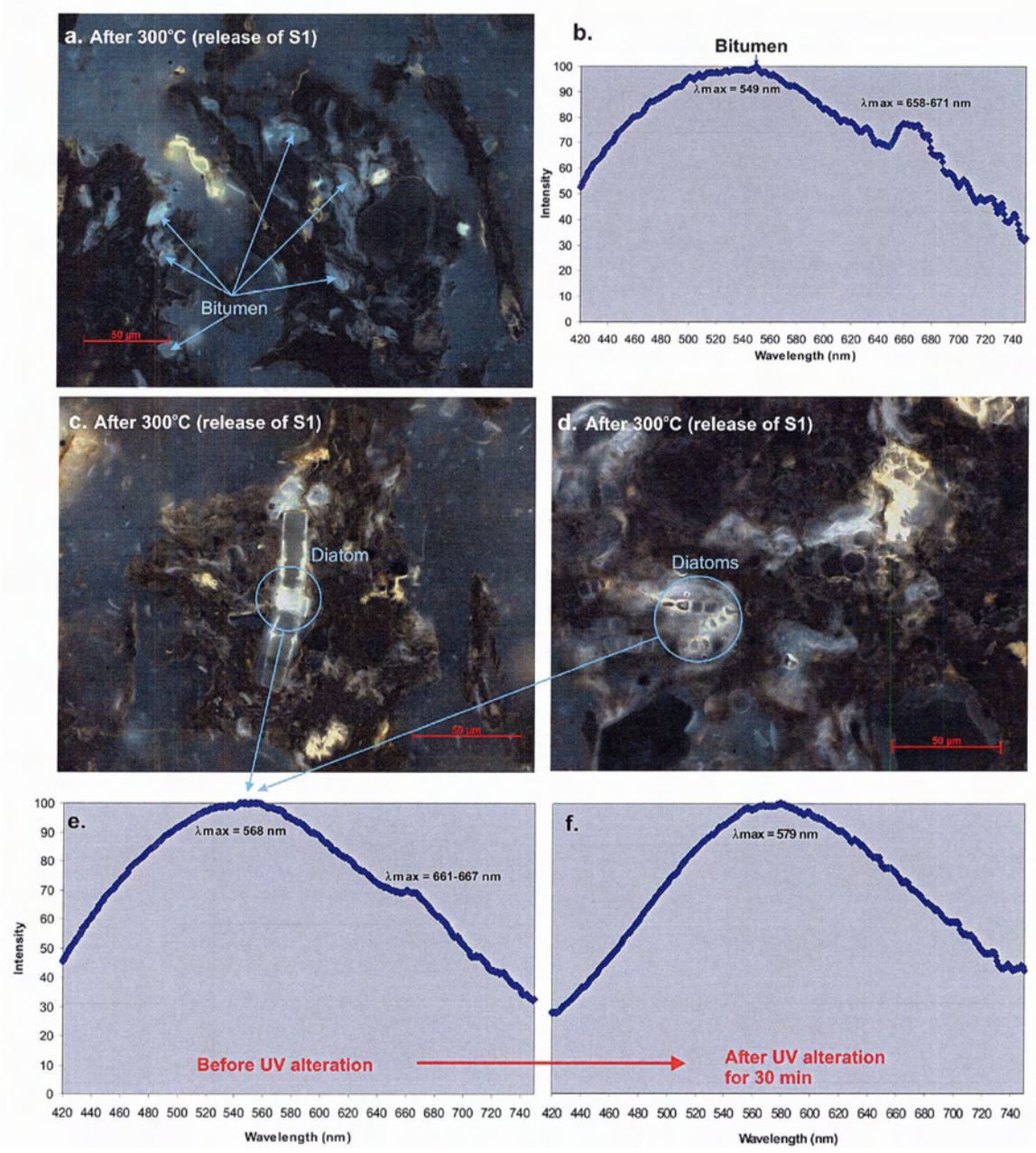

Figure 8.6.a-f. Fluorescence-light photomicrographs dispersed organic matter in Wabamun Lake sediments, after pyrolysis of up to 300 °C (release of S1-compounds). (a) Formation of blue-fluorescing bitumen within cell lumens and microfractures; (b) Fluorescence spectra corresponding to the bitumen with the inclusion of a secondary peak corresponding to the remnants of red-fluorescing chlorophyllinite; (c and d) Siliceous diatom frustules, possibly stained with blue-fluorescing bitumen; (e) Fluorescence spectra measured on a diatom frustule; (f) Slight shift of spectra towards the red-region measured on a diatom frustule after UV alteration for a period of 30 min.

Secondly, there are likely some new oily to semi-solid products formed from AOM even at the low temperatures of pyrolysis (e.g. from soluble algae-derived lipids-oils, branched alkanes) (Figure 8.6a). These products are hereafter referred to as secondary bitumen, which show a blue-green fluorescence with λ_{max} averaging ~ 550 nm (Figure 8.6b). The secondary bitumen tends to fill in the porosity and stain the cell structures of the liptinites (Figures 8.6a; 8.6c; 8.6d). Other, perhaps cyclic and aromatic components in the AOM, condensed into a non-volatile, non-fluorescing amorphous OM or kerogen fraction during low temperature S1 pyrolysis stage. This stage of Rock Eval of Recent sediments may be equivalent to the condensation of non-cellular, soluble OM (i.e. lipids etc) during the earliest stages of diagenesis forming an amorphinite kerogen commonly referred to in literature as bituminite (Teichmuller and Ottenjann, 1985; Stasiuk, 1993). By contrast, resistant biomacromolecules such as polymeric lipid-rich cell walls of *Botryococcus* or *Tasmanites* (e.g. Tegalaar et al., 1989; Stasiuk, 1999), have very high preservation potential simply by nature of their original chemical structure.

The alteration of blue fluorescing "oil" after 30 minutes of exposure to UV light shows a slight red shift of spectra to the higher wavelength (Figures 8.6e-f). The small secondary peak around 673nm (Figure 8.6e) corresponds to the trace of remaining chlorophyllinite within the diatom frustule, which is eliminated after alteration (Figure 8.6f).

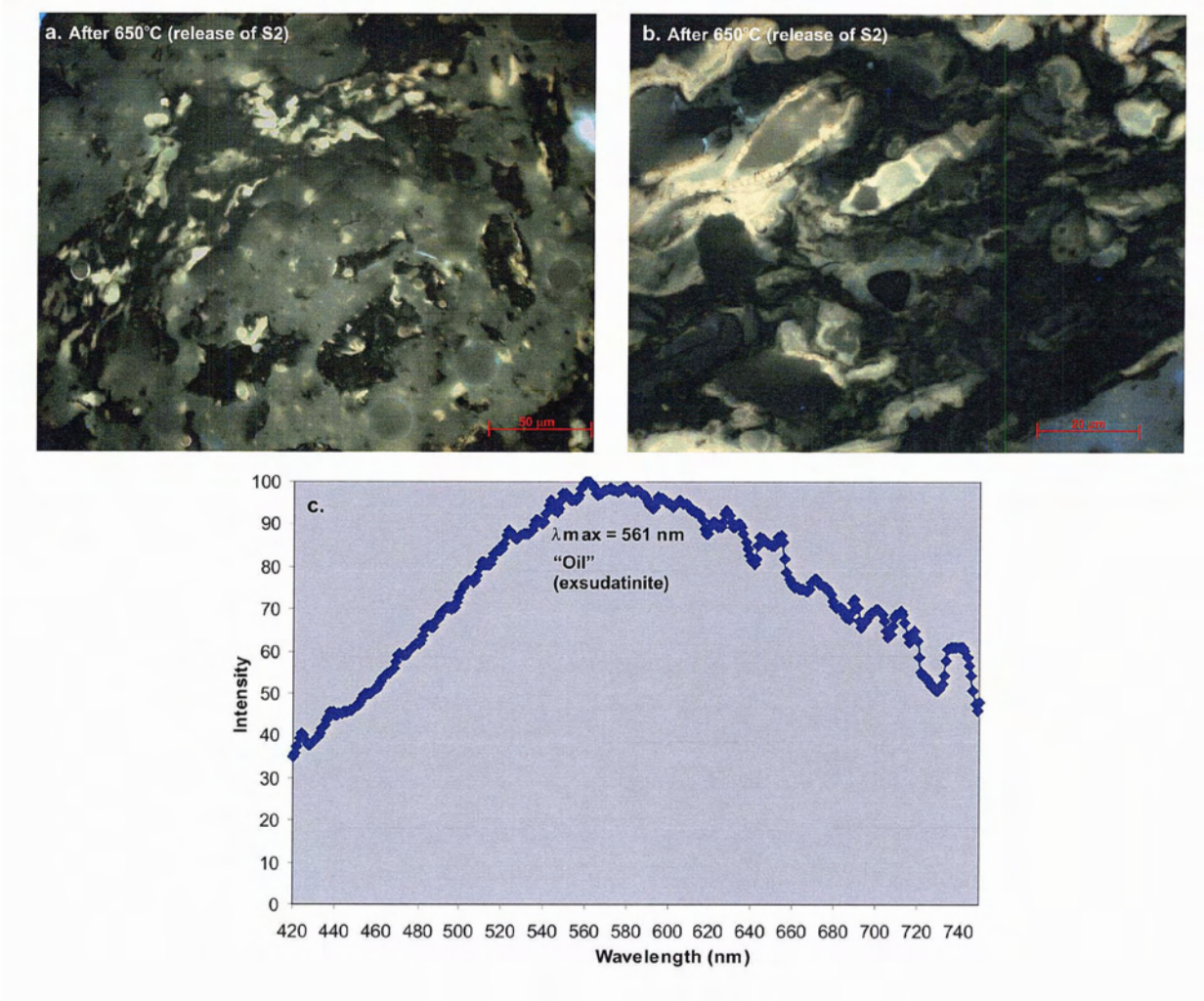

Figure 8.7: Fluorescence-light photomicrographs dispersed organic matter in Wabamun Lake sediments, after pyrolysis of up to 650 °C (release of S2-compounds). (a) yellow fluorescing "oily-organic matter" (generation of exsudatinite); (b) thermally altered remnants of diatoms and alginite structures exude a soluble yellow-fluorescing oil during UV exposure, as well as areas with very intense yellow fluorescence, which is likely the same oil trapped in mineral and porosity; (c) fluorescence spectra corresponding to the yellow fluorescing "oily-material".

8.3.3. Pyrolysis up to 650 °C

There is major thermal alteration of OM during this stage (Figures 8.3e-f; 8.7a-b). The particulate liptinites are transformed and 'broken down' under thermal stress, with significant

alteration to their morphology (Figures 8.3e-f; 8.7a-b). There are clear indications of formation of high reflecting, isotropic pyrobitumen and, typical anisotropic, mosaic-shaped pyrobitumen (e.g. fine to medium grained mosaic textures; Figures 8.8a-b). Surprisingly, even up to 650 °C, some of the liptinitic materials show a bright fluorescence color (Figures 6e; 9a-b) and exhibits oily exudation upon exposure to prolonged UV excitation.

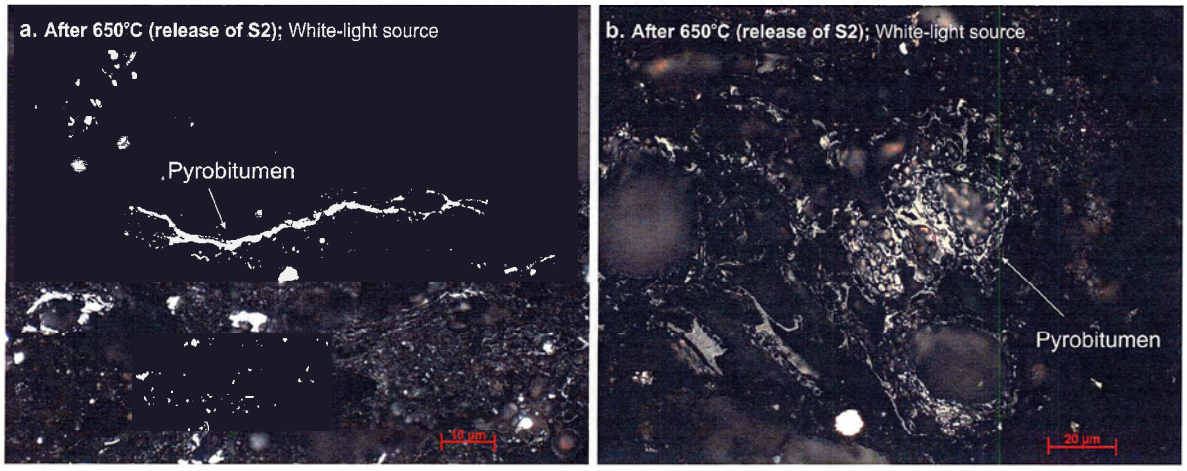

Figure 8.8: White-light photomicrographs of the Wabamun Lake sediments, showing the formation of high reflectance (a) pyribitumen; and (b) anisotropic, mosaic structure of pyribitumen formed due to the thermal alteration by temperatures up to 650 °C by Rock-Eval pyrolysis.

The observed yellow fluorescence likely corresponds to an "oily-material" formed during thermal transformation of oil-prone AOM, alginite, and other macerals in the sample. This is analogous to the stages of bituminite/amorphinite transforming into exsudatinite or bitumen, which occurs during diagenesis to catagenesis in sedimentary rocks (e.g., Goodarzi et al., 1987). The secondary oily material diffuses into the mineral matrix and "stains" diatom frustules as well as the resistant sporinite and remnants of liptinites (Figures 8.7a-b). This is evident as fluorescence spectra measured on various liptinitic materials (diatom frustules,

sporinite and organic debris) are all similar (λ_{max}=561-563 nm; Figures 8.4f and 8.7c), suggesting that a "homogenization" process has taken place at this stage.

The thermal effect at 650 °C on the recent sediments appear to have had more of an impact on smaller particulate liptinites with thin cell walls. This is shown in Figures 8.3e-f, in which a *Pediastrum* alginites lose their fluorescence with an evidently visible crumbled cell structure (Figure 8.3e). The white-light microscopy shows remnants of high-reflecting, *Pediastrum* alginite due to thermal alteration (Figures 8.3e-f). However, more resistant sporinite maintain their cell structure and show yellow fluorescence (Figure 8.4e). The fluorescence spectra measured at a sporinite cell wall shows a shift of spectra to the higher wavelength (λ_{max}=563 nm; Figure 8.4f) as compared to the previous stages (Figures 8.4b and 8.4d). However, this may not be from sporinite itself but rather from "oily-material" generated and absorbed by the maceral, since the λ_{max} are virtually identical.

The presence of fluorescing liptinites after release of S2-compounds is compelling evidence that suggests the rapid thermal alteration in Rock-Eval 6® may not be sufficient to break down all of the recent OM. This is because the Rock-Eval method is designed for rock samples that have previously undergone a thermal diagenetic history (Di-Giovanni et al, 1998; Disnar et al, 2003). The combination of heating rate and sample residence time during Rock-Eval pyrolysis is insufficient for complete thermal destruction of the OM in the recent sediments.

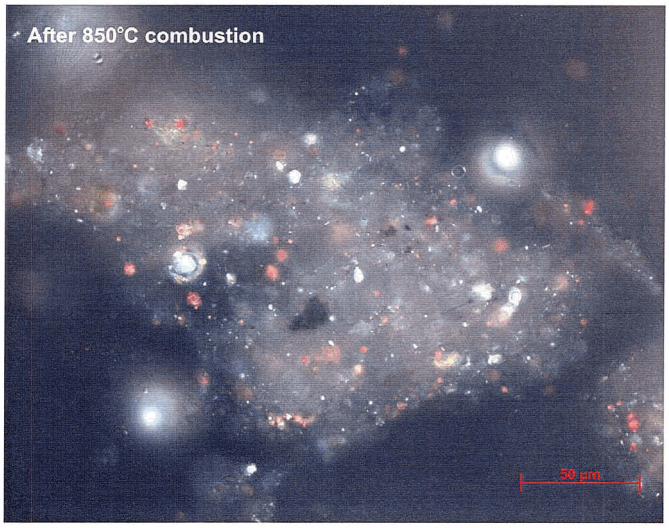

Figure 8.9: White-light photomicrograph of the Wabamun Lake sediments, after a complete Rock-Eval 6® run (pyrolysis and combustion up to 850 °C).

8.3.4. Combustion to 850°C

Microscopic observation under white reflected and fluorescent light confirms complete combustion of all OM in the sediment samples. The abundant red particles (under the reflected light) indicate the formation of iron oxides during combustion of the sediment. The mineral matrix appears to have disintegrated into small pieces due to devolatilization of the OM matrix (Figure 8.9).

8.4. CONCLUSIONS

This study documents systematic petrological changes occurring in OM from Recent lacustrine sediments during Rock-Eval pyrolysis. Important findings include the following:

- The S1-compounds are likely derived mainly from multicolored fluorescing, 'bitumen stain-like' amorphous organic matter. The fluid-like nature of the S1-compounds provides surface coating for the sediments grains, which accounts for the strong grain surface adsorption of organic matter.

- Thermal alteration of sediments at 300 °C results in the formation of blue-fluorescing bitumen, which has migrated into available free spaces (into microfractures).

- The release of S2-compounds during pyrolysis (between 300 °C to 650 °C) causes severe alterations in the morphology of the liptinitic OM and the formation of pyrobitumen. The bright yellow fluorescence appearing at this stage is likely due to the thermal transformation of macerals into "oil", which appears to be incorporated into remaining structure of some organic matter and mineral matrix. The rapid rates of heating (25 °C /min) and sample residence time during Rock-Eval pyrolysis are insufficient for complete thermal destruction of the secondary liquefied hydrocarbons in the sample.

APPENDIX A: METALS IN SEDIMENT AND POREWATER FROM WABAMUN LAKE

A.1. INTRODUCTION

Due to environmental concerns surrounding Wabamun Lake, this appendix provides a detailed breakdown of some trace metals as related to their temporal distributions found in the porewater and sediments of this Lake. Furthermore, the significance of these elements of environmental concern has been addressed as it pertains to environmental effects on Wabamun Lake.

A.2. TEMPORAL DISTRIBUTION OF METALS IN SEDIMENT AND POREWATER FROM WABAMUN LAKE

A.2.1. Arsenic (As)

The porewater profile of WAB1 shows an increase in concentration of dissolved As with increasing depth (Figure A.1a). The peak of dissolved As (37.7 ppb) occurs at the bottom of the porewater profile (at depth of 50 cm) (Table A.1a; Figure A.1a). The dissolved As content remains low (<3.2 ppb) in the upper section of the profile with a slight increase in the top 4 cm of porewater samples, below the SWI (3.2-5.2 ppb) (Table A.1a and Figure A.1a). The As concentration in the uppermost porewater samples (Table A.1a) slightly exceeds the As content of the lake water (average 2.5 ppb; Golder Associates, 2002).

Table A.1.a. The total concentrations of trace metals in sediments and porewater profiles from core WAB1.

Sediment intervals (cm)	Porewater As ppb	Sediment As ppm	Porewater Cd ppb	Sediment Cd ppm	Porewater Co ppb	Sediment Co ppm	Porewater Cr ppb	Sediment Cr ppm	Porewater Cu ppb	Sediment Cu ppm	Porewater Hg ppt	Sediment Hg ppm	Porewater Pb ppb	Sediment Pb ppm	Porewater Zn ppb
Wab1-01	5.2	11	< .05	0.42	0.03	11.3	1	68	0.8	30	< 2	0.02	< .1	16	0.5
Wab1-02	4.7	16	< .05	0.30	0.04	6.8	2.8	50	0.7	97	< 5	0.10	< .1	25	< .5
Wab1-03	3.9	16	< .05	0.34	0.04	6.9	2.4	54	0.7	103	< 2	0.08	< .1	22	< .5
Wab1-04	3.2	17	< .05	0.30	0.05	6.7	0.25	52	6.3	105	< 8	0.06	< .1	23	1
Wab1-05	3	18	< .05	0.34	0.05	6.9	2.3	52	0.7	108	< 2	0.06	< .1	23	< .5
Wab1-06	3	19	< .05	0.32	0.07	7.6	1.8	56	0.7	118	< 2	0.08	< .1	24	< .5
Wab1-07	3.2	20	< .05	0.37	0.07	7.8	1.5	58	0.8	121	< 2	0.06	3.4	25	0.5
Wab1-08	2.8	21	< .05	0.36	0.09	7.4	1.8	60	0.8	132	24	0.06	< .1	27	0.7
Wab1-09	2.9	23	< .05	0.42	0.11	7.3	2.1	61	1.5	157	16	0.06	0.1	30	0.6
Wab1-10	2.4	24	< .05	0.42	0.21	7.7	2.9	62	0.9	176	10	0.08	< .1	32	< .5
Wab1-12	3.2	25	< .05	0.46	0.18	7.6	1.5	55	0.9	149	10	0.06	< .1	30	< .5
Wab1-14	2.3	20	< .05	0.54	0.22	7.8	2.9	46	0.9	64	< 2	0.05	< .1	26	< .5
Wab1-16	2.5	17	< .05	0.47	0.25	7.4	2.5	42	0.8	41	11	0.05	0.1	23	< .5
Wab1-18	1.7	16	< .05	0.50	0.24	7.2	2.4	42	0.8	37	10	0.05	0.1	20	0.7
Wab1-20	1.8	15	< .05	0.50	0.26	7.5	3.5	41	0.8	38	< 5	0.05	0.1	18	< .5
Wab1-23	3.3	15	< .05	0.49	0.18	7.9	1	44	1.1	34	< 6	0.02	0.1	16	0.8
Wab1-26	3.9	12	< .05	0.40	0.21	7.5	2.7	42	0.9	31	10	0.03	1.2	14	0.9
Wab1-30	2.9	12	< .05	0.39	0.22	8.5	2.4	49	1	32	< 5	0.05	0.4	14	4.3
Wab1-34	6.7	10	< .05	0.38	0.13	9.1	0.5	52	0.9	31	< 6	0.04	0.9	14	1.4
Wab1-39	10	11	< .05	0.40	0.13	9.9	4.6	51	1.1	34	< 6	0.02	0.1	14	1.6
Wab1-44	20	12	< .05	0.44	0.12	9.4	2.9	51	5	34	< 4	0.03	0.1	14	0.9
Wab1-50	38	12	< .05	0.42	0.23	9.4	3.9	52	1.4	34	< 5	0.05	0.1	15	0.9
Wab1-56	13.2	9	< .05	0.43	0.13	8.3	2.5	48	1.4	34	< 5	0.04	0.1	15	1
Wab1-64	19	13	< .05	0.43	0.12	10.0	4.1	53	3.2	34	< 5	0.05	0.1	14	1.6
Min	1.7	9	ND	0.30	0.03	6.7	0.5	41	0.7	30	10	0.02	0.1	14	0.5
Median	3.2	16	ND	0.42	0.13	7.7	2.4	52	0.9	40	10	0.05	0.1	21	0.9
Max	38	25	ND	0.54	0.26	11.3	4.6	68	6.3	176	24	0.10	3.4	32	4.3
Mean	6.8	16	ND	0.41	0.14	8.1	2.4	52	1.4	74	13	0.05	0.5	21	1.16

Table A.1.b. The total concentrations of trace metals in sediments and porewater profiles from core WAB2.

Sediment intervals (cm)	Porewater As ppb	Sediment As ppm	Porewater Cd ppb	Sediment Cd ppm	Porewater Co ppb	Sediment Co ppm	Porewater Cr ppb	Sediment Cr ppm	Porewater Cu ppb	Sediment Cu ppm	Porewater Hg ppt	Sediment Hg ppm	Porewater Pb ppb	Sediment Pb ppm	Porewater Zn ppb
Wab2-01	9.8	16	< .05	0.39	0.02	6.3	1.5	62	0.8	92	< 5	0.06	0.1	20	1.6
Wab2-02	11.7	15	< .05	0.40	0.02	8.3	2.6	64	0.6	90	< 5	0.07	0.1	20	< .5
Wab2-03	7.7	14	< .05	0.37	0.03	8.0	2.5	63	0.6	95	< 5	0.06	0.1	21	< .5
Wab2-04	6	15	< .05	0.38	0.03	7.7	1.7	66	0.6	104	< 4	0.07	< .1	22	< .5
Wab2-05	7.3	15	< .05	0.39	0.04	8.3	2.5	67	0.6	104	< 4	0.06	< .1	23	< .5
Wab2-06	7.1	16	< .05	0.40	0.03	8.3	0.9	64	1	102	< 4	0.07	0.2	21	< .5
Wab2-07	7.3	18	< .05	0.38	0.03	8.6	0.9	60	1	102	< 6	0.05	0.2	21	< .5
Wab2-08	6.4	19	< .05	0.41	0.03	8.2	0.9	64	0.9	99	< 4	0.04	0.2	22	< .5
Wab2-09	6.7	21	< .05	0.41	0.03	8.3	0.8	60	0.9	88	< 3	0.02	0.1	21	< .5
Wab2-10	7.4	21	< .05	0.43	0.02	8.4	0.5	61	0.8	77	< 5	0.10	0.2	21	0.9
Wab2-12	7.6	19	< .05	0.44	0.03	8.9	0.8	56	1	46	< 5	0.08	0.1	17	< .5
Wab2-14	7.8	15	< .05	0.44	0.04	9.1	0.6	55	1	36	< 2	0.09	0.3	16	< .5
Wab2-16	6.7	12	< .05	0.43	0.05	9.2	0.6	58	1.1	30	< 4	0.07	0.1	16	< .5
Wab2-18	5.6	12	< .05	0.35	0.06	9.8	0.7	59	1.1	28	< 3	0.06	0.1	15	0.5
Wab2-20	3.2	10	< .05	0.37	0.07	9.4	0.7	58	1.2	26	< 3	0.07	0.1	15	1.1
Wab2-23	3.8	10	< .05	0.37	0.11	10.0	< .5	60	1.2	27	< 4	0.06	0.3	16	< .5
Wab2-26	5.8	10	< .05	0.42	0.1	9.5	< .5	58	1.2	28	< 4	0.07	0.3	16	0.5
Wab2-30	4.9	10	< .05	0.40	0.09	10.1	< .5	62	1.2	28	< 3	0.06	0.3	17	0.5
Wab2-35	5.5	9	< .05	0.44	0.05	10.4	0.7	61	2.1	29	< 3	0.06	0.2	17	6.9
Wab2-41	5.7	9	< .05	0.45	0.06	9.9	0.5	61	2.2	30	< 2	0.06	0.4	16	10.3
Wab2-47	11.9	8	< .05	0.41	0.07	9.9	< .5	57	2.6	27	< 3	0.05	0.3	15	6.2
Wab2-54	5.6	8	< .05	0.41	0.07	9.8	< .5	60	1.5	28	< 4	0.06	0.3	16	2.9
Min	3.2	8	ND	0.35	0.02	6.3	0.5	55	0.6	26	ND	0.02	0.1	15	0.5
Median	6.7	15	ND	0.41	0.04	9.0	0.8	61	1.0	41	ND	0.06	0.2	17	1.35
Max	11.9	21	ND	0.45	0.11	10.4	2.6	67	2.6	104	ND	0.10	0.4	23	10.3
Mean	6.9	14	ND	0.40	0.05	8.9	1.1	61	1.1	60	ND	0.06	0.2	18	3.14

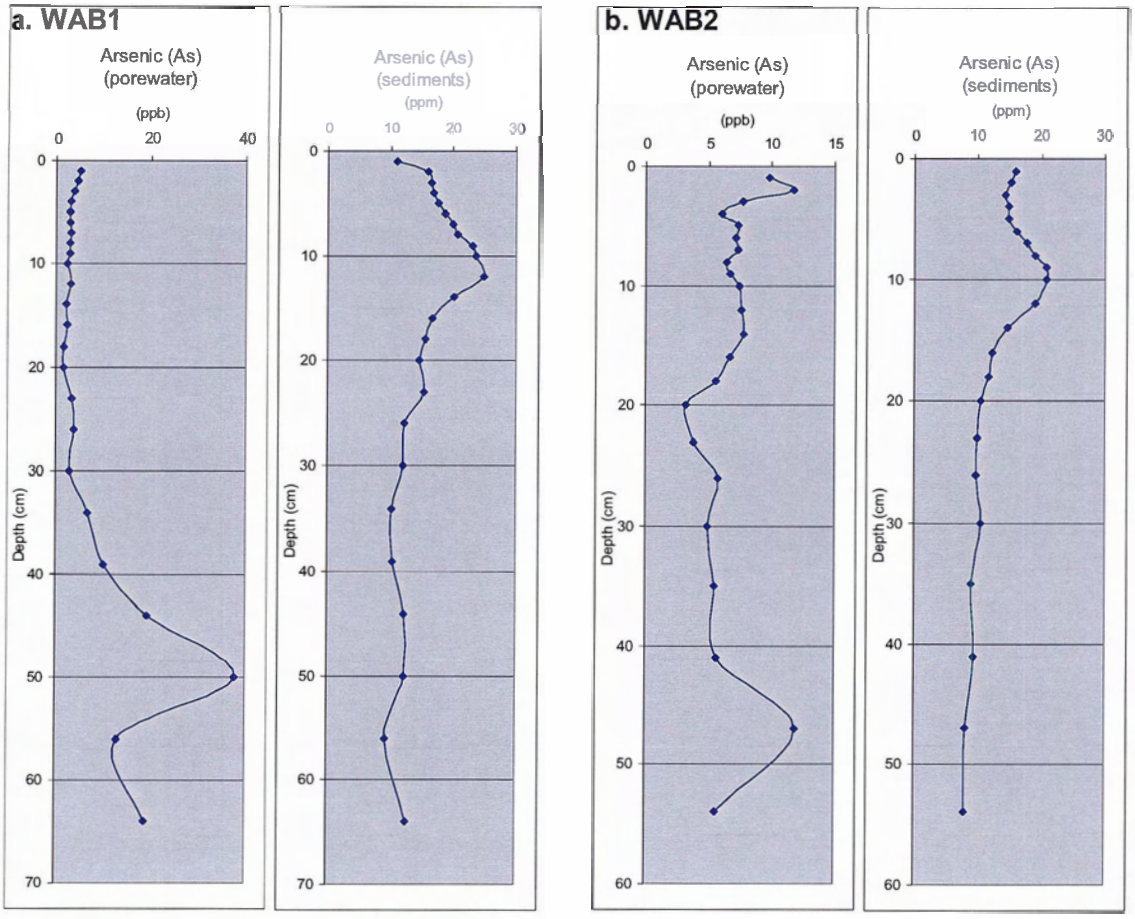

Figure A.1.a-b. The temporal distribution of arsenic (As) in porewater and sediment profiles from (a) WAB1 core and (b) WAB2 core.

The depth profile of As in sediment from the WAB1 core shows an inverse pattern as compared to that observed in the porewater profile (Figure A.1a). The As profile in sediments shows an upward increase up to the maximum concentration (24.9 ppm) at 12 cm. From that point, the As content tends to decrease towards the SWI (As content at SWI = 10.9 ppm) (Table A.1a; Figure A.1a). The range of total As in the upper section of the WAB1 sediment core exceeds the sediment quality guideline (5.9 ppm; CCME, 1999) (Table A.2).

The As profile in the WAB2 sediments show the same pattern observed in WAB1. The peak of arsenic content (21 ppm) in WAB2 sediment profile occurs between 9 and 10 cm (Table A.1b; Figure A.1b).

Table A.2. Canadian Sediment Quality Guidelines for the Protection of Aquatic Life (Freshwater).

Total metals	Units	ISQG [a]
Arsenic (As)	ppm	5.9
Cadmium (Cd)	ppm	0.6
Chromium (Cr)	ppm	37.3
Copper (Cu)	ppm	35.7
Lead (Pb)	ppm	35
Mercury (Hg)	ppm	0.17
Zinc (Zn)	ppm	123

[a] ISQG= interim sediment quality guideline (CCME 1999).

The increased concentration of dissolved As in the bottom section of the WAB2 porewater profile (Figure A.1b) suggests the dissolution of As-containing substrates in this part. Dissolution of As gradually declines upward until it reaches its minimum amount of 3.2 ppb at 18 cm (Table A.1b; Figure A.1b). Above 18 cm, the concentration of dissolved As tends to increase continually towards the SWI (Figure A.1b). The arsenic contents in the uppermost 3 cm of the porewater profile (7.7 to 11.7 ppb; Tables A.1b) exceeds the concentration of dissolved As for Wabamun Lake water (average 2.5 ppb) (Golder Associates, 2002).

As it was discussed in Chapter 3, the increased concentration of dissolved As in the deeper section of the porewater profiles may be related to dissolution/decomposition of Ca-

OM fraction and their subsequent release of adsorbed As into porewater. The dissolved As may move upward due to a concentration gradient and compaction of the sediments. It may, in turn, be fixed at the upper section of the profile by lime and/or freshly formed organic matter. Hence the porewater may act as a conveyer, moving the dissolved As from the bottom to the top of the core.

The higher concentration of dissolved As at surficial sediments of core WAB2 is also correlated with high concentrations of dissolved Fe and Mn near the SWI (Chapter 3). This suggests that As is possibly released into porewater along with reduced Fe and Mn under anoxic conditions. A high input of organic matter in the surface sediment layer may result in rapid depletion of O_2 in the surface sediments, which causes the reduction of Fe and Mn oxides (Appenidx B).

A.2.2. Cadmium (Cd)

The Cd content of the sediment in the Wabmaun Lake sediment cores (WAB1 and WAB2) ranges from 0.3 to 0.5 ppm (Table A.1a). The maximum Cd contents of 0.54 and 0.45 ppm were measured in WAB1 and WAB2, respectively, which are considered lower than the sediment guideline of 0.6 ppm (Tables A.1a-b; A.2).

The vertical variations of Cd in both WAB1 and WAB2 (Figures A.2a; A.2b) sediment cores lack any similarities with neither heavy metals nor other geochemical indicators (e.g, TOC, Total S, and Fe/Mn) (Figures 3.1-3.2). However, there are low, but statistically

significant, positive correlations between Cd and some lithophilic elements (e.g., Al, Zr, Ti) in WAB2 (Tables 3.9-3.10). This is an indication that the major influence, with respect to Cd concentration, is geogenic, masking the variations induced by other geochemical processes.

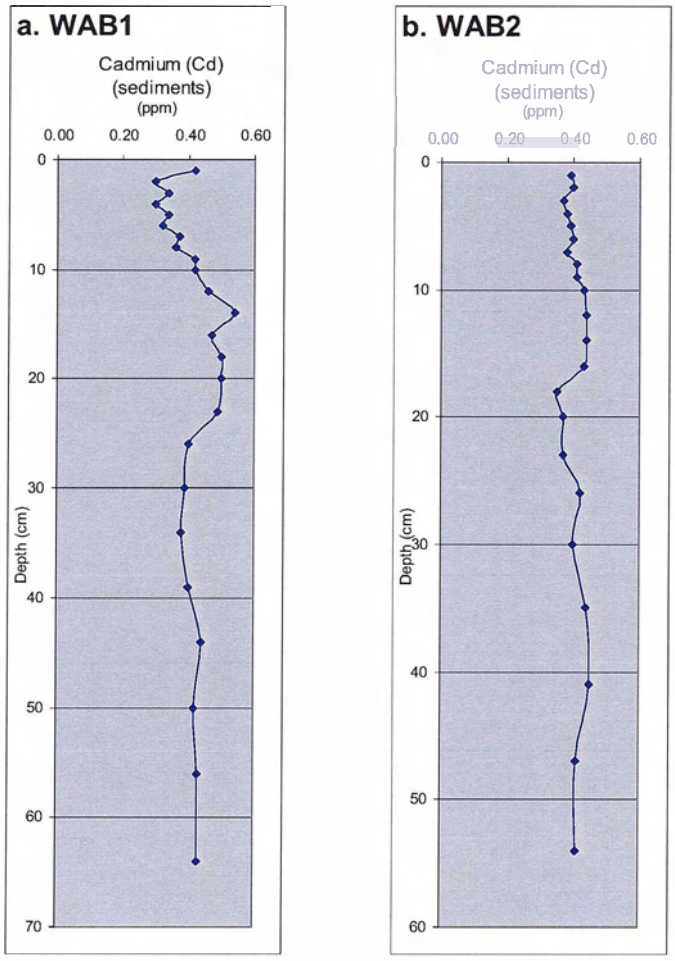

Figure A.2.a-b. The temporal distribution of cadmium (Cd) in sediment profiles from (a) WAB1 core and (b) WAB2 core.

Dissolved Cd was not detected in either WAB1 or WAB2 porewater profiles (Tables A.1a-b). This suggests very low dissolution of Cd, thus confirming that the dominant source of Cd in Wabamun sediments is geogenic. The geogenically-induced Cd is within the crystal

lattice of the lithophilic minerals and only leaches out under extreme pH condition (strong acid leaching; Sanei et al., 2001).

A.2.3. Cobalt (Co)

The Co contents of sediments in the Wabamun cores (WAB1 and WAB2) range from 6 to 11 ppm with the lower Co contents at upper sections of the cores (Figures A.3a-b; Tables A.1a-b). Temporal changes of Co in both sediment cores are very similar to those of geogenic elements (e.g., REEs, Th, Ti, etc.), showing increasing concentrations with increasing depth (Figures A.3a-b; Figures 3.1; 3.2) (Chapter 3). This pattern is likely the result of the dilution effect caused by organic matter (see Chapter 3 and Chapter 7 for details). The rapid increase of Co in the top 1 cm of the sediment sample in WAB1 (Figure A.3a) is possibly due to oxidation of the sample during sample handling and hence co-precipitation of Co along with redox Fe/Mn phase.

The dissolved concentration of Co in both WAB1 and WAB2 porewater ranges from 0.02 to 0.26 ppb (Tables A.1a-b), which is within the range of Co content for lake water (<0.2-0.7 ppb; Golder Associates, 2002). The dissolved Co in the WAB1 porewater profile increases with depth below the sediment-water interface, correlating with the observed trend for Mn in the porewater (Figures A.3a-b; 3.20). It appears that the cycling of Co in the sediments is related to Mn-redox processes. The strong affinity of Co with redox sensitive Fe/Mn oxides has been well described in scientific literature (Gendron et al. 1986; Shaw et al., 1990; ; Wallmann, 1990; Williams 1992; Wallmann 1992).

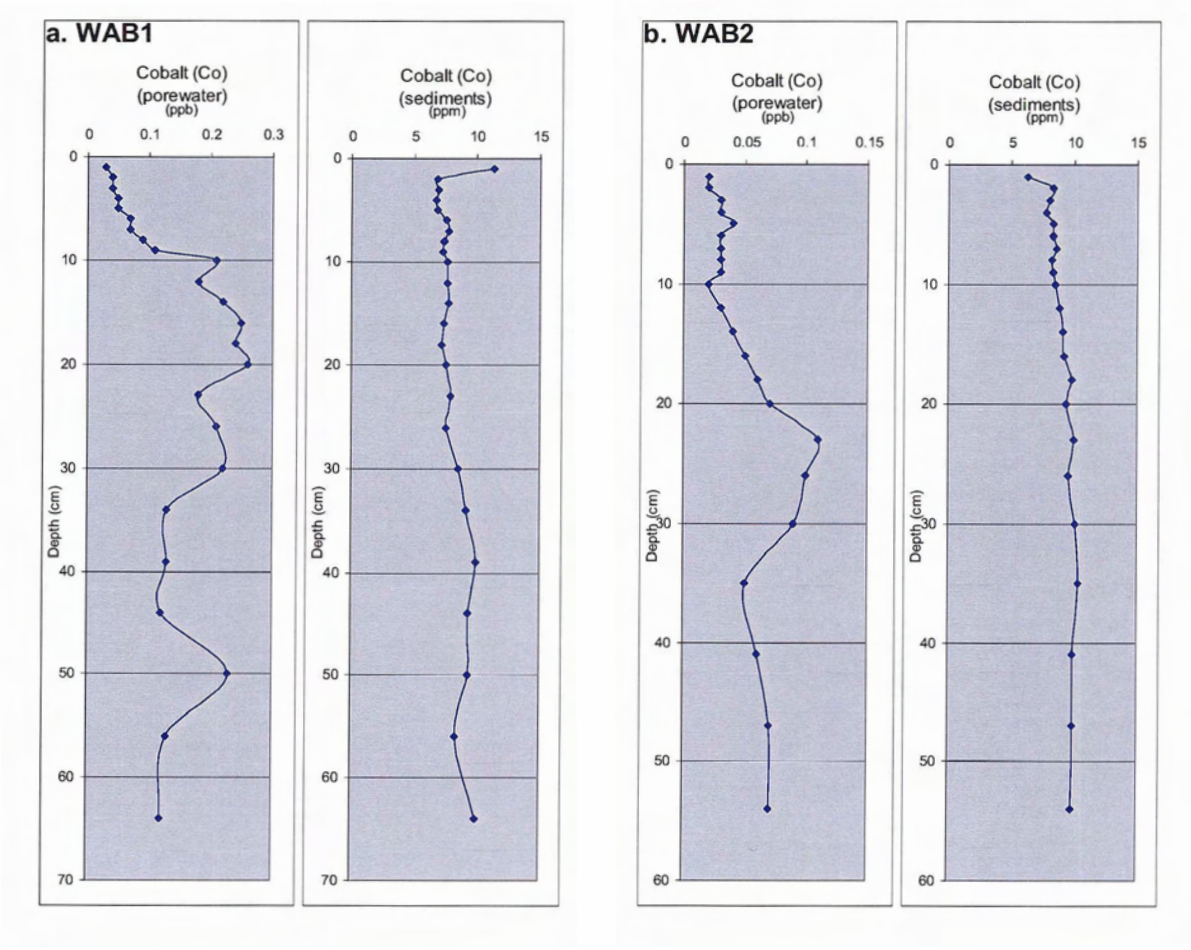

Figure A.3.a-b. The temporal distribution of cobalt (Co) in porewater and sediment profiles from (a) WAB1 core and (b) WAB2 core.

A.2.4. Chromium (Cr)

The Cr contents of Wabamun Lake sediments range from 41 to 68 ppm, which are distinctly higher than the 37.7 ppm outlined by the Canadian sediment quality guideline (Tables A.1a-b; A.2) (CCME, 1999). The depth profiles of Cr in both WAB1 and WAB2 sediment cores resemble the well-characterized episode of enrichment in the upper part of the profiles (Figures A.4a-b), similar to the other anthropogenically-induced elements (e.g., Pb, Cu, As) (Chapter 3.4.1). The peaks of Cr in the sediment profiles are followed by the gradual

decrease of Cr towards the SWI (Figures A.4a-b), possibly due to the decrease in external input of Cr or dissolution of Cr into porewater (Chapter 3.4.1). Below the Cr-enrichment in the upper part of the WAB1 and WAB2 sediment profiles, the Cr contents remain low with a gradual increase with depth (Figures A.4a-b), as typically seen for the geogenic elements (e.g., Zr) (Figure 3.1). It appears that the anthropogenic enrichment of Cr in the upper section of the sediment cores in Wabamun Lake is masking the geogenic pattern. This is an indication of the complexity of the sediment core interpretation.

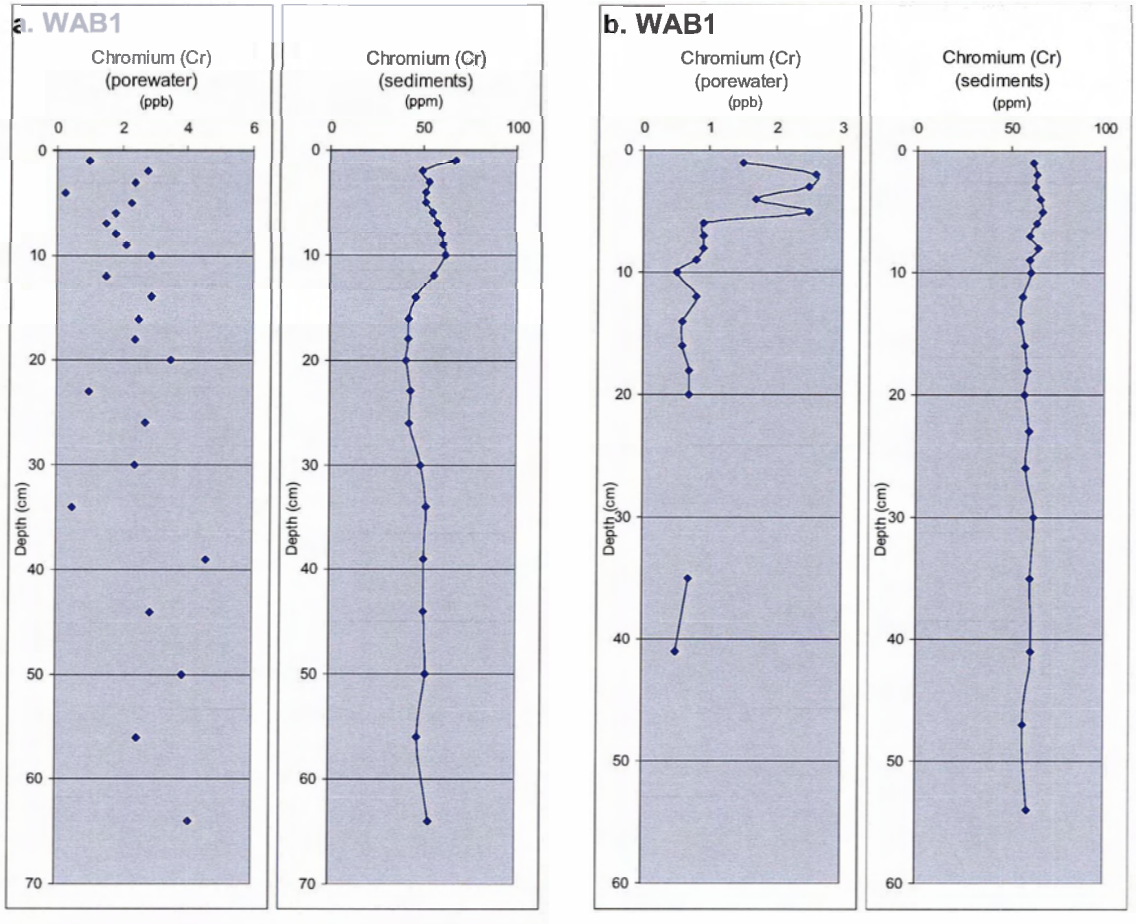

Figure A.4.a-b. The temporal distribution of chromium (Cr) in porewater and sediment profiles from (a) WAB1 core and (b) WAB2 core.

The concentrations of dissolved Cr range from less than 0.5 to 4.6 ppb in WAB1 and WAB2 porewater profiles (Tables A.1a-b), which is higher than the total Cr content of the lake water (<0.8-1.4 ppb; Golder Associates, 2002). This implies that dissolved Cr released from sediments may not have a direct influence on the quality of the overlying water.

The depth profiles of Cr and Mn, after being normalized to Zr (to remove the effect of the mineral matrix and geogenic dilution) show significant similarities in both sediments and porewater. Johnson et al., (1992) stated that the cycling of Cr is closely linked to the cycling of Mn.

A.2.5. Copper (Cu)

The sediment profile in WAB1 shows an episode of Cu enrichment in the upper section of the profile, above the depth of 15 cm (Figure A.5a and Table A.1a). The maximum concentration of Cu (176 ppm) in WAB1 sediment core is observed at the depth of 10 cm, which decreases to 30 ppm at the sediment-water-interface (Figure A.5a; Table A.1a).

The concentration of dissolved Cu in the WAB1 core ranges from 0.7 ppb in the upper portion of the porewater profile, to the maximum concentration of 5 ppb at a depth 44 cm (Figure A.5a and Table A.1a). The concentration of dissolved Cu in the upper portion of the porewater profile is within the range of Wabamun Lake water (<1-2 ppb) measured from various regions of the lake (Golder Associates, 2002).

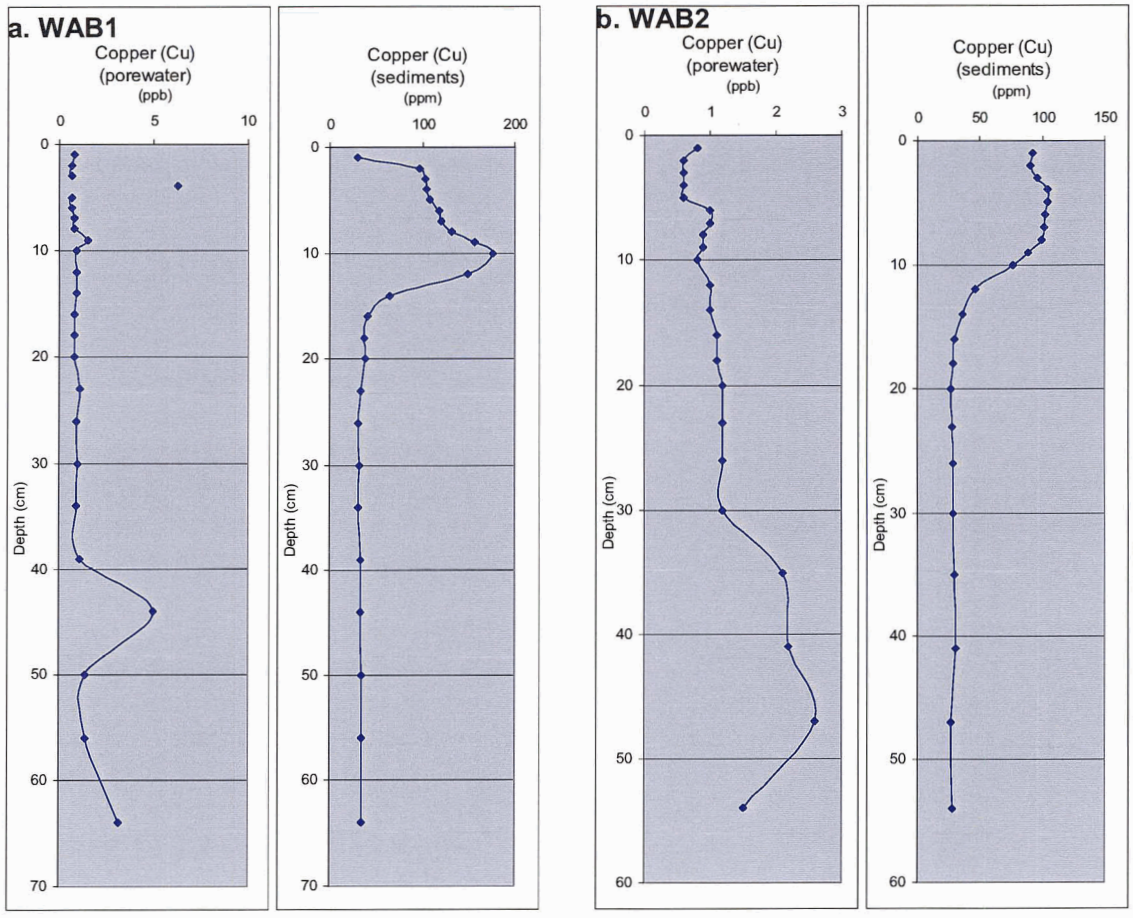

Figure A.5.a-b. The temporal distribution of copper (Cu) in porewater and sediment profiles from (a) WAB1 core and (b) WAB2 core.

The WAB2 porewater profile shows the minimum concentration of dissolved Cu (0.6 ppb) occurs at the uppermost samples followed by the gradual increase of dissolved Cu with increasing depth (Figure A.5b). The concentration of dissolved Cu in the top 10 cm of the porewater profile (0.6-1 ppb; Table A.1b) varies within the range of Cu content for Wabamun lake water (<1-2 ppb; Golder Associates, 2002). The peak of dissolved Cu (2.6 ppb) is located at the bottom of the porewater profile (47 cm) (Figure A.5b; Table A.1b).

The WAB2 sediment profile shows an inverse trend as compared to its porewater profile (Figure A.5b). Similar to the WAB1 sediment profile, the highest accumulation of Cu occurs in the upper part of the profile (above depth 15 cm) followed by a decreasing trend for the top three-centimeter sediment samples (Figure A.5b; Table A.1b).

Release of Cu in bottom sediments can be controlled by organic ligands, which are capable of forming highly soluble complexes with Cu (Gerringa, 1990), and could enhance the mobility of Cu throughout the sediment core. This explanation is confirmed with the observation that the distribution of Cu in sediments shows a strong correlation with labile S1-OM, which readily produces organic ligands (Chapter 3.4.1). Furthermore, the dissolution of lime in bottom sediment may partly release Cu from sediment into porewater (Chapter 3.4.1).

A.2.6. Mercury (Hg)

The depth profile of Hg in the WAB1 sediment core shows an increase in concentration with decreasing depth throughout the sediment profile (Figure A.6a). The increasing trend of Hg towards the upper part of the profile begins at the depth of 23 cm, which is significantly lower than the 1956 marker at 15 cm below the SWI (Figure A.6a) (Chapter 3.4.1). This indicates that accumulation of Hg in the WAB1 sediments does not necessarily coincide with the onset of coal-utilization activities in the region. At the depth of 23 cm, Hg content begins to increase steadily towards upper part of the profile until it reaches its maximum concentration (0.10 ppm) at 2 cm, just below the SWI (Figure A.6a). Subsequently, the sediment sample representing SWI (0-1 cm) shows a rapid decline in Hg concentration

(Figure A.6a and Table A.1a). Below the depth of 23 cm, the concentration of Hg remains low, ranging from 0.02 to 0.05 ppm (Figure A.6a and Table A.1a), which is regarded in some literature as the background level.

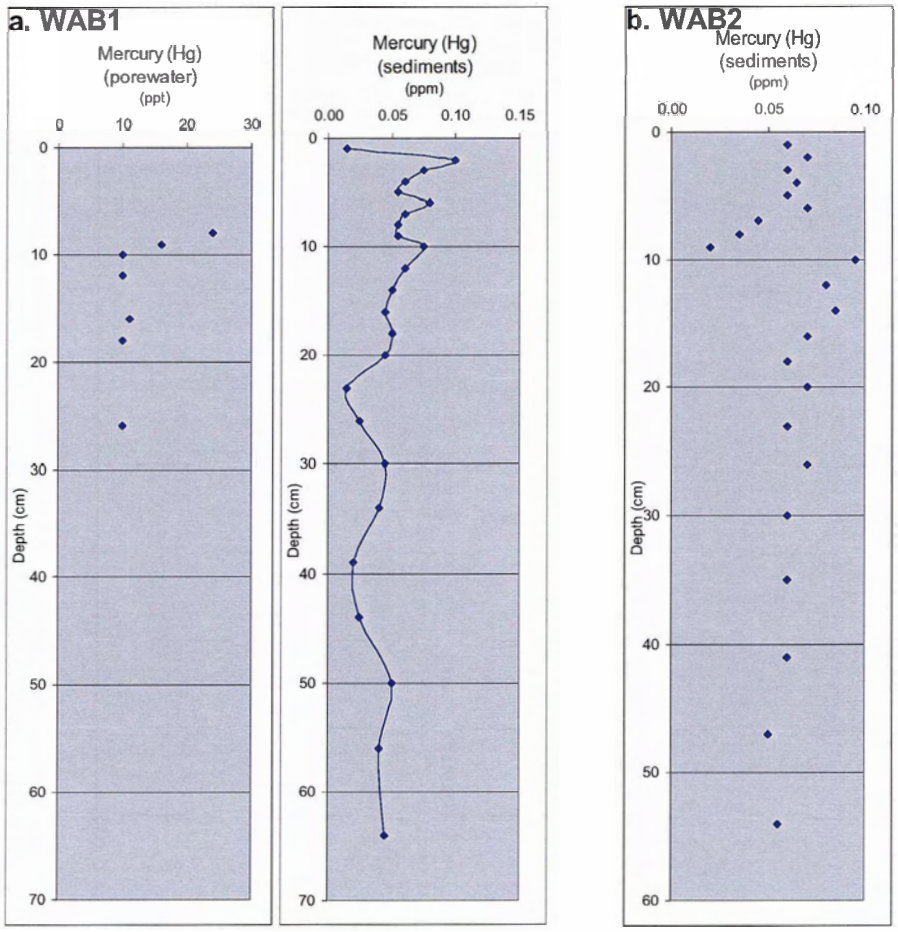

Figure A.6.a-b. The temporal distribution of mercury (Hg) in porewater and sediment profiles from (a) WAB1 core and (b) WAB2 core.

The difference in concentrations of Hg between the younger sediment layer and the older sediment layer is often attributed to anthropogenic impact. This reflects the idea of those researchers who believe that Hg accumulates in lake sediments without major digenetic

remobilization (e.g., Donahue 2002). The temporal distribution of Hg in the Wabamun Lake sediment shows the same pattern has been observed in many published results for cores retrieved from the bottom of natural lakes in the world. These cores are characterized by a sharp exponential-like increase above background concentrations in the upper portion of the profiles (e.g., Johansson 1985, Verta et al, 1990; Rada et al., 1989; Swain et al., 1992; Lockhart et al., 1995; Lucotte et al, 1995; Lucotte et al, 1999).

The increased concentration of Hg in the upper part of Wabamun Lake sediment profiles can partly be attributed to the cumulative effects of the power plant emissions since 1956 (Chapter 3.4.1.1). This may be partly true, as Hg is temporally associated with elements typically enriched in power plant emissions (Zn, As, Pb, and Sb). However, the similarities between the Hg profile and the marked diagenesis indicators such as Ca and OM suggest that various geochemical processes may also control the current temporal distribution of Hg throughout the sediment profile (Chapter 3.4.1.2).

The WAB1 porewater profile shows the detectable amount of Hg (7.5 ppb) is at 27 cm below the SWI, followed by a concentration increase towards the upper part of the profiles (Figure A.6a and Table A.1a). The maximum concentration of 21.5 ppt occurred at a depth of 8 cm (Table A.1a). The release of Hg into the porewater can be attributed to the decomposition of organic matter (Lindqvist, 1991; Dmytriw et al, 1995; EPRI, 1996). The dissolved Hg may migrate upward (due to the concentration gradient), where it can be fixed in the upper section of sediment profile.

The distribution pattern of Hg in WAB2 porewater and sediment profiles is different from those seen in the WAB1 core (Figure A.6b). The depth profile of dissolved Hg in WAB2 is below the detection limit (Table A.1b). The sediments in WAB2 show a steady pattern in regards with Hg concentration throughout the sediment profile. At 9 cm below the SWI, the Hg content declines to its minimum value of 0.02 ppm (Figure A.6b and Table A.1b). The temporal variation of Hg in the WAB2 sediment does not correlate with the emission histories of the coal-fired power plants in the study area (Figure 3.2). The Hg profile in the WAB2 core also appears decoupled from the marked diagenesis indicators such as Fe, Mn, S, Ca, OM (Figure 3.2). We could not find any explanation for the apparent temporal pattern of Hg in the WAB2 sediment cores.

A.2.7. Lead (Pb)

The Pb profile in WAB1 sediments shows very similar variation to the profiles of Sb, As, Zn, U, Hg, Se, Cu, W, Mo, Cr, and V (Figure 3.1). The temporal distribution of theses elements in Wabamun Lake sediment are characterized by low concentrations below 20 cm, followed by an upward increasing trend up to the SWI (Figure 3.1). The maximum concentration of Pb (32 ppm) was recorded 10 cm below the surface (Figure A.7a and Table A.1a). Above this depth, Pb concentration begins to decline towards the SWI (Figure A.7a). A similar trend was observed for the WAB2 sediment core (Figure A.7b). In general, the concentrations of Pb in the Wabamun sediment cores are relatively lower (WAB1: 32 ppm; WAB2: 23 ppm) than the sediment quality guideline (35 ppm; CCME, 1999) (Tables A.1a-b; A.2).

The concentration of dissolved Pb in WAB1 porewater samples was below the detection limit (<0.1 ppb) for all samples (Table A.1a). The porewater data from both WAB1 and WAB2 suggest low dissolution of Pb (Tables A.1a-b). In porewater samples near the SWI, Pb concentrations measured less than, or equal to 0.1 ppb (Table A.1a). This is distinctively lower than the average Pb content of the lake water (0.45 ppb; Golder Associates, 2002).

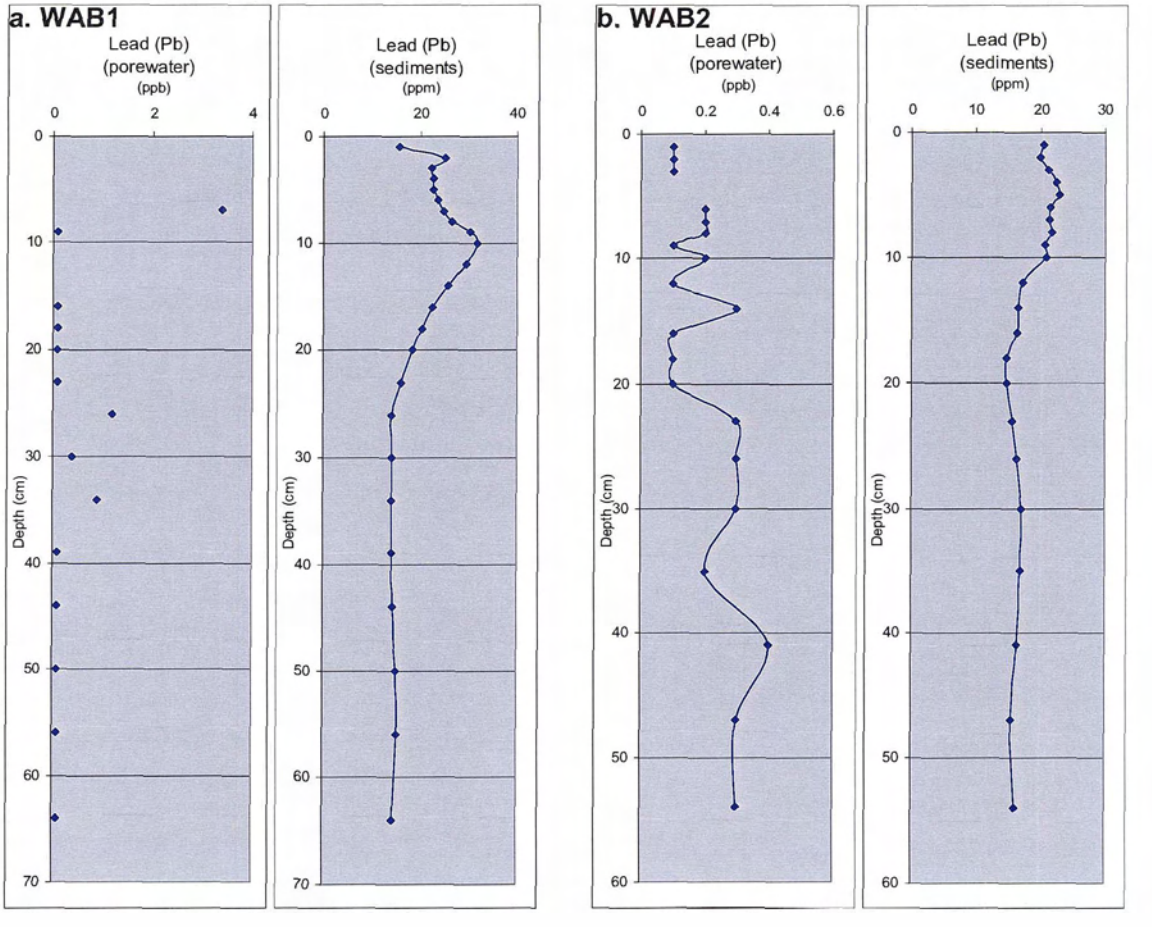

Figure A.7.a-b. The temporal distribution of lead (Pb) in porewater and sediment profiles from (a) WAB1 core and (b) WAB2 core.

The positive correlations between concentrations of Pb with Ca suggests (Tables 3.9; 3.10) that carbonates are substrates for lead in the Wabamun Lake sediment cores (Todorović et al., 2001). Lead found in association with carbonate minerals, precipitated as stable solid compounds and were less likely to be mobilized by resuspension of sediments or biological activity (Todorović et al., 2001). Furthermore, input of Pb into the Wabamun Lakes may be associated with deposition of calcareous flyash, emitting from the power plants located in the Wabamun area (Chapter 3.4.1.1). The Pb profiles in both WAB1 and WAB2 sediments coincide with the emission histories of the power plants in this region (Figure 3.9). Rapid increases in Pb concentration, from the depth of 15 cm to approximately 10 cm, in WAB1 and WAB2 sediment profiles correspond to the commencement of the Wabamun power plant (1956), as detected by ^{210}Pb data. Subsequently, the peaks of Pb concentrations in both sediment cores at the depth of 10.5 cm (Figures 3.1; 3.2) correspond to the peak emission in 1970 by the addition of the Sundance power plant on the Wabamun lakeshore (Chapter 3.4.1.1). This result suggests that the utilization of coal played an important role as an anthropogenic source of Pb in the sediments over the past few decades.

The decrease in Pb content in the uppermost sediments (below SWI, but above 10.5 cm) is unlikely to be the result of post-depositional mobility/migration of elements during early diagenesis processes (Figures A.7a-b). This can be confirmed as the dissolved Pb measured in uppermost WAB1 and WAB2 porewater profiles were both below the detection limit, ruling out the possibility of dissolution/mobilization of Pb below the SWI (Tables A.1a-b). Therefore, the decrease of Pb content in the most recent sediment samples is likely

the result of a decline in the external input of Pb, such as the reduction of emissions from the power plants in the region and/or the global reduction of leaded fuel (Chapter 3.4.1.1).

A.2.8. Zinc (Zn)

The average Zn concentration in the Wabamun Lake sediment cores is lower than the Canadian sediment quality guideline of 123 ppm (CCME 1999) (Tables A.1a-b; A.2). Depth profiles of Zn in WAB1 and WAB2 sediments (Figures 3.1; 3.2) follow the same pattern observed with other trace metals. The occurrence of Zn enrichment above 15 cm was also observed for other anthropogenically-induced elements such as Pb, As, Cu, Sb, Mo, and Se (Figures 3.1; 3.2).

The concentrations of dissolved Zn in porewater profiles from both WAB1 and WAB2 show an increase with increasing depth (Figures A.8a-b and Tables A.1a-b). Despite the relatively high concentrations of Zn in the Wabamun Lake sediment profiles, the Zn content of porewater registers very low amounts of dissolved Zn (Tables A.1a-b). The dissolved Zn in the uppermost porewater samples at both WAB1 and WAB2 is within or below the detection limit of 0.5 ppb (Tables A.1a-b). This is much lower than the average Zn content reported for the lake water (10 ppb; Golder Associates, 2002). The low amounts of dissolved Zn in surficial sediments indicate that the sediments act as a sink rather than as a source of Zn (Tables A.1a-b).

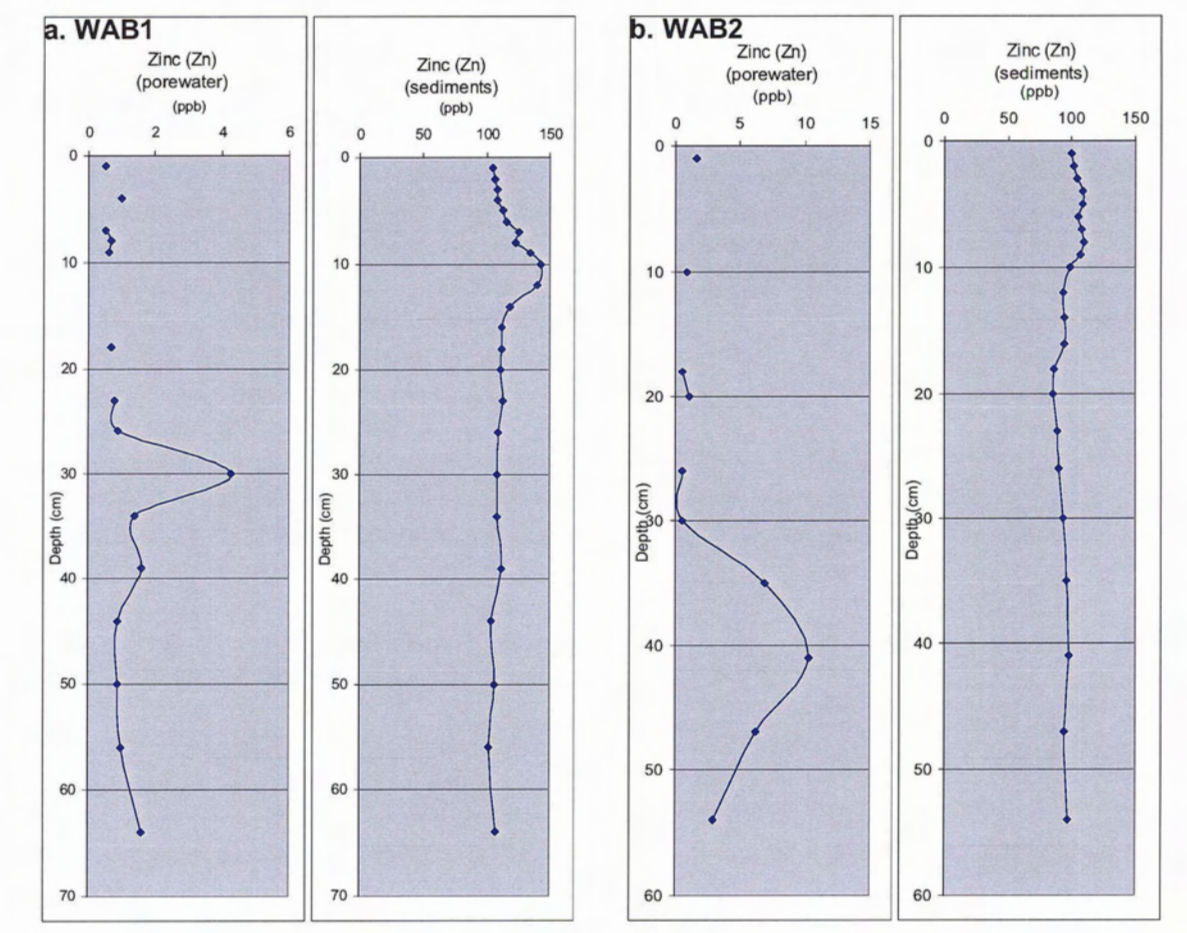

Figure A.8.a-b. The temporal distribution of zinc (Zn) in porewater and sediment profiles from (a) WAB1 core and (b) WAB2 core.

The depth profiles of Zn in Wabamun Lake sediment cores correlate with historical events as related to coal-fired power plants emissions in the study region. The increase in Zn concentration in the upper portion of the WAB1 and WAB2 sediment cores coincides with the 1956 marker representing the commencement of the Wabamun coal-fired power plant on the east shore of the lake. Similarly, the peaks of Zn in both WAB1 and WAB2 sediment cores coincide with the maximum emission period in 1970 by power plants (Figures 3.1; 3.2).

The current temporal pattern of Zn in the sediment profiles may also be explained due to the early diagenesis processes occurring between sediments and porewater. The release of Zn into porewater in the bottom section of the sediment cores may have occurred as a result of the decomposition of labile organic matter (S1) and/or dissolution of Ca (Chapter 3.4.1.1). The dissolved Zn will eventually move upward due to sediment compaction and the concentration gradient. As the Zn moved up in the profile, it would be immobilized by processes such as precipitation of lime or adsorption by freshly deposited organic matter at the upper part of the sediment profile (Chapter 3.4.1.2).

Like other trace metals, the Zn concentration rapidly decreases in the uppermost portion of the sediment cores (Figures A.8a-b and Tables A.1a-b). This is possibly due to the decrease in external input of Zn caused by the more rigorous emission control policy that recently was adopted by the power plants (Chapter 3.4.1.1). Low concentrations of dissolved Zn near the SWI rule out the possibility of dissolution/release of Zn from the upper sediments into the porewater.

APPENDIX B: ORGANIC MATTER DECOMPOSITION DURING EARLY DIAGENESIS

B.1. INTRODUCTION

Current information regarding early diagenesis in sediments is mostly based on the results of studies carried out by Bender et al., (1977); Froelich et al., (1979); Aller, (1980a; b); Berner, (1980); Elderfield et al., (1981); Jahnke et al., (1982); Balzer, (1984); Pettersson and Bostrom, (1986); Westerlund et al., (1986); Jahnke et al., (1989); McCorkle and Klinkhammer, (1990); Shaw et al., (1990); Bruland et al., (1991); Dahmke et al., (1991); Boudreau et al., (1992); and Wu et al., (1992).

Decomposition of organic matter during diagenesis results in a change in distribution of elements in porewater and sediment profiles (Froelich et al., 1979; Berner, 1980; Song and Müller, 1999). The degradation of organic matter is mediated by various aerobic and anerobic bacteria. Organic matter is oxidized by available oxidants with the highest Eh potential. Following the depletion of an oxidant in water, oxidation of organic matter will continue utilizing the next oxidant with the highest Eh potential.

The important processes involving bacterial degradation of organic matter include the following:

B.2. AEROBIC DECOMPOSITION OF ORGANIC MATTER

At the sediment-water interface, organic matter is rapidly oxidized by O_2 due to the activities of aerobic bacteria. The depth of O_2 penetration depends on its downward diffusion

- from the water above and the rate of consumption of O_2 by aerobic decomposition of organic matter. A high input of organic matter in the surface sediment of the studied lakes may be responsible for a rapid depletion of O_2 a few millimeters below the sediment-water interface (Jørgensen 1983).

B.3. ANAEROBIC DECOMPOSITION OF ORGANIC MATTER

Below the surface layer, where the O_2 is completely depleted, the organic matter is subsequently oxidized by anaerobic bacteria. These bacteria utilize alternative oxidants such as Mn oxide, NO_3, Fe oxide, SO_4^{2-} and CO_2 based on availability and Eh potentials.

B.3.1. Manganese oxide reduction and denitrification process

Oxidation of organic matter will utilize MnO_2 and NO_3 oxidants in the deeper suboxic layer. The processes of MnO_2 reduction and denitrification (NO_3 reduction) may occur simultaneously in this suboxic zone, where most of the microbes can tolerate aerobic conditions (Klinkhammer, 1980; Kerner, 1993). In most freshwater sediments, denitrification is not a dominating process because of the low concentration of NO_3 in the water and porewater (Bender and Heggie, 1984; Balzer, 1989).

B.3.2. Iron oxide reduction

Below the zone of MnO_2 reduction and denitrification, oxidation of organic matter continues by obligate anaerobes utilizing iron oxide as an oxidant. The iron oxide reduction process takes place only after the depletion of NO_3 and MnO_2 in the anoxic zone (Lovely and Phillips, 1988) and results in the release of ferrous iron into the porewater just below the SWI.

B.3.3. Sulphate reduction

In anoxic freshwater sediments, SO_4^{2-} reduction and CH_4 fermentation are the predominant processes in the mineralization of organic matter (Aller, 1980a; Billen, 1982; Klump and Martens, 1987; Barbanti et al., 1992).

Anaerobic, sulphate-reducing bacteria rapidly consume the dissolved SO_4^{2-} within the sediments to oxidize the organic matter (Aller, 1980a; Billen, 1982; Klump and Martens, 1987; Barbanti et al., 1992).

$$(CH_2O)_{113}(NH_3)_{15}H_3PO_4 + 56.5\ SO_4^{2-} \rightarrow 113\ HCO_3^- + 15\ NH_3 + H_3PO_4 + 56.5\ HS^- + 56.5H^+$$

B.3.4. Methanogenesis

In freshwater sediments, SO_4^{2-} may be depleted rapidly because of the oxidation of organic matter. As a result, methane fermentation becomes the dominating process (Jorgense, 1983; Mountfort and Asher, 1981; Kuivila et al., 1989; Winfrey and Zeikus, 1977; Capone et al., 1983). The methanogenic bacteria carry out the decomposition of organic matter during the CH4 fermentation process according to the following reaction:

$$(CH_2O)_{113}(NH_3)_{15}(H_3PO_4) \rightarrow 56.5\ CH_4 + 56.5\ CO_2 + 15\ NH_3 + H_3PO_4$$

Although the amount of labile S1-compound rapidly declines through the upper sections of all sediment profiles, there is still sufficient labile organic matter present after SO_4^{2-} depletion to support CH_4 fermentation.

The strong evidence of CH_4 production in Wabamun Lake is evident in the high-resolution seismic data from the bottom of the lake (Sanei et al., in prep). Due to the so-called "Chimney effect", caused by CH_4 emanation from the bottom sediments, a nuisance is created in the seismic data. This "chimney effect" was most evident in the deepest part of the lake where higher organic matter deposits and anaerobic conditions prevail (Sanei et al. in prep).

In this study, the sub-sampling resolution does not allow any distinction to be made between various oxidation zones resulting from bacterial activities.

A significant boundary between the oxic and anoxic zones was not found in any of the sediments. The mixing of the different zones would be caused by a high input of organic matter.

CONCLUDING REMARKS

The province of Alberta, Canada hast vast resources of fossil fuels, most importantly, coal deposits. Coal is being utilized in Alberta to generate electricity. There are a number of coal-fired power plants in the southern region of the province. However, the greatest coal-fired power generating activities are located in an area of central Alberta called Wabamun. The Wabamun area is uniquely located at the focal point of four major power plants producing the bulk portion of energy in the province. Wabamun area is covered by a number of fresh water lakes, which are extensively used for residential, agricultural, and recreational activities. Therefore, the impact of the power plants on these lakes is a major concern and has provoked many discussions and controversies.

The impact of coal-fired power plants occurs through aerial deposition, groundwater, and surface runoff. However, aerial deposition is of primary importance since it has regional impact through the emission of gas and flyash. Fly ash particles are spherical particles of calcium-rich aluminosilicates, which can settle within a proximal distance from the emission source and hence have a great aerial presence.

The objectives of this study were pursued in a two-phase project:

Phase I:

The first Phase aimed to address the regional impact of the coal-fired power plants on nine fresh water lakes in the Wabamun area. For this purpose, a comprehensive sediment isotopic dating was performed to determine the sediments deposited after the onset of coal-fired power plant activities in the region (Chapter 2). Therefore, the spatial distribution of trace elements in the post-coal utilizing era was investigated (Chapter 4). The results of this study indicate that the spatial distribution of Hg and most elements of environmental concern (e.g., Sb, As, Cu, Cd, Pb, Zn) in post-1956 deposited sediments do not show a so-called "bulls-eye" pattern around any of the power plants. The lack of such a pattern in the more recent sections of the lake sediment profiles suggests either an insignificant impact from the power plants in the study area or possible redistribution of elements throughout the sediment columns.

A significant negative correlation was found for elements Ce, Al, W, Hf, Ti, Nb, Ga, and Zr, which typically enrich in the siliceous structure of fly ash. The negative correlation is caused by a decrease in deposition loading of the given element with increasing distance from the power plants. Often this is a good indication of a possible link with emissions from the power plant.

Spatial dispersion patterns of Hg in post-1956 sediments obtained from 8 lakes in the study area do not show any clear relationship to the radial distance from the power plants, indicating the absence of significant influence by power plants in the study area, with respect

to Hg. This obscure relationship indicates that various geochemical processes may form the current spatial distribution of Hg in the sediments. These processes, in conjunction with the natural input of Hg into the sediments, determine the overall temporal and spatial distribution of Hg.

Similarly, the other trace elements such as As, Cd, Cu, Pb, and Zn demonstrate insignificant correlation coefficients to the radial distances from the power plants. This indicates that inputs of these elements in lakes are from mixed sources, both natural and anthropogenic, or their distribution is affected by the post-depositional diagenesis processes.

The SEM/EDX analyses of the sediments indicate that fly ash particles can be found in the post-industrial sediments of Wabamun Lake and Isle Lake. However, our study on the sediment samples of Lac Ste. Anne shows no evidence of fly ash deposition. This may suggest a localized area of influence by the power plants emission.

Phase II:

In the second Phase of this study, the detailed geochemistry (Chapters 3; 6; 7; Appendix A), mineralogy, and petrology (Chapters 5 and 8) of the recent sediments were addressed in three more important lakes (Wabamun Lake, Isle Lake, and Lac. Ste. Anne) in the study region. The detailed sampling of sediment and porewater under inert conditions was an important feature of Phase 1 study, which allowed the study of sediment–porewater interaction.

The results of this study show that the relative enrichment of trace elements (As, Sb, U, V, Cr, Cu, Mo, Pb, Se, Hg, and Zn) in the younger sediment layers of Wabamun Lake can be partly due to the emissions from the coal-fired power plants in the study area (as suggested by isotope dating data). The mineralogy and morphology of the post-industrial sediments (SEM/EDX) from Wabamun Lake is characterized by an abundant presence of spherical particles of fly ash. The size of fly ash particles tend to decrease (PM2.5) towards more recent part of the sediment profile indicating the effect of particle emission control measures adopted by the power plants (e.g., ESP technology), which filters the emission of larger particles. There is no evidence of fly ash particles in the sediments deposited prior to the commencement of coal-fired power plants in Wabamun Lake (before 1956).

Additionally, the study of porewater suggests that diagenetic dissolution/diffusion of some trace elements may have occurred at deeper part of the Wabamun sediment profile, acting as a conveyor of elements to the upper part of the sediment profile. This can also contribute to the elevated concentrations of trace elements near the surface sediments, which are often attributed solely to the activities of power plants in this region.

This study indicates that a combination of various biogeochemical processes may control the temporal distribution of elements and nutrients in sediment and porewater from the lakes in the study area. However, due to the alkalinity and eutrophic conditions of the studied lakes, and in particular Wabamun Lake, the Ca-OM fraction plays the most important role as substrate for trace elements and nutrients (e.g., P). Degradation of organic matter in

the deeper part of the sediment profile may result in the formation of highly soluble metal-organic complexes, which is responsible for the mobilization of trace elements during early diagenesis. The organic decomposition in deeper sediments may also cause dissolution of Ca-compounds and release of trace elements attached to Ca-minerals into the porewater. The dissolved metals may migrate upward in the column and immobilize again due to re-precipitation of calcium minerals in the upper section of the sediment profiles. The SEM/EDX results show the evidence of authigenic deposition of lime in the surficial sediments of especially Wabamun Lake and Lac Ste. Anne. These Ca deposits show an amorphous structure, which can be distinguished from the angular, crystalline calcite derived from geogenic sources. The presence of organic matter deposits in association with Ca (SEM/EDX results) is also strong evidence for the Ca-OM fraction, which is responsible for distribution of trace elements and nutrients (P) in the recent sediment from the study area.

The addition of calcium through aerial deposition of Ca-rich fly ash in the studied lakes, in particular Wabamun Lake, may serve as liming treatment for precipitation of soluble trace metal compounds and dissolved nutrients. The higher input of calcareous fly ash in Wabamun Lake as compared to Isle Lake and Lac Ste. Anne may cause higher scavenging of trace metals in this lake than the other two studied lakes.

The temporal distribution of lithophilic elements in the studied sediments is determined by the degree of dilution by organic matter in the sediment profiles. The variation of lithophilic elements throughout the sediment profiles can also be related to factors such as

fluctuation of detrital material from the watershed and dilution by other inorganic geochemical fractions such as carbonates and redox Fe/Mn.

The distributions of chondrite-normalized REEs in all studied sediment cores show a relative enrichment of LREEs versus HREEs throughout the sediment profiles, very similar to REEs patterns for upper earth crust and soil in Alberta, Canada. In contrast, porewater samples show relative enrichment of HREEs to LREEs.

The relative enrichment of HREEs to LREEs increases towards the upper parts of pore water columns, due to preferential release of HREEs into solution during the diagenesis process. There is more labile organic matter (S1-OM) available in the uppermost part of the sediment profiles, which form more soluble complexes with HREEs. The scavenging effect of carbonate ligands and iron oxides are also known to sequester LREEs preferentially to HREEs, resulting in negative LREEs anomalies in porewater.

In contrast to porewater samples, the sediments show little fractionation of REEs throughout the vertical profiles. This is possibly due to high clastic input of REEs-enriched clay minerals in the sediment that mask the patterns caused by diagenetic processes.

The relationships between temporal distribution of organic matter and concentrations of trace elements indicates that the significant positive correlation between TOC and metals in recent sediments arises mainly from the portion of organic matter related to the thermally labile compounds released during pyrolysis at 300 $^{\circ}$C (S1-OM). The higher molecular,

kerogen-derived hydrocarbons show consistently lesser correlation with trace elements. The strong affinity between temporal distribution of metals and thermally labile compounds is due to both the chemical reactivity and petrological characteristics of these amorphous compounds. They act as a stain by coating the outer part of fine sediment particles and concentrate in the finer sediment size fractions.

The organic petrology of the sediment indicates that the S1-OM compounds are likely derived mainly from multicolored fluorescing, 'bitumen stain-like' amorphous organic matter. The fluid-like nature of the S1-OM compounds provides surface coating for the sediments grains, which accounts for the strong grain surface adsorption of organic matter.

REFERENCES

Alberta Environment (1989), Lake Isle. Envir. Assess. Division, Envir. Qlty. Monit. Br., Edmonton.

AENV (Alberta Environment) (2002), Lake Wabamun water quality and sediment survey. Preliminary report. ISBN No. 0-7785-2297-0 (On-line Edition), Pub. No 1/919.

Albrecht, A., Reiser, R., Luck, A., Stoll, J-M.A., and Giger, W. (1998), Radiocesium dating of sediments from lakes and reservoirs. Environmental Science and Technology. 32, 1882-1887.

Ali, M.A. and Dzombak, D.A. (1996), Interactions of copper, organic acids, and sulfate in goethite suspensions. Geochimica et Cosmochimica Acta. 60(24), 5045-5053

Allan, R.J., Williams, J.D., Josh, S.R. and Warwick, W.F. (1980), Historical changes and relationship to internal loading of sediment phosphorus forms in hypertrophic Prairie lakes. Journal of Environmental Quality. 9, 199-206.

Aller, R.C. (1980a), Diagenetic processes near the sediment-water interface of Long Island Sound. I. Decomposition and nutrient element geochemistry (S, N, P), Advances in Geophysics. 22, 237-350.

Aller, R.C. (1980b), Diagenetic processes near the sediment-water interface of Long Island Sound. II. Fe and Mn. Advances in Geophysics. 22, 350-415.

Anderson, A. (2003), A Survey Of Metals And Trace Organic Compounds In Sediments From Wabamun Lake And Other Alberta Lakes; Environmental Monitoring and Evaluation Branch, Alberta Environment; Pub. No: T/693 ISBN: 0-7785-2501-5 (Printed Edition); p. 123

Andriashek, L.D., Fenton, M.M., and Root, J.D. (1979), Surficial geology, Wabamun Lake, Alberta, NTS 83G. Alberta Research Council, Edmonton.

Appleby, P.G. and Oldfield, F. (1978), The calculation of lead-210 dates assuming a constant rate of supply of unsupported ^{210}Pb to the sediment. Catena 5, 1-8

Appleby, P.G. and Oldfield, F. (1983), The assessment of ^{210}Pb data from sites with varying sediment accumulation rates. Hydrobiologia. 103, 29-35

Appleby, P.G., Nolan, P.J., Oldfield, F., Richardson, N., and Higgitt, S.R. (1988), ^{210}Pb dating of lake sediments and ombrotrophic peats by gamma essay. The Science of the Total Environment. 69, 157-177.

Åström, M. (2001), Abundance and fractionation patterns of rare earth elements in streams affected by acid sulphate soils. Chemical Geology, 175, 249-258.

Babin, J., Prepas, E.E., Murphy, T.P., Serediak, M., Curtis, P.J., Zhang, Y. and Chambers, P.A. (1994), Application of lime on sediment phosphorus release in hardwater lakes: the case of hypereutrophic Halfmoon Lake, Alberta. Lake and Reservoir Management. 8, 131-142.

Bau, M. (1996), Controls on the fractionation of isovalent trace elements in magmatic and aqueous systems: Evidence from Y/Ho, Zr/Hf, and lanthanide tetrad effect. Contrib. Mineral. Petrol. 123, 323-333.

Bau, M. (1999), Scavenging of dissolved yttrium and rare earths by precipitating iron oxyhydroxide: Experimental evidence of Ce oxidation, Y-Ho fractionation and lanthanide tetrad effect. Geochimica et Cosmochimica Acta, 63: 67-77.

Bau, M. and Dulski, P. (1999), Comparing yttrium and rare earths in hydrothermal fluids from the Mid-Atlantic Ridge: Implications for Y and REE behaviour during near-vent mixing and for the Y/Ho ratio of Proterozoic seawater. Chemical Geology, 155, 77-79.

Balzer, W. (1984), Organic matter degradation and biogenic element cycling in a nearshore sediment (Kiel Bight), Limnology and Oceanography, 29(6), 1231-1246.

Balzer, W. (1989), Chemische Reaktionen and Transportprozesse in oberfldchennahen Sedimenten borealer and polarer Meeresgebiete. Habilitationsschrift, Universitat Kiel. 312 S.

Barbanti, A., Ceccherelli, V.C., Frascari, F., Reggiani, G., and Rosso, G. (1992), Nutrient regeneration process in bottom sediments in a Po delta lagoon (Italy) and the role of bioturbation in determining the fluxes at the sediment-water interface. Hydrobiologia. 228, l-21.

Balistrieri, L.S., Murray, J.W., and Paul, B. (1992), The biogeochemical cycling of trace metals in the water column of Lake Sammamish, Washington: Response to seasonally anoxic conditions. Limnology and Oceanography, 37(3), 529-548.

Beak Consultants Ltd. (1980), The effect of thermal discharges on the aquatic plants and other biota of Wabamun Lake, Alberta. Prep. for Calg. Power Ltd., Calgary.

Bender, M.L., Fanning, K.A., Froelich, P.N., and Maynard, V. (1977), Interstitial nitrate profiles and oxidation of sedimentary organic matter in the Eastern Equatorial Atlantic. Science. 198, 605-609.

Bender, M.L. and Heggie, D.T. (1984), Fate of organic carbon reaching the deep sea floor: a status report. Geochemica et Cosmochimica Acta, 48, 977-986.

Berner, R.A. (1980), Early diagenesis. Princeton University Press, Princeton, N.J. 241 S.

Billen, G. (1982), Modelling the processes of organic matter degradation and nutrients recycling in sedimentary systems. in Sediment Microbiology. edited by Nedwell, D.B. and Brown, C.M. Academia Press, London.

Boudreau, B.P., Canfield, D.E., and Mucci, A. (1992), Early diagenesis in a marine sapropel, Mangrove Lake, Bermuda. Limnology and Oceanography, 37(8), 1738-1753.

Boulegue, J., Lord III. C.J., and Church, T.M. (1982), Sulfur speciation and associated trace metals (Fe, Cu) in the pore waters of Great Marsh, Delaware. Geochemica et Cosmochimica Acta, 46, 453-464.

Böers, P., Van der Does, J., Quaak, M. and Van der Vlugt, J. (1994), Phosphorus oxation with iron III chloride: a new method to combat internal phosphorus loading in shallow lakes, Archiv für Hydrobiologie, 129, 339-351.

Boström, B., Jansson, M. and Forsberg, C. (1982), Phosphorus release from sediments. Archiv für Hydrobiologie Supplement, 18, 5-59.

Boudreau, B.P. (1994), Is burial velocity a master parameter for bioturbation? Geochimica et Cosmochimica Acta. 58(4), 1243-1249.

Bruland, K.W., Donat, J.R., and Hutchins, D.A. (1991), Interactive influences of bioactive trace metals on biological production in oceanic waters. Limnology and Oceanography. 36(8),1555-1577.

Brunskill, G.J. (1969), Fayetteville Green Lake, New York. II. Precipitation and sedimentation of calcite in a meromictic lake with laminated sediments. Liminology and Oceanagraphy, 14: 830-847

Brunskill, J. G. and Wilkinson, P. (1987), Annual supply of U238, U234, Th230, Ra226, Pb210, Po210 and Th232 to lake 239 (ELA, Ontario) from terrestrial and atmospheric sources. Canadian Journal of Fisheries and Aquatic Sciences. 44, 215-230.

Buckland-Nicks, L. H. and Mitchell, P. A. (1990), Isle Lake. In Atlas of Alberta Lakes, edited by P. Mitchell and E. Prepas, pp. 394-400. University of Alberta Press, Edmonton, Alberta, Canada. AEU SCI GB 1630 A3 A8813 Information on current limnological conditions. Includes a bathymetric map.

Calmano, W., Hong J., and Förstner U. (1992), Influence of pH value and redox potential on binding and mobilization of heavy metals in contaminated sediments. Vom Wasser. 78, 245-257.

Capone, D.G., Reese, D.D., and Kiene, R.P. (1983), Effects of metals on methanogenesis, sulfate reduction, carbon dioxide evolution, and microbial biomass in anoxic salt marsh sediments. Appli. Environ. Microbiol. 45, 1586-1591.

Carignan, R and Nriagu, J.O. (1985), Trace metal deposition and mobility in the sediments of two lakes near Sudbury, Ontario. Geochemica et Cosmochimica Acta, 49, 1753-1764.

Carignan, R. and Lean, D.R.S. (1991), Regeneration of dissolved substances in a seasonally anoxic lake, The relative importance of processes occurring in the water column and in the sediments. Limnology and Oceanography, 36(43), 683-707.

CCME (Canadian Council of Ministers of the Environment). (1999), (with updates to 2001), Canadian Environmental Quality Guidelines. Winnipeg, MB.

Chin, Y. and Gschwend, P.M. (1991), The abundance, distribution, and configuration of porewater organic colloids in recent sediments. Geochemica et Cosmochimica Acta, 55, 1309-1317.

Cowan, C.E., Zachara, J.M., and Resch, C.T. (1991), Cadmium adsorption on iron oxides in the presence of alkaline-earth elements. Environmental Science & Technology, 25, 437-446.

Connan J., (1987), Regards sur la géochimie organique pétrolière d'augourd, Bull. Centre Rech. Explor.-Prod. Elf Aquitaine, 11(2), 181-219.

Cooke, G.D., Welch, E.B., Peterson, S.A., and Newroth, P.R. (1993), Restoration and Management of Lakes and Reservoirs, 2nd edn. Lewis Publishers, Boca Raton, FL, USA.

Cooke, G.D. (1993), Phosphorus inactivation and sediment oxidation. In: Restoration and Management of Lakes and Reservoirs, 2nd edn (Eds) G.D. Cooke E.B. Welch S.A.

Comans, R.N.J., Middleburg, J.J., Zonderhuis, J., Woittiez, J.R.W., De Lange, G.J., Das, H.A., and Van Der Weijden, C.H. (1989), Mobilization of radiocaesium in pore water of lake sediments. Nature, 339: 367-369.

Comans, R.N.J., Haller, M., and De Preter, P. (1991), Sorption of cesium on illite: Non-equilibrium behavior and reversibility. Geochimica et Cosmochimica, Acta, 55: 433-440.

Crosby, J. (1994), Pigeon Lake - A glimpse beneath the surface, Managing Western Canadian Lakes: demands, issues and solutions, In Proceedings of the Third Annual ALMS Conference, Edmonton, AB: Alberta Environmental Protection. 3, 19-22.

Dahmke, A., Schulz H.D., Kolling A., Kracht F., and Lucke A. (1991), Schwermetallspuren and geochemische Gleichgewichte zwischen Porenlosung and Sediment im Wesermundungsgebiet. Berichte, Fachbereich Geowissenschaften, Universitat Bremen, Nr. 12.

Danen-Louwerse, H.J., Lijklema, L., and Coenraats, M. (1995), Coprecipitation of phosphate with calcium carbonate in Lake Veluwe. Water Research, 29, 1781-1785.

Davis, J.A. (1984), Complexation of trace metals by adsorbed natural organic matter, Geochimica et Cosmochimica Acta, 48, 679-692.

Dean, W.E. and Gorham, E. (1976), Major chemical and mineral components of profundal surface sediments in Minnesota lakes, Liminology and Oceanography, 21(2), 259-284

Dean, W.E., and Schwalb, A. (2002), The lacustrine carbon cycle as illuminated by the waters and sediments of two hydrologically distinct headwater lakes in north-central Minnesota, USA. Journal of Sedimentary Research, 72, 416-431.

Dellapenna, T.M., Kuehl, S.A., and Schaffner, L.C. (1998), Sea-bed mixing and particle residence timesin biologically and physically dominated estuarine systems: a comparison of LowerChesapeake Bay and the York River subestuary. Est. Coast. Shelf Sci., 46, 777-795.

de Carlo E.H., Wen X.Y., and Irving M. (1998), The influence of redox reactions on the uptake of dissolved Ce by suspended Fe and Mn redox particles. Aquatic Geochemistry, 3, 357-389.

Dillon, P.J. and Rigler, F.H. (1974), The phosphorus-chlorophyll relationship in lakes. Limnology and Oceanography, 19, 767-773.

Di-Giovanni, C., Disnar, J.R., Bichet, V., Campy, M., and Guillet, B. (1998), Geochemical characterization of soil organic matter and variability of a postglacial detrital organic supply (Chaillexon Lake, France), Earth Surface Processes and Landforms, 23, 1057-1069.

Disnar, J.R., Guillet, B., Keravis, D., Di-Giovanni, C., and Sebag, D. (2003), Soil organic matter (SOM) characterization by Rock-Eval pyrolysis: scope and limitations, Organic Geochemistry, 34, 327-343.

Dmytriw, R., Mucci, A., Lucotte, M. and Pichet, P. (1995), The partitioning of mercury in the solidcomponents of dry and flooded forest soils and sediments from a hydroelectric reservoir, Quebec (Canada), Water, Air and Soil Pollution. 1099-1103

Donahue, W.F. (2002), An assessment of impacts of regional coal-burning power plants on metals accumulated in Lake Wabamun. Prepared for the Lake Wabamun Enhancement and Protection Association.

Douglas, G.S., Mills, G.L., and Quinn, J.G. (1986), Organic copper and chromium complexes in the interstitial waters of Narragansett Bay sediments. Marine Chemistry. 19, 161-174.

Driscoll, C.T., Effler, S.W., Auer, M.T., Doerr, S.M., and Penn, M.R. (1993), Supply of phosphorus to the water column of a productive hardwater lake: controlling mechanisms and management considerations. Hydrobiology, 253, 61-72.

Dukat, D.A. and Kuehl, S.A. (1995), Non-steady-state ^{210}Pb flux and the use of $^{228}Ra/^{226}Ra$ as a geochronometer on the Amazon continental shelf. Marine Geology, 125, 329–350.

Eck, G.T.M. van, and Smits, J.G.C. (1986), Calculation of nutrient fluxes across the sediment-water interface in shallow lakes. in Sediments and Water Interactions. edited by Sly, P.G. Springer-Verlag.

Edmonton Regional Planning Commission. (1983), Lake Isle management study. Edm. Reg. Plan. Commis., Edmonton.

El Bilali L., Rasmussen, P.E., Hall, G.E.M., and Fortin, D. (2002), Role of sediment composition in trace metal distribution in lake sediments. Applied Geochemistry, 17, 1171-1181.

Elderfield, H. and Hepworth, A. (1975), Diagenesis, Metal and Pollution in Estuaries.Marine Pollution Bulletin 6, 85-87

Elderfield H., Upstill-Goddard R., and Sholkovitz E.R. (1990), The rare earth elements in rivers, estuaries and coastal seas and their significance to the composition of ocean waters. Geochimica et Cosmochimica Acta, 54, 971-991.

Elderfield, H. (1981), Metal-organic associations in interstitial waters of Narragansett Bay sediments. American Journal of Science. 281, 1184-1196.

Emerson, S. (1976), Early diagenesis in anaerobic lake sediments: chemical equilibria in interstitial waters. Geochimica et Coschimica Acta. 40, 925-934.

Environment Canada. (1982), Canadian climate normals, Vol. 7: Bright sunshine (1951-1980), Prep. by Atm. Envir. Serv. Supply Serv. Can., Ottawa.

EPA (1996), Method 1631: Mercury in Water by Oxidation Purge and Trap and Cold Vapor Atomic Fluorescence Spectrometry, EPA number: 821R96012, p. 39

EPRI (1996), Mercury in the Environment – A Research Update, Final Report, Electric Power Research Institute, Palo Alto, CA, USA.

Evans, R. D., and Rigler, F.H. (1983), A test of lead-210 dating for measurement of whole lake soft sediment accumulation, Canadian Journal of Fisheries and Aquatic Sciences, 40, 506-515.

Farmer, J. G. and Lovell, M. A. (1986), Natural enrichment of arsenic in Loch Lomond sediments. Geochimica et Cosmochimica Acta, 50, 2059–2067.

Farmer, J.G. (1991), The perturbation of historical pollution records in aquatic systems: Environmental Geochemistry and Health, 13(2), 76-83.

Forstner, U. and Wittmann, G.T.W. (1979), Metal Pollution in the Aquatic Environment. Springer. Berlin, p. 367.

Francis, A.J. and Dodge, C.J. (1990), Anaerobic microbial remobilization of toxic metals coprecipitated with iron oxide. Environ. Sci. Technol, 24(3), 373-378.

Francis, C. W. and Brinkley, F. S. (1976), Preferential adsorption of ^{137}Cs to micaceous minerals in contaminated fresh water sediment. Nature, 260, 511-513

Froelich, F.N., Klinkhammer, G.P., Bender, M.L., Luedtke, N.A., Heath, G.R., Cullen, D., Dauphin, P., Hammond, D., Hartman, B., and Maynard, V. (1979), Early oxidation of organic matter in pelagic sediments of the eastern equatorial Atlantic: suboxic diagenesis. Geochemica et Cosmochimica Acta, 43, 1075-1090.

Gallup, D. N. and Hickman, M. (1973), Temperature and oxygen distribution in the mixing zone of a thermal discharge to Lake Wabamun, Alberta. Proceedings of a Symposium of Lakes in Western Canada, Water Resources Centre, University of Alberta, Edmonton, 285-303.

Gambrell, R.P., Wiesepape, J.B., Patrick, W.H., and Duff, M.C. (1991), The effects of pH, and salinity on metal release from a contaminated sediment. Water, Air, and Soil Pollution, 359-367.

Garrett, R.G. and Hornbrook, E.H.W. (1976), Relationship between zinc and organic content in center lake bottom sediments, Journal of Geochemical Exploration, 5(1), 31-38.

Gendron, A., Silverberg, N., Sundby, B., and Lebel, J. (1986), Early diagenesis of cadmium and cobalt in sediments of the Laurentian Trough. Geochemica et Cosmochimica Acta, 50, 741-747.

Gerringa, L.J.A. (1990), Aerobic degradation of organic matter and the mobility of Cu, Cd, Ni, Pb, Zn, Fe, and Mn in marine sediment slurries. Marine Chemistry, 29, 355-374

Gibbs, R. J. (1973), Mechanisms of trace metal transport in rivers. Science, 181, 71-73.

Gobeil, C., Silverberg, N., Sundby, B., and Cossa, D. (1987), Cadmium diagenesis in Laurentian Trough sediments. Geochemica et Cosmochimica Acta, 51, 589-596.

Goldberg, E.D. (1963), Geochronology with 210Pb. Radioactive Dating. Int. Atom. Energy Ag., Vienna, 121-131.

Golder Associates (2002), Water and sediment quality in Wabamun Lake and surrounding lakes, summer 2002; Report 022-7016; p.22

Golterman, H.L. (1977), Sediments as a source of phosphate for algal growth. In: Interactions Between Sediments and Freshwater; Amsterdam (September) 6-10, 1976 (Ed. H.L. Golterman), Dr W. Junk B.V., The Hague, pp. 286-293.

Goodarzi, F. (1996), Chemical characterization of milled-coal, ashes and stack emitted materials from the Genesee station, report, Geological Survey of Canada, Project 950001-07

Goodarzi, F. (2004), Speciation and mass-balance of mercury from pulverized coal fired power plants burning western Canadian subbituminous coals. Journal of Environmental Monitoring, 6, 792-798.

Goodarzi, F., Sanei, H. and Duncan, W.F. (2003), Deposition of trace elements in the Trail region, British Columbia; an assessment of the environmental effect of a base metal smelter on land. Geological Survey of Canada Bulletin 573, pp. 50.

Goodarzi, F., Sanei, H., and Garrett, R.G. (Submitted a), Deposition of metals around the Sheerness coal-fired generating station, Alberta, Canada, Journal of Environmental Monitoring.

Goodarzi, F., Sanei, H., and Garrett, R.G. (Submitted b), Distribution of trace elements in soil in the vicinity of Sheerness coal-fired power plant in Alberta, Canada, Journal of Environmental Monitoring.

Goodarzi, F., and Sanei, H. (Submitted c), Rare earth elements as tracers for the source of aerially deposited particles around a coal-fired power plant, Journal of Environmental Monitoring.

Goodarzi, F., Davies, G.R., Nassichuk, W.W., and Snowdon, L.R. (1987), Exsudatinite in carboniferous oil shales from Arctic Canada, Fuel, 66, 771-773.

Habgood, H. (1983), Lake Wabamun literature review. Prep. for L. Wabamun Watershed Advisory Committee, Edmonton.

Håkanson, L. and Jansson, M. (1983), Principles of lake sedimentology. Berlin: Springer-Verlag, p.316

Hall R.I., Leavitt, P.R., Quinlan, R., Dixit, A.S. and Smol, J.P. (1999), Effects of agriculture, urbanization, and climate on water quality in the northern Great Plains. Limnology and Oceanography, 44, 739-756.

Hall, G.E.M., Vaive, J.E., McConnell, J.W. (1995), Development and application of a sensitive and rapid analytical method to determine the rare earth elements in surface waters. Chemical Geology, 120, 91-109.

Hall, G.E.M. (1998), Cost-effective protocols for the collection, filteration and preservation of surface waters for detection of metals and metalloids at ppb and ppt levels, Phase I:

Evaluation of bottle type, bottle cleaning, filter and preservation technique. Prepared for Aquatic Effects Technology Evaluation Program (Task Force on Water Quality Issues), Geological Survey of Canada, Ottawa, Canada

Hall, G.E.M., Pelchat, J.C., Pelchat, P., and Vaive, E. (2002), Sample collection, filteration and preservation protocols for the determination of 'total dissolved' mercury in water. Analyst, 127, 674-680.

Hamilton, H. and T.B. Reynoldon. (1981), Lake Wabamun eutrophication study: Interim report on 1980 lake sediment studies. Alberta Envir., Poll. Contr. Division, Water Qlty. Contr. Br. Unpubl. rep., Edmonton.

Hamilton-Taylor, J. Millis, M., and Reynolds, C.S. (1984), Depositional fluxes of metals and phytoplankton in Windermere as measured by sediment traps. Limnology and Oceanography, 29 (4), 695-710.

Health and Safety Laboratory (1972), Health and Safety Laboratory Fallout Program.HASL-258, A-40-41, A-93-94, New York.

Henderson, P. (1984), General Geochemical Properties and Abundances of the Rare Earth Elements. In Rare Earth Geochemistry, P Henderson (ed.), Developments in Geochemistry 2, Elsevier, New York, New York, pp. 1-32.

Hirner, A., Kritsotakis, K., and Tobschall, H. (1990), Metal-organic associations in sediments - I, comparison of unpolluted recent and ancient sediments and sediments affected by anthropogenic pollution: Applied Geochemistry, 5, 491-506.

Holdren, G.C. and Armstrong, D.E. (1986), Interstitial ion concentrations as an indicator of phosphorus release and mineral formation in lake sediments. In: Sediments and Water Interactions, edited by Sly, P.G. Springer-Verlag.

Horowitz, A. (1990), The role of sediment-trace element chemistry in water-quality monitoring and the need for standard analytical methods, in, Hall, J., and Glysson, D., eds., Monitoring water in the 1990's: meeting new challenges, ASTM STP 1102, Philadelphia, American Society for Testing and Materials.

Horowitz, A. J. (1991), A primer on sediment-trace element chemistry, Lewis Publishers, Inc., USA, p. 136

Huc, A.Y. (1988), Sedimentology of organic matter, in: Frimmel, F.H. and Christman, R.F. (Eds.), Humic Substances and their relative role in the environment, Wiley, 215-243.

HydroQual Laboratories Ltd. (2003), Toxicity Assessment of Wabamun Lake Sediments, Prepared for: Alberta Environment, Pub. No: T/717; ISBN: 0-7785-3040-x (Printed Edition); p. 36

Ingri, J., Widerlund, A., Land, M., Gustafsson, Ö., Andersson, P., and Öhlander, B. (2000), Temporal variations in the fractionation of the rare earth elements in a boreal river; the role of colloidal particles. Chemical Geology, 166, 23-45.

Ishiwatari, R. (1985), Geochemistry of humic substances, 147-180. In: D. M. McKnight (Ed.), Humic Substances in Soil, Sediment, and Water: Geochemistry, Isolation, and Characterization, New York: John Wiley & Sons.

Ishikawa, M. and Ichikuni, M. (1981), Coprecipitation of phosphate with calcite. Geochemical Journal, 15, 283-288.

Ivert, S. (1990), Bestimmung der Porenwasserzusammensetzung mit Hilfe der Dialysetechnik and fruhdiagenetische Prozesse in Sedimenten der Eckemforder Bucht (Hausgarten), Diplomarbeit an der Christian-Albrechts-Universitat zu Kiel.

Jahnke, R.A., Emerson, S.R., and Murray, J.W. (1982), A model of oxygen reduction, denitrification, and organic matter mineralization in marine sediments. Limnology and Oceanography, 27(4), 610-623.

Jahnke, R.A., Emerson, S.R., Reimers, C.E., Schuffert, J., Ruttenberg, J., and Archer, D. (1989), Benthic recycling of biogenic debris in the eastern tropical Atlantic Ocean. Geochemica et Cosmochimica Acta, 53, 2947-2960.

Johansson, K. (1985), Mercury in sediment in Swedish forest lakes, Internationale Vereinigung für Theoretische und Angewandte Limnologie, Verhandlungen, 22, 2359-2363

Johannesson, K.H., Zhou, X., Guo, C., Stetzenbach, K.J., Hodge, V.F. (2000), Origin of rare earth element signatures in groundwaters of circumneutral from southern Nevada and eastern California. Chemical Geology, 164, 239-257.

Johnson, C.A., Sigg, L., and Lindauer, U. (1992), The chromium cycle in a seasonally anoxic lake. Limnology and Oceanography, 37(2), 315-321.

.Johnson-Prytle, A., Scott, M.R., Laing, T.E., and Smol, J.P. (2000), ^{137}Cs distribution and geochemistry of Lena River (Siberia) drainage basin lake sediments. The Science of the Total Environment, 255, 145-159.

Jonasson, I. (1977), Geochemistry of sediment/water interactions of metals, including observations on availability, in Shear, H., and Watson, A., eds., The fluvial transport of sediment-associated nutrients and contaminants, IJC/PLUARG, Windsor, Ontario, p. 255-271

Jørgensen, B.B. (1983), Processes at the sediment-water interface. in The Major Biogeochemical Cycles and their Interactions, edited by Bolin, B and Cook, R.B. John Wiley & Sons.

Jørgensen, B.B. and Sorensen, J. (1985), Seasonal cacles of O2, NO_3^- and SO_4^{2-} reduction in estuarine sediments: the significance of an N03- reduction maximum in spring. Mar. Ecol. Prog. Ser., 24, 65-74.

Kamp-Nielsen, L. (1974), Mud–water exchange of phosphate and other ions in undisturbed sediment cores and factors affecting the exchange rates. Arch. Hydrobiol., 73, 218–237.

Keil, R.G., Montlucon, D.B., Prahl, F.G., and Hedges, J. (1994), Sorptive preservation of labile organic matter in marine sediments. Nature, 370, 549-552.

Kerndorff, H. and Schnitzer, M. (1980), Sorption of metals on humic acid. Geochimica et Cosmochimica Acta, 44, 1701-1708.

Kerner, M. (1993), Coupling of microbial fermentation and respiration processes in an intertidal mudflat of the ELBE estuary, Liminology and Oceanography, 38, 314-330.

Kersten, M., Förstner, U., Calmano. W., and Ahlf, W. (1985), Release of metals during oxidation of sludges - Environmental chemical aspects of dredged material disposal. Vom Wasser. 65, 21-35.

Burley, K. L., Prepas, E. E., and Chambers, P. A. (2001), Phosphorus release from sediments in hardwater eutrophic lakes: the effects of redox-sensitive and -insensitive chemical treatments. Freshwater Biology, 46(8), 1061-1074

Klinkhammer, G. P. (1980), Early diagenesis in sediments fromthe eastern equatorial Pacific. 2. Trace metal results. EarthPlanet. Sci. Lett., 49, 81–101.

Klump, J.V. and Martens, C.S. (1987), Biogeochemical cycling in an organic-rich coastal marine basin. 5. Sedimentary nitrogen and phosphorus budgets based upon kinetic models, mass balances, and the stoichiometry of nutrient regeneration. Geochimica et Cosmochimica Acta, 51, 1161-1173.

Koschel, R.H. (1997), Structure and function of pelagic calcite precipitation in lake ecosystems. Verhandlungen der Internationalen Vereinigung für Theoretische und Angewandte Limnologie, 26, 343-349.

Koschel, R., Benndorf, G., Proft, G. and Rechnagel, F. (1983), Calcite precipitation as a natural control mechanism of eutrophication. Archiv für Hydrobiologie, 98, 380-408.

Krezoski, J. R., and Robbins, J.A. (1985), Vertical distribution of feeding and particle selective transport of 137Cs in lake sediments by lumbriculid oligochaetes. Journal of Geophysical Research, 90, 11999-12006.

Krom, M.D. and Berner, R.A. (1981), The diagenesis of phosphorus in a nearshore marine sediment. Geochemica et Cosmochimica Acta, 45, 207-216.

Kuivila, K.M., Murray, J.W., and Devol, A.H. (1989), Methane production, sulfate reduction and competition for substrates in the sediments of Lake Washington. Geochemica et Cosmochimica Acta, 53, 409-416.

Labonté, M. and Goodarzi, F. (1985), Application of statistical analyses (dendograph and correspondence analysis) in the geological sciences, Fuel, 64, 1177.

Lafargue, E., Espitalité, J., Marquis, F., and Pillot, D. (1998), Rock-Eval 6 applications in hydrocarbon exploration, production and soil contamination studies. Revue de L'institut Francais du Petrole, 53(4), 421-437.

Land, M., Öhlander, B., Ingri, J., and Thunberg, J. (1999), Solid speciation and fractionation of rare earth elements in a spodosol profile from northern Sweden as revealed by sequential extraction. Chemical Geology, 160, 121-138.

Lee, B. and Fisher, N.S. (1992), Degradation and elemental release rates from phytoplankton debris and their geochemical implications. Limnology and Oceanography, 37(7), 1345-1360.

Liebezeit, G. and Wiesner, M.G. (1990), Pyrolysis of recent marine sediments-I. Biopolymers, Org. Geochem., 16(4-6), 1179-1185.

Lijklema, L. (1976), The role of iron in the exchange of phosphate between water and sediments. In: Interactions between sediments and freshwater; Amsterdam, September 6-10, 1976 (Ed. H.L. Golterman), Dr. W. Junk B.V., The Hague, pp. 313-317.

Lindqvist, O. (1991), Mercury in the Swedish environment. Water Air Soil Pollut. 55, 23–32.

Lomenick, T.R. and Tamura, T. (1965), Naturally occurring fixation of cesium-137 on sediments of lacustrine origin. Soil Science Society of America Proceedings, 29, 383-386.

Lockhart, L. B. Jr., Patterson, R. L. Jr., and Saunders, A. W. (1965), The size distribution of radioactive atmospheric aerosols. Journal of Geophysical Research, 70, 6033-6041.

Lockhart, W.L., Wilkinson, B.N., Billeck, B.N., Hunt, R.V., Wagemannn, R., and Brunskill, G.J. (1995), Current and historical inputs of mercury to high-latitude lakes in Canada and to Hudson Bay, Water, Air, and Soil Pollution, 80, 539-551.

Longmore, M.E. (1982), Cesium-137 dating technique and associated applications in Australia- a review. In W. Ambrose and P. Euerden (Eds.) Archaeometry: An Australian Persepective. ANU Press, Canberra, Australia, pp. 310-321.

Longmore, M.E., O'Leary, B.M., and Rose, C.W. (1983), Cesium-137 profiles in the sediment of a partial-meromictic lake on Great Sandy Island, Queensland, Australia. Hydrobiologia, 103, 21-27.

Lovely, D.R. and Phillips, E.J.P. (1988), Manganese inhibitation of microbial iron reduction in anaerobic sediments. Geomicrobiology Journal . 6, 145-155.

Lucotte, M., Mucci, A., Hillaire-Marcel, C., Pichet, P., and Grondin, A. (1995), Anthropogenicmercury enrichment in remote lakes of northern Quebec (Canada), Water Air Soil Pollution, 80, 467-476.

Lucotte, M., Montgomery, S., Caron, B., and Kainz, M. (1999), Chapter 3: Mercury in natural lakes and unper-turbed terrestrial ecosystems of Northern Quebec. InMercury in the Biogeochemical Cycle, eds. M. Lucotte, R. Schetagne, N. Therien, C. Langlois, and A. Tremblay, Berlin, Springer-Verlag, pp. 55–87.

Lyth, M., Håkansson, K., and Sjöblom, Å. (2003), Effects of calcium on sorption and flocculation of trace metals in leachate from mine waste deposits, Sudbury, Canada, Mining and the Environment Conference III, 25th-28th May 2003 at Laurentian University in Sudbury, Ontario

Mackowsky, M.Th. (1982), Preparation of polished surfaces from Particulate samples. In: R. Stach, M.Th. Mackowsky, M.Teichmüller, G.H.Taylor, D.Chandra, and R. Teichmüller (Eds). Stach Textbook of Coal Petrology, Geberüder Borntrager, Berlin-Stuttgart. 4, 308-311.

Macyk, T.M., and Veauvy, C.F. (1977), Detailed soil survey of the Lac Ste. Anne area. Alberta Inst. Pedol. Rep. No. M-77-9. Alberta Research Council, Edmonton.

Manning P.G., Prepas, E.E. and Serediak, M.S. (1999), Pyrite and vivianite intervals in the bottom sediments of eutrophic Baptiste Lake, Alberta. Canadian Mineralogist, 37, 593-601.

Marinsky, J.A., Mathutu, A., Ephraim, J.H., and Reddy, M.M. (1999), Calcium ion binding to soil fulvic acid using a Donnan potential model. Radiochim. Acta, 84, 205 – 211.

Matisoff, G., Fisher, J.B., and McCall, P.L. (1981), Kinetics of nutrient and metal release from decomposing lake sediments. Geochemica et Cosmochimica Acta, 45, 2333-2347.

Matsuda, H., and Koyama, T. (1977a), Early diagenesis of fatty acids in lacustrine sediments-I, Identification and distribution of fatty acids in recent sediment from a fresh water lake. Geochimica et Cosmochimica Acta, 41, 777-783.

Matsuda, H. and Koyama, T. (1977b), Early diagenesis of fatty acids in lacustrine sediments-II, A statistical approach to changes in fatty acid composition from recent sediments and source materials. Geochimica et Cosmochimica Acta, Acta, 41, 1825-1834.

Matsunaga, T., Karametaxas, G., von Gunten, H.R., and Lichtner, P.C. (1993), Redox chemistry of iron and manganese minerals in river-recharged aquifers: A model interpretation of a column experiment. Geochemica et Cosmochimica Acta, 57, 16911704.

Mayer, L. M., and Rahaim, P. T., Guerin, W., Macko, S. A., Walting, L., and Anderson, F. E. (1985), Biological and granulometric controls on sedimentary organic matter of an intertidal mudflat. Estuarine Coastal Shelf Sci., 20, 491-504.

Mayer, L. M., Macko, S. A., and Gammen, L. (1988), Provenance, concentrations and nature of sedimentary organic nitrogen in the Gulf of Marine. Mar. Chem., 25, 291-304.

Mayer, L.M. (1993), Organic matter at the Sediment-Water Interface. In: Engel, M.H., Macko, S. A. (Eds.), Organic Geochemistry. Plenum, New York, pp. 171-183.

Meyers, P.A., Kawka, O. E., and Whitehead, D. R. (1984), Geolipid, pollen, and diatom stratigraphy in postglacial lacustrine sediments. Organic Geochemistry, 6, 727-732.

McCallan, M.E., O'Leary, B.M., and Rose, C.W. (1980), Redistribution of cesium-137 by erosion and deposition on an Australian soil. Australian Journal of Soil Research, 18, 119-128.

McCorkle, D.C. and Klinkhammer, G.P. (1990), Porewater cadmium geochemistry and the porewater cadmium: δ13C relationship. Geochemica et Cosmochimica Acta, 55, 161168.

Mitchell, P.A. (1984), The importance of sediment release in the assessment of a shallow, eutrophic lake for phosphorus control, p. 129-133. In Proceedings of the 3rd annual conference on lake and reservoir management, North American Lake Management Society. USEPA 440/5-84-001. Washington.

Mitchell, P. A. (1990a), Wabamun Lake. In Atlas of Alberta Lakes, edited by P. Mitchell and E. Prepas, pp. 438-445. University of Alberta Press, Edmonton, Alberta, Canada, AEU SCI GB 1630 A3 A8813 Information on current limnological conditions. Includes a bathymetric map.

Mitchell, P. A. (1990b), Lac Ste. Anne. In Atlas of Alberta Lakes, edited by P. Mitchell and E. Prepas, pp. 412-418. University of Alberta Press, Edmonton, Alberta, Canada. AEU SCI GB 1630 A3 A8813 Information on current limnological conditions. Includes a bathymetric map.

Mitchell, P. and Prepas, E.E. (1990), Atlas of Alberta Lakes. Edmonton: The University of Alberta Press.

Moffett, J.W. (1990), Microbially Mediated Cerium Oxidation in Sea Water, Nature, 345(6274), 421–423.

Moffett, J.W. (1994a), A radiotracer study of cerium and manganese uptake onto suspended particles in Chesapeake Bay. Geochimica et Cosmochimica Acta, 58(2), 695-703.

Moffett, J.W. (1994b), The relationship between cerium and manganese oxidation in the marine environment. Limnology and Oceanography, 39(6), 1309-1318.

Moore, J.N., Ficklin, W.H., and Johns, C. (1988), Partitioning of arsenic and metals in reducing sulfidic sediments. Environ. Sci. Technol., 22, 432-437.

Morfett, K., Davison, W., and Hamilton-Taylor, J. (1988), Trace metal dynamics in a seasonally anoxic lake. Environ. Geol. Water Sci., 11(1), 107-114.

Mortimer, C.H. (1941), The exchange of dissolved substances between mud and water in lakes. I and II. Journal of Ecology, 29, 280-329.

Mortimer, C.H. (1942), The exchange of dissolved substances between mud and water in lakes III. and IV. Journal of Ecology, 30, 147-201.

Mountfort, D.O. and Asher, R. (1981), Role of sulfate reduction versus methanogenesis in terminal carbon flow in polluted intertidal sediment of Waimea Inlet, Nelson, New Zealand. Appl. Environ. Microbiol., 42, 252-258.

Murphy, T.P, Prepas E.E., Lim, J.T., Crosby, J.M. and Walty, D.T. (1990), Evaluation of calcium carbonate and calcium hydroxide treatments of prairie drinking water dugouts. Lake Reserv. Manage. 6, 101-108.

Murray, J.W. (1975), The interaction of metal ions at the manganese dioxide-solution interface. Geochimica et Cosmochimica Acta, 39, 505-520.

Moss, B. (1985), Ecology of Fresh Waters. Blackwell Scientific Publications, London.

Murphy, T.P., Hall, K.J. and Yesaki, I. (1983), Co-precipitation of phosphate with calcite in a naturally eutrophic lake, Limnology and Oceanography, 28, 58-69.

Murphy, T.P., Hall, K.G., and Northcote, T.G. (1988), Lime treatment of a hardwater lake to reduce eutrophication. In Lake and Reserv. Manage., 4(2), 51-62.

Nelson, L. R., and Mitchell, P. A. (1988), Volunteer citizen's lake monitoring program (1988)-Lac Ste. Anne and Pigeon Lake. Alberta Environment, Envir. Assess. Division, Envir. Qlty. Monit. Br., Edmonton.

Nembrini, G., Capobianco, A., Garcia, J., and Jacquet, J.M. (1982), Interaction between interstitial water and sediment in two cores of Lac Leman, Switzerland. Hydrobiologia., 92, 363-375.

Nittrouer, C.A., DeMaster D.J., Mackee B.A., Cutshall N.H., and Larsen N.H. (1984), The effect of sediment mixing on ^{210}Pb accumulation rates for the Washington continental shelf. Marine Geology, 54, 201-221.

Nriagu, J.O. (1990), Global metal pollution: poisoning the biosphere? Environment, 32, 28-33.

Nriagu, J.O. (1994), Global inventory of natural and anthropogenic emissions of trace metals to the atmosphere; Nature, 279, 409-411.

Nriagu, J.O. and Pacyna, J.M. (1988), Quantitative assessment of worldwide contamination of air, water and soils by trace metals; Nature, 333, 134-139.

Noton, L.R. (1974), Phytoplankton productivity in Lake Wabamun, Alberta and the effect of thermal effluent. MSc thesis. Univ. Alberta, Edmonton.

Nriagu, J.O. and Dell, C.I. (1974), Diagenesic formation of iron phosphates in recent lake sediments. American Mineralogist. 59, 934-946.

Orem, W.H., Hatcher, P.G., Spiker, E.C., Szeverenyi, N.M., Maciel, G.E. (1986), Dissolved organic matter in anoxic waters from Mangrove Lake, Bermuda. Geochemica et Cosmochimica Acta, 50, 609-618.

Otsuki A. and Wetzel R.G. (1972), Coprecipitation of phosphate with carbonates in a marl lake. Limnology and Oceanography, 17, 763-767.

Park, S.W. and Huang, C.P. (1989), Chemical substitution reaction between Cu (II) and Hg (II) and hydrous US (s), Wat. Res. 23(12), 1527-1534.

Pedersen, T.F. and Price, N.B. (1982), The geochemistry of manganese carbonate in Panama Basin sediments. Geochemica et Cosmochimica Acta, 46, 59-68.

Penn, M.R., Auer, M.T., Doerr, S.M., Driscoll, C.T., Brooks, C.M., and Effler, S.W. (2000), Seasonality in phosphorus release rates from the sediments of a hypereutrophic lake under a matrix of pH and redox conditions. Canadian Journal of Fisheries and Aquatic Sciences, 57, 1033–1041.

Perkins, R. W., and Thomas, C. W. (1980), Worldwide fallout. Transuranic Elements in the Environment. W. C. Hanson, ed., USDOE/TIC-22800, 55-82.

Pettersson, K. (1986), The fractional composition of phosphorus in lake sediments of different characteristics. In Sediment and Water Interactions, edited by Sly, P.G. Springer-Verlag.

Pettersson, K. and Bostrom, B. (1986), Phosphorus exchange between sediment and water in Lake Balaton. In Sediment and Water Interactions, edited by Sly, P.G. Springer-Verlag.

Prapaipong, P., Shock, E. L., and Korestky, C. (1999), Metal-or ganic complexes in geochemical processes: Temperature dependence of the standard thermodynamic properties of aqueous complexes between metal cations and dicarboxylate ligands. Geochimica et Cosmochimica Acta, 63(17), 2547-2577.

Premuzic, E. T., Benkovitz, C. M., Gaffney, J. S., and Walsh, J. J. (1982), The nature and distribution of organic matter in the surface sediments of world oceans and Seas, Org. Geochem, 4, 63-77.

Prepas E.E. (1983), Orthophosphate turnover time in shallow productive lakes. Canadian Journal of Fisheries and Aquatic Sciences, 40, 1412-1418.

Prepas, E.E. and Trew, D.O. (1983), Evaluation of the phosphorus-chlorophyll relationship for lakes off the Precambrian Shield in western Canada. Canadian Journal of Fisheries and Aquatic Sciences, 40, 27-35.

Prepas, E.E. and Trimbee, A.M. (1988), Evaluation of indicators of nitrogen limitation in deep prairie lakes with laboratory bioassays and limnocorrals. Hydrobiologia, 159, 269-276.

Prepas, E.E., Murphy, T.P., Dinsmore, W.P., Burke, J.M., Chambers, P.A., and Reedyk, S. (1997), Lake management based onlime application and hypolimneticoxygenation: The experience in eutrophichardwater lakes in Alberta. Water Qual.Res. J. Canada, 32, 273-293.

Prepas, E.E., Babin, J., Murphy, T.P., Chambers, P.A., Sandland, G.J., Ghadouani, A., Serediak, M. (2001), Long-term effects of successive $Ca(OH)_2$ and $CaCO_3$ treatments on the water quality of two eutrophic hardwater lakes, Freshwater Biology, 46 (8) 1089-1103

Prepas, E.E., Pinel-Alloul, B., Chambers, P.A., Murphy, T.P., Reedyk, S., Sandland, G.J. and Serediak, M. (2001), Lime treatment and its effects on the chemistry and biota of hardwater eutrophic lakes. Freshwater Biology, 46 (8), 1049-1060.

Prepas, E.E., Murphy, T.P., Crosby, J.M., Walty, D.T., Lim, J.T., Babin, J., and Chambers, P.A. (1990), Reduction of phosphorus and chlorophyll a concentrations following $CaCO_3$ and

$Ca(OH)_2$ additions to hypereutrophic Figure Eight Lake, Alberta. In Environ. Sci. Technol., 24(8), 1252-1258.

Postma, D. (1981), Formation of siderite and vivianite and the porewater composition of a recent bog sediment in Denmark. Chemical Geology, 31, 225-244.

Rada R.G., Wiener, J.G., Winfrey, M.R., and Powell, D.E. (1989), Recent increases in atmospheric deposition of mercury toNorth-Central Wisconsin lakes inferred from sediment analyses.Arch. Environ. Contam. Toxicol., 18, 175-181.

Rasmussen, P.E. (1996), Trace metals in the environment: a geological perspective; Geological Survey of Canada, Bulletin 429, p. 26.

Rasmussen, P.E. (1998), Long range atmospheric transport of trace metals: the need for geoscience perspectives. Environmental Geology, 33(2/3), 96-107.

Reedyk, S., Prepas, E.E. and Chambers, P.A. (2001), Effects of single $Ca(OH)_2$ doses on phosphorus concentration and macrophyte biomass of two boreal eutrophic lakes over 2 years. Freshwater Biology, 46(8), 1075-1087.

Reid Crowther and Partners Ltd. (1973), Lake Wabamun Study. Prep. for Alberta Envir., Edmonton.

Renewable Resources Consulting Services Ltd. (1971), An ecological study of the wildlife and fisheries in the Pembina and Sturgeon River basins. Prepared for Alberta Environment, Water Resources Division, Edmonton.

Reynoldson, T.B., (1981), A reassessment of phosphorus inputs to Lake Isle, or Lake Isle revisited. Alta. Envir., Poll. Contr. Division, Water Qlty. Contr. Br., Edmonton.

Riley, E.T. and Prepas, E.E. (1984), Role of internal phosphorus loading in two shallow productive lakes in Alberta, Canada. Canadian Journal of Fisheries and Aquatic Sciences, 41, 845-855.

Ritchie, J.C., and McHenry, J.R. (1990), Application of radioactive fallout cesium-137 for measuring soil erosion and sediment accumulation rates and patterns: a review. Journal of Environmental Quality, 19, 215-233.

R.L. & L. Environmental Services Ltd. (1987), County of Parkland fisheries inventory: Lake Wabamun. Prep. for Alberta For. Ld. Wild., Fish Wild. Division and Rec. Parks Wild. Foundation, Edmonton.

Robbins, J.A. (1978), Geochemical and Geophysical Applications of Radioactive Lead. In: J.O. Nriagu (ed.), The Biogeochemistry of Lead in the Environment, Elsevier/North-HollandBiomedical Press New York, N.Y. pp. 285-393.

Robbins, J. A., Edgington, D. N., and Kemp, A. L. W. (1978), Comparative ^{210}Pb, ^{137}Cs and pollen geochronologies of sediments from lake Ontario and Erie. Quaternary Research, 10, 256-278.

Robbins, J.A., and Edgington, D.N. (1975), Determination of recent sedimentation rates using lead-210 and cesium-137. Geochimica et Cosmochimica Acta, 39, 285-304.

Robbins, J. A. and Herche, L. R. (1993), Radiochemical limnology: Models and uncertainty in ^{210}Pb dating of sediments. Verh. Internat. Verein. Limnol., 25, 217–222.

Robbins, J. A., Holmes, C., Halley, R., Bothner, M., Shinn, E., Graney, J., Keeler, G., TenBrink, M., Orlandini, K. A., and Rudnick, D. (2000), Time-averaged fluxes of lead and fallout radionuclides to sediments in Florida Bay, J. Geophys. Res. Vol. 105 , No. C12 , p. 28,805, In Environmental Changes and Radioactive Tracers, Proceedings of the South Pacific Environmental Radioactivity Association (SPERA) 2000 (J. M. Fernandez and R. Fichez, Eds.) IRD Editions, Paris, 2002, pp. 532.

Rosen, M.R., Turner, J.V., Coshell, L., and Gailitis, V. (1995), The effects of water temperature, stratification, and biological activity on the stable isotope composition and timing of carbonate precipitation in a hypersaline lake. Geochimica et Cosmochimica Acta, 59, 979-990.

Salmon, V. Derenne, S., Lallier-Verges, E., Largeau, C. and Beaudoin, B. (2000), Protection of organic matter by mineral matrix in a Cenomanian shale. Organic Geochemistry, 31, 463-474.

Sanei H., Goodarzi F., Snowdon L.R., Stasiuk L.D., and Van Der Flier-Keller E. (2000), Characterizing the Recent sediments from Pigeon Lake Alberta as related to anthropogenic and natural fluxes. Environmental Geosciences (AAPG). 7(4), 177-189.

Sanei, H., Goodarzi, F., Snowdon, and Van der Flier Keller, E. (2001), Historical variation of elements with respect to different geochemical fractions in recent sediments from Pigeon Lake, Alberta, Canada. Journal of Environmental Monitoring, 3(1), 27-36.

Saxby, J. (1969), Metal-organic chemistry of the geochemical cycle: Reviews of Pure and Applied Chemistry, 19, 131-150.

Schindler, D.W. (1977), Evolution of phosphorus limitation in lakes. Science, 195, 260-262.

Schwedhelm, E., Vollmer, M. and Kersten, M. (1988), Determination of dissolved heavy metal gradients at the sediment-water interface by use of a diffusioncontrolled sampler. Fresenius Z. Anal. Chem., 332, 756-763.

Shaw, J.F.H. and Prepas, E.E. (1990), Relationship between phosphorus in shallow sediments and in the trophogenic zone of seven Alberta Lakes. Wat. Res., 24, 551556.

Shirahata, H.R., Elias, R.W., Patterson, C.C. (1980), Chronological560variations in concentrations and isotope compositions of anthro-561pogenic atmospheric lead in sediments of a remote sub-alpine562pond. Geochimica et Cosmochimica Acta, 44, 149–162.

Sigg, L. (1986), Metal transfer mechanisms in lakes; the role of settling particles. In Chemical Processes in Lakes. edited by Werner Stumm. John Wiley & Sons.

Sholkowitz, E.R. (1976), Flocculation of dissolved organic and inorganic matter during the mixing of river water and sea water. Geochimica et Cosmochimica Acta, 40, 831-845.

Sholkovitz, E.R. and Copland, D. (1981), The coagulation, solubility and adsorption properties of Fe, Mn, Cu, Ni, Cd, Co and humic acids in a river water. Geochimica et Cosmochimica Acta, 45, 181–189.

Sigg, L., Stumm, M., and Kistler, D. (1987), Vertical transport of heavy metals by settling particles in Lake Zurich. Limnology and Oceanography, 32(l), 112-130.

Sloss, L. L. and Gardner, C. A. (1995), Sampling and Analysis of Trace Emissions from Coal-Fired Power Stations, IEA Coal Research Publication, International Energy Agency, London, p.74.

Smedley, P.L. (1991), The geochemistry of rare earth elements in groundwater from the Carnmenellis area, southwest England. Geochimica et Cosmochimica Acta, 55, 2767-2779.

Song, Y. and Müller, G. (1999), Sediment-water interactions in anoxic freshwater sediments; mobility of heavy metals and nutrients. Springer, Berlin. p. 111

Stabel, H. (1986), Calcite precipitation in Lake Constance:chemical equilibrium, sedimentation, and nucleation byalgae. Limnology and Oceanography, 31, 1081-1093.

Stasiuk, L.D. (1993), Algal bloom episodes and the formation of bituminite and micrinite in hydrocarbon source rocks: evidence from the Devonian and Mississippian, northern Williston Basin. International Journal of Coal Geology, 24, 195-210.

Stasiuk, L.D. (1999), Confocal laser scanning fluorescence microscopy of Botryococcus alginite from boghead oil shale, Boltysk, Ukraine: selective preservation of various micro-algal components. Organic Geochemistry, 30, 1021-1026.

Stasiuk, L.D. and Sanei, H. (2001), Characterization of diatom-derived lipids and chlorophyll within Holocene laminites, Saanich Inlet, British Columbia, using conventional and laser scanning fluorescence microscopy. Organic Geochemistry, 32, 1417-1428.

Stoeppler, M. (1992), Hazardous Metals in the Environment, Elsevier Science Publishers, London, p. 97-122, and 157-164.

Suess, E. (1979), Mineral phases formed in anoxic sediments by microbial decomposition of organic matter. Geochemica et Cosmochimica Acta, 43, 339-352.

Sundby, B., Gobeil, C., Silverberg, N., and Mucci, A. (1992), The phosphorus cycle in coastal marine sediments. Limnology and Oceanography, 37(6), 1129-1145.

Swain, E.B., Engstrom, D.R., Bringham, M.E., Henning, T.A., Breznik P.L. (1992), Increasing rates of atmospheric Mercury depsotion in midcontinental North America, Science, 257, 784-787.

Swanson, V., Frist, L., Radar, R., Jr., and Huffman, C., Jr. (1966), Metal sorption by northwest Florida humate: U.S. Geological Survey Professional, Paper 550-C, p. 174-177.

Sykes, R. and Snowdon, L.R. (2002), Guidelines for assessing the petroleum potential of coaly source rocks using Rock-Eval pyrolysis, In: Advances in organic geochemistry 2001; proceedings of the 20th international meeting on Organic geochemistry. (Ed) Di-Primio-R, Connan J., Eganhouse R., Schaeffer P., and van-Bergen P., Organic Geochemistry. 33(12), 1441-1455. Pergamon. Oxford-New York, International. 2002.

Takahashi, Y., Minai, Y., Ambe, S., Makide, Y. and Ambe, F. (1999), Comparison of adsorption behavior of multiple inorganic ions on kaolinte and silica in the presence of humic acid using the multitracer technique. Geochimica et Cosmochimica Acta, 63, 815-836.

Tamura, T. (1964), Selective sorption reactions of cesium with soil minerals. Nuclear Safety, 5(3), 262-265.

Tanoue, E. and Handa, N. (1979), Differential sorption of organic matter by various sized sediment particles in recent sediment from the Bering Sea. J. Oceanogr. Soc. J., 35, 199-208.

Taylor, S. R. and S. M. McClennan, (1985), The Continental Crust: Its Composition and Evolution, Blackwell, Cambridge.

Taylor, S.R. and McClennan, S.M, (1988), The significance of the rare earths in geochemistry. In: Gschneider Jr., K.A., Eyring, L. (Eds.), Handbook on the Physics and Chemistry of the Rare Earths, vol. 11, Elsevier, pp. 465-479.

Tegelaar, E. W., de Leeuw, J. W., Derenne, S., and Largeau, C. (1989), A reappraisal of kerogen formation. Geochimica et Cosmochimica Acta. 53, 3103-3106.

Telmer K, Bonham-Carter GF, and Kliza DA, (2004), The atmospheric transport and deposition of smelter emissions: Evidence from the multi-element geochemistry of snow, Quebec, Canada, Geochemica et Cosmochimica Acta. 68 (14), 2961-2980

Telmer, K., Kliza, D.A., Bonham-Carter, G.F., and Hall, G.E.M. (1999), Multi element environmental geochemical database for the Rouyn-Noranda region, Eastern Ontario and Western Quebec: Lake water and sediment chemistry, GSC open file.

Telmer, K. (1999), Interpretation of trace metals from natural and anthropogenic sources: Lake sediment studies. Metals In The Environment [MITE] Program Progress Report. Geological Survey of Canada.

Telmer, K. (Submitted). Spatial and temporal distribution of metals in the sediments of 99 lakes around the Horne Smelter, Quebec: the relationship between smelter emissions and lake sediment concentrations.

Telmer, K., Desjardins, M., and Ferguson, P. (in press a), Mercury in Lake Sediments and Porewaters: Multiple Evidence for Remobilization. In: A Multidisciplinary Study of Mercury Cycling in a Wetland Dominated Ecosystem: Kejimkujik Park, Nova Scotia. Eds. Ancitew Rencz and Nelson O'Driscoll. Society of Environmental Toxicology and Chemistry.

Telmer, K., Sanborn, M., and Rayne, S. (in press b), Sediment and Porewater Sampling for Trace Metal Concentrations in Lakes and Estuaries: Novel Coring, Extruding, and Dialysis Methods. Journal of Paleolimnology.

Tessier, A., Fortin, D., Belzile, N., DeVitre, R.R., Leppard, G.G. (1996), Metal sorption to diagenetic iron and manganese oxyhydroxides and associated organic matter: Narrowing the gap between field and laboratory measurements, Geochimica et Cosmochimica Acta, 60 (3), 387-404

Tipping, E. (1993), Modeling the competition between alkaline earth cations and trace metal species for binding of humic substances. Environmental Science & Technology, 27, 520-529.

Tissot, B.P. and Welte, D.H. (1985), Petroleum formation and occurrence, Journal of Sedimentary Petrology, 55(6), 942-943.

Todorović, Z., Polić, P., Djordjević, D. and Antonijević, S. (2001), Lead distribution in water and its association with sediment constituents of the "Barje" lake (Leskovac, Yugoslavia), J.Serb.Chem.Soc., 66(10), 697–708

Turekian, K.K., Nozaki, Y., and Benninger, L.K. (1977), Geochemistry of atmospheric radon and radon products. Ann. Rev. Earth Planet. Sci., 5, 227-255

Twardy, A.G. and Brocke, L.K. (1978), Soil survey and land suitability evaluation of the Isle Lake study area. Prepared for Alberta Environment by Pedol. Consult., Edmonton.

Tyson, R. V. (1995), Sedimentary Organic Matter, Organic Facies and Palynofacies. London: Chapmann and Hall.

Tyson, R. V. (2001), Sedimentation rate, dilution, preservation and total organic carbon: some results of a modeling study, Organic Geochemistry, 32, 333-339

Vanderploeg, H.A., Eadie, B.J., Lieberg, J.R., Tarapchak, S.J., and Glover, R.M. (1987), Contribution of calcite to the particle-size spectrum of Lake Michigan seston and its interactions with the plankton. Canadian Journal of Fisheries and Aquatic Sciences, 44, 1898-1914.

van den Berg, C.M.G. and Dharmvanij, S. (1984), Organic complexation of zink in estuarine interstitial and surface water samples. Limnology and Oceanography, 29(5), 1025-1036.

Verta, M. (1990), Mercury in Finnish forest lakes and resevoirs: Anthropogenic contribution to the load and accumulation in fish. Doctoral dissertation, Univ. of Helsinki. Publication of the Water and Environmantal Research Inst., Nat. Board of Waters and the Environ. Finland.

Vile, M.A., Wieder, R.K., Novak, M. (2000), 200 years of Pb deposition throughout the Czech Republic: Patterns and sources. Environ. Sci. Technol., 34(1), 12-21

Vuynovich, D. (1989), Geochemische Untersuchungen an Porenwassern im BodenseeSediment. Dissertation am Institut fur Sedimentforschung, Heidelberg Universitat.

Wallmann, K. (1990), Die Fruhdiagenese and ihr EinfluB auf die Mobilitat der Spurenelemente As, Cd, Co, Cu, Ni, Pb and Zn in Sediment- and SchwebstoffSuspensionen. Dissertation. Universitat Hamburg-Harburg. 195 S.

Wallmann, K. (1992), Solubility of cadmium and cobalt in a post-oxic or sub-oxic sediment suspension. Hydrobiologia, 235/236, 611-622.

Weiler, R. R., and Mills, A. A. (1965), Surface properties and pore structure of marine sediments. Deep-Sea Res., 12, 511-529.

Westerlund, S.F.G., Anderson, L.G., Hall, P.O.G., Iverfeldt, A., van der Loeff, M.M., and Sundby, B. (1986), Benthic fluxes of cadmium, copper, nickel, zinc and lead in the coastal environment. Geochemica et Cosmochimica Acta. 50, 1289-1296.

Williams, T.M. (1992), Diagenetic metals profiles in recent sediments of a Scottish Freshwater Loch. Environ. Geol. Water Sci., 20(2), 117-123.

Winfrey, M.R. and Zeikus, J.G. (1977), Effect of sulfate on carbon and electron flow during microbial methanogenesis in freshwater sediments. Appli. Environ. Microbiol., 33, 275-281.

Wu, Y., Lin, Y., Guo, T., Wang, L., and Zheng, Z. (1992), Mechanisms of phosphorus released from the sediment-water interface in Xiamen Bay, Fujian, China. Science of the Total Environment, Supplement, 1087-1097.

Zielinski, R.A. and Budahn, J.R. (1998), Radionuclides in fly ash and bottom ash: improved characterization based on radiography and low energy gamma-ray spectrometry, Fuel, 77(4), 259-267.